University Of Nottingham

School of Mathematical Sciences

Applications of Perturbation Theory to Power Electronic Converters

Author:

Marta Laterza

Supervisors:

Dr Stephen C. Creagh

Prof Pericle Zanchetta

Dr Martin Richter

Thesis submitted to the University of Nottingham for the degree of Doctor of Philosophy

24th August 2022

To Alessandro

Abstract

Power Electronic converters usually require complex controllers, involving large numbers of state-space variables; their models, moreover, tend to include multiple nonlinearities. These characteristics make assessing the stability of systems dominated by power electronics converters particularly challenging.

This work concerns the application of mathematical methods (in particular, attention focused on Singular Perturbation Theory) to power electronic systems, in order to model effectively their behaviour, reduce the size of their state-space systems, and assess their operating stability using simplified methods.

Some preliminary work was performed on the ripple modelling of a DC-DC boost converter and a single-phase full-bridge inverter; second-order approximations of the ripple and average behaviour, computed by applying Singular Perturbation methods, were found to agree very well to the solutions computed for the initial-value problem ODEs.

Singular Perturbation theory was subsequently applied to perform model reductions of power-electronic-based systems. First, a single-phase rectifier was considered, then AC microgrids. From a mathematical point of view, a similar approach was adopted in both cases to achieve the model reduction, but, given the different technical nature of such systems, they required separate literature reviews and preparatory work. The reductions were performed gradually, and several stages are here presented; results were tested in simulations, and stability analyses were compared to analogous analyses performed on the non-reduced full-sized systems.

Acknowledgements

I would like to start this thesis with thanking everyone who has supported me through my PhD journey.

First, I would like to thank my supervisors: Dr Stephen M. Cox, who guided most of my work, for patiently instilling mathematical rigour into my research; I am very grateful I had the opportunity to work with him; Dr Alessandro Costabeber, for his enthousiasm and insight in Power Electronics — time will not be enough to forget; Prof Pericle Zanchetta, who was my first contact in Nottingham, for welcoming me in England and supporting my application; Dr Andrea Formentini, for his contribution during a difficult change of topic; Dr Stephen C. Creagh, for his persistence in helping me get to the end and polish every chapter; Dr Martin Richter, for stepping in when we needed. This thesis could not exist without the contribution of each of them.

I would like to thank my Internal Examiner Prof Richard Graham and my Second Advisor Dr Gabriele Gradoni, for the feedback and encouragement I received during each Annual Review.

I would like to thank my External Examiner Prof Paolo Mattavelli, for dedicating time and attention to this thesis, and providing me with in-depth comments about my work.

I would like to thank my friends in Nottingham, who have been for me like a second family: my dear neighbour Mauro, who, with a broken arm, heroically pushed me in a trolley around the hospital emergency section; Gianluca, who first made me feel welcome when I moved to Nottingham; Giacomo, Davide, Luca, Massimo, Daniele, Alessandro, Alessandra, Luca, Con, Giulia, Gustavo, Jesu, Nicolas, Mattia, Giorgio, Luca, Manjusha, Xu Chen, Baya, Chris, Ellen, Fabio, Davide, Eugenio, Carmine, Giorgio, Charline, Tali, Grace, Bassem, Jordi, Tony, Liliana, Rasha.

The aim of branches is to grow away from roots, seeking more light, but they always need to keep a link with them. In the same way, I would like to thank my motherland Italy, that still provides its kids with high-level affordable education,

for raising and educating me, and generously granting me the freedom to choose any path I preferred as the next stage of my life and career. I would like to thank my friends from home, who did not let the physical distance compromise our connection: Sergio, Giulia, Davide, Luigi, Francesco, Emanuele, Arianna, Cesare, Kant, Kati, Marina, Andrea, Valentina, Laura, Sara, Alice, Marco, Beatrice, Giuliana, Sara, Stefania, Marianna, Luigi, Paolo, Riccardo, Yue, Luca. I would like to thank Marco for his generosity in helping me stay (in)sane.

I would like to thank my extended family, a bit scattered around Europe, as we like keeping in touch during easy times, but I am also sure we can count on each other when times are hard.

I would like to thank Savvas for his love and support during the last three years.

Finally, I would like to thank my parents, for being uninterruptedly encouraging and proud, and brave enough to teach me to be independent since early age (even though I know two parachutes might pop out if I were in need). It must have been hard to let the tiny eight-year-old me walk to school on her own, it must have been hard, later in life, to see me fly away.

Contents

List of Figures

List of Tables

List of Acronyms

AC alternating current.

AFE Active-Front-End.

BW bandwidth.

DC direct current.

HV high voltage.

HVDC high-voltage direct current.

LTP Linear Time-Periodic.

LV low voltage.

ODE ordinary differential equation.

PI Proportional-Integral.

PLL phase-locked loop.

PWM pulse-width modulation.

SP single-phase.

ZOH Zero-Order Hold.

Chapter 1

Introduction

This thesis concerns the application of mathematical methods to power electronic systems, in order to obtain effective models of such systems, perform reliable model reductions and assess their operating stability. Power electronic converters, introduced in §1.1, in general, need complex controllers to operate effectively; the state-space systems describing their behaviour tend to be "large". Hence, power-electronic-based systems could particularly benefit from the application of techniques aimed at reducing the number of their variables without compromising the accuracy of their models.
In particular, in this work attention is focused on:

- Mathematical modelling of the ripple of a Boost direct current (DC)-DC converter and a single-phase (SP) Full-Bridge inverter;
- Model reduction of a Single-Phase Active-Front-End (AFE);
- Model reduction of alternating current (AC) microgrids.

The present chapter contains theoretical introductions to both mathematical and engineering topics. §1.1 gives a short induction to Power Electronics, while the mathematical bases for the different parts of the project will be given at the beginning of the relevant chapters, together with the corresponding literature review.
§2 concerns the application of perturbation theory to a DC-DC boost converter and a Single-Phase Full-Bridge inverter, presenting different approximations of their average behaviour and ripple.
In §3, a model reduction of a Single-Phase Active-Front-End rectifier is presented.

A literature review opens the chapter, where nonlinear and linear time-periodic systems are analysed. Results are achieved through the application of perturbation theory, and different levels of reduction are treated, according to different choices that can be performed during nondimensionalisation. Stability analyses are performed to full and reduced systems according to Linear Time-Periodic theory.

§4 contains an introduction to AC microgrids, together with a relevant literature review.

An analysis of the controller structure of inverters connected to AC microgrids is presented in §5. After discussing each part of the controller, a model reduction is performed on a system formed by a single inverter operating as an AC microgrid converter.

§6 concerns the model reduction of an AC microgrid formed by two inverters. Results are achieved by applying perturbation theory to the system, and different degrees of reduction are proposed. Time-domain simulations and stability analyses are used to compare the reduced models with the full-model behaviour.

Conclusions and potential future work topics are summarised in §7.

1.1 Brief introduction to Power Electronics and main challenges of operating power electronic converters

Power electronic converters are semiconductor-based devices which are employed to control and convert electrical power by high-frequency switching [1] [2]. As power can flow through alternating current (AC) or direct current (DC), conversions are needed in order to make voltages and currents meet the requirements of the load or a certain section of the considered electrical systems. Conversions are possible when a change from DC to AC or vice versa is needed, but also if a different value of the voltage or current is demanded without changing the type of flow, as in DC-DC and AC-AC conversions. In particular, applications of rectifiers (AC-DC converters) include: supplying power to electronic devices (e.g. computer, phones, televisions, etc.), DC electrical motors and some railway

and metro lines, charging batteries, feeding high-voltage direct current (HVDC) transmission systems, which are in general employed for underwater power cables. Inverters, instead, are DC-AC converters and are necessary to connect DC-generated power (e.g. power from photovoltaic systems) to the grid, or to link DC storages, consisting of batteries or other charge accumulators, to AC loads.

The switching frequency used by power electronic converters is usually of the order of 10 kHz; the switching period tends then to be at least one or two orders smaller than the other time scales of the electrical systems connected to the switches, which are, in general, a low-pass filter followed by the grid or a load (e.g. resistive load, inductive-resistive load, electrical motor, etc.).

The presence of a parameter that is small compared to the others of the system (e.g. the ratio of the switching period to the other time scales) suggests that perturbation methods could be applied to generate simpler models. This could be achieved by averaging (or a generalisation of averaging) and/or by model reduction, reducing the number of governing ordinary ordinary differential equations (ODEs) if some variables appear to be "slaved" to others.

Traditionally, electrical engineers compute an averaged system of converters by applying an averaging method (such as state-space averaging, Krylov-Bogoliubov-Mitropolsky theories, [3, 4, 5]). The so-obtained simplified systems are free from high-frequency oscillations and are characterised by having fewer nonlinearities; they can be utilised in model implementation and controller design ([6], [7], [8], [9], etc.). Neglecting the ripple caused by the high-frequency switching, it is possible to work with an average model where the system evolution is noticeable only on a larger time scale (e.g. the AC grid period or other time scales of the same order of the system time constants), while they are quasi-constant if a single switching period is considered. Considering the average behaviour only, though, can lead to the formulation of an inaccurate controller and to possible errors in the prediction of the system stability. ([6], [8], [10]).

When symmetric three-phase systems are considered (i.e., each phase carries an alternating current of the same frequency and voltage amplitude relative to

a common reference, with a phase difference of $2\pi/3$), a direct-quadrature-zero (DQ0) transformation can often be applied (in the case of negligible harmonics with order greater than one, compared to the amplitude of the fundamental). DQ0 transformation projects a three-phase quantity onto a rotating reference frame whose frequency is equal to that of the alternating voltage. This procedure allows one, in steady-state, to consider two constant values instead of three sinusoidal quantities [11][12].

However, if a single-phase converter is considered or if in the analysed system some harmonics of order greater than one cannot be neglected, DQ0 transformation cannot be applied. Therefore, even though the system model can be simplified by averaging it and neglecting high frequencies, stability analysis is algebraically involved. Indeed, when state-space systems are computed for control and stability purposes, some of their variables are characterised by time-periodic behaviours. Those systems, moreover, are often nonlinear. Performing their linearisation, then, includes the computation of time-periodic steady-states. When looking at the behaviour of perturbations of the steady-state, a linearised system with time-periodic coefficients is obtained, in the form of a Linear Time Periodic (LTP) system. The stability analysis, thus, follows from Floquet theory [13] [14].

Engineering custom tends to deal with dimensional systems and to apply ad-hoc approximations. For the purpose of performing perturbation methods or other reduction techniques, the system parameter magnitudes must be compared to each other, in order to identify relatively big and small quantities. Keeping the system dimensional, however, makes this comparison hard because of the inconsistency between the parameters.

To improve those results and obtain a more systematic way of approximating and reducing power electronic models, a different approach has been considered here. Nondimensionalisation has been applied to power electronic systems in order to identify small parameters and to lead to the formulation of systematic reduction techniques.

Chapter 2

DC-DC Boost Converter and Single-Phase Full-Bridge Inverter Analysis

In this chapter, the behaviour of a DC-DC converter and a single-phase inverter are analysed through the computation of the averaged state-space ODEs and of the ripple. Those systems are relatively simple from an engineering point of view, but were chosen for familiarising with the application of perturbation theories to power electronics, as a preliminary step before moving to more complex systems described in the following chapters.
In §2.1 is given an introduction to singular perturbed systems and their averaging, while 2.2 reports some examples of averaged systems from the engineering literature. The following sections contain the averaging and ripple modelling of the two analysed converters.

2.1 Averaging of Singular Perturbed Systems

According to the Krylov-Bogoliubov-Mitropolsky (KBM) technique, the exact differential equation describing a singularly perturbed system can be decomposed into the approximation of its averaged ODEs and the approximation of its ripple. The averaged problem and the ripple can each be further decomposed into a series, whose terms decrease according to the power of a small scalar parameter ϵ. The terms of each series can be computed sequentially by an iterative method, as shown below. Iterating the computation of the averaged system and the ripple leads the sum of the series terms to converge to the exact system solution ([3],

[4], [5], [10]).

If a system can be described by

$$\dot{\boldsymbol{w}} \;=\; \epsilon\, \boldsymbol{h}(t,\; \boldsymbol{w})\;, \tag{2.1}$$

where $\boldsymbol{h}$ is a continuous function and ϵ is a small scalar parameter, the following change of variables can be considered:

$$\boldsymbol{w}(t) \;=\; \boldsymbol{y}(t) \;+\; \epsilon\; \boldsymbol{\Psi}_1(t,\; \boldsymbol{y}) \;+\; \epsilon^2\; \boldsymbol{\Psi}_2(t,\; \boldsymbol{y}) \;+\; \cdots\;, \tag{2.2}$$

where $\boldsymbol{\Psi}_i$ are functions with a zero average with respect to t and are continuous in t, $\boldsymbol{y}$.

In (2.2), $\boldsymbol{y}$ behaves like the average of $\boldsymbol{w}$, while $\sum_{i=1}^{N} \epsilon^i\; \boldsymbol{\Psi}_i$ represents the ripple of $\boldsymbol{x}$.

The averaged-variables vector $\boldsymbol{y}$ can be computed as the solution of a time-invariant system

$$\dot{\boldsymbol{y}} \;=\; \epsilon\, \boldsymbol{G}_1(\boldsymbol{y}) \;+\; \epsilon^2\, \boldsymbol{G}_2(\boldsymbol{y}) \;+\; \cdots\;. \tag{2.3}$$

Therefore, (2.2) can be differentiated with respect to time, substituting $\dot{\boldsymbol{y}}(t)$ with (2.3):

$$\dot{\boldsymbol{w}}(t) \;=\; \sum_{i=1}^{N} \epsilon^i \boldsymbol{G}_i(\boldsymbol{y}) \;+\; \sum_{i=1}^{N} \epsilon^i \left\{ \frac{\partial\, \boldsymbol{\Psi}_i}{\partial\, t} \;+\; \frac{\partial\, \boldsymbol{\Psi}_i}{\partial \boldsymbol{y}} \left[\sum_{m=1}^{N} \epsilon^m\, \boldsymbol{G}_m(\boldsymbol{y}) \right] \right\}\;. \tag{2.4}$$

The computation of $\boldsymbol{G}_i$ and $\boldsymbol{\Psi}_i$ can be performed by equating identical powers of ϵ and setting the average value of $\boldsymbol{\Psi}_i$ equal to $\mathbf{0}$, as follows.

$$\langle\, \boldsymbol{\Psi}_i(t,\; \boldsymbol{y}) \rangle \;=\; \langle\, \boldsymbol{\Psi}_i \rangle \;=\; \mathbf{0}\;, \tag{2.5}$$

where

$$\langle\, \boldsymbol{\Psi}_i(t,\; \boldsymbol{y}) \rangle \;=\; \frac{1}{T} \int_{n}^{n+T} \boldsymbol{h}(\boldsymbol{w})\; \mathrm{d}t \tag{2.6}$$

and T is the period of the ripple.

While a short time scale in variations of $\boldsymbol{h}$ needs to be resolved in (2.1), no short time scale has to be resolved in (2.3), requiring a smaller computational effort.

2.2 Applications of Singular Perturbation Theory in the Power Electronics Literature

Since in a power electronic converter the switching period is small compared to the system time constants, voltages and currents measured on the passive components (i.e. resistors, capacitors, inductors) are never allowed to complete their exponential-shaped transients after a switch changes its position from open to closed or vice versa. Long before the system reaches its steady state, the switches change their configuration again, leading to a high-frequency oscillatory behaviour. Due to the different order of the switching period and the system time constants, the shape of the ripple looks almost like a triangle wave. After the switches, capacitive and/or inductive filters are usually placed to obtain smoother voltages and currents: high-frequency ripples are an unwanted consequence of the switching and are added to the desired output values, which are in general constant (AC-DC and DC-DC cases) or sinusoidal (DC-AC and AC-AC cases).

The KBM averaging method has been applied to DC-DC converters in [7], [8] and [9]. In particular, [8] highlights how the application of KBM averaging to closed-loop systems allows a better stability than the utilisation of other, heuristic methods. In [9], a separation between "slow" and "fast" variables is applied and some considerations about the system stability are given. The system (2.1) is then split into

$$\dot{\boldsymbol{x}} = \boldsymbol{f}(\boldsymbol{x}, \boldsymbol{z}, \epsilon), \tag{2.7a}$$

$$\epsilon\dot{\boldsymbol{z}} = \boldsymbol{g}(\boldsymbol{x}, \boldsymbol{z}, \epsilon) \tag{2.7b}$$

where the variables of $\boldsymbol{w}$ are split into $\boldsymbol{x}$, the vector of "slow" variables, and $\boldsymbol{z}$,

the vector of "fast" ones. On the fast timescale, $\boldsymbol{x}$ are considered as constant and only the dynamics of $\boldsymbol{z}$ are taken into account.

The same separation of variables is performed in [15], where a DC-AC converter is modelled as a singularly perturbed system and a stability analysis has been performed. In both cases, stability has not been studied for systems in which the separation of variables is not possible due to excessively close time scales.
In none of the cited articles has nondimensionalisation been performed and the choice of the small scalar parameter ϵ is sometimes not clear. Traditionally, indeed, the engineering modelling procedures tend to deal with dimensional systems; this can sometimes obscure any separation of fast and slow dynamics and make the identification of small parameters harder. By contrast, in mathematical methods the systems tend to be nondimensionalised, which allows a clear indication of any small or large parameter groups. In [7], for example, ϵ results from an inconsistent comparison between quantities with differing dimensions, while in [8] and [9] it is defined as "small", but its relation to the system constants is not explicitly clarified; in [15], ϵ is declared as being not scalar and is dimensionally an inductance.

2.3 Boost DC-DC Converter Analysis

This section describes the work performed on a standard boost DC-DC converter. The presented analysis aims to study its behaviour applying perturbation theory. The system is first described in §2.3.1, and is then nondimensionalised as explained in §2.3.2. Its averaged are computed, and its ripple is approximated. The proposed model is tested in simulations.

2.3.1 Model Description

Figure 2.1 depicts a standard boost DC-DC converter. Boost converters are used to increase the value of a DC voltage to a desired reference. V_{in} is the input DC voltage; V_{out} is the output voltage; q is a silicon-based controllable switch.

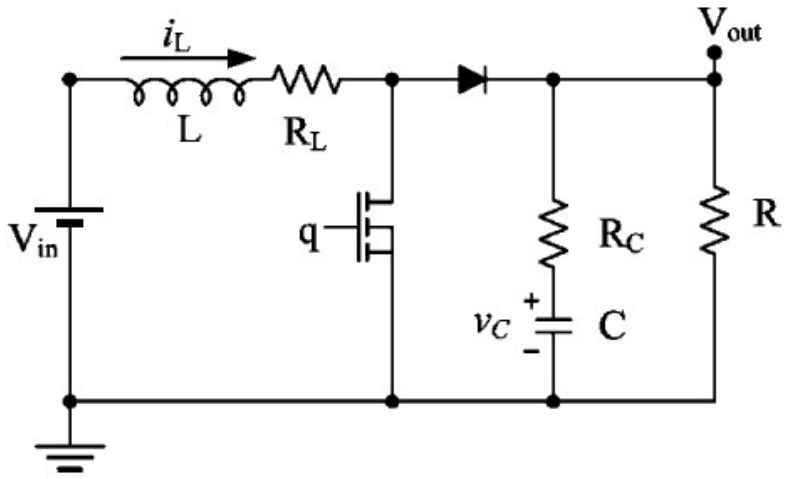

Figure 2.1: Boost DC-DC converter scheme

An inductor, whose inductance and parasitic resistance are denoted by L and R_L, respectively, is placed between the input voltage source and the switch; a capacitor, with capacitance C and parasitic resistance R_C, is in parallel with the load resistor. The values of the system parameters used in simulations are listed in Table 2.1.

T_S	Switching period	[s]	$4.00 \cdot 10^{-5}$
R	Load resistance	[Ω]	100
L	Inductor inductance	[H]	$657 \cdot 10^{-6}$
R_L	Inductor resistance	[Ω]	0.584
C	Capacitor capacitance	[F]	$77 \cdot 10^{-6}$
R_C	Capacitor resistance	[Ω]	0.381
V_{in}	Input DC voltage	[V]	12

Table 2.1: System parameters used to model a boost DC-DC converter.

The inductor current i_L and the capacitor voltage v_C are the chosen state variables.

Applying Kirchhoff laws to the depicted circuit, it is possible to compute the

following state-space equations:

$$\frac{\mathrm{d}v_C(t)}{\mathrm{d}t} = -\frac{1}{C(R+R_C)}v_C(t) + h(t)\frac{R}{C(R+R_C)}i_L(t), \tag{2.8a}$$

$$\frac{\mathrm{d}i_L(t)}{\mathrm{d}t} = -h(t)\frac{R}{L(R+R_C)}v_C(t) - h(t)\frac{RR_C}{L(R+R_C)}i_L - \frac{R_L}{L}i_L(t) + \frac{v_{\text{in}}(t)}{L}, \tag{2.8b}$$

where $h(t)$ is a switching function, whose value depends on the state of the switch q: h is equal to 1 when q is open (OFF) and equal to 0 when it is closed (ON), as shown in Figure 2.2.

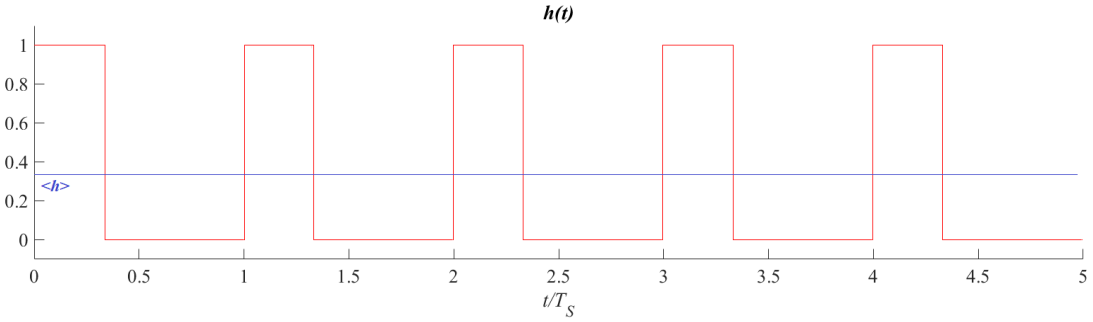

Figure 2.2: Behaviour of $h(t)$

Then, in steady-state, $h(t)$ can be expressed as

$$h(t) = \begin{cases} 1 & \text{if } nT_S < t < (n+\langle h\rangle)T_S, \\ 0 & \text{if } (n+\langle h\rangle)T_S < t < (n+1)T_S, \end{cases} \qquad n \in \mathbb{N}. \tag{2.9}$$

In (2.9), T_S is the switching period, while $\langle h\rangle$ is the average value of h, given by

$$\langle h\rangle = \frac{1\cdot t_{OFF}}{T_S} = \frac{1\cdot(T_S - t_{ON})}{T_S} = 1 - \delta\,, \tag{2.10}$$

where δ is the duty cycle of the switch.

2.3.2 Nondimensionalisation

Let V_b, I_b, T_b be the base unit values for voltage, current and time, respectively, and let $I_b = V_b/R$.

The system variables can then be expressed as

$$v_C = \hat{v}_C\, V_b\ , \tag{2.11a}$$

$$i_L = \hat{i}_L\, I_b\ = \hat{i}_L \frac{V_b}{R}\ , \tag{2.11b}$$

$$t = \hat{t}\, T_b\ , \tag{2.11c}$$

$$V_{in} = \hat{w}\, V_b\ , \tag{2.11d}$$

where $\hat{v}_C$, $\hat{i}_L$, $\hat{t}$ and $\hat{w}$ are nondimensional time-dependent variables.

Substitution of (2.11a)-(2.11d) into (2.8) leads to

$$\frac{\mathrm{d}\hat{v}_C(\hat{t})}{\mathrm{d}\hat{t}} = -\frac{T_b}{C(R+R_C)}\,\hat{v}_C(\hat{t}) + h(\hat{t})\frac{T_b}{C(R+R_C)}\,\hat{i}_L(\hat{t}) \tag{2.12a}$$

$$\begin{aligned}\frac{\mathrm{d}\hat{i}_L}{\mathrm{d}\hat{t}} = -h(\hat{t})\frac{R^2\,T_b}{L(R+R_C)}\hat{v}_C(\hat{t}) - h(\hat{t})\frac{RR_CT_b}{L(R+R_C)}\hat{i}_L(\hat{t}) - \frac{R_LRT_b}{LR}\hat{i}_L(\hat{t}) \\ + \frac{R\,T_b}{L}\hat{w}(\hat{t}).\end{aligned} \tag{2.12b}$$

Now, let the time constant τ_1, τ_2 and their ratio k_{12} be defined as

$$\tau_1 = C(R + R_C)\ , \tag{2.13a}$$

$$\tau_2 = \frac{L}{R}\ , \tag{2.13b}$$

$$k_{12} = \frac{\tau_2}{\tau_1}\ . \tag{2.13c}$$

Then, using (2.13a)-(2.13c), and dropping the hats from the notation, equations (2.12) can be written as

$$\frac{\mathrm{d}v_C(t)}{\mathrm{d}t} = -\frac{T_b}{\tau_1}\,v_C + h(t)\frac{T_b}{\tau_1}\,i_L \tag{2.14a}$$

$$\begin{aligned}\frac{\mathrm{d}i_L(t)}{\mathrm{d}t} = -h(t)\frac{R}{(R+R_C)}\frac{T_b}{k_{12}\tau_1}v_C(t) - h(t)\frac{R_C}{R+R_C}\frac{T_b}{k_{12}\tau_1}i_L(t) + \\ - \frac{R_L}{R}\frac{T_b}{k_{12}\tau_1}i_L(t) + \frac{T_b}{k_{12}\tau_1}w(t).\end{aligned} \tag{2.14b}$$

System (2.14) is the dimensionless system corresponding to (2.8).

2.3.3 Small Parameter and Perturbed System Definition

Since the system is considered to be "fast switching" (i.e. the switching period is negligible compared to the other time constants characteristic of the system), the small dimensionless parameter ϵ is set to be proportional to T_S and inversely proportional to one of the system time constants.
For the considered system, the following values are chosen as the time base unit and ϵ, respectively:

$$T_b = T_S \,, \tag{2.15a}$$

$$\epsilon = \frac{T_S}{\tau_1} \,. \tag{2.15b}$$

The choice of setting the time base unit equal to the switching period, moreover, allows one to compute the average values in a nondimensional time interval from 0 to 1.
For the values listed in Table 2.1, ϵ is equal to $5.2 \cdot 10^{-3}$. Therefore, substitution of (2.15) into (2.14) leads to

$$\frac{\mathrm{d}v_C(t)}{\mathrm{d}t} = -\epsilon\, v_C(t) + h(t)\,\epsilon\, i_L(t), \tag{2.16a}$$

$$\frac{\mathrm{d}i_L(t)}{\mathrm{d}t} = -h(t)\,\frac{\epsilon}{k_{12}}\,\frac{R}{R+R_C}\,v_C(t) - h(t)\,\frac{\epsilon}{k_{12}}\,\frac{R_C}{R+R_C}\,i_L(t) + \frac{\epsilon}{k_{12}}\,w(t), \tag{2.16b}$$

which, in matrix form, corresponds to

$$\begin{bmatrix} \dot{v}_C(t) \\ \dot{i}_L(t) \end{bmatrix} = \epsilon \left\{ \left(\begin{bmatrix} -1 & 0 \\ 0 & -\dfrac{R_L}{k_{12}R} \end{bmatrix} + h(t) \begin{bmatrix} 0 & 1 \\ -\dfrac{R}{k_{12}(R+R_C)} & -\dfrac{R_C}{k_{12}(R+R_C)} \end{bmatrix} \right) \begin{bmatrix} v_C(t) \\ i_L(t) \end{bmatrix} + \begin{bmatrix} 0 \\ \dfrac{w(t)}{k_{12}} \end{bmatrix} \right\} . \tag{2.17}$$

Let M_1, M_2 and $\boldsymbol{b}$ be defined, respectively, as:

$$M_1 = \begin{bmatrix} -1 & 0 \\ 0 & -\dfrac{R_L}{k_{12}R} \end{bmatrix}, \tag{2.18a}$$

$$M_2 = \begin{bmatrix} 0 & 1 \\ -\dfrac{R}{k_{12}(R+R_C)} & -\dfrac{R_C}{k_{12}(R+R_C)} \end{bmatrix}, \tag{2.18b}$$

$$\boldsymbol{b}(t) = \begin{bmatrix} 0 \\ \dfrac{w(t)}{k_{12}} \end{bmatrix}. \tag{2.18c}$$

Then, substitution of (2.18) into (2.17) allows (2.17) to be written in the following more compact form:

$$\dot{\boldsymbol{x}}(t) = \epsilon\Big[\Big(M_1 + h(t)\,M_2\Big)\boldsymbol{x}(t) + \boldsymbol{b}(t)\Big], \tag{2.19}$$

where

$$\boldsymbol{x}(t) = \Big[v_C(t) \quad i_L(t)\Big]^T. \tag{2.20}$$

2.3.4 Average System and Ripple Computation

According to the procedure explained in §2.1, the averaged system can be found by equating the RHS of (2.4) and (2.19):

$$\sum_{i=1}^{N} \epsilon^i \boldsymbol{G}_i(\boldsymbol{y}) + \sum_{i=1}^{N} \epsilon^i \left\{ \frac{\partial \boldsymbol{\Psi}_i}{\partial t} + \frac{\partial \boldsymbol{\Psi}_i}{\partial \boldsymbol{y}} \left[\sum_{m=1}^{N} \epsilon^m \boldsymbol{G}_m(\boldsymbol{y}) \right] \right\} = \\ = \epsilon\left[\left(M_1 + h(t)\,M_2\right)\boldsymbol{x}(t) + \boldsymbol{b}(t)\right]. \tag{2.21}$$

Moreover, substituting (2.2) into the RHS of (2.21) leads to

$$\sum_{i=1}^{N} \epsilon^i \left\{ \boldsymbol{G}_i(\boldsymbol{y}) + \frac{\partial \boldsymbol{\Psi}_i}{\partial t} + \frac{\partial \boldsymbol{\Psi}_i}{\partial \boldsymbol{y}} \left[\sum_{m=1}^{N} \epsilon^m \boldsymbol{G}_m(\boldsymbol{y}) \right] \right\} =$$

$$= \epsilon \left[\Big(M_1 + h(t)\, M_2 \Big) \left(\boldsymbol{y} + \sum_{i=1}^{N} \epsilon^i \, \boldsymbol{\Psi}_i \right) + \boldsymbol{b}(t) \right] . \quad (2.22)$$

Equation (2.22) corresponds to equation (2.4). Then, its LHS terms can be equated to the RHS terms according to the power order of ϵ, allowing the explicit computation of $\boldsymbol{G}_i$ and $\boldsymbol{\Psi}_i$.

2.3.4.1 Ripple computation, O(ϵ) terms and first-order approximation

Selection in (2.22) of the terms of order ϵ leads to

$$\boldsymbol{G}_1(\boldsymbol{y}) + \frac{\partial \boldsymbol{\Psi}_1}{\partial t} = \Big(M_1 + h(t)\, M_2 \Big) \boldsymbol{y} + \boldsymbol{b}(t) . \quad (2.23)$$

Since, according to (2.15), the time base unit has been set equal to the switching period, the average value of (2.23) can be computed by integrating each term with respect to the nondimensionalised time from 0 to 1:

$$\int_0^1 \boldsymbol{G}_1(\boldsymbol{y})\, \mathrm{d}t + \int_0^1 \frac{\partial \boldsymbol{\Psi}_1}{\partial t}(t,\, \boldsymbol{y})\, \mathrm{d}t = \int_0^1 \Big(M_1 + h(t)\, M_2 \Big) \boldsymbol{y}\, \mathrm{d}t + \int_0^1 \boldsymbol{b}\, \mathrm{d}t , \quad (2.24)$$

where $\displaystyle\int_0^1 \frac{\partial \boldsymbol{\Psi}_1}{\partial t}(t,\, \boldsymbol{y})\, \mathrm{d}t = \boldsymbol{0}$ and $\boldsymbol{G}_1(\boldsymbol{y})$ and $\boldsymbol{b}$ are time invariant by definition. Therefore,

$$\boldsymbol{G}_1(\boldsymbol{y}) = \int_0^1 \Big(M_1 + h(t)\, M_2 \Big) \boldsymbol{y}\, \mathrm{d}t + \boldsymbol{b} = \Big(M_1 + \langle h \rangle\, M_2 \Big) \boldsymbol{y} + \boldsymbol{b} . \quad (2.25)$$

Thus, in first approximation, the averaged system can be expressed as

$$\dot{\boldsymbol{y}} = \epsilon \Big[\Big(M_1 + \langle h \rangle M_2 \Big) \boldsymbol{y} + \boldsymbol{b} \Big] + o(\epsilon) . \quad (2.26)$$

$\boldsymbol{\Psi}_1$ can be computed by substituting (2.25) in (2.23) and integrating the resulting

equation with respect to time, as shown below.

$$\Big(M_1 + \langle h \rangle M_2\Big)\boldsymbol{y} + \boldsymbol{b} + \frac{\partial \boldsymbol{\Psi}_1(t,\boldsymbol{y})}{\partial t} = \Big(M_1 + h(t)\, M_2\Big)\boldsymbol{y} + \boldsymbol{b} \tag{2.27}$$

$$\implies \frac{\partial \boldsymbol{\Psi}_1(t,\boldsymbol{y})}{\partial t} = \Big(h(t) - \langle h \rangle\Big) M_2\, \boldsymbol{y} \tag{2.28}$$

Let now the scalar function $f_1(t)$ be continuous in t and defined as follows:

$$f_1'(t) = h(t) - \langle h \rangle \,, \tag{2.29a}$$

$$\langle f_1 \rangle = 0 \,, \tag{2.29b}$$

where $\langle f_i \rangle$ is the average value of f_i.

The derivative of $\boldsymbol{\Psi}_1$ with respect to time, displayed in (2.28), then, can also be written as:

$$\frac{\partial \boldsymbol{\Psi}_1}{\partial t}(t,\boldsymbol{y}) = f_1'(t)\, M_2\, \boldsymbol{y} \,. \tag{2.30}$$

Integrating (2.30) leads to

$$\boldsymbol{\Psi}_1(t,\, \boldsymbol{y}) = \int f_1'(t)\, M_2\, \boldsymbol{y}\, \mathrm{d}t = \left(\int f_1'(t)\, \mathrm{d}t\right) M_2\, \boldsymbol{y} = f_1(t)\, M_2\, \boldsymbol{y} \,. \tag{2.31}$$

Since $\boldsymbol{\Psi}_1$ is an approximation of the ripple, it is defined as a zero-average function; f_1 is the only element in (2.31) directly dependent on time. Then, f_1 must be chosen by integrating the first equation of (2.29) and imposing that the function should have a zero average between 0 and 1.

Considering that the equation of h displayed in (2.9) can be expressed for the nondimensional time as

$$h(t) = \begin{cases} 1 & \text{if } n < t < n + \langle h \rangle \\ \\ 0 & \text{if } n + \langle h \rangle < t < n + 1 \end{cases} \qquad n \in \mathbb{N} \,, \tag{2.32}$$

substitution of (2.32) into (2.29) leads to

$$f_1'(t) = \begin{cases} 1 - \langle h \rangle & \text{if } n < t < n + \langle h \rangle \\ \\ -\langle h \rangle & \text{if } n + \langle h \rangle < t < n + 1 \end{cases} \tag{2.33}$$

Therefore, f_1 can be computed integrating (2.33) with respect to time:

$$f_1(t) \;=\; \begin{cases} (1 \,-\, \langle h \rangle)\,(t \,-\, n) \,+\, c_1 & \text{if } \; n \,<\, t \,<\, n + \langle h \rangle \\ \\ -\,\langle h \rangle\;(t \,-\, n) \,+\, c_2 & \text{if } \; n + \langle h \rangle \,<\, t \,<\, n + 1\;, \end{cases} \tag{2.34}$$

where c_1 and c_2 are constants of integration, which can be computed by imposing continuity in t and a zero average between 0 and 1. The result is

$$f_1(t) \;=\; \begin{cases} (1 \,-\, \langle h \rangle)(t - n \,-\, 1/2\langle h \rangle) & \text{if } \; n \,<\, t \,<\, n + \langle h \rangle \\ \\ \langle h \rangle \left(\dfrac{\langle h \rangle + 1}{2} \,-\, t + n \right) & \text{if } \; n + \langle h \rangle \,<\, t \,<\, n + 1 \end{cases} \tag{2.35}$$

Finally, $\boldsymbol{x}$ can be approximated to first order as follows:

$$\boldsymbol{x} \;=\; \boldsymbol{y} \;+\; \epsilon\, f_1(t)\, M_2\, \boldsymbol{y} \;+\; o(\epsilon)\;, \tag{2.36}$$

where $\boldsymbol{y}$ is the solution of (2.26). An explicit solution for $\boldsymbol{y}$ is not explicitly found here, but the ODE of (2.26) has been solved numerically as an initial value problem by MATLAB, and its results are shown in §2.3.5.

2.3.4.2 Ripple computation, $O(\epsilon^2)$ terms and second-order approximation

This section concerns the computation of second-order terms of the approximation of the ripple, performed in an analogous manner of first-order terms. Analogously to (2.23), terms of order ϵ^2 are selected in (2.22):

$$\boldsymbol{G}_2(\boldsymbol{y}) \,+\, \frac{\partial\, \boldsymbol{\Psi}_2(t,\, \boldsymbol{y})}{\partial \boldsymbol{y}} \boldsymbol{G}_1(\boldsymbol{y}) \,+\, \frac{\partial\, \boldsymbol{\Psi}_2(t,\, \boldsymbol{y})}{\partial t} \;=\; \Big(M_1 \,+\, h(t)\, M_2 \Big)\, \boldsymbol{\Psi}_1(t,\, \boldsymbol{y})\;. \tag{2.37}$$

Substituting $\boldsymbol{\Psi}_1$ from (2.31) and averaging (2.37) from 0 to 1 leads to

$$\int_0^1 \boldsymbol{G}_2(\boldsymbol{y})\, \mathrm{d}t \;+\; \int_0^1 \frac{\partial\, \boldsymbol{\Psi}_2(t,\, \boldsymbol{y})}{\partial t}(t,\, \boldsymbol{y})\, \mathrm{d}t \;=$$

$$= \int_0^1 M_1 \Big[f_1(t)\, M_2\, \boldsymbol{y} \Big]\, \mathrm{d}t \;+\; \int_0^1 h(t)\, f_1(t)\, M_2^2\, \boldsymbol{y}\, \mathrm{d}t\,, \quad (2.38)$$

where $\boldsymbol{G}_1$ and $\boldsymbol{G}_2$ are time-invariant, and

$$\int_0^1 \frac{\partial\, \boldsymbol{\Psi}_2(t,\, \boldsymbol{y})}{\partial t} = \boldsymbol{0}, \quad (2.39a)$$

$$\int_0^1 f_1(t)\, \mathrm{d}t = \int_0^1 f_2(t)\, \mathrm{d}t = 0\,. \quad (2.39b)$$

Hence, the second term in the LHS of (2.38) and the first of the RHS are equal to $\boldsymbol{0}$. $\boldsymbol{G}_2$ can be computed using the expression for h and f_1 displayed in (2.32) and (2.35), respectively, as follows

$$\begin{aligned}
\boldsymbol{G}_2(\boldsymbol{y}) \;&=\; \int_0^1 h(t) f_1(t) M_2^2 \boldsymbol{y} \mathrm{d}t \\
&= \left[\int_0^{\langle h \rangle} \Big(1 - \langle h \rangle\Big) \left(t - n - \frac{1}{2}\langle h \rangle \right) \mathrm{d}t - \int_{\langle h \rangle}^1 0 \cdot \langle h \rangle \left(\frac{\langle h \rangle + 1}{2} - t + n \right) \mathrm{d}t \right] M_2^2 \boldsymbol{y} \\
&= \frac{(1 - \langle h \rangle)}{2} \left[\left(t - n - \frac{1}{2}\langle h \rangle \right)^2 \right]_0^{\langle h \rangle} M_2^2 \boldsymbol{y} \;=\; \frac{(1 - \langle h \rangle)}{2} \left[\frac{\langle h \rangle^2}{4} - \frac{\langle h \rangle^2}{4} \right] M_2^2 \boldsymbol{y} \\
&= \boldsymbol{0}\,.
\end{aligned} \quad (2.40)$$

Since $\boldsymbol{G_2}$ is identically equal to $\boldsymbol{0}$, the expression for $\boldsymbol{y}$ at second order remains of the form given in (2.26):

$$\dot{\boldsymbol{y}} \;=\; \epsilon\, \boldsymbol{G}_1 \;+\; o(\epsilon^2) \;=\; \epsilon \Big[\Big(M_1 \;+\; \langle h \rangle M_2 \Big) \boldsymbol{y} \;+\; \boldsymbol{b} \Big] \;+\; o(\epsilon^2)\,. \quad (2.41)$$

The second-order ripple contribution $\boldsymbol{\Psi}_2$ can then be computed by substitut-

ing the respective expressions for $\boldsymbol{G}_1$, $\boldsymbol{G}_2$ and $\boldsymbol{\Psi}_1$ into (2.37):

$$f_1(t)\,M_2\Big[(M_1\,+\,\langle h\rangle M_2)\boldsymbol{y}\,+\,\boldsymbol{b}\Big]\,+\,\frac{\partial\,\boldsymbol{\Psi}_2(t,\,\boldsymbol{y})}{\partial t}\;=\;\Big(M_1\,+\,h(t)\,M_2\Big)f_1(t)\,M_2\,\boldsymbol{y}\;. \tag{2.42}$$

Therefore, the partial derivative of $\boldsymbol{\Psi}_2$ with respect to time is equal to

$$\frac{\partial\,\boldsymbol{\Psi}_2(t,\,\boldsymbol{y})}{\partial t}\;=\;f_1(t)\Big(M_1\,M_2\,-\,M_2\,M_1\Big)\boldsymbol{y}\,+\,f_1(t)\Big(h(t)\,-\,\langle h\rangle\Big)M_2^2\,\boldsymbol{y}\,-\,f_1(t)M_2\boldsymbol{b}\;, \tag{2.43}$$

where, according to (2.29), $h(t)-\langle h\rangle = f_1'(t)$.

Let the auxiliary scalar function $f_2(t)$ be defined by the conditions

$$f_2'(t) = f_1(t)\,, \tag{2.44a}$$

$$\langle f_2\rangle = 0\,. \tag{2.44b}$$

Integrating (2.43) with respect to time leads to

$$\boldsymbol{\Psi}_2(t,\,\boldsymbol{y})\;=\;f_2(t)\Big[(M_1\,M_2\,-\,M_2\,M_1)\boldsymbol{y}\,-\,M_2\boldsymbol{b}\Big]\,+\,\frac{1}{2}\,[f_1(t)]^2\,M_2^2\,\boldsymbol{y}\;. \tag{2.45}$$

Analogously to (2.34), f_2 can be found by integrating (2.35) with respect to time:

$$f_2(t)\;=\;\begin{cases}(t\,-\,n)\left(\dfrac{t\,-\,n\,-\,\langle h\rangle}{2}\right)\Big(1\,-\,\langle h\rangle\Big)\,+\,c_3 & \text{if}\;\; n\,<\,t\,<\,n+\langle h\rangle\\[2ex] \langle h\rangle(t\,-\,n)\left(\dfrac{\langle h\rangle\,+\,1\,-\,t\,+\,n}{2}\right)\,+\,c_4 & \text{if}\;\; n+\langle h\rangle\,<\,t\,<\,n+1\,,\end{cases} \tag{2.46}$$

where c_3 and c_4 are constants of integration and can be computed analogously to c_1 and c_2 by imposing continuity in $t=\langle h\rangle$ and the average from 0 to 1 to be null.

Then, f_2 is found to be equal to

$$f_2(t) \;=\; \begin{cases} \dfrac{1}{2}\Big(t \,-\, n\Big)\Big(t \,-\, n \,-\, \langle h\rangle\Big)\Big(1 \,-\, \langle h\rangle\Big) \,-\, \dfrac{\langle h\rangle^3}{6} \,+\, \dfrac{\langle h\rangle^2}{4} \,-\, \dfrac{\langle h\rangle}{12} \\ \qquad\qquad\qquad\qquad\qquad\qquad\qquad\qquad\qquad \text{if } \; n \,<\, t \,<\, n + \langle h\rangle, \\ \dfrac{\langle h\rangle}{2}\Big(t \,-\, n\Big)\Big(\langle h\rangle \,+\, 1 \,-\, t \,+\, n\Big) \,-\, \dfrac{\langle h\rangle^3}{6} \,-\, \dfrac{\langle h\rangle^2}{4} \,-\, \dfrac{\langle h\rangle}{12} \\ \qquad\qquad\qquad\qquad\qquad\qquad\qquad\qquad\qquad \text{if } \; n + \langle h\rangle \,<\, t \,<\, n + 1. \end{cases} \tag{2.47}$$

2.3.4.3 Ripple computation, $O(\epsilon^3)$ terms and third-order approximation

This section regards the computation of third-order approximation of the ripple, following the same method shown for first and second-order approximation. Analogously to (2.23), and (2.37), terms of order ϵ^3 can be isolated in (2.22) as follows:

$$\boldsymbol{G}_3(\boldsymbol{y}) \;+\; \frac{\partial\, \boldsymbol{\Psi}_1(t,\, \boldsymbol{y})}{\partial \boldsymbol{y}} \boldsymbol{G}_2(\boldsymbol{y}) \;+\; \frac{\partial\, \boldsymbol{\Psi}_2(t,\, \boldsymbol{y})}{\partial \boldsymbol{y}} \boldsymbol{G}_1(\boldsymbol{y}) \;+\; \frac{\partial\, \boldsymbol{\Psi}_3(t,\, \boldsymbol{y})}{\partial t} \;= \\ = \; \Big(M_1 \;+\; h(t)\, M_2\Big)\, \boldsymbol{\Psi}_2(t,\, \boldsymbol{y})\;, \tag{2.48}$$

where, according to (2.40), $\boldsymbol{G}_2(\boldsymbol{y}) = \boldsymbol{0}$.

Averaging (2.48) with respect to t leads to

$$\int_0^1 \boldsymbol{G}_3(\boldsymbol{y})\, \mathrm{d}t \;+\; \int_0^1 \frac{\partial\, \boldsymbol{\Psi}_2(t,\, \boldsymbol{y})}{\partial \boldsymbol{y}}(t,\, \boldsymbol{y}) \boldsymbol{G}_1(\boldsymbol{y})\, \mathrm{d}t \;+\; \int_0^1 \frac{\partial\, \boldsymbol{\Psi}_3(t,\, \boldsymbol{y})}{\partial t}(t,\, \boldsymbol{y}) \;= \\ = \int_0^1 (M_1 \;+\; h(t)\, M_2)\, \boldsymbol{\Psi}_2\, \mathrm{d}t\;. \tag{2.49}$$

Solving (2.49) for $\boldsymbol{G}_3$ gives

$$\boldsymbol{G}_3 \;=\; -\,\frac{\langle h\rangle^2}{12}(1-\langle h\rangle)^2 M_2\Big[(M_1\, M_2 - M_2 M_1)\boldsymbol{y} - M_2 \boldsymbol{b}\Big] + \frac{\langle h\rangle^3}{24}(1-\langle h\rangle) M_2^3 \boldsymbol{y}\;. \tag{2.50}$$

Therefore, $\boldsymbol{y}$ can be approximated as

$$\dot{\boldsymbol{y}} \;=\; \epsilon\, \boldsymbol{G}_1 \;+\; \epsilon^3\, \boldsymbol{G}_3 \;+\; o(\epsilon^3). \tag{2.51}$$

2.3.5 Constant $\langle h \rangle$: Simulations

In this section, some results from simulations are displayed. Ordinary differential equations (ODEs) describing the behaviour of the system, its average, and its ripple, as computed in the previous sections, have been solved by MATLAB as initial value problems. The results have been re-dimensionalised and plotted in the figures below.

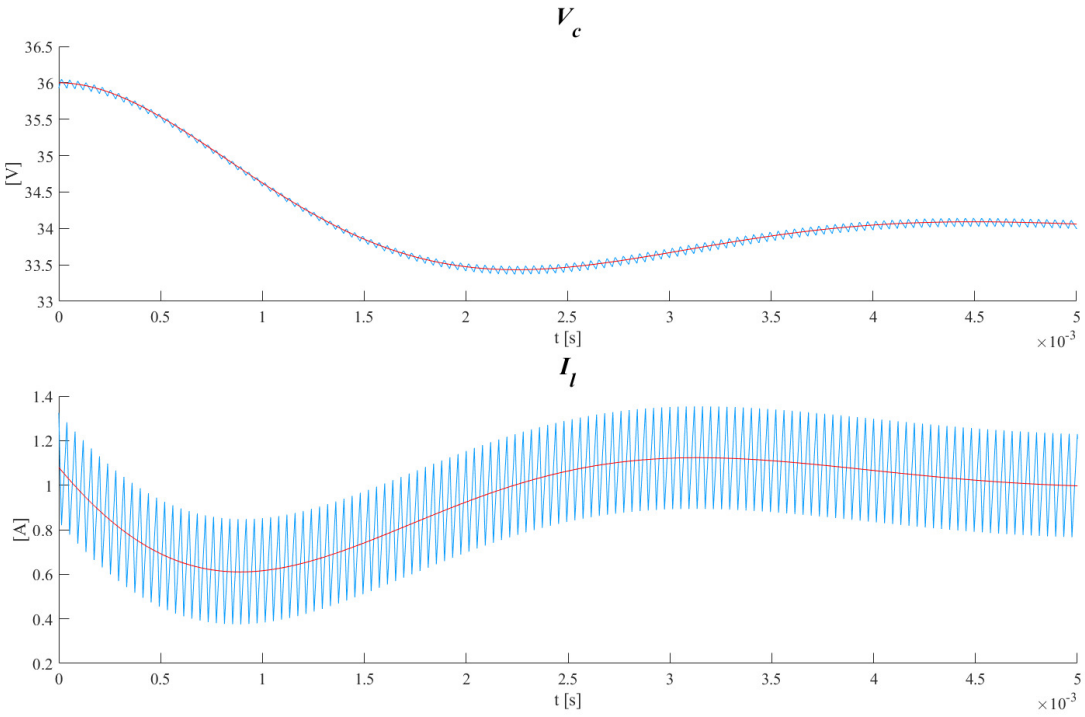

Figure 2.3: DC-DC converter, constant $\langle h \rangle$: comparison between the solution of the exact differential equation (blue) and the solution of the averaged system (red)

As shown in Figure 2.3 and according to (2.2), the solution of the exact differential equation (2.19) behaves like the sum of the solution of the averaged system (2.26) and a periodic ripple.

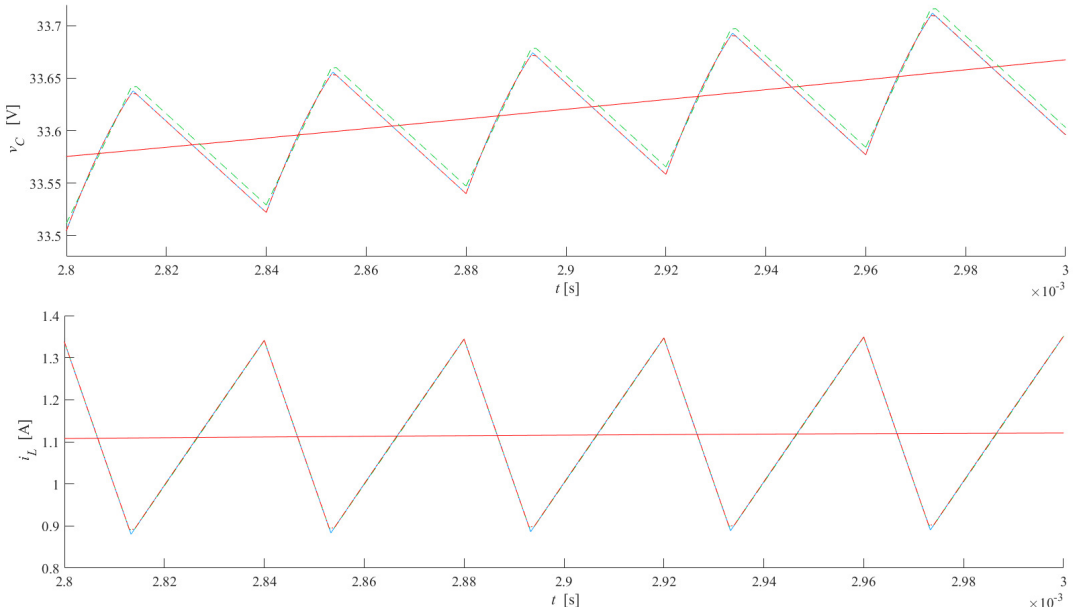

Figure 2.4: DC-DC converter, constant $\langle h \rangle$: exact solution (blue) compared with the averaged one (red) plus the first approximation of the ripple (green dashes) and the second approximation of the ripple (magenta dash-dots).

The first approximation of the ripple, presented in (2.36) and depicted in Figure 2.4 with green dashes, agrees with the behaviour of the exact solution, even though some small discrepancies can be observed in the capacitor voltage plot (never exceeding 0.01 V). A better agreement can be observed in the same figure between the second approximation and the exact solution.
The addition of the time-invariant function $\boldsymbol{G}_3$, shown in (2.50), for the computation of the average vector $\boldsymbol{y}$, does not bring significant improvements and has been neglected: $\boldsymbol{y}$ has been computed first according to (2.26), using $\boldsymbol{G}_1$ only, then according to (2.51), adding $\epsilon^3 \boldsymbol{G}_3$. The difference between the results is plotted in Figure 2.5: even in the worst cases, occurring during transients, the discrepancy keeps its values two orders of magnitude below the amplitude of the ripple.

As shown in Figure 2.6, the steady-state average value of the system variables depends also on the switching period: when T_S increases, the equilibrium values drift away from those of the averaged system (2.26). Moreover, since, according to its definition (2.15), the small parameter ϵ is proportional to T_S, if the latter increases, ϵ can lose its negligibility if compared with the other parameters of the system and the assumptions of (2.2) are not valid any more.

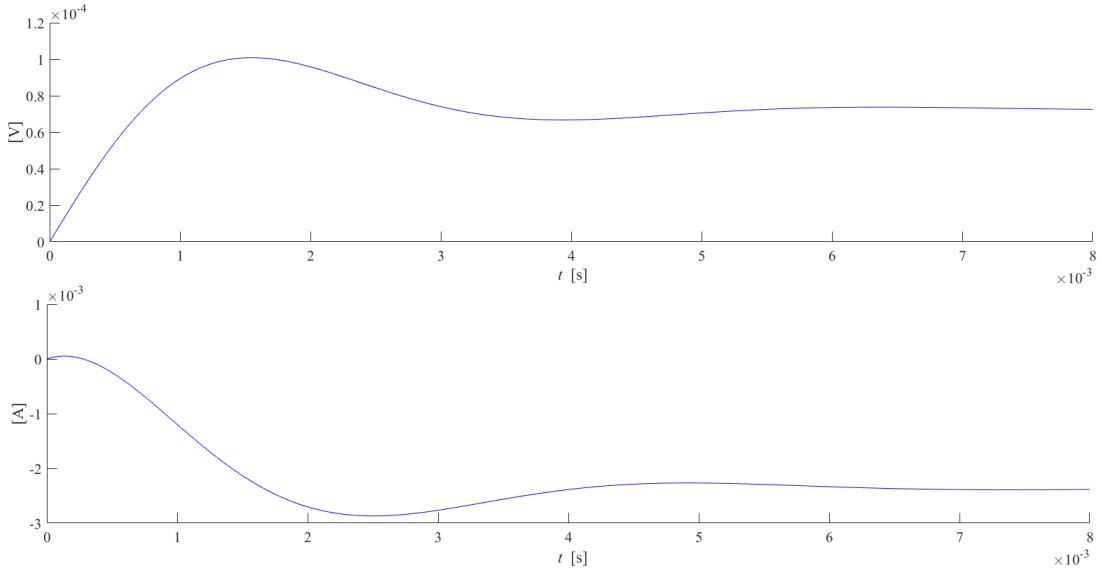

Figure 2.5: DC-DC converter, constant $\langle h \rangle$: error between voltage (top) and current (bottom) of the exact system and the approximated system

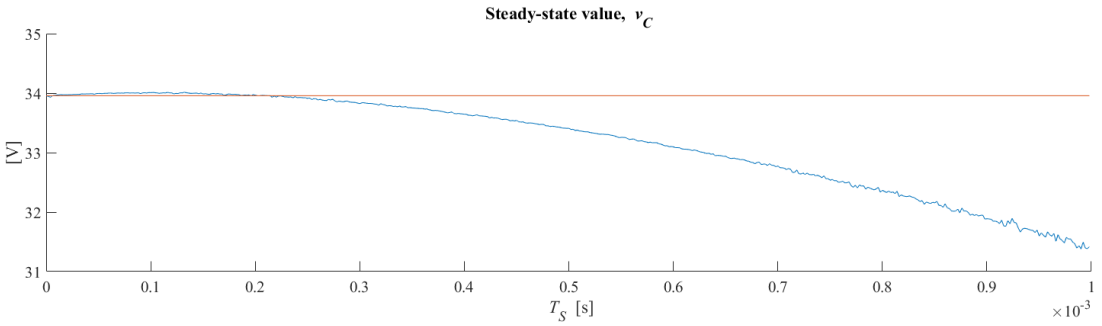

Figure 2.6: DC-DC converter, constant $\langle h \rangle$: equilibrium value computed by solving the exact differential equation (2.8) and the averaged system (2.26), depending on the switching period T_s.

In Figure 2.7 is depicted the behaviour of the system obtained by using a switching period ten times bigger than the nominal one.

In Figure 2.8, T_S has been kept equal to the nominal switching period, while the time constant τ_1, inversely proportional to ϵ, has been reduced by setting the capacitance C equal to a tenth of the nominal value. Hence, in this case ϵ is increased by ten times, as well as in Figure 2.7, while T_S is still equal to $4.0 \cdot 10^{-5}$ s.

These results highlight the importance of checking that enough difference is present between "fast" and "slow" time scales, in case a similar technique is applied to model average and ripple.

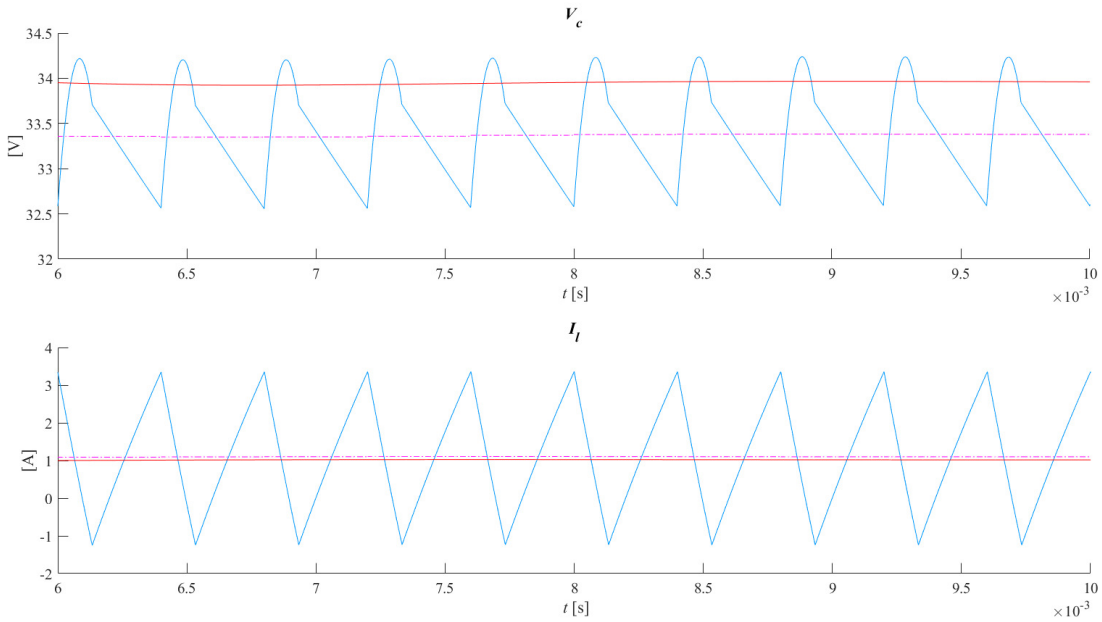

Figure 2.7: DC-DC converter, constant $\langle h \rangle$: comparison between the exact solution (blue), its average (magenta dash-dots) and the averaged solution (red). $T_S = 4.0 \cdot 10^{-4}$ s

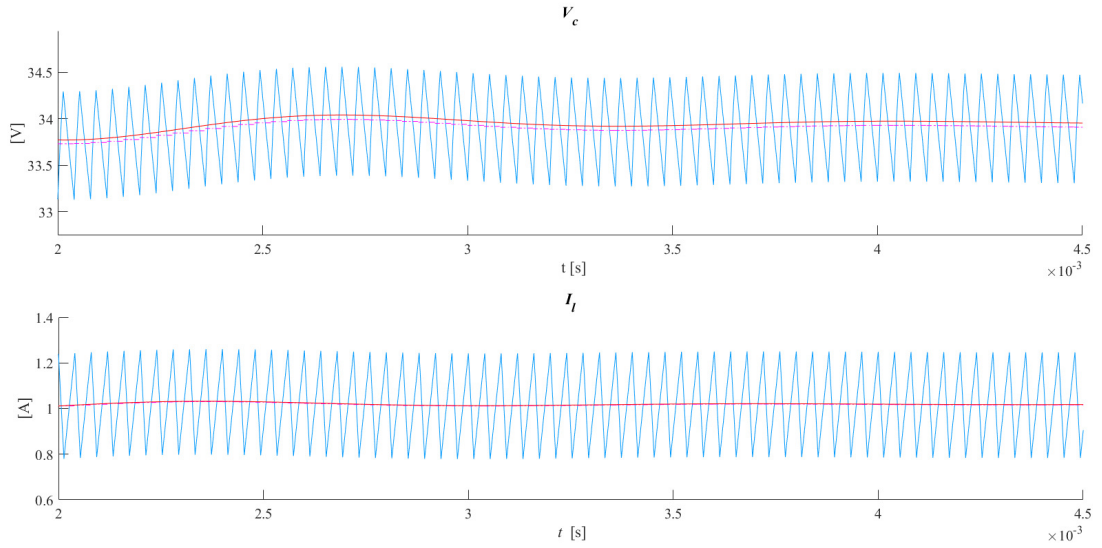

Figure 2.8: DC-DC converter, constant $\langle h \rangle$: comparison between the system exact solution (blue), its average (magenta dash-dots) and the averaged system solution (red). $C = 7.7$ μF

2.3.6 Varying duty-cycle

In closed-loop systems, the average value $\langle h \rangle$ of the switching function h is computed by the controller in order to obtain an output voltage as close as possible to a set reference. In this case, $\langle h \rangle$ cannot be considered as constant. To model this, the expression (2.9) is changed into:

$$h(t,\,\tau) \;=\; \begin{cases} 1 & \text{if } \; n\,T_S \;<\; t \;<\; (n+q(\tau))\,T_S \\ \\ 0 & \text{if } \; (n+q(\tau))\,T_S \;<\; t \;<\; (n+1)\,T_S \end{cases} , \quad n \in \mathbb{N}, \tag{2.52}$$

where $q(\tau)$ is a scalar function: $0 \leq q(\tau) \leq 1$.
In the examined model, the switching behaviour is supposed to be "fast" if compared to the electrical transients or $q(\tau)$. Then, τ is a slow time scale, defined as

$$\tau \;=\; k_t\,\epsilon\,t, \tag{2.53}$$

where k_t is a scalar constant and ϵ is a "small" scalar parameter, as defined in (2.15).

After performing nondimensionalisation, the system equations can be written in terms of t and τ, as follows:

$$\frac{\mathrm{d}\boldsymbol{x}}{\mathrm{d}t}(t,\,\tau) \;=\; \epsilon\Big[(M_1 \;+\; h(t,\,\tau)\,M_2)\,\boldsymbol{x}(t,\,\tau) \;+\; \boldsymbol{b}\Big]\,, \tag{2.54}$$

where M_1, M_2, $\boldsymbol{b}$ and $\boldsymbol{x}$ are as defined in in (2.18) and (2.20).
According to the Krylov-Bogoliubov-Mitropolsky averaging method, $\boldsymbol{x}$ can be approximated as

$$\boldsymbol{x}(t,\,\tau) \;=\; \boldsymbol{y}(t,\,\tau) \;+\; \epsilon\,\boldsymbol{\Psi}_1(t,\,\boldsymbol{y},\,\tau) \;+\; \epsilon^2\,\boldsymbol{\Psi}_2(t,\,\boldsymbol{y},\,\tau) \;+\; \ldots\,, \tag{2.55}$$

where $\boldsymbol{y}$ is the average of $\boldsymbol{x}(t,\,\tau)$ over t and is the solution of the system of differential equations shown in (2.56), analogously to (2.3). Since $\sum_{i=1}^{N} \epsilon^i\,\boldsymbol{\Psi}_i(t,\,\boldsymbol{y},\,\tau)$ represents the ripple of $\boldsymbol{x}$, functions $\boldsymbol{\Psi}_i$ have zero average. Hence,

$$\frac{\mathrm{d}\boldsymbol{y}}{\mathrm{d}t}(\tau) \;=\; \epsilon\,\boldsymbol{G}_1(\boldsymbol{y},\,\tau) \;+\; \epsilon^2\,\boldsymbol{G}_2(\boldsymbol{y},\,\tau) \;+\; \ldots\,. \tag{2.56}$$

Differentiation of (2.55) with respect to time leads to

$$\frac{\mathrm{d}\boldsymbol{x}}{\mathrm{d}t}(t,\,\tau) \;=\; \frac{\mathrm{d}\boldsymbol{y}}{\mathrm{d}t}(\tau) \;+\; \epsilon\left[\frac{\partial\,\boldsymbol{\Psi}_1}{\partial t} \;+\; \frac{\partial\,\boldsymbol{\Psi}_1}{\partial\,\boldsymbol{y}}\frac{\partial\boldsymbol{y}}{\partial t} \;+\; \frac{\partial\,\boldsymbol{\Psi}_1}{\partial\tau}\frac{\partial\tau}{\partial t}\right] \;+ \\ +\; \epsilon^2\left[\frac{\partial\,\boldsymbol{\Psi}_2}{\partial t} \;+\; \frac{\partial\,\boldsymbol{\Psi}_2}{\partial\,\boldsymbol{y}}\frac{\partial\boldsymbol{y}}{\partial t} \;+\; \frac{\partial\,\boldsymbol{\Psi}+2}{\partial\tau}\frac{\partial\tau}{\partial t}\right] \;+\; \ldots \quad (2.57)$$

According to (2.53),

$$\frac{\partial\tau}{\partial t} \;=\; k_t\epsilon. \quad (2.58)$$

Substitution of (2.56) and (2.58) into (2.57) leads to

$$\frac{\mathrm{d}\boldsymbol{x}}{\mathrm{d}t}(t,\,\tau) \;=\; \sum_{i=1}^{N}\epsilon^i\boldsymbol{G}_i(\boldsymbol{y},\,\tau) \;+ \\ +\; \sum_{i=1}^{N}\epsilon^i\left\{\frac{\partial\,\boldsymbol{\Psi}_i}{\partial\,t} \;+\; \frac{\partial\,\boldsymbol{\Psi}_i}{\partial\,\boldsymbol{y}}\left[\sum_{m=1}^{N}\epsilon^m\,\boldsymbol{G}_m(\boldsymbol{y})\right] \;+\; \epsilon\,k_t\frac{\partial\,\boldsymbol{\Psi}_i}{\partial\tau}\right\}. \quad (2.59)$$

Moreover, (2.55) can be substituted also into (2.54). Equation (2.60) can then be obtained by equating the RHS of the modified equation (2.54) to (2.59), as shown below:

$$\epsilon\left\{[M_1 \;+\; h(t,\,\tau)\,M_2]\left[\boldsymbol{y}(\tau) \;+\; \sum_{i=1}^{N}\epsilon^i\,\boldsymbol{\Psi}_i(t,\,\boldsymbol{y},\,\tau)\right] \;+\; \boldsymbol{b}\right\} \;= \\ =\; \sum_{i=1}^{N}\epsilon^i\left\{\boldsymbol{G}_i(\boldsymbol{y},\tau) \;+\; \frac{\partial\,\boldsymbol{\Psi}_i}{\partial\,t}(t,\boldsymbol{y},\tau) \;+\; \frac{\partial\,\boldsymbol{\Psi}_i}{\partial\,\boldsymbol{y}}(t,\boldsymbol{y},\tau)\left[\sum_{m=1}^{N}\epsilon^m\,\boldsymbol{G}_m(\boldsymbol{y},\tau)\right] \;+ \\ +\;\epsilon\,k_t\frac{\partial\,\boldsymbol{\Psi_i}}{\partial\tau}(t,\boldsymbol{y},\tau)\right\}, \quad (2.60)$$

where $\boldsymbol{G}_i$ and $\boldsymbol{\Psi}_i$ can be computed analogously to the fixed $\langle h\rangle$ case, selecting in each member of (2.60) terms with the same power of ϵ and solving the resulting equations.

2.3.6.1 First-order approximation of the ripple, O(ϵ) terms

This section and the following proceed analogously to the ripple computation for constant $\langle h \rangle$. Selection in (2.60) of the terms of order ϵ leads to

$$\boldsymbol{G}_1(\boldsymbol{y},\,\tau) \;+\; \frac{\partial\,\boldsymbol{\Psi}_1}{\partial t}(t,\,\boldsymbol{y},\,\tau) \;=\; \Big(M_1 \;+\; h(t,\,\tau)\,M_2\Big)\boldsymbol{y} \;+\; \boldsymbol{b}\,. \tag{2.61}$$

Comparison between (2.61) and (2.23) allows one to notice that the two equations have the same structure and, then, to write $\boldsymbol{G}_1(t,\,\tau)$ similarly to (2.25), as shown below:

$$\boldsymbol{G}_1(\boldsymbol{y},\,\tau) \;=\; \int_0^1 \Big(M_1 + h(t,\,\tau)\,M_2\Big)\boldsymbol{y}\;\mathrm{d}t \;+\; \boldsymbol{b} \;=\; \Big(M_1 + q(\tau)\,M_2\Big)\boldsymbol{y} + \boldsymbol{b}\,. \tag{2.62}$$

In this case, $\boldsymbol{G}_1$ depends on τ in addition to $\boldsymbol{y}$, since the average value of h computed in one switching period is not fixed, but depends in turn on τ.
The averaged system can then be expressed in first approximation as

$$\dot{\boldsymbol{y}}(\tau) \;=\; \epsilon\,\boldsymbol{G}_1(\boldsymbol{y},\,\tau) \;+\; o(\epsilon) \;=\; \epsilon\Big[\Big(M_1 \;+\; q(\tau)M_2\Big)\boldsymbol{y} \;+\; \boldsymbol{b}\Big] \;+\; o(\epsilon)\,. \tag{2.63}$$

Equations (2.64) and (2.65), where only $\boldsymbol{\Psi}_1$ is unknown, can be obtained by substituting the expression of $\boldsymbol{G}_1$ shown in (2.62) into (2.61). Then

$$\Big(M_1 \;+\; q(\tau)M_2\Big)\boldsymbol{y} \;+\; \boldsymbol{b} \;+\; \frac{\partial\,\boldsymbol{\Psi}_1(t,\boldsymbol{y},\,\tau)}{\partial t} \;=\; \Big(M_1 \;+\; h(t,\,\tau)\,M_2\Big)\boldsymbol{y} \;+\; \boldsymbol{b}, \tag{2.64}$$

$$\Longrightarrow\quad \frac{\partial\,\boldsymbol{\Psi}_1(t,\boldsymbol{y},\,\tau)}{\partial t} \;=\; \Big(h(t) \;-\; q(\tau)\Big)M_2\,\boldsymbol{y}. \tag{2.65}$$

Let the auxiliary scalar function $f_1(t,\,\tau)$, defined in (2.66), be continuous in t and τ.

$$\frac{\partial f_1(t,\,\tau)}{\partial t} = h(t,\,\tau) - q(\tau)\,, \tag{2.66a}$$

$$\langle f_1 \rangle = 0\,, \tag{2.66b}$$

where $\langle f_i \rangle$ is the average value of f_i computed for one switching period and h has

been nondimensionalised.

Then, (2.65) can also be stated as:

$$\frac{\partial \boldsymbol{\Psi}_1(t, \boldsymbol{y}, \tau)}{\partial t} = \frac{\partial f_1(t, \tau)}{\partial t} M_2 \boldsymbol{y} \,. \tag{2.67}$$

Integrating (2.67) leads to

$$\boldsymbol{\Psi}_1(t, \boldsymbol{y}, \tau) = \int \frac{\partial f_1(t, \tau)}{\partial t} M_2 \boldsymbol{y} \, \mathrm{d}t = \left(\int \frac{\partial f_1(t, \tau)}{\partial t} \, \mathrm{d}t \right) M_2 \boldsymbol{y} = f_1(t, \tau) M_2 \boldsymbol{y} \,. \tag{2.68}$$

Analogously to (2.33)-(2.35), f_1 can be found by integrating the first equation of (2.66) with respect to time t and imposing both continuity and zero-average conditions. Then

$$\frac{\partial f_1(t, \tau)}{\partial t} = \begin{cases} 1 - q(\tau) & \text{if } n < t < n + q(\tau) \\ \\ -q(\tau) & \text{if } n + q(\tau) < t < n + 1 \,, \end{cases} \tag{2.69}$$

so,

$$f_1(t, \tau) = \begin{cases} (1 - q(\tau))(t - n) + c_1 & \text{if } n < t < n + q(\tau) \\ \\ -q(\tau)(t - n) + c_2 & \text{if } n + q(\tau) < t < n + 1 \,, \end{cases} \tag{2.70}$$

$$\Rightarrow f_1(t, \tau) = \begin{cases} \left(1 - q(\tau)\right) \left(t - n - \dfrac{q(\tau)}{2}\right) & \text{if } n < t < n + q(\tau) \\ \\ q(\tau) \left(\dfrac{q(\tau) + 1}{2} - t + n\right) & \text{if } n + q(\tau) < t < n + 1 \,. \end{cases} \tag{2.71}$$

Therefore, $\boldsymbol{x}$ at first order is approximated by

$$\boldsymbol{x}(t, \tau) = \boldsymbol{y}(\tau) + \epsilon f_1(t, \tau) M_2 \boldsymbol{y} + o(\epsilon) \,, \tag{2.72}$$

where $\boldsymbol{y}$ is the solution of (2.63). Also in this case, an explicit solution of (2.63) has not been computed, but the ODE has been solved numerically in MATLAB, and the results are presented in §2.3.6.3.

2.3.6.2 Second-order approximation of the ripple, $O(\epsilon^2)$ terms

This section contains the second-order approximation of the system ripple. It follows the same methodology applied for the first-order approximation.
Selection of terms of order ϵ^2 in (2.60) leads to

$$\boldsymbol{G}_2(\boldsymbol{y},\,\tau)\;+\;\frac{\partial\,\boldsymbol{\Psi}_1(t,\,\boldsymbol{y},\,\tau)}{\partial\boldsymbol{y}}\boldsymbol{G}_1(\boldsymbol{y},\,\tau)\;+\;k_t\frac{\partial\,\boldsymbol{\Psi_1}(t,\,\boldsymbol{y},\,\tau)}{\partial\tau}\;+\;\frac{\partial\,\boldsymbol{\Psi}_2(t,\,\boldsymbol{y},\,\tau)}{\partial t}\;=\;$$
$$=\;\Big(M_1\;+\;h(t,\,\tau)\,M_2\Big)\,\boldsymbol{\Psi}_1(t,\,\boldsymbol{y},\,\tau). \tag{2.73}$$

Equations (2.62) and (2.68) are now substituted into (2.73) for $\boldsymbol{G}_1$ and $\boldsymbol{\Psi}_1$, respectively, while (2.73) is integrated from 0 to 1 with respect to time. Since in §2.3.4.2 all the other terms are found to have a null average, $\boldsymbol{G}_2$ is equal to

$$\boldsymbol{G}_2(\boldsymbol{y},\,\tau)\;=\;-\,k_t\int_0^1\frac{\partial\,\boldsymbol{\Psi}_1(t,\,\boldsymbol{y},\,\tau)}{\partial\tau}\,\mathrm{d}t\;=\;-\,k_t\int_0^1\frac{\partial f_1(t,\,\tau)}{\partial\tau}\mathrm{d}t\,M_2\,\boldsymbol{y}\;. \tag{2.74}$$

The partial derivative $\dfrac{\partial\,\boldsymbol{\Psi}_1}{\partial\tau}$ has been computed by applying the definition of derivative as the limit of the increment ratio. Modifying (2.71) for the instant $\tau+\delta\tau$ leads to

$$f_1(t,\,\tau{+}\delta\tau)\;=\;\begin{cases}\Big(1\;-\;q(\tau+\delta\tau)\Big)\Big(t\;-\;n\;-\;\dfrac{1}{2}q(\tau+\delta\tau)\Big) & \\ \qquad\qquad\qquad\qquad\text{if}\;\;n\;<\;t\;<\;n+q(\tau+\delta\tau) & \\ q(\tau+\delta\tau)\left(\dfrac{q(\tau+\delta\tau)+1}{2}\;-\;t\;+\;n\right) & \\ \qquad\qquad\qquad\qquad\text{if}\;\;n+q(\tau+\delta\tau)\;<\;t\;<\;n+1\;. & \end{cases}. \tag{2.75}$$

For small $\delta\tau$,

$$q(\tau+\delta\tau)\;=\;q(\tau)\;+\;\delta\tau\,q'(\tau)\;, \tag{2.76}$$

where

$$q'(\tau)\;=\;\frac{\mathrm{d}q(\tau)}{\mathrm{d}\tau}\;. \tag{2.77}$$

$\dfrac{\partial\,\boldsymbol{\Psi}_1}{\partial\tau}$ has then been computed for both $q(\tau)$ increasing and decreasing, substitut-

ing (2.71) and (2.75) in (2.78).

$$\frac{\partial f_1(t,\,\tau)}{\partial \tau} \;=\; \lim_{\delta\tau\to 0} \frac{f_1(t,\,\tau+\delta\tau) \;-\; f_1(t,\,\tau)}{\delta\tau} \tag{2.78}$$

For the sake of clarity, computations are performed separately, considering first a decreasing q, then an increasing q. This is needed because f_1 is defined by parts, but the time extrema of each part differ according to the sign of q', as observable in (2.79) and (2.80).

1. $q'(\tau) > 0$

$$\frac{\partial f_1(t,\,\tau)}{\partial \tau} = \begin{cases} -\dfrac{1}{2}\,q'(\tau) \;+\; q(\tau)\,q'(\tau) \;-\; (t \;-\; n)\,q'(\tau) \\ \qquad\qquad\qquad\qquad \text{if } n < t < n + q(\tau) \\ \left(\lim\limits_{\delta\tau\to 0} \dfrac{t-n-q(\tau)}{\delta\,\tau}\right) - \dfrac{1}{2}q'(\tau) + q(\tau)q'(\tau) - (t-n)q'(\tau) \\ \qquad\qquad\qquad\qquad \text{if } n + q(\tau) < t < n + q(\tau+\delta\tau) \\ q(\tau)\,q'(\tau) \;+\; \dfrac{1}{2}\,q'(\tau) \;-\; (t \;-\; n)\,q'(\tau) \\ \qquad\qquad\qquad\qquad \text{if } n + q(\tau+\delta\tau) < t < n + 1 \end{cases} \tag{2.79}$$

2. $q'(\tau) < 0$

$$\frac{\partial f_1(t,\,\tau)}{\partial \tau} = \begin{cases} -\dfrac{1}{2}\,q'(\tau) \;+\; q(\tau)\,q'(\tau) \;-\; (t \;-\; n)\,q'(\tau) \\ \qquad\qquad\qquad\qquad \text{if } n < t < n + q(\tau+\delta\tau) \\ \left(\lim\limits_{\delta\tau\to 0} \dfrac{q(\tau)-t+n}{\delta\,\tau}\right) - \dfrac{1}{2}q'(\tau) + q(\tau)q'(\tau) - (t-n)q'(\tau) \\ \qquad\qquad\qquad\qquad \text{if } n + q(\tau+\delta\tau) < t < n + q(\tau) \\ q(\tau)\,q'(\tau) \;+\; \dfrac{1}{2}\,q'(\tau) \;-\; (t \;-\; n)\,q'(\tau) \\ \qquad\qquad\qquad\qquad \text{if } n + q(\tau) < t < n + 1 \end{cases} \tag{2.80}$$

Therefore, using (2.79) and (2.80) in (2.74) leads to the computation of $\boldsymbol{G}_2$, which, in both cases, is equal to a null vector:

$$\boldsymbol{G}_2(\boldsymbol{y},\,\tau)\;=\;\boldsymbol{0}\,. \tag{2.81}$$

Substituting (2.81) and (2.68) in (2.73) leads to

$$\begin{aligned}\frac{\partial\,\boldsymbol{\Psi}_2(t,\boldsymbol{y},\,\tau)}{\partial t}\;&=\;-\,f_1(t,\tau)\,M_2\,\boldsymbol{G}_1(\boldsymbol{y},\tau)\;-\;k_t\frac{\partial\,\boldsymbol{\Psi_1}(t,\boldsymbol{y},\tau)}{\partial\tau}\,+\\&\quad+\;f_1(t,\tau)\Big(M_1\;+\;h(t,\tau)\,M_2\Big)M_2\,\boldsymbol{G}_1(\boldsymbol{y},\tau)\\&=\;f_1(t,\tau)\Big[(M_1\,M_2\;-\;M_2\,M_1)\boldsymbol{y}\;-\;M_2\,\boldsymbol{b}\Big]\,+\\&\quad+\;f_1(t,\tau)\frac{\partial f_1(t,\tau)}{\partial t}M_2^2\,\boldsymbol{y}\;-\;k_t\frac{\partial f_1(t,\tau)}{\partial\tau}M_2\,\boldsymbol{y}\,.\end{aligned} \tag{2.82}$$

Thus, $\boldsymbol{\Psi}_2$ can be obtained by integrating (2.82) with respect to time:

$$\begin{aligned}\boldsymbol{\Psi}_2(t,\,\boldsymbol{y},\,\tau)\;&=\;f_2(t,\tau)\Big[(M_1\,M_2\;-\;M_2\,M_1)\boldsymbol{y}\;-\;M_2\,\boldsymbol{b}\Big]\,+\\&\quad+\;\frac{1}{2}\,f_1^2(t,\tau)M_2^2\,\boldsymbol{y}\;-\;k_t\int\frac{\partial f_1(t,\tau)}{\partial\tau}\mathrm{d}t\,M_2\,\boldsymbol{y}\,,\end{aligned} \tag{2.83}$$

where the auxiliary scalar function $f_2(t,\,\tau)$ is defined by the conditions

$$\frac{\partial f_2(t,\tau)}{\partial t}=f_1(t,\,\tau)\,, \tag{2.84a}$$

$$\langle f_2\rangle=0\,, \tag{2.84b}$$

and can be computed analogously to (2.47), giving

$$f_2(t,\tau)\;=\;\begin{cases}\dfrac{1}{2}\Big(t\;-\;n\Big)\Big(t\;-\;n\;-\;q(\tau)\Big)\Big(1\;-\;q(\tau)\Big)\;-\;\dfrac{q^3(\tau)}{6}\;+\;\dfrac{q^2(\tau)}{4}\;-\;\dfrac{q(\tau)}{12}\\[2ex]\qquad\qquad\qquad\qquad\qquad\qquad\text{if } n<t<n+q(\tau)\\[2ex]\dfrac{q(\tau)}{2}\Big(t\;-\;n\Big)\Big(q(\tau)\;+\;1\;-\;t\;+\;n\Big)\;-\;\dfrac{q^3(\tau)}{6}\;-\;\dfrac{q^2(\tau)}{4}\;-\;\dfrac{q(\tau)}{12}\\[2ex]\qquad\qquad\qquad\qquad\qquad\qquad\text{if } n+q(\tau)<t<n+1\end{cases} \tag{2.85}$$

Considering

$$\frac{\partial f_1(t,\,\tau)}{\partial \tau} \;=\; \lim_{\delta\tau\to 0} \frac{f_1(t,\,\tau+\delta\tau) \;-\; f_1(t,\,\tau)}{\delta\tau}, \tag{2.86}$$

and defining another auxiliary scalar function $f_{1\tau}$ by the conditions

$$\frac{\partial f_{1\tau}(t,\tau)}{\partial t} = \frac{\partial f_1(t,\,\tau)}{\partial \tau}\,, \tag{2.87a}$$

$$\langle f_{1\tau}\rangle = 0, \tag{2.87b}$$

it can be observed that $f_{1\tau}$ can be computed by integrating (2.79) and (2.80) with respect to time. Again, the computation is split into increasing and decreasing q, due to the different integration extrema of the two cases.

1. $q'(\tau) > 0$

$$f_{1\tau}(t,\tau) = \begin{cases} \left[-\dfrac{1}{2}\,q'(\tau) \;+\; q(\tau)\,q'(\tau)\right](t \;-\; n) \;-\; \dfrac{(t \;-\; n)^2}{2}\,q'(\tau) \;+\; c_1 \\ \qquad\qquad\qquad\qquad\qquad\qquad \text{if } n < t < n + q(\tau) \\ \left[-\dfrac{1}{2}q'(\tau) + q(\tau)q'(\tau) - \dfrac{q(\tau)}{\delta\tau}\right](t-n) + \dfrac{(t-n)^2}{2}\left[\dfrac{1}{2\delta\tau} - q'(\tau)\right] + c_2 \\ \qquad\qquad\qquad\qquad\qquad\qquad \text{if } n + q(\tau) < t < n + q(\tau+\delta\tau) \\ \left[q(\tau)\,q'(\tau) \;+\; \dfrac{1}{2}\,q'(\tau)\right](t \;-\; n) \;-\; \dfrac{(t \;-\; n)^2}{2}\,q'(\tau) \;+\; c_3 \\ \qquad\qquad\qquad\qquad\qquad\qquad \text{if } n + q(\tau+\delta\tau) < t < n + 1 \end{cases} \tag{2.88}$$

2. $q'(\tau) < 0$

$$f_{1\tau}(t,\tau) = \begin{cases} \left[-\frac{1}{2}q'(\tau) + q(\tau)\,q'(\tau)\right](t-n) - \frac{(t-n)^2}{2}q'(\tau) + c_4 \\ \qquad\qquad \text{if } n < t < n + q(\tau+\delta\tau) \\ \left[-\frac{1}{2}q'(\tau) + q(\tau)q'(\tau) + \frac{q(\tau)}{\delta\tau}\right](t-n) - \frac{(t-n)^2}{2}\left[\frac{1}{2\delta\tau} + q'(\tau)\right] + c_5 \\ \qquad\qquad \text{if } n + q(\tau+\delta\tau) < t < n + q(\tau) \\ \left[q(\tau)\,q'(\tau) + \frac{1}{2}q'(\tau)\right](t-n) - \frac{(t-n)^2}{2}q'(\tau) + c_6 \\ \qquad\qquad \text{if } n + q(\tau) < t < n+1 \end{cases} \tag{2.89}$$

Continuity of (2.88) and (2.89) cannot be achieved in $n+q(\tau)$ and $n+q(\tau+\delta\tau)$, but setting all the constants of integration equal to zero allows to obtain a zero average.

Finally, (2.83) can then be rewritten as

$$\begin{aligned} \boldsymbol{\Psi}_2(t,\,\boldsymbol{y},\,\tau) \;=\; & f_2(t,\tau)\Big[(M_1\,M_2 - M_2\,M_1)\boldsymbol{y} - M_2\,\boldsymbol{b}\Big] + \\ & + \frac{1}{2}\,f_1^2(t,\tau)M_2^2\,\boldsymbol{y} - k_t\,f_{1\tau}(t,\tau)\,M_2\,\boldsymbol{y}\,. \end{aligned} \tag{2.90}$$

The expression (2.90) for $\boldsymbol{\Psi}_2$ has the same structure of (2.45), but with an additional term $-\,k_t\,f_{1\tau}(t,\tau)\,M_2\,\boldsymbol{y}$.

2.3.6.3 Varying duty-cycle: simulations

Some MATLAB simulations have been performed, solving the system ODEs numerically as initial value problems. The results are shown below.

In particular, attention focused on the evaluation of the contribution of the term $-\,k_t\,f_{1\tau}(t,\tau)\,M_2\,\boldsymbol{y}$, which is not present in case the duty cycle is constant. The contribution of that term is found to be relatively small, as shown in Figure 2.10 for the voltage. The first and second-order approximations found in the previous sections for a constant duty cycle system, then, are found to be in general good enough also for the case of a varying duty cycle.

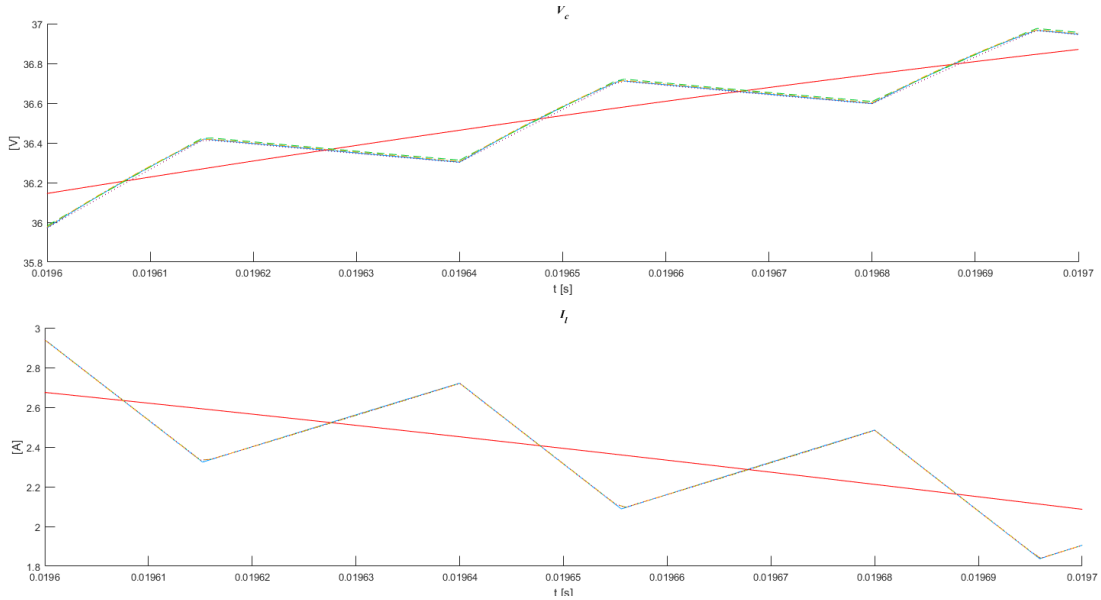

Figure 2.9: DC-DC converter, varying $\langle h \rangle$: comparison between the system exact solution (blue), its average (red), its average plus the first approximation of ripple (green dashes), its average plus the second approximation of ripple neglecting the derivative $\dfrac{\partial f_1}{\partial \tau}$ (yellow dash-dots) and its average plus the complete second approximation of the ripple (magenta dots)

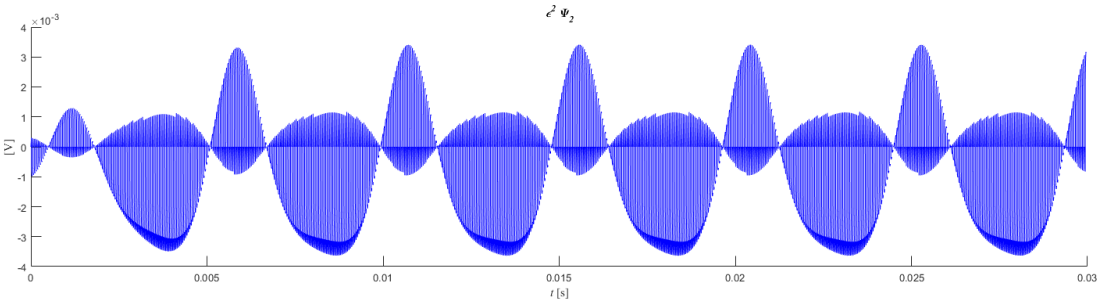

Figure 2.10: DC-DC converter, varying $\langle h \rangle$: Contribution of $-k_t\, f_{1\tau}(t,\tau)\, M_2\, \boldsymbol{y}$ on the voltage.

2.4 Single Phase Full-Bridge Inverter Analysis

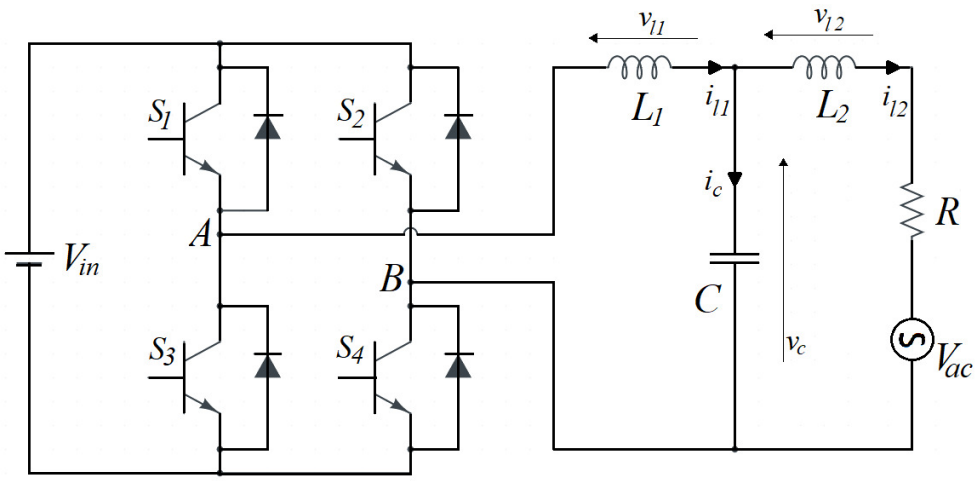

Figure 2.11: Full-bridge inverter model

The second analysed system is a single-phase full-bridge inverter, whose scheme is depicted in Figure 2.11. Inverters are in general used as DC-AC converters, but they can be controlled in order to obtain a DC output. In the AC case, another time scale is introduced in the system, since the period of the output voltage, which is in general the grid period, is "big" if compared with the switching period of the device. The filter and load time constants can be small if compared with the output period or of the same order. Both cases have been taken into consideration for the perturbed system analysis described in the following sections.

T_S	Switching period	[s]	$4.00 \cdot 10^{-5}$
R	Load resistance	[Ω]	100
L_1	First inductor inductance	[H]	$657 \cdot 10^{-6}$
L_2	Second inductor inductance	[H]	$500 \cdot 10^{-6}$
C	Capacitor capacitance	[F]	$77 \cdot 10^{-6}$
V_{ac}	Grid RSM voltage	[V]	230
V_{in}	Input DC voltage	[V]	400

Table 2.2: System parameters used to model a single-phase full-bridge inverter.

2.4.1 Model Formulation

The considered state-space system describes the behaviour of the system shown in Figure 2.11, and whose parameters are listed in table 2.2. In this case, the inverter is connected to an AC grid, whose voltage amplitude is $\sqrt{2}V_{\text{ac}}$. Considering i_c, i_{l1} and i_{l2} as state variables leads to the following model

$$\frac{\mathrm{d}v_c(t)}{\mathrm{d}t} = \frac{i_{l1(t)}(t) - i_{l2}(t)}{C} \tag{2.91a}$$

$$\frac{\mathrm{d}i_{l1}(t)}{\mathrm{d}t} = \frac{-v_c(t) + h(t)\,V_{\text{in}}}{L_1} \tag{2.91b}$$

$$\frac{\mathrm{d}i_{l2}(t)}{\mathrm{d}t} = \frac{v_c(t) - \sqrt{2}\,V_{\text{ac}}\sin(\omega\,t)}{L_2} \tag{2.91c}$$

where ω is the grid angular frequency and $h(t)$ is the switching function, given by a Pulse-Width Modulator (PWM). This modulation is performed by comparing a sine wave with the same frequency of the desired AC output, while the triangle wave is characterised by high frequency. The output signal of the PWM is then given by

$$h(t) = \begin{cases} 1 & m(\omega\,t) > p(t) \\ -1 & m(\omega\,t) < p(t) \end{cases}, \tag{2.92}$$

where m and p are the sinusoids and the triangular wave, respectively, and are defined by.

$$m(\omega\,t) = A_m \sin(\omega\,t), \tag{2.93}$$

$$p(t) = \begin{cases} -\dfrac{4\,A_P}{T_P}\,(t - n\,T_P) + A_P, & T_P\,n < t < T_P\left(n + \dfrac{1}{2}\right), \\ \dfrac{4\,A_P}{T_P}\,(t - n\,T_P) - 3\,A_P, & T_P\left(n + \dfrac{1}{2}\right) < t < T_P\,(n+1)\,. \end{cases} \tag{2.94}$$

According to Figure 2.11, h is equal to 1 when S_1 and S_4 are closed and to -1 when S_2 and S_3 are closed.

The behaviour of m, p and h is displayed in Figure 2.12.

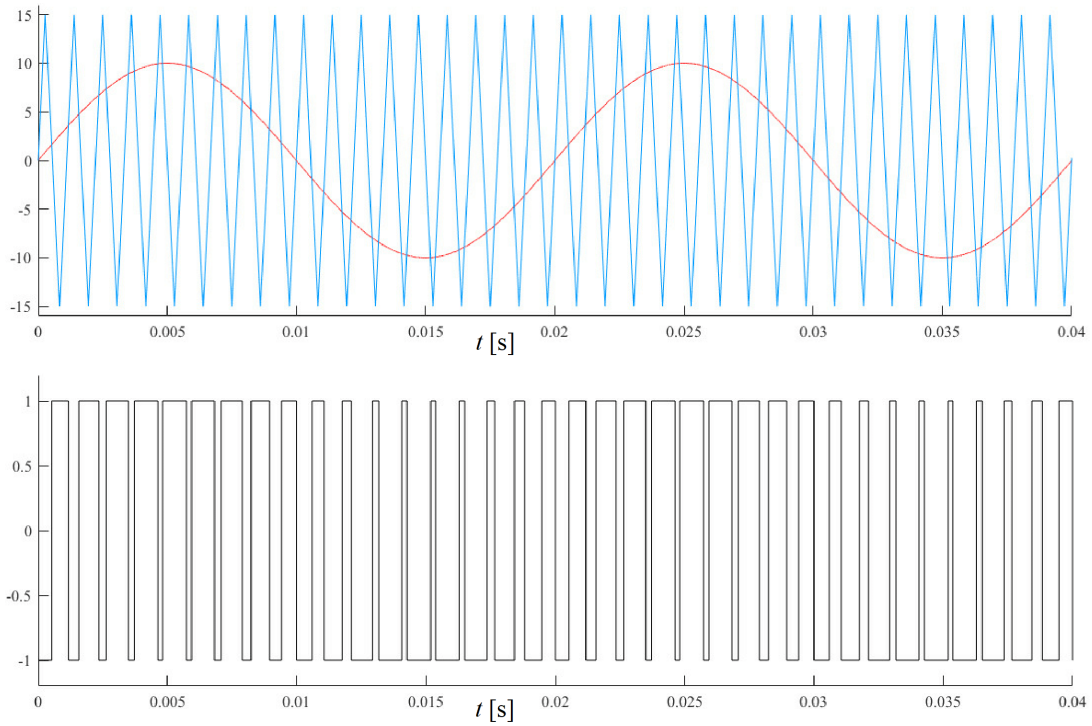

Figure 2.12: PWM - $m(\omega\ t)$ (red), $p(t)$ (blue), $h(t)$ (black), plotted for:$\omega = 2\pi 50$ rad/s, $A_P = 15$, $A_M = 10$, $T_P = \dfrac{1}{18\, f_m} \approx 1.11 \cdot 10^{-3}$s

2.4.2 Nondimensionalisation and singular perturbed model

Let V_b, I_b, T_P be the base unit values for voltage, current and time, respectively. Thus, the system variables can be expressed as

$$v_c = \hat{v}_c\, V_b\,, \tag{2.95a}$$

$$i_{l1} = \hat{i}_{l1}\, I_b\,, \tag{2.95b}$$

$$i_{l2} = \hat{i}_{l2}\, I_b\,, \tag{2.95c}$$

$$V_{in} = \hat{v}_{in}\, V_b\,, \tag{2.95d}$$

$$t = \hat{t}\, T_P\,. \tag{2.95e}$$

The nondimensional variable for time, $\hat{t}$, is thus scaled according to the triangle wave period.

Substitution of (2.95) into (2.91) leads to

$$\frac{V_b}{T_P}\frac{\mathrm{d}\hat{v}_c(\hat{t}T_P)}{\mathrm{d}\hat{t}} = \frac{I_b}{C}\Big(\hat{i}_{l1}(\hat{t}T_P) - \hat{i}_{l2}(\hat{t}T_P)\Big)\,, \tag{2.96a}$$

$$\frac{I_b}{T_P}\frac{\mathrm{d}\hat{i}_{l1}(\hat{t}T_P)}{\mathrm{d}\hat{t}} = \frac{V_b}{L_1}\Big(- \hat{v}_c(\hat{t}T_P) + h(T_P\,\hat{t})\,\hat{v}_{\text{in}}\Big)\,, \tag{2.96b}$$

$$\frac{I_b}{T_P}\frac{\mathrm{d}\hat{i}_{l2}(\hat{t}T_P)}{\mathrm{d}\hat{t}} = \frac{V_b}{L_2}\Big(\hat{v}_c(\hat{t}T_P) - \sqrt{2}\,\hat{v}_{ac}\sin(\omega\,T_P\,\hat{t})\,.\Big) \tag{2.96c}$$

Let the hats drop from the notation. Let also T_C, T_1, T_2, k_1 and k_2 be defined as

$$T_C = \frac{V_b\,C}{I_b}, \tag{2.97a}$$

$$T_1 = \frac{I_b\,L_1}{V_b} = k_1\,T_C \tag{2.97b}$$

$$k_1 = \frac{L_1}{C}\left(\frac{I_b}{V_b}\right)^2, \tag{2.97c}$$

$$T_2 = \frac{I_b\,L_2}{V_b} = k_2\,T_C \tag{2.97d}$$

$$k_2 = \frac{L_2}{C}\left(\frac{I_b}{V_b}\right)^2. \tag{2.97e}$$

Then, (2.96) can be rewritten as

$$\frac{\mathrm{d}v_c(tT_P)}{\mathrm{d}t} = \frac{T_P}{T_C}\Big(i_{l1}(tT_P) - i_{l2}(tT_P)\Big), \tag{2.98a}$$

$$\frac{\mathrm{d}i_{l1}(tT_P)}{\mathrm{d}t} = \frac{T_P}{k_1\,T_C}\Big(- v_c(tT_P) + h(T_P t)\,v_{\text{in}}\Big), \tag{2.98b}$$

$$\frac{\mathrm{d}i_{l2}(tT_P)}{\mathrm{d}t} = \frac{T_P}{k_2\,T_C}\Big(v_c(tT_P) - \sqrt{2}v_{\text{ac}}\sin(\omega\,T_P\,t)\Big). \tag{2.98c}$$

Let $\epsilon \ll 1$ be a scalar parameter. In PWM converters, the period of the triangular wave T_P is usually "small" if compared to the one of the sinusoidal wave, leading to multiple intersections of m and p in each period of m. Depending on the kind of system, its time constants can be "fast", if compared to the grid period, or of its same order. Hence, two different cases are analysed.

2.4.3 Large capacitor, $T_C \sim T_g$

The first case analyses a system with "slow" time constants, which are assumed to be of the same order of the grid period T_g. Therefore, the scalar parameter ϵ can be defined as

$$\epsilon \;=\; \frac{T_P}{T_C}\,. \tag{2.99}$$

Let also θ be the "slow" time scale, given by

$$\theta \;=\; \omega\, t \;=\; \omega\, T_P\, \hat{t} \;=\; \epsilon\, k_\theta\, \hat{t}\,, \tag{2.100}$$

where

$$k_\theta \;=\; \frac{\omega\, T_P}{\epsilon} \;=\; \omega\, T_C \;=\; \omega \frac{V_b\, C}{I_b}\,. \tag{2.101}$$

Substituting (2.99) and (2.100) in (2.98) leads to

$$\frac{\mathrm{d}\boldsymbol{x}}{\mathrm{d}t} \;=\; \epsilon\Big[M\,\boldsymbol{x}(t,\,\theta) \;+\; h(t,\,\theta)\,\boldsymbol{b}_1 \;+\; \sin(\theta)\,\boldsymbol{b}_2\Big]\,, \tag{2.102}$$

where

$$\boldsymbol{x} \;=\; \begin{bmatrix} v_c \\ i_{l1} \\ i_{l2} \end{bmatrix}\,, \qquad \boldsymbol{b}_1 \;=\; \begin{bmatrix} 0 \\ \dfrac{v_{in}}{k_1} \\ 0 \end{bmatrix}\,, \qquad \boldsymbol{b}_2 \;=\; \begin{bmatrix} 0 \\ 0 \\ -\dfrac{\sqrt{2} v_{ac}}{k_2} \end{bmatrix}\,,$$

$$M \;=\; \begin{bmatrix} 0 & 1 & -1 \\ -\dfrac{1}{k_1} & 0 & 0 \\ \dfrac{1}{k_2} & 0 & 0 \end{bmatrix}\,, \tag{2.103}$$

$$h(\theta,\,t) \;=\; \begin{cases} 1 & m(\theta) \;>\; p(t) \\ -1 & m(\theta) \;<\; p(t) \end{cases}\,, \tag{2.104}$$

$$m(\theta) = A_m \sin(\theta)\,, \tag{2.105}$$

$$p(t) \;=\; \begin{cases} -\,4\,A_P\,(t\;-\;n)\;+\;A_P & n\;<\;t\;<\;n\;+\;1/2 \\ \\ 4\,A_P\,(t\;-\;n)\;-\;3\,A_P & n\;+\;1/2\;<\;t\;<\;n\;+\;1\,. \end{cases} \tag{2.106}$$

Both m and p can be further rescaled by A_P:

$$\hat{m}(\theta) \;=\; \frac{A_m}{A_P}\sin(\theta) \;=\; \mu\,\sin(\theta) \;=\; \gamma(\theta), \tag{2.107}$$

$$\hat{p}(t) \;=\; \begin{cases} -\,4\,(t\;-\;n)\;+\;1 & n\;<\;t\;<\;n\;+\;1/2 \\ \\ 4\;(t\;-\;n)\;-\;3 & n\;+\;1/2\;<\;t\;<\;n\;+\;1\,. \end{cases} \tag{2.108}$$

2.4.3.1 First approximation, O(ϵ) terms

In this section, the first approximation of the average and ripple of the system are computed. Applying the same procedure of §2.3.4, and equating the RHS of (2.102) to the RHS of (2.2) gives

$$M\,\boldsymbol{y}\;+\;h(t,\,\theta)\,\boldsymbol{b}_1\;+\;\sin(\theta)\,\boldsymbol{b}_2\;=\;\boldsymbol{G}_1(\theta,\,\boldsymbol{y})\;+\;\frac{\partial\,\boldsymbol{\Psi}_1(t,\,\theta,\,\boldsymbol{y})}{\partial t} \tag{2.109}$$

Averaging (2.109) for $0\;<\;t\;<\;1$ leads to

$$\boldsymbol{G}_1(\boldsymbol{y},\,\theta)\;=\;M\,\boldsymbol{y}\;+\;\langle h\rangle\,\boldsymbol{b}_1\;+\;\sin\left(\theta\;+\;\frac{\epsilon\,k_\theta}{4}\right)\,\boldsymbol{b}_2\,, \tag{2.110}$$

where

$$\langle h\rangle\;=\;\langle h\rangle(\theta)\;=\;\gamma(\theta)\;\;. \tag{2.111}$$

Substituting (2.110) into (2.109) leads to

$$\frac{\partial\,\boldsymbol{\Psi}_1(t,\,\theta,\,\boldsymbol{y})}{\partial t}\;=\;\Big[h(\theta,\,t)\;-\;\langle h\rangle\Big]\boldsymbol{b}_1\;. \tag{2.112}$$

Hence, $\boldsymbol{\Psi}_1$ can be obtained by integrating (2.112) with respect to t:

$$\boldsymbol{\Psi}_1(\theta,\,t,\,\boldsymbol{y})\;=\;f_1(\theta,\,t)\,\boldsymbol{b}_1\;, \tag{2.113}$$

where $f_1(\theta,\, t)$ is a scalar zero-average function, defined by the conditions

$$\frac{\partial f_1(\theta,\, t)}{\mathrm{d}t} \;=\; h(\theta,\, t) \;-\; \langle h \rangle(\theta)\;, \tag{2.114a}$$

$$\langle f_1 \rangle \;=\; 0\;. \tag{2.114b}$$

Integrating (2.114) with respect to t and using (2.111) leads to

$$f_1(\theta,\, t) \;=\; \begin{cases} -(1\,+\,\gamma)(t\,-\,n)\;+\;f_1(\theta,\,0) & \\ & n \;<\; t \;<\; n + \dfrac{1-\gamma}{4} \\ (1\,-\,\gamma)\left(t\,-\,n\,-\,\dfrac{1-\gamma}{4}\right)\;+\;f_1\left(\theta,\,\dfrac{1-\gamma}{4}\right) & \\ & n + \dfrac{1-\gamma}{4} \;<\; t \;<\; n + \dfrac{3+\gamma}{4} \\ -(1\,+\,\gamma)\left(t\,-\,n\,-\,\dfrac{3+\gamma}{4}\right)\;+\;f_1\left(\theta,\,\dfrac{3+\gamma}{4}\right) & \\ & n + \dfrac{3+\gamma}{4} \;<\; t \;<\; n+1\;, \end{cases} \tag{2.115}$$

where the dependence of γ on θ has been dropped from the notation.

Imposing both continuity and zero-average on f_1 leads to

$$f_1(\theta,\, t) \;=\; \begin{cases} -(1\,+\,\gamma)(t\,-\,n) & n \;<\; t \;<\; n + \dfrac{1-\gamma}{4} \\ (1\,-\,\gamma)\,(t\,-\,n)\;+\;\dfrac{\gamma\,-\,1}{2} & n + \dfrac{1-\gamma}{4} \;<\; t \;<\; n + \dfrac{3+\gamma}{4} \\ -(1\,+\,\gamma)\,(t\,-\,n)\;+\;1\;+\;\gamma & n + \dfrac{3+\gamma}{4} \;<\; t \;<\; n+1 \end{cases} \tag{2.116}$$

2.4.3.2 Second approximation, $O(\epsilon^2)$ terms

Proceeding analogously with the terms $\mathcal{O}(\epsilon^2)$ gives

$$\boldsymbol{G}_2(\theta,\, \boldsymbol{y}) \;+\; \frac{\partial\, \boldsymbol{\Psi}_2(\theta,\, t,\, \boldsymbol{y})}{\partial t} \;+\; \frac{\partial\, \boldsymbol{\Psi}_1(\theta,\, t,\, \boldsymbol{y})}{\partial \boldsymbol{y}} \boldsymbol{G}_1(\theta,\, \boldsymbol{y}) \;+\; k_\theta \frac{\partial\, \boldsymbol{\Psi}_1(\theta,\, t,\, \boldsymbol{y})}{\partial \theta} \;= \;= \;M\; \boldsymbol{\Psi}_1(\theta,\, t,\, \boldsymbol{y})\;, \tag{2.117}$$

where

$$\frac{\partial \boldsymbol{\Psi}_1(\theta,\, t,\, \boldsymbol{y})}{\partial \boldsymbol{y}} \;=\; \mathbf{0}\,. \tag{2.118}$$

Following the same method as applied to (2.110)-(2.112) leads to

$$\boldsymbol{G}_2(\theta,\, \boldsymbol{y}) \;=\; -\,k_\theta \int_0^1 \frac{\partial \boldsymbol{\Psi}_1(t,\, \theta,\, \boldsymbol{y})}{\partial \theta}\,\mathrm{d}t \;=\; -\,k_\theta \int_0^1 \frac{\partial f_1(\theta,\, t)}{\partial \theta}\mathrm{d}t\,\boldsymbol{b}_1\,. \tag{2.119}$$

Applying the definition of γ shown in (2.111), γ' can be defined as

$$\gamma'(\theta) \;=\; \frac{\mathrm{d}\gamma(\theta)}{\mathrm{d}\theta} \;=\; \frac{\mathrm{d}}{\mathrm{d}\theta}\left[\mu \sin\left(\theta \,+\, \frac{\epsilon\, k_\theta}{4}\right)\right] \;=\; \mu \cos\left(\theta \,+\, \frac{\epsilon\, k_\theta}{4}\right). \tag{2.120}$$

Therefore, the partial derivative of f_1 with respect to θ can be expressed as

$$\frac{\partial f_1(\theta,\, t)}{\partial \theta} \;=\; \begin{cases} -\,(t \,-\, n)\,\gamma' & n \,<\, t \,<\, n + \dfrac{1-\gamma}{4} \\[2ex] -\,(t \,-\, n)\,\gamma' \,+\, \dfrac{\gamma'}{2} & n + \dfrac{1-\gamma}{4} \,<\, t \,<\, n + \dfrac{3+\gamma}{4} \\[2ex] -\,(t \,-\, n)\,\gamma' \,+\, \gamma' & n + \dfrac{3+\gamma}{4} \,<\, t \,<\, n+1 \end{cases} \tag{2.121}$$

Hence, the expression of $\boldsymbol{G}_2$ can then be computed by integrating (2.121) for $0 < t < 1$:

$$\boldsymbol{G}_2(\theta,\, \boldsymbol{y}) \;=\; -\,k_\theta \int_0^1 \frac{\partial f_1(\theta,\, t)}{\partial \theta}\mathrm{d}t\,\boldsymbol{b}_1 \;=\; \mathbf{0}\,. \tag{2.122}$$

Substitution of (2.122) and (2.113) in (2.119) leads to

$$\frac{\partial \boldsymbol{\Psi}_2(t,\, \theta,\, \boldsymbol{y})}{\partial t} \;=\; M\; \boldsymbol{\Psi}_{\mathbf{1}}(t,\, \theta,\, \boldsymbol{y}) \;-\; k_\theta \frac{\partial \boldsymbol{\Psi}_1(t,\, \theta,\, \boldsymbol{y})}{\partial \theta}\,. \tag{2.123}$$

Integrating (2.21) with respect to t leads to

$$\boldsymbol{\Psi}_2(t,\, \theta,\, \boldsymbol{y}) \;=\; [f_2(\theta,\, t)M \;-\; k_\theta\, f_{1\theta}(\theta,\, t)]\,\boldsymbol{b}_1\,, \tag{2.124}$$

where f_2 and $f_{1\theta}$ are defined, respectively, by

$$\frac{\partial f_2(t,\, \theta)}{\partial t} \;=\; f_1(\theta,\, t)\,, \qquad \langle f_2 \rangle \;=\; 0 \tag{2.125}$$

and

$$\frac{\partial f_{1\theta}(t,\,\theta)}{\partial t} \;=\; \frac{\partial f_1(\theta,\,t)}{\partial \theta}\,, \qquad \langle f_{1\theta}\rangle \;=\; 0\,. \tag{2.126}$$

Imposing both the zero-average condition and continuity on f_2 leads to the following equation:

$$f_2(t,\,\theta) \;=\; \begin{cases} -\dfrac{1}{2}(1\,+\,\gamma)(t\,-\,n)^2\,+\,c_1 \\ \qquad\qquad\qquad\qquad\qquad\qquad n\,<\,t\,<\,n+\dfrac{1-\gamma}{4} \\ \dfrac{1}{2}(1\,-\,\gamma)\,(t\,-\,n)^2\,+\,\dfrac{\gamma\,-\,1}{2}(t\,-\,n)\,+\,c_2 \\ \qquad\qquad\qquad\qquad\qquad\qquad n+\dfrac{1-\gamma}{4}\,<\,t\,<\,n+\dfrac{3+\gamma}{4} \\ -\dfrac{1}{2}(1\,+\,\gamma)\,(t\,-\,n)^2\,+\,(1\,+\,\gamma)(t\,-\,n)\,+\,c_3 \\ \qquad\qquad\qquad\qquad\qquad\qquad n+\dfrac{3+\gamma}{4}\,<\,t\,<\,n+1 \end{cases}, \tag{2.127}$$

where

$$c_1 \;=\; \frac{(3\,+\,\gamma)(1\,-\,\gamma)(1\,+\,\gamma)}{96}\,, \tag{2.128}$$

$$c_2 \;=\; \frac{(3\,+\,\gamma)(1\,-\,\gamma)(1\,+\,\gamma)}{96}\,+\,\left(\frac{1\,-\,\gamma}{4}\right)^2\,, \tag{2.129}$$

and

$$c_3 \;=\; \frac{(3\,+\,\gamma)(1\,-\,\gamma)(1\,+\,\gamma)}{96}\,+\,\left(\frac{1\,-\,\gamma}{4}\right)^2\left(\frac{3\,+\,\gamma}{4}\right)^2\,. \tag{2.130}$$

Proceeding analogously for $f_{1\theta}$ leads to

$$f_{1\theta}(t,\,\theta) \;=\; \begin{cases} -\dfrac{1}{2}(t\,-\,n)^2\,\gamma' \,+\, c_{1\theta} & \\ & n \,<\, t \,<\, n+\dfrac{1-\gamma}{4} \\ -\dfrac{1}{2}(t\,-\,n)^2\,\gamma' \,+\, \dfrac{\gamma'}{2}(t\,-\,n) \,+\, c_{2\theta} & \\ & n+\dfrac{1-\gamma}{4} \,<\, t \,<\, n+\dfrac{3+\gamma}{4} \\ -\dfrac{1}{2}(t\,-\,n)^2\,\gamma' \,+\, \gamma'(t\,-\,n) \,+\, c_{3\theta} & \\ & n+\dfrac{3+\gamma}{4} \,<\, t \,<\, n+1 \end{cases}, \tag{2.131}$$

where

$$c_{1\theta} \;=\; \gamma'\left(\frac{16\,-\,3\gamma^2}{96}\right)\,, \tag{2.132}$$

$$c_{2\theta} \;=\; \gamma'\left(\frac{4\,+\,12\gamma\,-\,3\gamma^2}{96}\right)\,, \tag{2.133}$$

$$c_{3\theta} \;=\; -\,\gamma'\left(\frac{32\,+\,3\,\gamma^2}{96}\right)\,. \tag{2.134}$$

Then, some continuous functions are found that satisfy the conditions for the second approximation of the average and ripple of the system.

2.4.4 Small capacitor, $T_P \ll T_C \ll T_g$

In the second case, the triangular wave period T_P is assumed to be negligible compared to the time constants of the systems, which are, in turn, negligible compared to the grid period T_g, as expressed in (2.135).

$$T_P \ll T_C \ll T_g. \tag{2.135}$$

According to the definition of ϵ and $\hat{t}$ shown in (2.95) and (2.99), respectively, in this case θ can be defined as

$$\theta \;=\; \omega\,t \;=\; \omega\,T_P\,\hat{t} \;=\; \epsilon^2\,k_\theta\,\hat{t}\,, \tag{2.136}$$

where

$$k_\theta \;=\; \frac{\omega\, T_P}{\epsilon^2} \;=\; \frac{\omega\, T_C^2}{T_P}\;. \tag{2.137}$$

Substituting (2.99) and (2.136) into (2.98) and dropping the hats from the notation leads to

$$\frac{\mathrm{d}\boldsymbol{x}}{\mathrm{d}t} \;=\; \epsilon\Big[M\,\boldsymbol{x}(t,\,\theta) \;+\; h(t,\,\theta)\,\boldsymbol{b}_1 \;+\; \sin(\theta)\,\boldsymbol{b}_2\Big]\;, \tag{2.138}$$

where $\boldsymbol{x}$, $\boldsymbol{b}_1$, $\boldsymbol{b}_2$, M, h, m and p are as defined in (2.103)-(2.106). Furthermore, $\hat{m}$ and $\hat{p}$ are obtained by rescaling m and p by A_P, analogously to (2.107) and (2.108). Equation (2.138) is found to be the same as (2.102), but approximation terms might differ due to the different orders of the system time scales.

2.4.4.1 First approximation, O(ϵ) terms

Analogously to the previous cases,

$$M\,\boldsymbol{y} \;+\; h(t,\,\theta)\,\boldsymbol{b}_1 \;+\; \sin(\theta)\,\boldsymbol{b}_2 \;=\; \boldsymbol{G}_1(\theta,\,\boldsymbol{y}) \;+\; \frac{\partial\,\boldsymbol{\Psi}_1(t,\,\theta,\,\boldsymbol{y})}{\partial t}. \tag{2.139}$$

Averaging (2.139) for $0 < t < 1$ leads to

$$\boldsymbol{G}_1(\boldsymbol{y},\,\theta) \;=\; M\,\boldsymbol{y} \;+\; \langle h\rangle\,\boldsymbol{b}_1 \;+\; \sin\left(\theta \;+\; \frac{\epsilon\, k_\theta}{4}\right)\,\boldsymbol{b}_2\;, \tag{2.140}$$

where

$$\langle h\rangle \;=\; \langle h\rangle(\theta) \;=\; \gamma(\theta)\;. \tag{2.141}$$

Substituting (2.140) into (2.139) leads to

$$\frac{\partial\,\boldsymbol{\Psi}_1(t,\,\theta,\,\boldsymbol{y})}{\partial t} \;=\; \Big[h(\theta,\,t) \;-\; \langle h\rangle\Big]\boldsymbol{b}_1\;, \tag{2.142}$$

while integrating (2.16) with respect to t gives

$$\boldsymbol{\Psi}_1(\theta,\,t,\,\boldsymbol{y}) \;=\; f_1(\theta,\,t)\,\boldsymbol{b}_1\;, \tag{2.143}$$

where $f_1(\theta,\,t)$ is defined in (2.116).

Therefore, $\boldsymbol{G}_1$ and $\boldsymbol{\Psi}_1$ have the same structure in both of the analysed cases, and no difference is found so far due to the system time constant being negligible

compared to the grid period.

2.4.4.2 Second approximation, $O(\epsilon^2)$ terms

The same method is applied here to compute the second-order terms. Equating the $\mathcal{O}(\epsilon^2)$ terms leads to

$$\boldsymbol{G}_2(\theta,\, \boldsymbol{y}) \,+\, \frac{\partial\, \boldsymbol{\Psi}_2(\theta,\, t,\, \boldsymbol{y})}{\partial t} \,+\, \frac{\partial\, \boldsymbol{\Psi}_1(\theta,\, t,\, \boldsymbol{y})}{\partial \boldsymbol{y}} \boldsymbol{G}_1(\theta,\, \boldsymbol{y}) \;=\; M\; \boldsymbol{\Psi}_1(\theta,\, t,\, \boldsymbol{y})\;, \tag{2.144}$$

where

$$\frac{\partial\, \boldsymbol{\Psi}_1(\theta,\, t,\, \boldsymbol{y})}{\partial \boldsymbol{y}} \;=\; \mathbf{0}\;. \tag{2.145}$$

Equation (2.144) has one term less than its equivalent with the previous scaling. Averaging (2.144) for $0 < t < 1$ gives

$$\boldsymbol{G}_2(\theta,\, \boldsymbol{y}) \;=\; \mathbf{0}\;. \tag{2.146}$$

Substitution of (2.146) and (2.143) in (2.144) then leads to

$$\frac{\partial\, \boldsymbol{\Psi}_2(t,\, \theta,\, \boldsymbol{y})}{\partial t} \;=\; M\; \boldsymbol{\Psi}_1(t,\, \theta,\, \boldsymbol{y})\;, \tag{2.147}$$

and integrating (2.147) with respect to τ leads to

$$\boldsymbol{\Psi}_2(t,\, \theta,\, \boldsymbol{y}) \;=\; f_2(t,\, \theta) M\, \boldsymbol{b}_1\;, \tag{2.148}$$

where f_2 is defined in (2.127). Again, no difference is found so far in the approximation of systems with "big" or "small" capacitors.

2.4.5 PI controller implementation

Inverters need a controller which regulates their duty cycle. In general, it is not possible to operate an inverter in open loop, and the controller output depends on the value of selected variables of the system.

Hence, a Proportional-Integral (PI) controller has been implemented for the

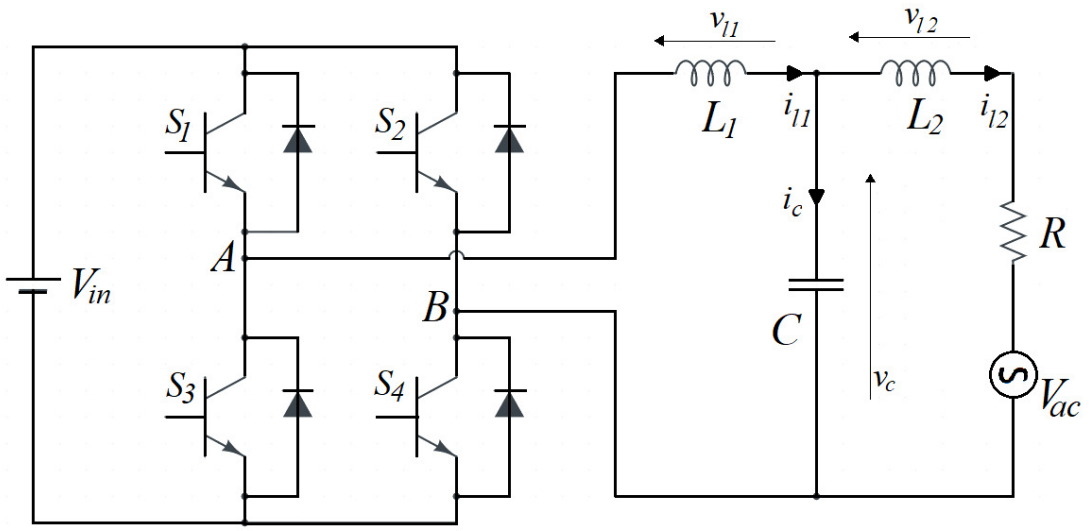

Figure 2.13: Full-bridge grid-connected inverter

model analysed in the previous sections, re-displayed in Figure 2.13 for the sake of clarity. Different hypotheses have been considered in each case concerning the system parameters and the output voltage v_C, while the complete state-space system is given by

$$\frac{\mathrm{d}v_c(t)}{\mathrm{d}t} = \frac{i_{l1}(t) - i_{l2}(t)}{C}, \tag{2.149a}$$

$$\frac{\mathrm{d}i_{l1}(t)}{\mathrm{d}t} = \frac{h(\theta, t)V_{\mathrm{in}} - v_c(t)}{L_1}, \tag{2.149b}$$

$$\frac{\mathrm{d}i_{l2}(t)}{\mathrm{d}t} = \frac{v_c(t) - R\, i_{l2}(t) - \sqrt{2}V_{\mathrm{ac}}\, \sin(\omega t)}{L_2}. \tag{2.149c}$$

2.4.5.1 Inverter operating in DC-DC

The first system taken into account is not connected to the grid and supplies a purely resistive load with a DC voltage. In this case, then, $L_2 = 0$ and $V_{\mathrm{ac}} = 0$, as shown in figure 2.14.

Since, in this case, the current i_{l2} is proportional to the voltage v_C with proportional constant R, the third equation of (2.149) can be eliminated from the

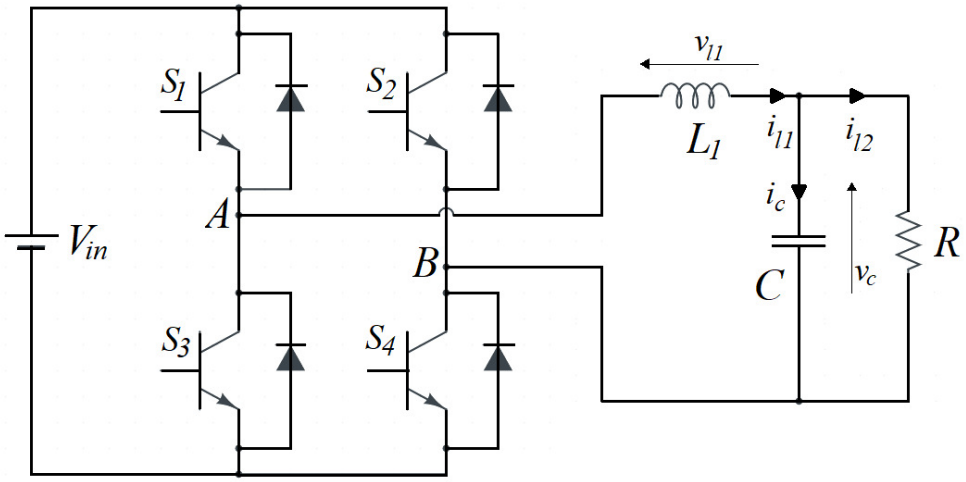

Figure 2.14: Full-bridge inverter operating as a DC-DC converter, $L_2 = 0$, $V_{ac} = 0$

system, in order to remove the linear dependence between two state variables:

$$i_{l2} = \frac{v_c}{R} \implies \frac{\mathrm{d}i_{l2}}{\mathrm{d}t} = \frac{1}{R}\frac{\mathrm{d}v_c}{\mathrm{d}t} \tag{2.150}$$

The final system is hence given by

$$\frac{\mathrm{d}v_c}{\mathrm{d}t} = \frac{R\, i_{l1} - v_c}{R\, C}, \tag{2.151a}$$

$$\frac{\mathrm{d}i_{l1}}{\mathrm{d}t} = \frac{h(t)\, V_{in} - v_c}{L_1}. \tag{2.151b}$$

For the DC-DC conversion, the switching function h is

$$h(t) = \begin{cases} 1 & \text{if } t - n\, T_S < \langle h \rangle \\ -1 & \text{if } t - n\, T_S > \langle h \rangle \end{cases}, \tag{2.152}$$

where T_S is the switching period of the switches and $\langle h \rangle$ is the duty cycle, whose value is equal to the average of h computed in the considered period.
The nondimensionalisation procedure follows 2.4.2, and the following base values are chosen:

$$V_b = V_{\text{in}}, \tag{2.153a}$$

$$R_b = R, \tag{2.153b}$$

$$T_b = T_s \ . \tag{2.153c}$$

Let additional time constants and dimensionless parameter be defined by

$$T_C = RC, \tag{2.154a}$$
$$T_1 = \frac{L_1}{R}, \tag{2.154b}$$
$$k_1 = \frac{T_1}{T_C} \ . \tag{2.154c}$$

If $T_C >> T_s$, the small dimensionless parameter ϵ is computed as

$$\epsilon = \frac{T_s}{T_C} \ . \tag{2.155}$$

Therefore, the nondimensionalised system is

$$\frac{\mathrm{d}v_c(t)}{\mathrm{d}t} = \epsilon\Big(i_{l1}(t) - v_c(t)\Big), \tag{2.156a}$$
$$\frac{\mathrm{d}i_{l1}(t)}{\mathrm{d}t} = \frac{\epsilon}{k_1}\Big(h(t)v_{in} - v_c(t)\Big), \tag{2.156b}$$

where all the variables and parameters are dimensionless. (2.156) can be written in matrix form as

$$\frac{\partial \boldsymbol{x}(t)}{\partial t} = \epsilon\Big[M\,\boldsymbol{x}(t) + h(t)\boldsymbol{b}_1\Big] \ , \tag{2.157}$$

where

$$\boldsymbol{x}(t) = \begin{bmatrix} v_c(t) \\ i_{l1}(t) \end{bmatrix}, \quad M = \begin{bmatrix} 1 & -1 \\ -\dfrac{1}{k_1} & 0 \end{bmatrix}, \quad \boldsymbol{b}_1 = \begin{bmatrix} 0 \\ \dfrac{v_{in}}{k_1} \end{bmatrix} \ . \tag{2.158}$$

Since, from a control point of view, working with transfer functions is in general easier than dealing with differential equations, the Laplace transform has been applied to the system (2.156) to facilitate the controller design. This has been possible thanks to the system being linear. First, the average equations of the system are computed, in order to remove the discontinuities of the switching

function h. A proportional-integral controller is then implemented to force the average of the capacitor voltage v_C to follow a reference signal and obtain a null steady-state error. The ripple is computed in simulations on the side and added to the average, but is not directly controlled. The average value of the duty cycle $\langle h \rangle$ is the output of the PI controller and the input of the switching function h. Averaging (2.157) for $0 < \tau < 1$ leads to

$$\boldsymbol{G}_1 \;=\; M\boldsymbol{y} \;+\; \langle h \rangle \boldsymbol{b}_1 \;. \tag{2.159}$$

As shown in (2.159), the average values of the system variables depend on the average value $\langle h \rangle$ of the duty cycle h. A controller is designed to act on the value of $\langle h \rangle$, and the design is performed in the Laplace domain.

Applying the Laplace transform to (2.159) leads to

$$s\, V_c(s) \;=\epsilon\Big(I_{l1}(s) \;-\; V_c(s)\Big), \tag{2.160a}$$

$$s\, I_{l1}(s) \;=\frac{\epsilon}{k_1}\Big(\langle h \rangle V_{\text{in}}(s) \;-\; V_c(s),\Big) \tag{2.160b}$$

where, about the notation, the Laplace transform of a time-domain variable $a(t)$ is denoted as $A(s)$.

The Laplace transform of the current $I_{l1}(s)$ can be expressed as a function of the duty cycle $\langle h \rangle$ and the transform of the output voltage $V_c(s)$:

$$I_{l1}(s) \;=\; \frac{\epsilon}{s\, k_1}\Big(\langle h \rangle V_{\text{in}}(s) \;-\; V_c(s)\Big) \;. \tag{2.161}$$

Substituting (2.161) into the first equation of (2.160) leads to

$$V_c(s)\left(1 \;+\; \frac{\epsilon}{s} \;+\; \frac{\epsilon^2}{k_1\, s^2}\right) \;=\; \frac{\epsilon^2\, \langle h \rangle\, V_{\text{in}}(s)}{k_1\, s^2} \quad . \tag{2.162}$$

Let $G(s)$ be the transfer function between the output voltage V_c and the switches duty cycle $\langle h \rangle$. Then, from (2.162) it can be expressed as

$$G(s) \;=\; \frac{V_c(s)}{\langle h \rangle} \;=\; \frac{\epsilon^2 V_{\text{in}}(s)}{k_1\, s^2 \;+\; k_1\, \epsilon\, s \;+\; \epsilon^2} \quad . \tag{2.163}$$

The transfer function $G(s)$ has two poles, p_1 and p_2, located in the left-hand plane

as shown by

$$p_{1,2} \;=\; \frac{\epsilon}{2}\left(-1 \pm \sqrt{1 - \frac{4}{k_1}}\right) \quad . \tag{2.164}$$

Computing their values using the current parameters ($L_2 = 0$, $V_{\text{ac}} = 0$, all the other parameters according to table 2.2), p_1 and p_2 can be approximated as

$$p_{1,2} \;=\; -0.0361 \;\pm\; 0.4232\,\text{j} \quad , \tag{2.165}$$

where j is the imaginary unit.

Bode diagrams of $G(s)$ are depicted in Figure 2.15.

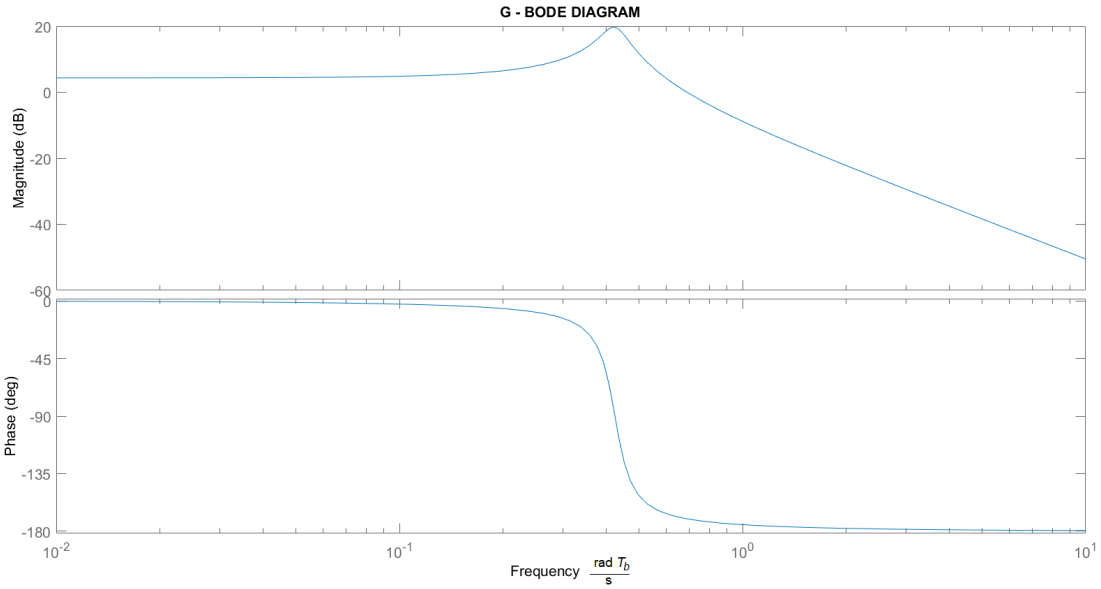

Figure 2.15: Bode diagram of the transfer function G

Let e be the error in the capacitor voltage v_c compared to its reference value v_{ref}. A Proportional-Integral (PI) controller can be implemented to obtain a desired behaviour of v_c. It modifies the duty cycle $\langle h \rangle$ of the switches according to the value of e:

$$\langle h \rangle \;=\; C(s)\,e(s) \;=\; \left(K_p \;+\; \frac{K_i}{s}\right) e(s) \quad , \tag{2.166}$$

where K_p and K_i are the proportional and the integral constants, whose settings depend on the desired bandwidth[1] or other requirements chosen by the user.

According to the scheme depicted in Figure 2.16, the closed-loop equation of the

[1] A definition of bandwidth is given in §.1

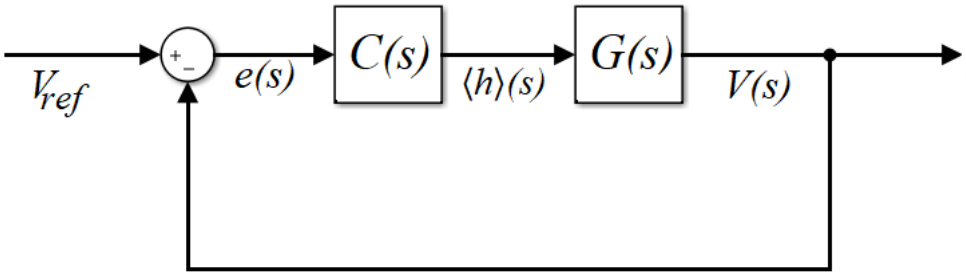

Figure 2.16: Control block scheme

system can be expressed as

$$V_c(s) \;=\; G(s)\,C(s)\Big(V_{\text{ref}} \;-\; V_c(s)\Big) \;\;, \tag{2.167}$$

and the closed-loop transfer function $F(s)$ between V_c and V_{ref} can be defined as

$$F(s) \;=\; \frac{V_c}{V_{\text{ref}}} \;=\; \frac{G(s)\,C(s)}{1 \;+\; G(s)\,C(s)} \;=\; \frac{L(s)}{1 \;+\; L(s)} \;\;, \tag{2.168}$$

where $L(s)$ is defined by

$$L(s) \;=\; G(s)C(s) \;\;. \tag{2.169}$$

Substituting the expressions for $G(s)$ and $C(s)$ shown in (2.163) and (2.166), respectively, for the examined system, $L(s)$ and $F(s)$ are equal to

$$L(s) \;=\; \frac{\epsilon^2\,V_{\text{in}}(s)(K_p\,s \;+\; K_i)}{k_1\,s^3 \;+\; k_1\,\epsilon\,s^2 \;+\; \epsilon^2\,s} \tag{2.170}$$

and

$$F(s) \;=\; \frac{\epsilon^2\,V_{\text{in}}(s)\Big(K_p\,s \;+\; K_i\Big)}{k_1\,s^3 \;+\; k_1\,\epsilon\,s^2 \;+\; \epsilon^2\Big(1 \;+\; V_{\text{in}}(s)K_p\Big)s \;+\; \epsilon^2\,V_{\text{in}}\,K_i} \;\;. \tag{2.171}$$

The open-loop transfer function L has the same poles as G and another at the origin, while a zero is located at $-\,K_i/K_p$.

To reduce the system oscillations, the following bounds on the gain margin and the phase margin are set:

$$\gamma_m \;\geq\; 3 \;, \qquad \phi_m \;\geq\; 90^\circ \;\;, \tag{2.172}$$

where γ_m is the gain margin and ϕ_m is the phase margin. Moreover, a minimum bandwidth has been imposed for the closed-loop system:

$$BW_{min} \;=\; 10^{-2} \;\; \frac{\mathrm{rad}\, T_b}{\mathrm{s}} \;\; , \tag{2.173}$$

where BW is the nondimensionalised bandwidth.

Choosing

$$K_p \;=\; 0.010 \;\; , \qquad K_i \;=\; 0.015 \;\; , \tag{2.174}$$

the following values can be obtained for phase margin, gain margin and bandwidth, respectively:

$$\begin{aligned} \phi_m \;\; &= \; 90.3780^\circ \; , \\ \gamma_m \;\; &= \; 3.0589 \text{ dB} \; , \\ BW \;\; &= \; 0.0246 \; \frac{\mathrm{rad}\, T_b}{\mathrm{s}} \; . \end{aligned} \tag{2.175}$$

In Figure 2.17 and Figure 2.18 are depicted, respectively, the Bode diagram and the zeros and poles location of the open-loop transfer function L for the selected valued of K_p and K_i, while Figure 2.19 shows the Bode diagram of the closed-loop transfer function F. Since the PI controller defined in (2.166) is continuous, but

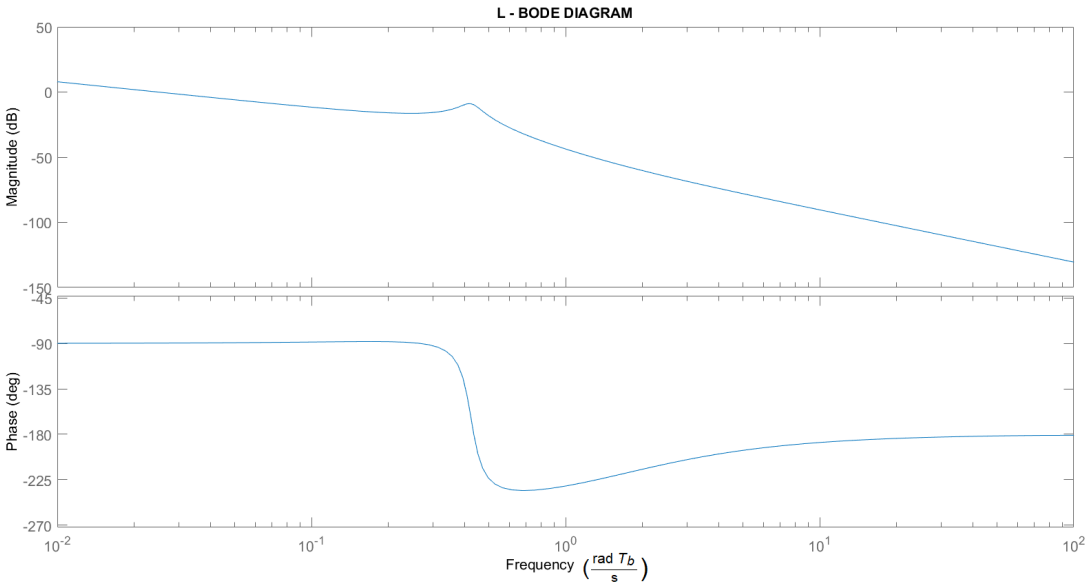

Figure 2.17: Bode diagram of the transfer function L

the average value $\langle h \rangle$ can be modified once during each sample interval, $C(s)$ has been discretised according to the Tustin method. During MATLAB simula-

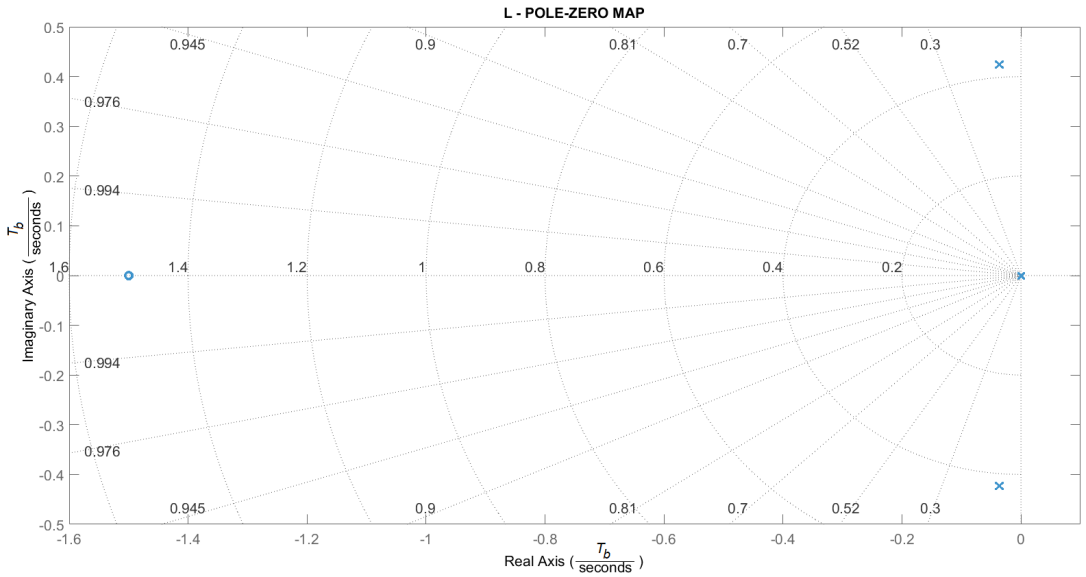

Figure 2.18: Plot of zeros and poles of L

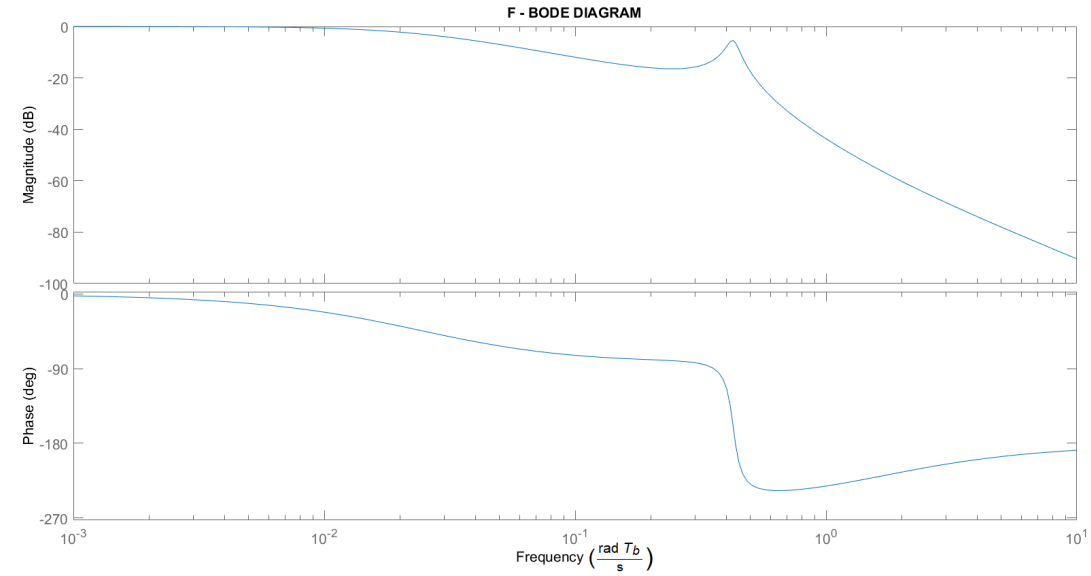

Figure 2.19: Bode diagram of the transfer function F

tions, the system variables have been computed by solving the continuous-time differential equations (2.151), while a discrete-time controller has been utilised to impose the capacitor voltage v_c to follow the reference value.
According to (2.166),

$$s\,\langle h\rangle(s) \;=\; K_p\,e(s)\,s \;+\; K_i\,e(s)\;. \tag{2.176}$$

Therefore, applying the Tustin bilinear discretisation method, the control equation becomes

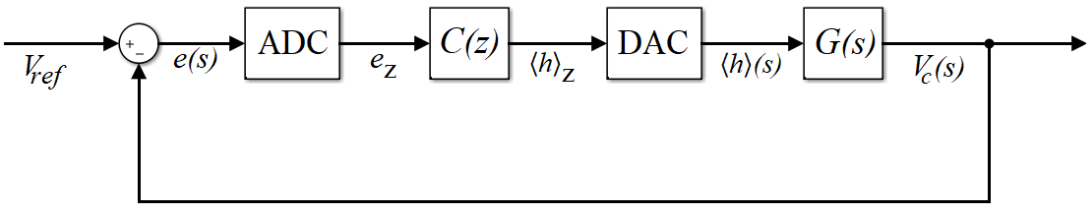

Figure 2.20: Overall control block scheme

$$\frac{\langle h \rangle_{z+1} - \langle h \rangle_{z-1}}{2\,T_d} = \frac{K_p(e_{z+1} - e_{z-1})}{2\,T_d} + K_i\,e_z\,. \tag{2.177}$$

Hence, operating a shift equal to 1 to z in (2.177) and computing $\langle h \rangle_z$ leads to

$$\langle h \rangle_z = \langle h \rangle_{z-2} - K_p\,e_{z-2} + 2\,K_i\,T_d\,e_{z-1} - K_p\,e_z\,, \tag{2.178}$$

where T_d is the sampling time used for the discretisation.
The transfer functions are computed by applying the Laplace transform to the nondimensional system (2.151), where the base value for time T_b is set equal to the switching period T_s. In this case, therefore, T_d has been set equal to 1. The selected value is compatible with the bandwidth, since it is of a greater order.

The overall control scheme, including the Analog-to-Digital-Converter and the Digital-to-Analog-Converter blocks, is depicted in Figure 2.20. The discretisation is performed according to Tustin method to avoid the occurrance of instabilities, while the DAC block operates a zero-order-hold conversion, since $\langle h \rangle$ is piecewise constant. The system's re-dimensionalised response after a step in the reference voltage from 230 V to 150 V is shown in Figure 2.21.

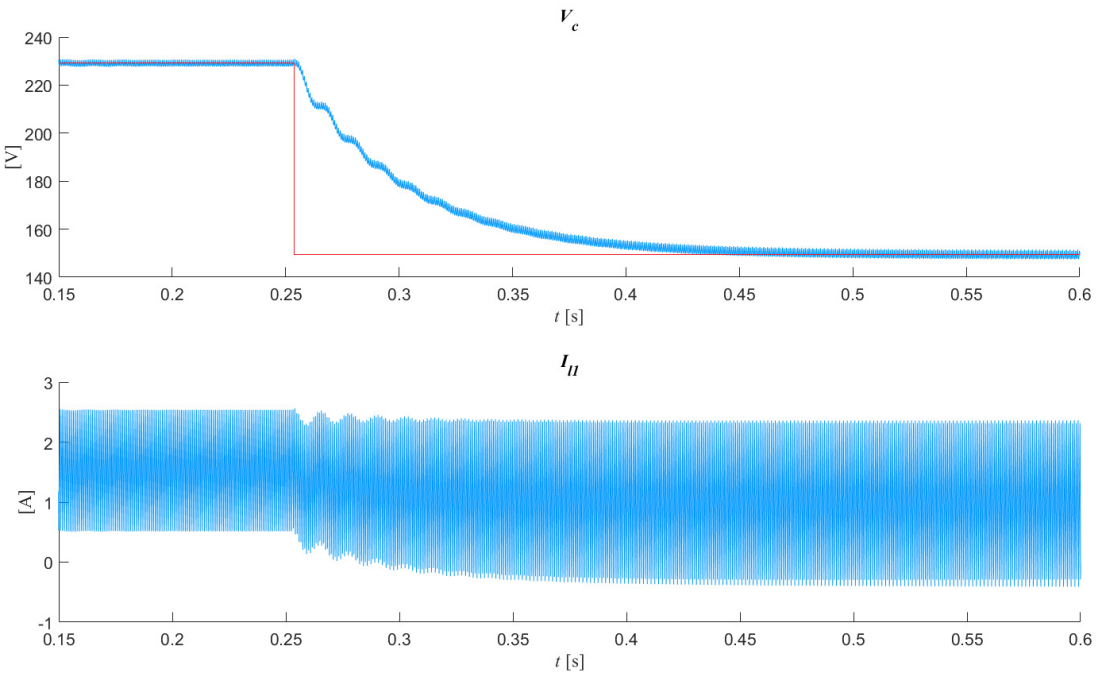

Figure 2.21: Closed-loop inverter operating in DC-DC - System behaviour (blue) after a step in the reference voltage value (red)

2.4.5.2 DC-AC conversion

This system is the same as depicted in Figure 2.14, but this time an alternate voltage is required on the load. As well as in the DC-DC case, the second inductor L_2 is set equal to 0 and the inverter is not connected to the grid (i.e. $V_{\text{ac}} = 0$ in the equations).

In this case, the switching function is given by

$$h(t) = \begin{cases} 1 & \hat{m}(t) > \hat{p}(t) \\ -1 & \hat{m}(t < \hat{p}(t) \end{cases}, \tag{2.179}$$

where $\hat{p}(\tau)$ is the nondimensionalised triangular carrier wave defined in (2.108) and $\hat{m}(\tau)$ is a piecewise constant function, whose value is the output of the controller and can vary once in each period of the carrier.

Since, according to (2.111), the average of the switching function h computed in one switching period is equal to the nondimensional value $\hat{m}$ in the same period, the output of the controller directly changes $\langle h \rangle$. Therefore, the block scheme shown in Figure 2.20 is still valid. In the previous example, the reference voltage

was constant, while V_{ref} is now sinusoidal, with a frequency equal to 50 Hz.
A first attempt is made by applying the same PI controller of the DC-DC case. However, even though the system is stable, it does not appear fast enough to effectively follow a sinusoidal reference: the output voltage wave has a delay of about $\frac{\pi}{2}$, and its amplitude is less than half of the reference. The system behaviour is depicted in Figures 2.22 and 2.23.

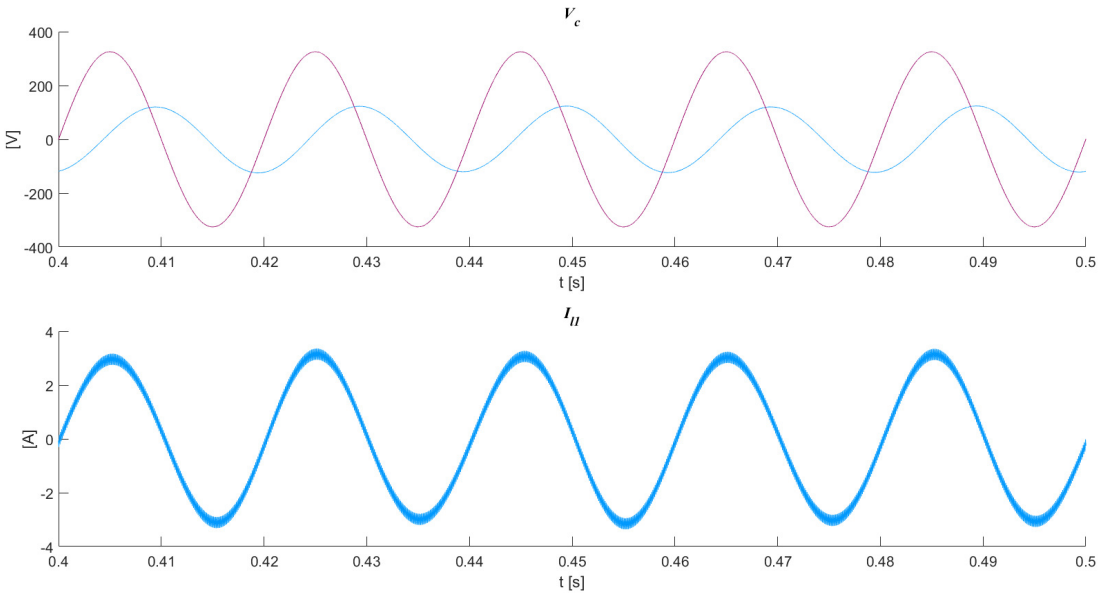

Figure 2.22: System behaviour (blue) with a 50 Hz sinusoidal reference voltage (purple)

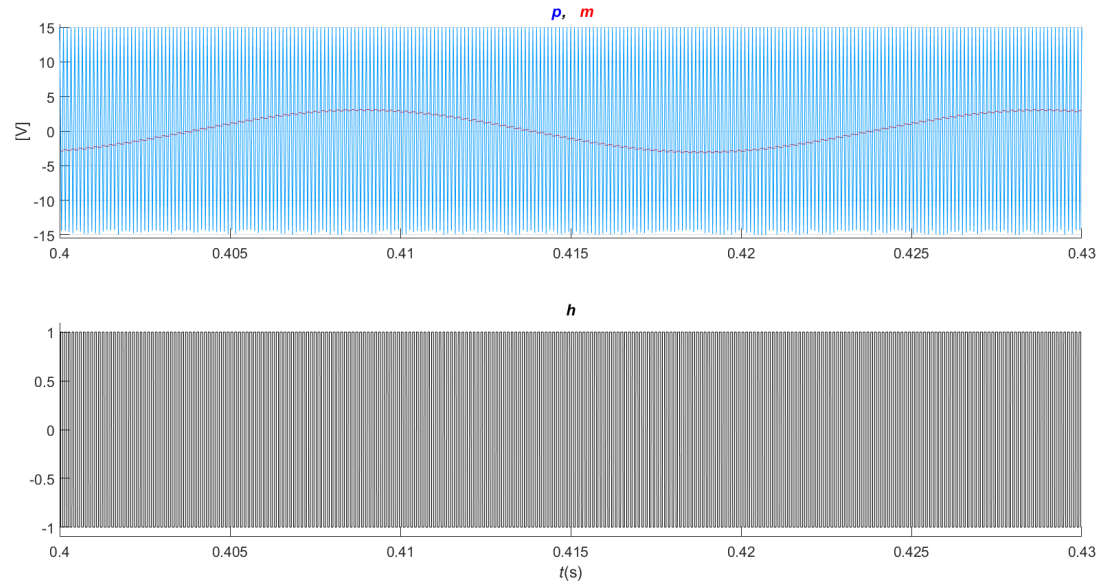

Figure 2.23: Carrier wave (blue), dimensionalised $\langle h \rangle$ (red), switching signal (black)

Applying a PI controller on the capacitor voltage only, indeed, is in general not sufficient to achieve a good performance from a power electronic converter, as

the bandwidth cannot be increased significantly without compromising stability. More complex controllers are usually required, and some examples are included in the next chapters.

In particular, §3 concerns the analysis of the behaviour of an inverter working as a single-phase rectifier. In that case, singular perturbation is applied in order to achieve a model reduction in the state-space analyses of the system.

In the following chapters, the switching behaviour of power electronic converters will not be taken into account directly, and further analyses will be performed on the average systems. This is possible thanks to the preliminary work described in the first two chapters: if the switching period is negligible compared to the other time constants of the system, and if the considered phenomena occur over time intervals much longer than a switching period, then the average model approximates well enough the overall behaviour of the system.

Chapter 3

Model Reduction of a Single-Phase Active Front-End

This chapter concerns the work which was performed on a single phase rectifier. These kinds of devices, despite being structurally simple and being formed of few components, present some challenges when their stability needs evaluation. Their state-space systems, indeed, are characterised by nonlinear time-periodic behaviours. Their models are usually linearised, and Linear Time-Periodic (LTP) analyses are employed to evaluate the stability of the linearised systems. This overall process is more complicated than that of other power electronic converters, and dealing with fewer variables and ODEs could be beneficial for the simplification of this process.

§3.1 gives an introduction to the topic of LTP theory; §3.2 illustrates a literature review about the application of LTP techniques in engineering. The following sections regards the examined case: first, the single-phase rectifier is described, and its state-space system is presented; the state-space system is then linearised and nondimensionalised; singular perturbation is then applied to the system, and a model reduction is performed. Initial-value problem solutions (i.e. time-domain simulations) and stability analyses are computed for both full and reduced system, in order to validate the model reduction. Good agreement is found in both simulations and stability analyses, whose results are shown in §3.3.3.

3.1 Linear Time Periodic Theory

A Linear Time-Periodic (LTP) system of period T is defined by

$$\dot{\boldsymbol{x}}(t) \;=\; A(t)\boldsymbol{x}(t)\;, \tag{3.1}$$

where $\boldsymbol{x}(t) \in \mathbb{R}^n$ and $A(t) \in \mathbb{R}^{n\times n}$ is a T-periodic matrix.
Now, let (3.1) be expressed in matrix form as

$$\dot{\boldsymbol{x}}(t) \;=\; \sum_{n=-\infty}^{+\infty} A_n\, \mathrm{e}^{\mathrm{j}\, n\,\omega_g\, t}\; \boldsymbol{x}(t)\;, \tag{3.2}$$

where j is the imaginary unit, $\mathrm{j}^2 \;=\; -1$.
According to Floquet theory, solutions of (3.2) can be found in the form

$$\boldsymbol{x}(t) \;=\; P(t)\,\mathrm{e}^{Rt}\;, \tag{3.3}$$

where $P(t+T) \;=\; P(t)$ and R is some constant matrix. Assuming the eigenvalues of R to be distinct leads one to seek so-called exponentially modulated time-periodic signals as solutions of (3.2). These are of the form

$$\boldsymbol{x}(t) \;=\; \sum_{m=-\infty}^{+\infty} \boldsymbol{x}_m\, \mathrm{e}^{(\sigma\,+\mathrm{j}\,m\,\omega_g)t}\;. \tag{3.4}$$

The eigenvalues σ must in general be determined numerically, as described later. From (3.4), the derivative $\dot{\boldsymbol{x}}(t)$ can be computed in two ways: first, by differentiating (3.4) as shown below:

$$\dot{\boldsymbol{x}}(t) \;=\; \mathrm{e}^{\sigma\, t} \sum_{m=-\infty}^{+\infty} (\sigma \;+\; \mathrm{j}\, m\, \omega_g)\boldsymbol{x}_m \mathrm{e}^{\mathrm{j}\, m\,\omega_g\, t}\;, \tag{3.5}$$

then by substituting (3.4) into (3.2):

$$\begin{aligned} \dot{\boldsymbol{x}}(t) \;&=\; \sum_{n=-\infty}^{+\infty} A_n\, \mathrm{e}^{\mathrm{j}\, n\, w_g t} \sum_{m=-\infty}^{+\infty} \boldsymbol{x}_m\, \mathrm{e}^{(\sigma\,+\mathrm{j}\, m\,\omega_g t)} \\ &= \mathrm{e}^{\sigma t} \sum_{n=-\infty}^{+\infty} \sum_{m=-\infty}^{+\infty} A_m \boldsymbol{x}_{n-m} \mathrm{e}^{\mathrm{j}\, n\,\omega_g t}. \end{aligned} \tag{3.6}$$

Equating the RHS of (3.5) and (3.6) leads to

$$(\sigma + \mathrm{j}\, n\, \omega_g)\boldsymbol{x}_n = \sum_{m=-\infty}^{+\infty} A_m \boldsymbol{x}_{n-m} \,. \tag{3.7}$$

In solving (3.7), it is useful to introduce the infinite matrices $\mathcal{A}$, $\mathcal{N}$ and $\mathcal{X}$, which are defined, respectively, by

$$\mathcal{A} = \begin{bmatrix} \ddots & \vdots & \vdots & \vdots & \\ \cdots & A_0 & A_{-1} & A_{-2} & \cdots \\ \cdots & A_1 & A_0 & A_{-1} & \cdots \\ \cdots & A_2 & A_1 & A_0 & \cdots \\ & \vdots & \vdots & \vdots & \ddots \end{bmatrix}, \tag{3.8}$$

$$\mathcal{N} = \begin{bmatrix} \ddots & & & & & & \\ & -2j\omega_g I & & & & 0 & \\ & & -j\omega_g I & & & & \\ & & & Z & & & \\ & & & & j\omega_g I & & \\ & 0 & & & & 2j\omega_g I & \\ & & & & & & \ddots \end{bmatrix}, \tag{3.9}$$

$$\mathcal{X} = \begin{bmatrix} \vdots \\ x_{-2} \\ x_{-1} \\ x_0 \\ x_1 \\ x_2 \\ \vdots \end{bmatrix}, \tag{3.10}$$

where I is an identity matrix of suitable dimensions and Z a zero matrix of suitable dimensions.

Then, (3.7) can be expressed in matrix form as

$$\sigma\mathcal{X} \;=\; (\mathcal{A} \;-\; \mathcal{N})\mathcal{X}\;. \tag{3.11}$$

From (3.11), solutions σ are the eigenvalues of $(\mathcal{A} - \mathcal{N})$. The system is stable if $\Re(\sigma) < 0$ for all σ [13] [14].

For the LTP system (3.2), if σ is an eigenvalue, then so is $\sigma + \mathrm{j}\,n\,\omega_g$ for any given integer n. Therefore, the eigenvalues form columns parallel to the imaginary axis when plotted in the complex plane. For practical purposes, the system (3.7), and hence the infinite matrix problem (3.11), is truncated. As a result, the eigenvalue columns distorted far from the real axis as an artefact of truncation.

3.2 Applications of Linear Time-Periodic Theories in the Power Electronics Literature

LTP systems are ubiquitous in physics and dynamical systems theory (e.g. Hill's equation [16], Arnol'd tongues [17], etc). In engineering applications, a LTP stability analysis, as presented in [13] and [14], was initially developed for aeronautical applications characterised by periodic behaviour. In particular, they focused on helicopter blades and the forces applied to them.

In the last two decades, the same techniques have begun to be applied to power electronic systems too. A general method to derive harmonic state-space models for linear and switching subsystems is explained in [18]. More specific examples are given in [19] and [20], where harmonic state-space models are computed for a thyristor-controlled reactor and a grid-connected converter, respectively.

Stability analysis through LTP techniques is performed on a locomotive single-phase grid-connected inverter in [21]. Stability is analogously assessed in [20], [22] and [23] for different kinds of power electronic systems. In [23] a comparison between stability analysis carried out through linear time-invariant (LTI) and LTP approaches is shown, highlighting the limits and inaccuracies that are obtained

when the harmonic behaviour of the system is neglected. Even though from a mathematical point of view it is obvious that the time-periodic nature of the steady-state solution must be taken into account when assessing its stability, engineers often ignore this and try to apply techniques to LTP problems which are suitable only for problems with constant steady-states, where the coefficients in the linearised problem are constant. In [23], stability analyses performed with this approximation are close to the LTP ones only if relatively big filtering components (e.g. inductors, capacitors, ...) are added to reduce the ripple amplitudes and the controller behaviour is kept slow by reducing its bandwidth[1]. Consequently, the system cost increases because of the increased size of passive components and its performance deteriorates through the controller slowness. Therefore, this engineering ad hoc approximation is not good enough for practical purposes and will not be used in this work. When nonlinear time-periodic (NLTP) systems are analysed, time-periodic steady states will be computed and the LTP system stability will be assessed as explained in §3.1.

A stability analysis based on LTP techniques is presented in [24] for a modular multilevel converter (MMC), even though time-domain simulations of the considered systems do not completely agree with the stability analysis previously performed. These discrepancies are not further discussed or justified in the paper. In general, power-electronic-based systems can be modelled as NLTI or LTI systems when they are three-phase and symmetrical. In order to do so, a DQ0 transform is usually applied to the ABC sinusoidal model. When single-phase systems are taken into account, though, or in case a three-phase system is unbalanced, the DQ0 Park transform cannot be applied effectively to the models. State-space variables, then, will show periodic behaviours, and the models will be LTP or NLTP.

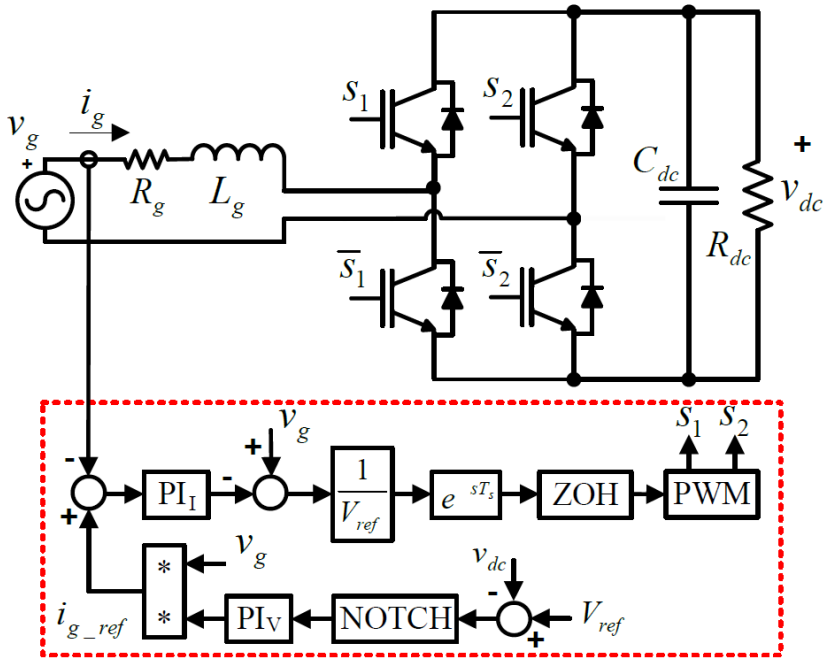

Figure 3.1: Scheme of the SP-AFE converter and relative controller (red dashed box)

3.3 Single-Phase Active-Front-End Model Formulation

In this section, a brief introduction of the analysed power electronic system is given and the different procedures used to evaluate its stability are summarised.

The system depicted in Figure 3.1 shows a standard AC-DC converter and its control scheme. A standard device has been chosen to allow us to focus on developing techniques for a model reduction. Parameters and controllers are as explained in [23], so that an easy comparison can be made between the results of non-reduced and reduced models.

In this case, the conversion is performed by a Single-Phase Active Front End (SP-AFE); both the grid voltage v_g and grid current i_g are measured and their values are sent to a feedback controller, whose aim is to keep the voltage on the DC-link capacitor C_{dc} as close as possible to a reference V_{ref}. First, the error on the DC-link voltage v_{dc} is computed and then filtered by a notch filter to attenuate the voltage ripple at $2\omega_g$ (the harmonic at $2\omega_g$ is the main component of the ripple on the capacitor voltage, as further explained in 3.3.2.2). The filtered signal constitutes the input of a Proportional-Integral (PI) controller, while its

[1]See Appendix A

output is suitably scaled by the value of v_g to compute a reference for i_g. The error on i_g enters a further PI, whose output is subtracted from the grid voltage v_g, rescaled by V_{ref}, and discretised by a Zero-Order Hold. The exponential $\mathrm{e}^{-\mathrm{s}T_s}$ is added due to computational delays happening with sampling period T_s. The resulting signal is finally sent to a PWM in order to obtain the control signals for the four switches S_1, $\bar{S}_1$, S_2 and $\bar{S}_2$.

The state-space model of the system, including the control variables, is formed of eight ODEs and eight independent variables, which, in this case, are chosen as follows:

- x_1, x_2 are additional variables describing the dynamics of the notch filter;
- x_3 and x_4 are the states associated with the voltage PI control and the current PI control, respectively (they behave like the integral of the error between the value of the current or voltage and its respective reference);
- x_5 and x_6 represent the internal dynamics involving the computational delay, Zero-Order Hold discretiser and PWM;
- x_7 is the current i_g drawn from the grid;
- x_8 is the voltage v_{dc} measured on the DC-link capacitor;
- $v_g(t)$ is the alternating grid voltage, which is assumed to be purely sinusoidal and is given by

$$v_g(t) \;=\; V_g \sin(\omega_g t)\;. \tag{3.12}$$

In practice, the assumption stated in (3.12) is valid since v_g is taken from an AC grid: this makes eventual deviations from the sinusoidal shape extremely small.

The delays due to both discretised control and PWM Zero-Order Hold are approximated by the continuous-time transfer function

$$H(s) \;=\; \frac{\mathrm{e}^{-sT_s}\left[1 \;-\; \mathrm{e}^{sT_s}\right]}{\mathrm{s}\,T_s}\,. \tag{3.13}$$

If the complex exponential in (3.13) is replaced by a first-order Padé approxima-

tion of the form

$$\mathrm{e}^{-sT_s} = \frac{n_1 s + n_0}{d_1 s + d_0}, \tag{3.14}$$

where n_1, n_0, d_1, and d_0 are suitable real coefficients, then (3.13) becomes

$$H(s) = \frac{\gamma_1 s + \gamma_0}{s^2 + \sigma_1 s + \sigma_0}, \tag{3.15}$$

where γ_1, γ_0, σ_1, and σ_0 can be derived from (3.13) and (3.14).

The notch filter transfer function is given by

$$N(s) = k_n + \frac{p_1 s + p_0}{s^2 + q_1 s + q_0}, \tag{3.16}$$

where p_1, p_0, q_1, q_0, and k_n are real parameters tuned to attenuate functions with frequency $2\omega_g$.

Transforming $H(s)$ and $N(s)$ as expressed in (3.15) and (3.16), respectively, into time domain, and neglecting the switching behaviour of the converter leads to the following average state-space system:

$$\dot{x}_1 = x_2 \,, \tag{3.17a}$$

$$\dot{x}_2 = -q_0 x_1 - q_1 x_2 + V_{\text{ref}} - x_8 \,, \tag{3.17b}$$

$$\dot{x}_3 = p_0 x_1 + p_1 x_2 + k_n(V_{\text{ref}} - x_8) \,, \tag{3.17c}$$

$$\dot{x}_4 = k_{iv} v_g(t) x_3 + k_{pv} p_0 v_g(t) x_1 + k_{pv} p_1 v_g(t) x_2 + k_{pv} k_n (V_{\text{ref}} - x_8) v_g(t) - x_7, \tag{3.17d}$$

$$\dot{x}_5 = x_6 \,, \tag{3.17e}$$

$$\begin{aligned}\dot{x}_6 = {} & -\sigma_0 x_5 - \sigma_1 x_6 + V_{\text{ref}}^{-1}\{v_g(t) - [k_{ii} x_4 + k_{pi} k_{iv} v_g(t) x_3 + k_{pi} k_{pv} p_0 v_g(t) x_1 + \\ & + k_{pi}\, k_{pv}\, p_1\, v_g(t)\, x_2 + k_{pi}\, k_{pv}\, v_g(t)(V_{\text{ref}} - x_8) - k_{pi}\, x_7]\} \,,\end{aligned} \tag{3.17f}$$

$$\dot{x}_7 = L_g^{-1}\,[v_g(t) - R_g\, x_7 - (\gamma_0\, x_5 + \gamma_1\, x_6)\, x_8] \,, \tag{3.17g}$$

$$\dot{x}_8 = C_{dc}^{-1} \left[(\gamma_0 x_5 + \gamma_1 x_6) x_7 - R_{dc}^{-1} x_8 \right] . \tag{3.17h}$$

In general, the approximations which have been employed both above and in what follows are ad hoc more than systematic and follow electrical engineering custom. However, each of them will be explained and justified and comparative plots will be shown to demonstrate their effectiveness.

The meanings and respective values of parameters in (3.17) are reported in Table 3.1. Explicit mention of the time dependency of the state variables has been omitted in (3.17), for the sake of notational brevity.

V_g	Peak grid voltage	$115\sqrt{2}$ V
f_g	Grid frequency	50 Hz
T_g	Grid period	0.020 s
L_g	Grid inductance	0.87 mH
R_g	Grid resistance	0.2 Ω
R_{dc}	Load resistance	120 Ω
C_{dc}	DC-link capacitance	600 μF
f_{pwm}	PWM frequency	1000 Hz
f_s	Sampling frequency	2000 Hz
V_{ref}	Reference DC-link voltage	300 V
γ_0	Zero-order hold parameter	$1.6 \cdot 10^9$ s^{-2}
γ_1	Zero-order hold parameter	$-4.0 \cdot 10^4$ s^{-1}
σ_0	Zero-order hold parameter	$1.6 \cdot 10^9$ s^{-2}
σ_1	Zero-order hold parameter	$8.0 \cdot 10^4$ s^{-1}
p_0	Notch filter parameter	0 s^{-2}
p_1	Notch filter parameter	-31.4159 s^{-1}
q_0	Notch filter parameter	$3.9 \cdot 10^5$ s^{-2}
k_n	Notch filter parameter	1
q_1	Notch filter parameter	31.4159 s^{-1}
k_{pi}	Current PI proportional coefficient	5.009 Ω
k_{ii}	Current PI integral coefficient	1279.3 Ωs^{-1}
k_{iv}	Voltage PI proportional coefficient	0.0079 (ΩV)$^{-1}$
k_{pv}	Voltage PI integral coefficient	2.0609 (ΩVs)$^{-1}$

Table 3.1: System parameters

In the engineering literature, the ODE system (3.17) is referred to as a Non-linear Time Periodic (NLTP) system. To analyse such a system, a "steady-state" time-periodic solution is first found, then its stability is examined by linearising the system about that solution.

Let the following more compact notation be used to express the NLTP system (3.17):

$$\dot{\boldsymbol{x}}(T+t) \;=\; \dot{\boldsymbol{x}}(t) \;=\; \boldsymbol{f}(\boldsymbol{x}(t),\, u(t))\;, \tag{3.18}$$

where $\boldsymbol{x} \in \mathbb{R}^n$ is the state vector and the input $u(t)$ is here the grid voltage $v_g(t)$. Since $v_g(t)$ is the grid sinusoidal voltage, the input $u(t)$ is T_g-periodic:

$$u(t \,+\, T_g) \;=\; u(t)\;. \tag{3.19}$$

Given the signal x_i, its steady-state component can be separated from the perturbation as follows

$$x_i(t) \;=\; \bar{x}_i(t) \;+\; \tilde{x}_i(t)\;, \tag{3.20}$$

where $\bar{x}_i$ is the steady state of x_i and $\tilde{x}_i$ its perturbation.
Then, the corresponding linearised system is given by

$$\dot{\tilde{\boldsymbol{x}}}(t) \;=\; \left.\frac{\partial \boldsymbol{f}}{\partial \boldsymbol{x}}\right|_{\bar{\boldsymbol{x}},\,\bar{u}} \tilde{\boldsymbol{x}}(t) \;+\; \left.\frac{\partial \boldsymbol{f}}{\partial u}\right|_{\bar{\boldsymbol{x}},\,\bar{u}} u(t)\;. \tag{3.21}$$

Assuming that the perturbations are small if compared with the steady-state values and applying linearisation to (3.17) lead to

$$\dot{\tilde{x}}_1 = \; \tilde{x}_2\;, \tag{3.22a}$$

$$\dot{\tilde{x}}_2 = \; -\,q_0\,\tilde{x}_1 \;-\; q_1\,\tilde{x}_2 \;-\; \tilde{x}_8\;, \tag{3.22b}$$

$$\dot{\tilde{x}}_3 = \; p_0\,\tilde{x}_1 \;+\; p_1\,\tilde{x}_2 \;-\; k_n\,\tilde{x}_8\;, \tag{3.22c}$$

$$\dot{\tilde{x}}_4 = k_{pv}p_0v_g(t)\tilde{x}_1 + k_{pv}p_1v_g(t)\tilde{x}_2 + k_{iv}v_g(t)\tilde{x}_3 - \tilde{x}_7 - k_{pv}k_nv_g(t)\tilde{x}_8, \tag{3.22d}$$

$$\dot{\tilde{x}}_5 = \; \tilde{x}_6\;, \tag{3.22e}$$

$$\dot{\tilde{x}}_6 = -\sigma_0\,\tilde{x}_5 - \sigma_1\,\tilde{x}_6 + V_{ref}^{-1}\,[-k_{ii}\,\tilde{x}_4 - k_{pi}\,k_{iv}\,v_g(t)\,\tilde{x}_3 - k_{pi}\,k_{pv}\,p_0\,v_g(t)\,\tilde{x}_1 + - k_{pi}\,k_{pv}\,p_1\,v_g(t)\,\tilde{x}_2 + k_{pi}\,k_{pv}\,v_g(t)\,\tilde{x}_8 + k_{pi}\,\tilde{x}_7]\,, \tag{3.22f}$$

$$\dot{\tilde{x}}_7 = L_g^{-1}[-\gamma_0\bar{x}_8(t)\tilde{x}_5 - \gamma_1\bar{x}_8(t)\tilde{x}_6 - R_g\tilde{x}_7 - (\gamma_0\bar{x}_5(t) + \gamma_1\bar{x}_6(t))\tilde{x}_8], \tag{3.22g}$$

$$\dot{\tilde{x}}_8 = C_{dc}^{-1}\left[\gamma_0\bar{x}_7(t)\tilde{x}_5 + \gamma_1\bar{x}_7(t)\tilde{x}_6 + (\gamma_0\bar{x}_5(t) + \gamma_1\bar{x}_6(t))\tilde{x}_7 - R_{dc}^{-1}\tilde{x}_8\right]\,, \tag{3.22h}$$

where $\bar{x}_i$ denotes the steady state of x_i and $\tilde{x}_i$ its perturbation.
In (3.22), the grid voltage and the steady states are explicitly written as time-dependent to highlight the LTP nature of the system.

To evaluate the steady-state stability of (3.22), various approximations have been considered (some systematic, some ad hoc). In §3.3.2, their effect on the steady-state and its stability is analysed.

3.3.1 Procedure Summary

For the sake of clarity, the steps for performing a system reduction and its relative validation are depicted in Figure 3.2 and summarised below.

- First, the "exact" solution of the initial-value problem composed by the ODEs of (3.17) has been obtained by solving the state-space equations through high-accuracy simulations (in the present case, MATLAB ode45 has been used). The simulations have been run for a time-span long enough to assume that the system transients have finished. The so-obtained time-domain results, therefore, can be considered as steady-state solutions.
- The solution in time domain of the full system has been sampled and its Fourier coefficients have been found by applying the MATLAB function for the Fast Fourier Transform fft to the sampled values of the variables.
- The Fourier coefficients for the steady states of system (3.17) have also been computed by truncating and then solving numerically a system of equations obtained by substituting each state variable of (3.17) with the corresponding Fourier series, as explained in §3.3.2.1. In the present case, the MATLAB function fsolve has been used to solve the resulting system of equations.
- Due to the difficulty of finding a suitable starting point for fsolve (and to the non-convexity of the problem), another approach for finding the Fourier coefficients of the steady-states has been applied. As shown in §3.3.2.2 , some engineering approximations, suggested by experimental evidence, have been investigated. The corresponding approximate Fourier coefficients have been compared with both the coefficients from fsolve and the coefficients obtained by sampling the time domain steady-state solution. Those comparisons are given in §3.3.2.3.
- After assessing the validity of the steady states obtained from engineering approximations, the full state-space system (3.17) has been linearised about these steady -states and its corresponding LTP system has been computed.
- By applying LTP techniques, the eigenvalues of the so-obtained full LTP system have been found and stability of the full LTP system has been analysed.

– As explained in §3.3.3, the full state-space system has been nondimensionalised, small parameters have been identified and a model reduction has been performed. Time-domain simulations of the reduced system have been obtained through MATLAB ode45. These results have then been compared with the corresponding time domain results of the full system. Different possibilities have been explored for the reduction, leading to reduced systems with a different number of ODEs and different levels of approximation.

– The time-domain simulations for the reduced models have been sampled and the Fourier coefficients have been computed by applying MATLAB fft, analogously to the procedure followed for the full system. The coefficients of the full and the reduced models have been compared.

– The steady-state expressions for the reduced model have been found by applying the same engineering approximations that have been validated for the full system.

– The reduced systems have been linearised about those approximated steady states and the corresponding reduced LTP system has been computed.

– The eigenvalues for the reduced models have been computed and then compared with the eigenvalues of the full system. Stability analyses have been compared for different values of the controller parameters.

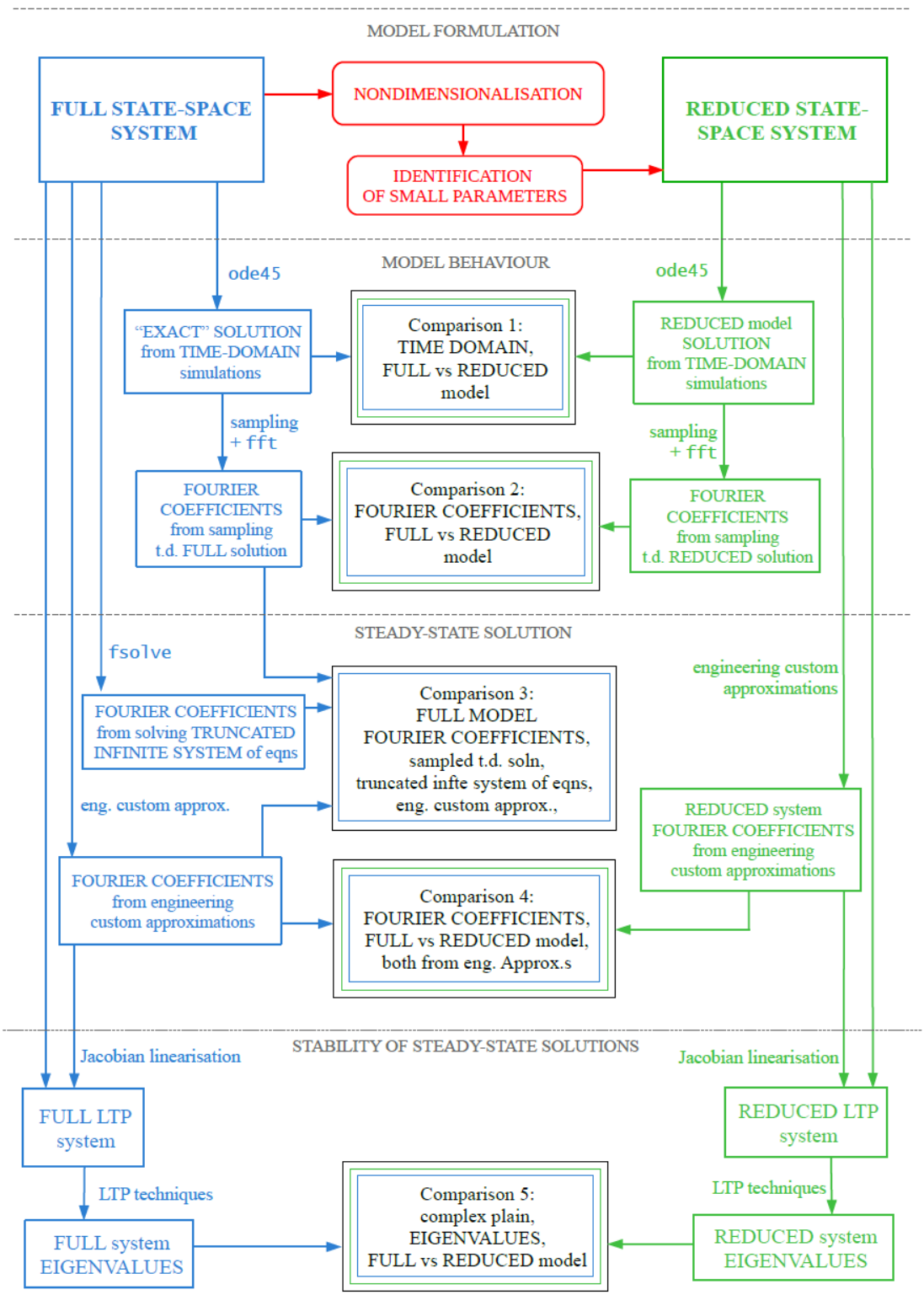

Figure 3.2: Scheme of the overall analyses performed on the SP-AFE

3.3.2 Computation of the Steady-State Operating Point

In this subsection, the steady-state operating points of the full system (3.17) are computed in two different ways, later compared.

First, as explained in §3.3.2.1, the time-periodic steady-states and input v_g are written as Fourier series; by substituting those expressions into the state-space system, an infinite system of algebraic equations is derived; truncating and solving numerically, the so-obtained system leads to the computation of the Fourier coefficients of the unknown steady-states.

As a second approach to computing the steady states of the analysed system, detailed in §3.3.2.2,, the "power balance approach" from engineering has been applied. This includes a drastic truncation of the Fourier series of the system based on engineering insight for the computation of the Fourier coefficients.

These two ways of approximating the system steady-states are compared in §3.3.2.3, where their corresponding Fourier coefficients are plotted, together with the Fourier coefficients obtained from sampling the steady-state time domain simulations of the system and processing the values applying the MATLAB function fft.

Only the steady-state solutions $\bar{x}_5(t)$, $\bar{x}_6(t)$, $\bar{x}_7(t)$ and $\bar{x}_8(t)$ appear in the linearised time-periodic system (3.22). Therefore, attention has been mainly focused on the computation of these, rather than on the steady states of the other four state variables.

3.3.2.1 Steady-State Point from Truncated Infinite System of Equations

Assuming that the steady-state solution of the NLTP system (3.17) is periodic, each variable can be written as a Fourier series

$$\bar{x}_i(t) \;=\; \langle \bar{x}_i \rangle \;+\; \sum_{n=-\infty}^{+\infty}{}' \; \bar{x}_i^{(n)} \, \mathrm{e}^{\mathrm{j}\, n\, \omega_g t} \;, \tag{3.23}$$

where

- $i = 1, 2, ..., 8$ labels the state degrees of freedom;

- $\langle \bar{x}_i \rangle$ is the average of $\bar{x}_i(t)$;
- $\bar{x}_i^{(n)}$ are its Fourier coefficients;
- $\sum_{n=-\infty}^{+\infty}{}' a_n = \sum_{n=-\infty}^{-1} a_n + \sum_{n=+1}^{+\infty} a_n$.

Defining $\bar{x}_i^{(0)}$ as

$$\bar{x}_i^{(0)} = \langle \bar{x}_i \rangle , \tag{3.24}$$

the equation (3.23) can be written more compactly as

$$\bar{x}_i(t) = \sum_{n=-\infty}^{+\infty} \bar{x}_i^{(n)} \, \mathrm{e}^{\mathrm{j}\, n\, \omega_g t} . \tag{3.25}$$

Differentiating (3.25) with respect to time leads to

$$\dot{\bar{x}}_i(t) = \sum_{n=-\infty}^{+\infty} \mathrm{j}\, n\, \omega_g \, \bar{x}_i^{(n)} \, \mathrm{e}^{\mathrm{j}\, n\, \omega_g t} . \tag{3.26}$$

The input voltage v_g can be written exponentially according to Euler's formula:

$$v_g(t) = \frac{V_g}{2\mathrm{j}} (\mathrm{e}^{\mathrm{j}\, \omega_g\, t} - \mathrm{e}^{-\mathrm{j}\, \omega_g\, t}) . \tag{3.27}$$

Now, substitution of (3.25), (3.26) and (3.27) into (3.17) leads to a new system whose equations are composed of constant parameters and parameters modulated by time-dependent exponential signals $\mathrm{e}^{\mathrm{j}\, n\, \omega_g\, t}$. The system unknowns are the infinite number of Fourier coefficients of the steady-state solution, $\bar{x}_i^{(n)}$.

For practical purposes, it is necessary to truncate the Fourier series up to a positive integer N, obtaining $8(2N+1)$ unknowns. Selecting in each equation the terms of the same frequency, $8(2N+1)$ equations can be written.

For example, for the first equation of (3.17), this gives rise to

$$\dot{\bar{x}}_1(t) = \bar{x}_2(t), \tag{3.28}$$

$$\sum_{n=-\infty}^{+\infty} \mathrm{j}\, n\, \omega_g \, \bar{x}_1^{(n)} \, \mathrm{e}^{\mathrm{j}\, n\, \omega_g\, t} = \sum_{n=-\infty}^{+\infty} \bar{x}_2^{(n)} \mathrm{e}^{\mathrm{j}\, n\, \omega_g\, t} . \tag{3.29}$$

Truncation of (3.29) at $n = \pm N$ leads to

$$\sum_{n=-N}^{+N} \mathrm{j}\, n\, \omega_g\, \bar{x}_1^{(n)}\, \mathrm{e}^{\mathrm{j}\, n\, \omega_g\, t} \;=\; \sum_{n=-N}^{+N} \bar{x}_2^{(n)} \mathrm{e}^{\mathrm{j}\, n\, \omega_g\, t}\;. \tag{3.30}$$

Equating the LHS and RHS terms with the same frequency leads to

$$\mathrm{j}\, n\, \omega_g\, \bar{x}_1^{(n)} \;=\; \bar{x}_2^{(n)}\;, \tag{3.31}$$

where

$$n \;=\; -N,\, -N+1, ...,\, N-1,\, N\;. \tag{3.32}$$

The same procedure can be applied to all the equations of (3.17), obtaining a system of $8(2N+1)$ time-invariant equations in $8(2N+1)$ unknowns. The equations originating from the last two equations of (3.17), which are nonlinear, are still nonlinear in this spectral representation. The system can be solved numerically: in the considered case, the MATLAB function fsolve has been used. However, this function needs an initial guess to operate. If the problem is not convex and the absolute minimum is far from the initial condition, some local minima can be mistaken for optimal points by the function, leading to inaccuracies.

Since stating an initial guess for big systems is in general hard, in the engineering practice a more approximated method for computing the steady-states is usually applied, as described in §3.3.2.2. In order to validate this approximated technique, the infinite system of equations obtained by substituting (3.25), (3.26) and (3.27) into (3.17) has been truncated at $n = \pm 4$ and solved by fsolve. The resulting Fourier coefficients have been compared with the Fourier coefficients obtained by following the method illustrated in §3.3.2.2. The values obtained by applying the engineering custom approximations have also been used as an initial guess for fsolve: the Fourier coefficients which are neglected by this method have been set equal to 0 in the initial guess.

In order to reduce the number of unknowns, the grid current $i_g(t)$ has been assumed to be mainly constituted by odd harmonics, and the voltage v_{dc} by even

harmonics; this approximation is common in engineering and is supported by experimental evidence. Following these assumptions and observing the ODEs of the full system (3.17), only the odd harmonics have been considered for x_4, x_5, x_6 and x_7, while only even harmonics have been considered for x_1, x_2, x_3 and x_8. All the other harmonic contributions have been treated and approximated as equal to 0.

Considering x_7 as constituted by odd harmonics only and x_8 by even only, indeed, forces x_5 and x_6 to be formed by odd harmonics to avoid imbalances in (3.17g) and (3.17h). Considering x_5 and x_6 as odd-harmonics-only, moreover, and observing (3.17f), leads to treating x_4 as composed by odd harmonics and x_1, x_2, x_3 by even. These choices are consistent if (3.17a), (3.17b), (3.17c), (3.17d) and (3.17e) are also taken into account.

This approximation has been validated by sampling the steady-state time-domain solutions from MATLAB ode45: the harmonics which have been considered equal to zero in solving the truncated infinite system are verified in this way to be negligible compared to the other harmonic amplitudes.

The comparison between the steady-state computation methods explained in §3.3.2.1 and §3.3.2.2 is shown in §3.3.2.3. The engineering custom approximations have been considered good enough for the computation of the steady-states and have been used for the formulation of LTP systems in the following subsections.

3.3.2.2 Approximated Steady-State Point

Since x_5 and x_6 represent the internal dynamics of the computational delay, they can be considered "slow" compared to the other states. Corroboration for this assumption will be provided later, after performing nondimensionalisation of the system.

Grouping the last terms of (3.17f), a variable d is defined by

$$d(t) = V_{\text{ref}}^{-1}\Big\{v_g(t)[1 - k_{pi}\,k_{pv}(p_0\,x_1 + p_1\,x_2 + k_n\,V_{\text{ref}} - k_n\,x_8) - k_{pi}\,k_{iv}\,x_3] - k_{ii}\,x_4 + k_{pi}\,x_7\Big\}. \tag{3.33}$$

By comparing the equation of d and the scheme depicted in Figure 3.1, the mean-

ing of d can be identified with the controller action, but without considering its internal delays, described by the fifth and sixth ODEs of (3.17).

The fifth and sixth equations from (3.17), for the steady-state case, lead to the state-space system

$$\begin{bmatrix} \dot{\bar{x}}_5(t) \\ \dot{\bar{x}}_6(t) \end{bmatrix} = \boldsymbol{A}_\sigma \begin{bmatrix} \bar{x}_5(t) \\ \bar{x}_6(t) \end{bmatrix} + \boldsymbol{B}_\sigma \, \bar{d}(t) \, , \tag{3.34}$$

where

$$\boldsymbol{A}_\sigma = \begin{bmatrix} 0 & 1 \\ -\sigma_0 & -\sigma_1 \end{bmatrix} , \qquad \boldsymbol{B}_\sigma = \begin{bmatrix} 0 \\ 1 \end{bmatrix} . \tag{3.35}$$

Since (3.34) is linear, it can be solved in terms of the Laplace transforms of $\bar{x}_5(t)$, $\bar{x}_6(t)$ and $\bar{d}(t)$, denoted by $X_5(s)$, $X_6(s)$ and $D(s)$, respectively. The transfer function $\boldsymbol{H}_\sigma(s)$ between $[X_5(s) \;\; X_6(s)]^{\mathrm{T}}$ and $\bar{D}(s)$ can be computed by applying the Laplace transform to (3.34) and isolating $[X_5(s) \;\; X_6(s)]^{\mathrm{T}}$ in the LHS:

$$\begin{bmatrix} X_5(s) \\ X_6(s) \end{bmatrix} = \boldsymbol{H}_\sigma(s) \, D(s) = (s \, \boldsymbol{I} - \boldsymbol{A}_\sigma)^{-1} \boldsymbol{B}_\sigma \, D(s) \, , \tag{3.36}$$

where $s = \mathrm{j}\omega_g$ and $\boldsymbol{I}$ is an identity matrix of suitable dimensions.

An ad hoc approximation is now introduced for $\bar{d}(t)$ and equates it to the ratio of the input voltage to the reference value for the DC-link voltage:

$$\bar{d}(t) \sim \frac{v_g(t)}{V_{\mathrm{ref}}} . \tag{3.37}$$

This approximation leading to (3.37) can be intuitively justified by interpreting $d(t)$ as the controller action before considering the internal delays of the system. It can be considered valid only if $x_5(t)$ and $x_6(t)$ are slow if compared with the other variables implicitly contained in $d(t)$.

Therefore, substituting equation (3.12) for v_g and (3.37) into (3.36) and ap-

plying an inverse Laplace transform, $\bar{x}_5(t)$ and $\bar{x}_6(t)$ are found to be of the forms

$$\begin{aligned}
\bar{x}_5(t) &\sim |H_5(\mathrm{j}\,\omega_g)|\,\frac{V_g}{V_{ref}}\sin\left(\omega_g\,t \;+\; \underline{/H_5(\mathrm{j}\,\omega_g)}\right) \;=\; \Im\left(H_5(\mathrm{j}\,\omega_g)\,\frac{V_g}{V_{ref}}\mathrm{e}^{\mathrm{j}\,\omega_g\,t}\right)\,, \\
\bar{x}_6(t) &\sim |H_6(\mathrm{j}\,\omega_g)|\,\frac{V_g}{V_{ref}}\sin\left(\omega_g\,t \;+\; \underline{/H_6(\mathrm{j}\,\omega_g)}\right) \;=\; \Im\left(H_6(\mathrm{j}\,\omega_g)\,\frac{V_g}{V_{ref}}\mathrm{e}^{\mathrm{j}\,\omega_g\,t}\right)\,,
\end{aligned} \tag{3.38}$$

where $\underline{/H_i}$ denotes the phase of H_i, and the transfer function $\boldsymbol{H}_\sigma(s)$ has been split into

$$\boldsymbol{H}_\sigma(s) \;=\; \begin{bmatrix} H_5(s) \\ \\ H_6(s) \end{bmatrix}\,. \tag{3.39}$$

Due to the nonlinearity of the system, additional approximations are adopted for the computation of $\bar{x}_7$ and $\bar{x}_8$. In particular, $\bar{x}_7$ is approximated by a pure sinusoid with period equal to T_g and peak value I_g:

$$\bar{x}_7(t) \;\sim\; \bar{\imath}_g(t) \;=\; I_g\,\sin(\omega_g\,t)\,, \tag{3.40}$$

where I_g is unknown and needs to be estimated.

This choice is originated by the need for the grid current to be a sinusoid in phase with the grid voltage in order to maximise the efficiency of the system and to have a power factor equal to one. The power factor (PF) is defined as the ratio of the real power to the apparent power entering the system and its value should lie between -1 and 1. If the input voltage v_g is a sinusoid with period T_g, a unity PF can be demonstrated to be possible only by absorbing from the grid a current i_g that is sinusoidal, in phase with v_g and free from further harmonics, as shown below.

If, in an AC system of angular frequency ω_g, if voltage and current are given, respectively, by

$$v(t) = V\,\sin(\omega_g t + \theta_v), \tag{3.41a}$$

$$i(t) = I\,\sin(\omega_g t + \theta_i), \tag{3.41b}$$

then the average active power is equal to

$$P_{\text{ave}} = \frac{1}{2} V\, I\, \cos(\phi)\,, \tag{3.42}$$

where ϕ is the phase shift between current and voltage, defined as $\phi = \theta_v - \theta_i$. In this case, the PF is equal to $\cos(\phi)$.

Analogously, if harmonics of order greater then 1 are present, the average active power is given by

$$P_{\text{ave}} = \frac{1}{2} \sum_{k=1}^{+\infty} V_k\, I_k\, \cos(\phi_k)\,, \tag{3.43}$$

where V_k, I_k and ϕ_k are, respectively, the voltage amplitude, current amplitude and phase shift for the k-th order harmonic.

From (3.43), it follows that, if the voltage is constituted by a pure sinusoid, as assumed in (3.12) for the grid voltage, the current harmonics of order greater than 1 do not contribute in the active power computation. Moreover, to obtain a PF equal to 1, the current fundamental must be in phase with v_g, leading to (3.40). Therefore, the approximation on $\bar{x}_7$ implies neglecting its eventual phase shift and its harmonics of order greater than one. This assumption will be checked by simulating the system (3.17) and comparing the amplitudes of the steady-state fundamental of i_g with its higher-order harmonics.

In order to determine $\bar{x}_7(t)$ and $\bar{x}_8(t)$, the so-called power balance approach has been applied. This method, based on engineering approximations, originates from neglecting the converter internal losses and equating the input and the output power of the system. In the next few paragraphs, the power balance approach will be explained.

The input power of the system is defined as the product of the AC variables i_g and v_g. The output power is defined as the power flowing downstream of the switches, absorbed by the DC-link and the load resistor.

The input steady-state power $\bar{P}_{\text{in}}$ can be computed as the product of v_g and

$\bar{\imath}_g$, as given in (3.12) and (3.40):

$$\begin{aligned}\bar{P}_{\text{in}}(t) &= v_g(t)\,\bar{\imath}_g(t) \;=\; V_g\,I_g\sin^2(\omega_g\,t)\\ &= V_g\,I_g\left[\frac{1\;-\;\cos(2\,\omega_g\,t)}{2}\right] \;=\; \frac{V_g\,I_g}{2}\;-\;\frac{V_g\,I_g}{2}\cos(2\,\omega_g t)\,.\end{aligned} \tag{3.44}$$

The output steady-state power $\bar{P}_{out}$, instead, can be computed by applying Ohm's law on the DC-resistor and DC-link and is equal to

$$\begin{aligned}\bar{P}_{\text{out}}(t) &= \bar{x}_8(t)\left[C_{dc}\frac{\mathrm{d}\bar{x}_8(t)}{\mathrm{d}t}\;+\;\frac{\bar{x}_8(t)}{R_{dc}}\right]\\ &= \bar{x}_8(t)\left\{\Big[\gamma_0\,\bar{x}_5(t)\;+\;\gamma_1\,\bar{x}_6(t)\Big]\bar{x}_7(t)\;-\;\frac{\bar{x}_8(t)}{R_{dc}}\;+\;\frac{\bar{x}_8(t)}{R_{dc}}\right\}\\ &= \bar{x}_7(t)\,\bar{x}_8(t)\Big[\gamma_0\,\bar{x}_5(t)\;+\;\gamma_1\,\bar{x}_6(t)\Big]\,.\end{aligned} \tag{3.45}$$

Comparing (3.45) and (3.17g) leads to

$$\begin{aligned}\bar{P}_{\text{out}}(t) &= \bar{x}_7(t)\left[-L_g\frac{\mathrm{d}\bar{x}_7(t)}{\mathrm{d}t}\;+\;v_g(t)\;-\;R_g\,\bar{x}_7(t)\right]\\ &= v_g(t)\bar{x}_7(t)\;-\;L_g\,\bar{x}_7(t)\frac{\mathrm{d}\bar{x}_7(t)}{\mathrm{d}t}\;-\;R_g\,\bar{x}_7^2(t)\\ &= v_g(t)\bar{\imath}_g(t)\;-\;\frac{1}{2}L_g\frac{\mathrm{d}\bar{\imath}_g^2(t)}{\mathrm{d}t}\;-\;R_g\,\bar{\imath}_g^2(t)\,.\end{aligned} \tag{3.46}$$

Hence, in steady state, the difference between input and output power is given by

$$\bar{P}_{\text{in}}(t)\;-\;\bar{P}_{\text{out}}(t)\;=\;\frac{1}{2}L_g\frac{\mathrm{d}\bar{\imath}_g^2(t)}{\mathrm{d}t}\;+\;R_g\,\bar{\imath}_g^2(t)\,, \tag{3.47}$$

where

- $\frac{1}{2}L_g\frac{\mathrm{d}\bar{\imath}_g^2(t)}{\mathrm{d}t}$ is the power stored in the grid inductance L_g;
- $R_g\,\bar{\imath}_g^2(t)$ is the power dissipated on the grid resistance R_g.

The power balance approach ignores those fluctuations in the power to equate input and output power and to compute an approximation for the steady states.

Considering the RHS of (3.47) as negligible,

$$\bar{P}_{\text{in}}\;\sim\;\bar{P}_{\text{out}}. \tag{3.48}$$

Assuming the steady state of v_{dc} to be equal to its reference value plus a

ripple, and then averaging (3.48), leads to

$$\frac{V_g\, I_g}{2} \;\sim\; \frac{V_{\text{ref}}^2}{R_{dc}}\,. \tag{3.49}$$

In (3.49), I_g is the only unknown; isolating it leads to

$$I_g \;\sim\; \frac{2\, V_{\text{ref}}^2}{V_g\, R_{dc}}\,. \tag{3.50}$$

Then, the approximated steady-state equation of i_g is given by

$$\bar{x}_7(t) \;=\; \bar{\imath}_g(t) \;\sim\; \frac{2\, V_{\text{ref}}^2}{V_g\, R_{dc}}\, \sin(\omega_g t)\,. \tag{3.51}$$

The ripple on $\bar{P}_{\text{in}}$ is assumed to be equal to the power periodically absorbed and released by the DC-link capacitor, while the power flowing through L_g and R_g is neglected. Assuming also $\bar{v}_{dc} \sim V_{\text{ref}}$ leads to

$$\bar{P}_{\text{in, ripple}}(t) \;\sim\; V_{\text{ref}}\, C_{dc}\, \frac{\mathrm{d}\bar{v}_{dc}(t)}{\mathrm{d}t}\,. \tag{3.52}$$

Substitution of (3.50) in the non-constant part of (3.44) leads to

$$\bar{P}_{\text{in,ripple}}(t) \;=\; -\,\frac{V_{\text{ref}}^2}{R_{dc}}\, \cos(2\,\omega_g\, t)\,. \tag{3.53}$$

The derivative of $\bar{v}_{dc}$ with respect to time can be obtained by equating the RHS of (3.52) and (3.53) and is given by

$$\frac{\mathrm{d}\bar{v}_{dc}(t)}{\mathrm{d}t} \;=\; -\,\frac{V_{\text{ref}}}{C_{dc}\, R_{dc}}\, \cos(2\,\omega_g\, t)\,. \tag{3.54}$$

Integrating (3.54) with respect to time and assuming the constant component of $\bar{v}_{dc}(t)$ to be equal to V_{ref} leads to

$$\bar{x}_8(t) \;=\; \bar{v}_{dc}(t) \;=\; -\,\frac{V_{\text{ref}}}{2\,\omega_g\, C_{dc}\, R_{dc}}\, \sin(2\,\omega_g\, t) \;+\; V_{\text{ref}}\,. \tag{3.55}$$

Then, since also $\bar{x}_7(t)$ and $\bar{x}_8(t)$ are T_g-periodic, in the linearised system (3.22) all the coefficients are constant or T_g-periodic, (3.22) is an LTP system and each variable can be written as a Fourier series.

3.3.2.3 Comparison Between the two Approximations for the Steady-State

In Figure 3.3 are depicted the steady-state behaviours of i_g and v_{dc} in the time domain: solutions obtained by applying MATLAB ode45 to (3.17) and the approximated steady-state from the engineering custom are shown, while the errors are plotted in Figure 3.4. The error amplitudes are small if compared with the current amplitude and the voltage ripple amplitude (about 2% and 4%, respectively).

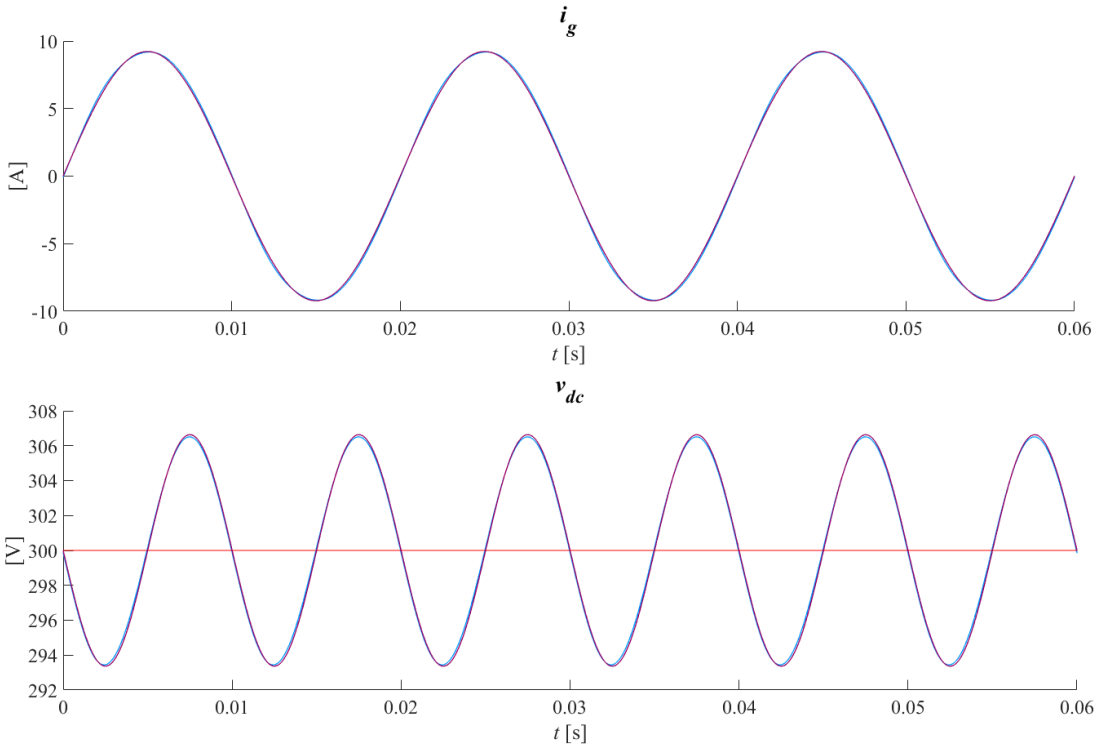

Figure 3.3: i_g and v_{dc} behaviour: comparison between time-domain solution (blue), the reference (red) and the steady-state solution obtained through engineering approximations

An harmonic analysis has been performed on the state variables of the system by solving it first in the time domain by applying MATLAB ode45 (the chosen time span has been assumed to be long enough to consider the transients finished at the end), then sampling each variable and finally applying the MATLAB fast Fourier transform fft to compute the Fourier coefficients. Simulations have been run for an integer number of grid periods and final state values have been

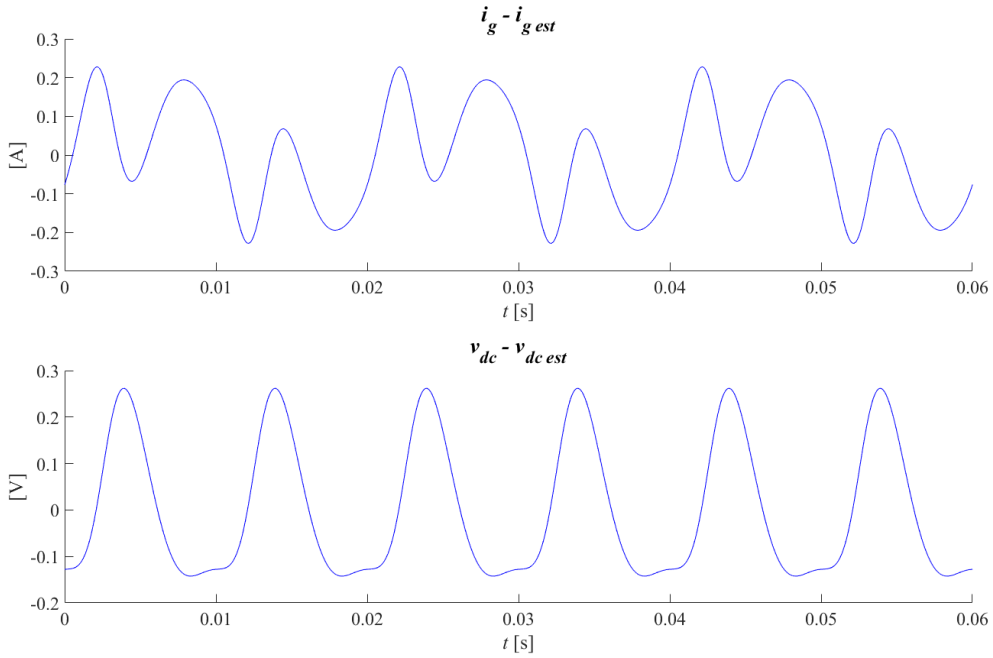

Figure 3.4: Errors between the time-domain steady-state solution of i_g and v_{dc} and the steady-states obtained through engineering approximations

compared with the initial ones: as the difference between initial and final value is negligible, the system can be considered to be in steady state and free from transients. Figure 3.5 shows the absolute values of the Fourier coefficients computed for i_g and v_{dc} and validate the assumption explained in §3.3.2.1 about their harmonic content: i_g shows only odd harmonics with a non-negligible absolute value, decaying geometrically with the harmonic order n; the voltage v_{dc}, on the contrary, shows just even harmonics decaying with n, while the odd harmonics are negligible.

The Fourier coefficients obtained by sampling the time-domain solutions have been compared with the corresponding coefficients computed as described in both §3.3.2.1 and §3.3.2.2. The comparative plot is depicted in Figure 3.6.

To validate the harmonic analysis performed by sampling and fft, i_g and v_{dc} have been reconstructed in time domain from their relative Fourier coefficients by adding first, third and fifth harmonic for the former and continuous component, second, fourth and sixth harmonic for the latter, as shown in Figure 3.7.

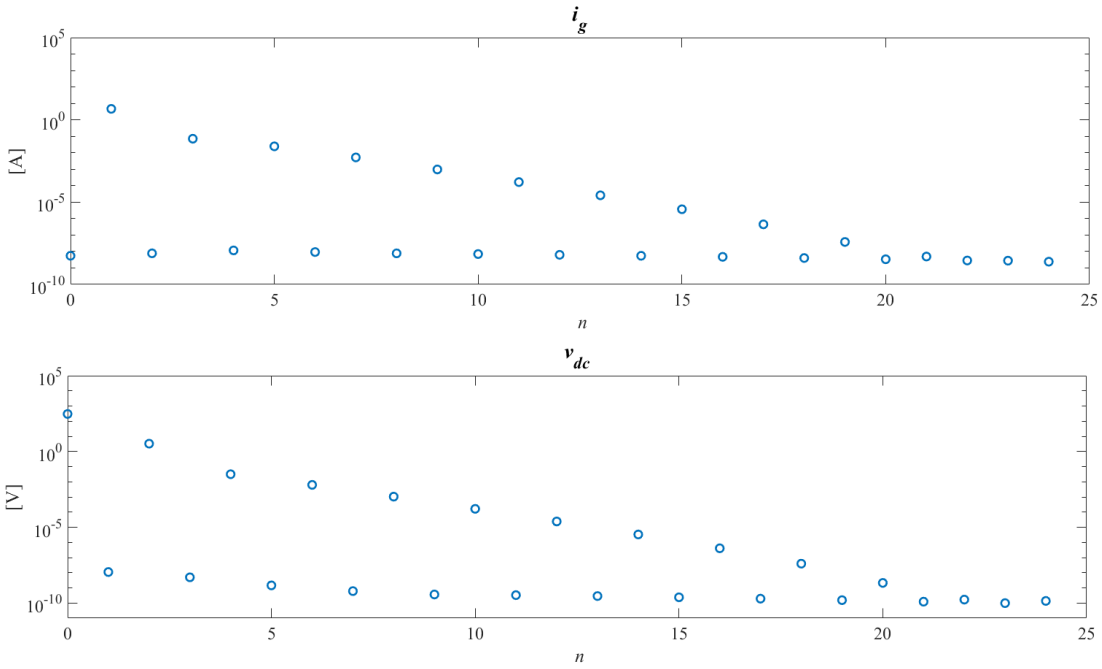

Figure 3.5: Semi-logarithmic plots of the absolute values of the Fourier coefficients computed for i_g and v_{dc} in SF-ETS

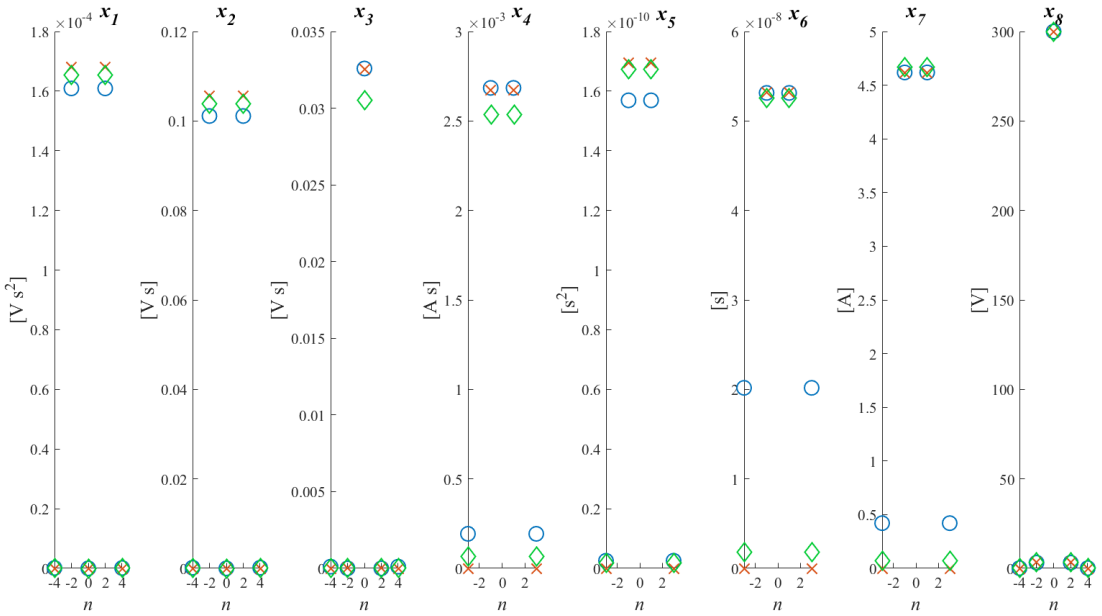

Figure 3.6: Fourier coefficients comparison of steady-state solutions - Absolute values: samples of time-domain simulations after the end of transients (green diamonds), non-approximated steady-state Fourier coefficients (blue circles), approximated solution (red crosses)

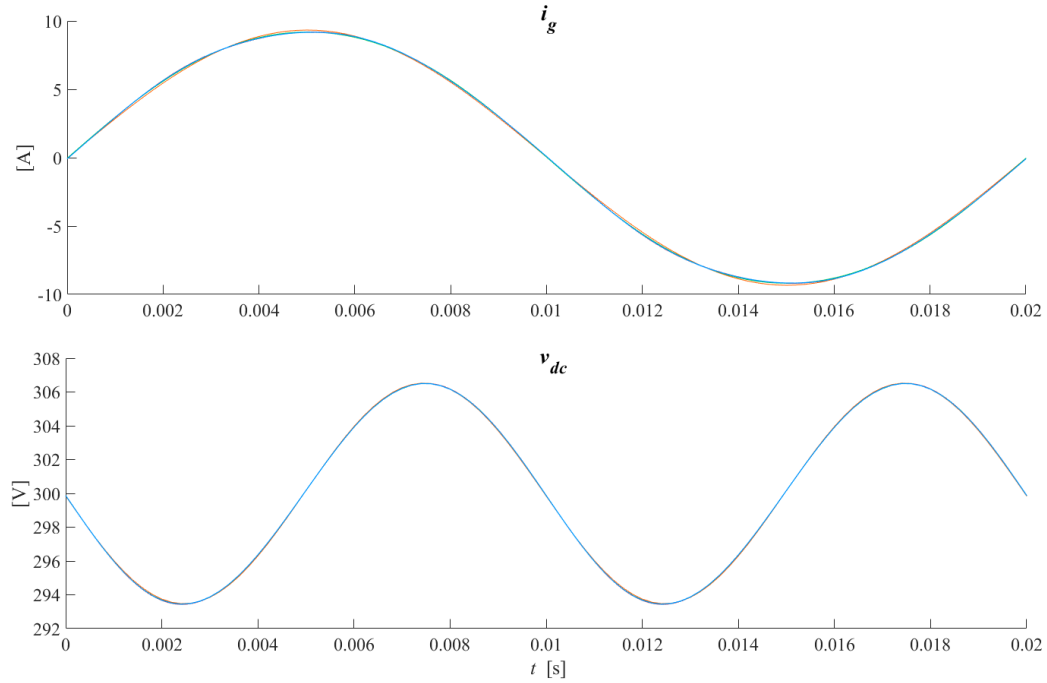

Figure 3.7: SP-AFE time-domain simulations and harmonic contributions comparison. For i_g (only odd harmonics): ode45 solution (red), $i_{g1}(t)$ (orange), $i_{g1}(t)+i_{g3}(t)$ (green), $i_{g1}(t)+i_{g3}(t)+i_{g5}(t)$ (blue); for v_{dc} (only even harmonics): ode45 solution (red), $v_{dc0}+v_{dc2}(t)$ (orange), $v_{dc0}+v_{dc2}(t)+v_{dc4}(t)$ (green), $v_{dc0}+v_{dc2}(t)+v_{dc4}(t)+v_{dc6}(t)$ (blue)

3.3.3 Nondimensionalisation and System Reduction

In this subsection, nondimensionalisation has been applied to the ODE system (3.17), in order to allow the clearer identification of small (dimensionless) parameters.

By evaluating the numerical values of the various dimensionless parameters for typical values of the system parameters, it is possible to identify likely candidates to be considered "small" dimensionless parameters.

While performing nondimensionalisation, V_g, R_{dc} and T_g have been chosen as base values for voltage, resistance and time, respectively. The nondimensional variables and parameters of the system are reported in the second column of Table 3.2. The nondimensionalised system is then

$$\dot{\hat{x}}_1 = \hat{x}_2 \tag{3.56a}$$

$$\dot{\hat{x}}_2 = -\hat{q}_0\,\hat{x}_1 - \hat{q}_1\,\hat{x}_2 + \hat{V}_{\text{ref}} - \hat{x}_8\,, \tag{3.56b}$$

$$\dot{\hat{x}}_3 = \hat{p}_0\,\hat{x}_1 + \hat{p}_1\,\hat{x}_2 + \hat{k}_n(\hat{V}_{\text{ref}} - \hat{x}_8)\,, \tag{3.56c}$$

$$\dot{\hat{x}}_4 = \hat{v}_g(\hat{t})[\hat{k}_{iv}\,\hat{x}_3 + \hat{k}_{pv}\,\hat{p}_0\,\hat{x}_1 + \hat{k}_{pv}\,\hat{p}_1\,\hat{x}_2 + \hat{k}_{pv}(\hat{V}_{\text{ref}} - \hat{x}_8)] - \hat{x}_7\,, \tag{3.56d}$$

$$\dot{\hat{x}}_5 = \hat{x}_6\,, \tag{3.56e}$$

$$\dot{\hat{x}}_6 = -\hat{\sigma}_0\,\hat{x}_5 - \hat{\sigma}_1\,\hat{x}_6 + \hat{d}(\hat{t})\,, \tag{3.56f}$$

$$\dot{\hat{x}}_7 = \hat{L}_g^{-1}(\hat{v}_g(\hat{t}) - \hat{R}_g\,\hat{x}_7 - \hat{\gamma}_0\,\hat{x}_5\,\hat{x}_8 - \hat{\gamma}_1\,\hat{x}_6\,\hat{x}_8)\,, \tag{3.56g}$$

$$\dot{\hat{x}}_8 = \hat{C}_{dc}^{-1}[(\hat{\gamma}_0\,\hat{x}_5 + \hat{\gamma}_1\,\hat{x}_6)\hat{x}_7 - \hat{R}_{dc}^{-1}\,\hat{x}_8]\,, \tag{3.56h}$$

where the nondimensional variable $\hat{d}(\hat{t})$ is defined by

$$\hat{d}(\hat{t}) = \hat{V}_{\text{ref}}^{-1}\Big\{\hat{v}_g(\hat{t})[1-\hat{k}_{pi}\hat{k}_{pv}(\hat{p}_0\hat{x}_1+\hat{p}_1\hat{x}_2+\hat{k}_n\hat{V}_{\text{ref}}-\hat{k}_n\hat{x}_8)-\hat{k}_{pi}\hat{k}_{iv}\hat{x}_3]-\hat{k}_{ii}\hat{x}_4+\hat{k}_{pi}\hat{x}_7\Big\}\,, \tag{3.57}$$

and the nondimensional expression of the grid voltage $\hat{v}_g(\hat{t})$ is given by

$$\hat{v}_g(\hat{t}) = \hat{V}_g\,\sin(\hat{\omega}_g\,\hat{t}) = \hat{V}_g\,\sin(2\,\pi\,f_g\,T_b\,t\,T_b^{-1}) = \hat{V}_g\,\sin(\omega_g\,t)\,. \tag{3.58}$$

A small parameter ϵ is now introduced, in order to assign to each dimensionless

State-Space Variables	$\hat{x}_1 = x_1(V_g T_g^2)^{-1}$ $\hat{x}_2 = x_2(V_g T_g)^{-1}$ $\hat{x}_3 = x_3(V_g T_g)^{-1}$ $\hat{x}_4 = x_4 R_{dc}(V_g T_g)^{-1}$ $\hat{x}_5 = x_5(T_g)^{-2}$ $\hat{x}_6 = x_6 T_g^{-1}$ $\hat{x}_7 = x_7 R_{dc} V_g^{-1}$ $\hat{x}_8 = x_8 V_g^{-1}$	
Grid Parameters	$\hat{L}_g = L_g(R_{dc} T_g)^{-1} = 3.6250 \cdot 10^{-4}$ $\hat{R}_{dc} = R_g R_{dc}^{-1} \approx 1.6667 \cdot 10^{-3}$ $\hat{V}_g = V_g V_g^{-1} = 1$ $\hat{f}_g = f_g T_g = 1$	$\mathcal{O}(1)$ or $\mathcal{O}(\epsilon)$ $\mathcal{O}(\epsilon)$ $\mathcal{O}(1)$ $\mathcal{O}(1)$
Load Parameters	$\hat{C}_{dc} = C_{dc} R_{dc} T_g^{-1} \approx 3.6000$ $\hat{R}_{dc} = R_{dc} R_{dc}^{-1} = 1$	$\mathcal{O}(1)$ $\mathcal{O}(1)$
PWM and Switch Parameters	$\hat{f}_{pwm} = f_{pwm} T_g = 200$ $\hat{f}_s = f_s T_g = 400$	$\mathcal{O}(1)$ $\mathcal{O}(1)$
Zero-Order Hold and Delay Parameters	$\hat{\gamma}_0 = \gamma_0 T_g^2 = 640000$ $\hat{\gamma}_1 = \gamma_1 T_g = -800$ $\hat{\sigma}_0 = \sigma_0 T_g^2 = 640000$ $\hat{\sigma}_1 = \sigma_1 T_g = 1600$	$\mathcal{O}(\epsilon^{-2})$ $\mathcal{O}(\epsilon^{-1})$ $\mathcal{O}(\epsilon^{-2})$ $\mathcal{O}(\epsilon^{-1})$
Notch Filter Parameters	$\hat{p}_0 = p_0 T_g^2 = 0$ $\hat{p}_1 = p_1 T_g \approx -0.6283$ $\hat{q}_0 = q_0 T_g^2 = 156$ $\hat{q}_1 = q_1 T_g \approx 0.6283$ $\hat{k}_n = k_n = 1$	$\mathcal{O}(1)$ $\mathcal{O}(1)$ $\mathcal{O}(1)$ or $\mathcal{O}(\epsilon^{-1})$ $\mathcal{O}(1)$ $\mathcal{O}(1)$
Voltage PI Parameters	$\hat{k}_{pv} = k_{pv} R_{dc} V_g \approx 154.3091$ $\hat{k}_{iv} = k_{iv} R_{dc} V_g T_g \approx 804.4166$	$\mathcal{O}(1)$ $\mathcal{O}(1)$
Current PI Parameters	$\hat{k}_{pi} = k_{pi} R_{dc}^{-1} \approx 4.2236 \cdot 10^{-2}$ $\hat{k}_{ii} = k_{ii} T_g R_{dc}^{-1} \approx 0.2132$	$\mathcal{O}(1)$ $\mathcal{O}(1)$
Reference	$\hat{V}_{\text{ref}} = V_{\text{ref}} V_g^{-1} \approx 1.8466$	$\mathcal{O}(1)$

Table 3.2: Nondimensionalised system variables and parameters

group a "size" (i.e. assign some power α to each, so that it is $\mathcal{O}(\epsilon^\alpha)$). This assignment is somewhat arbitrary and subjective. In the present case, significant progress in this regard can be made by supposing ϵ to be of order 10^{-3}, which is typical of values found in detailed calculation later. The orders of the system parameters have been assigned based on this choice and are listed in the third column of Table 3.2. Some variables have a clear suggestion for their associated "size" (e.g. $\hat{\gamma}_0$, $\hat{\sigma}_0$, $\hat{\sigma}_1$), while others require a greater degree of judgement.
In particular, $\hat{k}_{iv}$ is considered to be of order 1, despite being closer to ϵ^{-1}, because its value can vary depending on the selected control bandwidth[2]. Even though in this example $\hat{p}_0 = 0$, in order to retain flexibility, $\hat{p}_0$ is assigned the size $\hat{p}_0 = \mathcal{O}(1)$. About the order of $\hat{L}_g$ and $\hat{q}_0$, two options have been considered for each, leading to different possible approximations of the system.

To clarify the size of the various dimensionless groups, some $\mathcal{O}(1)$ parameters are now introduced by factoring out the assumed ϵ-dependence of the "raw" hatted dimensionless parameters. Hence, $\bar{\sigma}_0$, $\bar{\sigma}_1$, $\bar{\gamma}_0$, $\bar{\gamma}_1$, $\bar{R}_g$, $\bar{L}_g$ and $\bar{q}_0$ are defined by:

$$\begin{aligned} \bar{\sigma}_0 &= \hat{\sigma}_0\,\epsilon^2\,, \\ \bar{\sigma}_1 &= \hat{\sigma}_1\,\epsilon\,, \\ \bar{\gamma}_0 &= \hat{\gamma}_0\,\epsilon^2\,, \\ \bar{\gamma}_1 &= \hat{\gamma}_1\,\epsilon\,, \\ \bar{R}_g &= \hat{R}_g\,\epsilon^{-1}\,, \\ \bar{L}_g &= \hat{L}_g\,\beta\,, \\ \bar{q}_0 &= \hat{q}_0\,\alpha^{-1}\,, \end{aligned} \tag{3.59}$$

where

$$\begin{aligned} \alpha = 1 \quad \text{or} \quad \alpha = \epsilon^{-1}, \\ \beta = 1 \quad \text{or} \quad \beta = \epsilon^{-1}\,. \end{aligned} \tag{3.60}$$

Then, substitution of (3.59) into (3.56) leads to

$$\dot{\hat{x}}_1 = \hat{x}_2 \tag{3.61a}$$

[2]See Appendix .1

$$\dot{\hat{x}}_2 = -\alpha\,\bar{q}_0\,\hat{x}_1 - \hat{q}_1\,\hat{x}_2 + \hat{V}_{\text{ref}} - \hat{x}_8\,, \tag{3.61b}$$

$$\dot{\hat{x}}_3 = \hat{p}_0\,\hat{x}_1 + \hat{p}_1\,\hat{x}_2 + \hat{k}_n(\hat{V}_{\text{ref}} - \hat{x}_8)\,, \tag{3.61c}$$

$$\dot{\hat{x}}_4 = \hat{v}_g(\hat{t})[\hat{k}_{iv}\,\hat{x}_3 + \hat{k}_{pv}\,\hat{p}_0\,\hat{x}_1 + \hat{k}_{pv}\,\hat{p}_1\,\hat{x}_2 + \hat{k}_{pv}(\hat{V}_{\text{ref}} - \hat{x}_8)] - \hat{x}_7\,, \tag{3.61d}$$

$$\dot{\hat{x}}_5 = \hat{x}_6\,, \tag{3.61e}$$

$$\dot{\hat{x}}_6 = -\epsilon^{-2}\,\bar{\sigma}_0\,\hat{x}_5 - \epsilon^{-1}\,\bar{\sigma}_1\,\hat{x}_6 + \hat{d}(\hat{t})\,, \tag{3.61f}$$

$$\dot{\hat{x}}_7 = \beta\,\bar{L}_g^{-1}(\hat{v}_g(\hat{t}) - \epsilon\,\bar{R}_g\,\hat{x}_7 - \epsilon^{-2}\,\bar{\gamma}_0\,\hat{x}_5\,\hat{x}_8 - \epsilon^{-1}\,\bar{\gamma}_1\,\hat{x}_6\,\hat{x}_8)\,, \tag{3.61g}$$

$$\dot{\hat{x}}_8 = \hat{C}_{dc}^{-1}[(\epsilon^{-2}\,\bar{\gamma}_0\,\hat{x}_5 + \epsilon^{-1}\,\bar{\gamma}_1\,\hat{x}_6)\hat{x}_7 - \hat{R}_{dc}^{-1}\,\hat{x}_8]\,, \tag{3.61h}$$

where $\hat{d}$ has been defined in (3.57).

Now, the equations (3.61) are considered for model reduction. Different cases have been taken into account according to the different "sizes" which can be attributed to $\hat{L}_g$ and $\hat{q}_0$.

Since (3.61e) and (3.61f) are the only ODEs of the system which do not depend on α or β, they will be considered first. After that, (3.61g) and (3.61h) will follow, as they depend on the value of β and contain only the state variables $\hat{x}_5$, $\hat{x}_6$, $\hat{x}_7$ and $\hat{x}_8$. Then, (3.61a) and (3.61b), according to the selected value of α, will be taken into account. Last, (3.61c) and (3.61d) will be considered, since they depend both on α and on the expressions for $\hat{x}_1$ and $\hat{x}_2$ following from the reduction of (3.61a) and (3.61b).

EQUATIONS FOR x_5 AND x_6

Since $d(t)$ has the physical meaning of a controller action neglecting the internal delays of the system, $\hat{d}(t)$ is assumed to be $\mathcal{O}(1)$, along with its steady-state $\bar{d}(t)$. Thus, to avoid imbalance in (3.61f),

$$\hat{x}_5 = \mathcal{O}(\epsilon^2)\,. \tag{3.62}$$

Therefore, $\hat{x}_5$ can be expressed as

$$\hat{x}_5 = \epsilon^2\,\hat{x}_{52} + \mathcal{O}(\epsilon^3) \tag{3.63}$$

and, correspondingly,

$$\hat{x}_6 \;=\; \epsilon^2\,\hat{x}_{62} \;+\; \mathcal{O}(\epsilon^3). \tag{3.64}$$

Then, the governing equations from (3.61e) and (3.61f) are, respectively,

$$\hat{x}_{62} = \;\dot{\hat{x}}_{52}\;, \tag{3.65a}$$

$$\hat{x}_{52} = \;\frac{\hat{d}}{\bar{\sigma}_0}\;. \tag{3.65b}$$

With the chosen value for ϵ, the system size can therefore be reduced by two degrees of freedom irrespective of the values of α and β.

EQUATIONS FOR x_7 AND x_8

The leading order of the eighth ODE, irrespective of the orders of α and β, is

$$\dot{\hat{x}}_8 \;=\; C_{dc}^{-1}\left(\bar{\gamma}_0\,\hat{x}_{52}(\hat{t})\,\hat{x}_7 \;-\; \hat{R}_{dc}^{-1}\hat{x}_8\right) \;+\; \mathcal{O}(\epsilon). \tag{3.66}$$

At leading order, the seventh equation is

$$\dot{\hat{x}}_7 \;=\; \beta\,\bar{L}_g^{-1}\left(\hat{v}_g(\hat{t}) \;-\; \bar{\gamma}_0\,\hat{x}_{52}(\hat{t})\,\hat{x}_8\right) \;+\; \mathcal{O}(\epsilon), \tag{3.67}$$

which for $\beta = 1$ leads to the ODE

$$\dot{\hat{x}}_7 \;=\; \bar{L}_g^{-1}\left(\hat{v}_g(\hat{t}) \;-\; \bar{\gamma}_0\,\hat{x}_{52}(\hat{t})\,\hat{x}_8\right) \;=\; \hat{L}_g^{-1}\left(\hat{v}_g(\hat{t}) \;-\; \bar{\gamma}_0\,\hat{x}_{52}(\hat{t})\,\hat{x}_8\right) \;+\; \mathcal{O}(\epsilon), \tag{3.68}$$

while for $\beta = \epsilon^{-1}$ it leads to the algebraic equation

$$0 \;=\; \hat{v}_g(\hat{t}) \;-\; \bar{\gamma}_0\,\hat{x}_{52}(\hat{t})\,\hat{x}_8 \;+\; \mathcal{O}(\epsilon)\;. \tag{3.69}$$

Therefore, if $\hat{L}_g$ is considered of $\mathcal{O}(\epsilon)$, the system can be reduced by one further degree of freedom.

EQUATIONS FOR x_1 AND x_2

In the case $\alpha = 1$, no reduction is possible of the first two ODEs of the system,

leading to

$$\begin{aligned} \dot{\hat{x}}_1 &= \hat{x}_2\,, \\ \dot{\hat{x}}_2 &= -\bar{q}_0\,\hat{x}_1 - \hat{q}_1\,\hat{x}_2 + \hat{V}_{ref} - \hat{x}_8\,. \end{aligned} \tag{3.70}$$

If, instead, $\alpha = \epsilon^{-1}$, the second equation becomes

$$\dot{\hat{x}}_2 = \epsilon^{-1}\,\bar{q}_0\,\hat{x}_1 - \hat{q}_1\,\hat{x}_2 + \hat{V}_{\text{ref}} - \hat{x}_8\,. \tag{3.71}$$

To avoid imbalance,

$$\hat{x}_1 = \mathcal{O}(\epsilon)\,, \tag{3.72}$$

and $\hat{x}_1$ can be expressed as

$$\hat{x}_1 = \epsilon\,\hat{x}_{11} + \mathcal{O}(\epsilon^2) + \dots\,, \tag{3.73}$$

where $\hat{x}_{11} = \mathcal{O}(1)$. Substituting (3.73) into (3.61a) leads to

$$\epsilon\,\dot{\hat{x}}_{11} = \hat{x}_2 + \mathcal{O}(\epsilon^2)\,. \tag{3.74}$$

Therefore, $\hat{x}_2$ must be $\mathcal{O}(\epsilon)$ and can be analogously written as

$$\hat{x}_2 = \epsilon\,\hat{x}_{21} + \mathcal{O}(\epsilon^2) + \dots\,. \tag{3.75}$$

Thus, substituting (3.73) and (3.75) into (3.71) and selecting the leading order terms leads to

$$\bar{x}_1 = \frac{\hat{V}_{\text{ref}} - \hat{x}_8}{\bar{q}_0}\,. \tag{3.76}$$

From (3.61a),

$$\bar{x}_2 = \dot{\bar{x}}_1 = -\frac{\dot{\hat{x}}_8}{\bar{q}_0} = -\frac{1}{C_{dc}\,\bar{q}_0}\left[\bar{\gamma}_0\,\hat{x}_{52}\left(\hat{t}\right)\hat{x}_7 - \hat{x}_8\right]\,. \tag{3.77}$$

In this case, both ODEs are turned into algebraic equations. Moreover, since $\hat{x}_1$ and $\hat{x}_2$ are of $\mathcal{O}(\epsilon)$, they are not present in the leading order expression for $\hat{d}$, which is simplified as

$$\hat{d}(\hat{t}) = \hat{V}_{ref}^{-1}\Big[\hat{v}_g\left(\hat{t}\right) - \hat{k}_{pi}\hat{k}_{iv}\hat{v}_g\left(\hat{t}\right)\hat{x}_3 \\ -\hat{k}_{ii}\hat{x}_4 + \hat{k}_{pi}\hat{x}_7 - \hat{k}_n\hat{k}_{pi}\hat{k}_{pv}\hat{v}_g\left(\hat{t}\right)\left(\hat{V}_{ref} - \hat{x}_8\right)\Big] + \mathcal{O}(\epsilon). \tag{3.78a}$$

EQUATIONS FOR x_3 AND x_4

Following from (3.70), if $\alpha = 1$, (3.61c) and (3.61d) become

$$\dot{\hat{x}}_3 = \hat{p}_0\,\hat{x}_1 \;+\; \hat{p}_1\,\hat{x}_2 \;+\; \hat{k}_n\left(\hat{V}_{\text{ref}} \;-\; \hat{x}_8\right), \tag{3.79a}$$

$$\dot{\hat{x}}_4 = \hat{k}_{pv}\,\hat{v}_g\left(\hat{t}\right)\left[\hat{p}_0\,\hat{x}_1 \;+\; \hat{p}_1\hat{x}_2 \;+\; \hat{k}_n\left(\hat{V}_{\text{ref}} \;-\; \hat{x}_8\right)\right] \;+\; \hat{k}_{iv}\,\hat{v}_g\left(\hat{t}\right)\hat{x}_3 \;-\; \hat{x}_7\,. \tag{3.79b}$$

For $\alpha = \epsilon^{-1}$, $\hat{x}_1$ and $\hat{x}_2$ are $\mathcal{O}(\epsilon)$, leading to

$$\dot{\hat{x}}_3 = \hat{k}_n\left(\hat{V}_{\text{ref}} \;-\; \hat{x}_8\right) \;+\; \mathcal{O}(\epsilon)\,, \tag{3.80a}$$

$$\dot{\hat{x}}_4 = \hat{v}_g\left(\hat{t}\right)\left[\hat{k}_{iv}\,\hat{x}_3 \;+\; \hat{k}_{pv}\left(\hat{V}_{\text{ref}} \;-\; \hat{x}_8\right)\right] \;-\; \hat{x}_7 \;+\; \mathcal{O}(\epsilon)\,. \tag{3.80b}$$

Reduction Summary

The reduced system size varies according to the different combinations of choices for α and β values. A summary of the possible cases is displayed in Table 3.3 and their respective agreement with the full system behaviour is shown in the next subsections.

	$\alpha = 1$	$\alpha = \epsilon^{-1}$
$\beta = 1$	6	4
$\beta = \epsilon^{-1}$	5	3

Table 3.3: Number of system ODEs depending on the chosen values of α and β

From a physical point of view, in the 6-equations-reduced model, the ODEs describing the behaviour of the internal delays and ZOH are not present (despite their contribution being represented by the algebraic term $\hat{x}_{52}(t)$). This reduction

is included in all four of the possibilities shown in Table 3.3.
Making the assumption that $\alpha = \epsilon^{-1}$ leads to neglect of the first two ODEs of the full system, corresponding to the dynamics of the notch filter. When $\beta = \epsilon^{-1}$, one equation modelling the control on the grid current i_g is not included in the reduced system.

3.3.3.1 6-Equation Reduced Model

In the case $\alpha = \beta = 1$, then both $\hat{L}_g$ and $\hat{q}_0$ are of $\mathcal{O}(1)$. Let now the hats drop from the notation. Therefore, substituting (3.63) and (3.64) into the system (3.61), selecting the leading order terms and neglecting the terms of $\mathcal{O}(\epsilon)$ and $\mathcal{O}(\epsilon^2)$ leads to

$$\dot{x}_1 = x_2 \,, \tag{3.81a}$$

$$\dot{x}_2 = -q_0\, x_1 - q_1\, x_2 + V_{\text{ref}} - x_8 \,, \tag{3.81b}$$

$$\dot{x}_3 = p_0\, x_1 + p_1\, x_2 + k_n(V_{\text{ref}} - x_8) \,, \tag{3.81c}$$

$$\begin{aligned}\dot{x}_4 = {} & k_{iv}\, v_g(t)\, x_3 + k_{pv}\, p_0\, v_g(t)\, x_1 + k_{pv}\, p_1\, v_g(t)\, x_2 \\ & + k_{pv}\, k_n(V_{\text{ref}} - x_8) v_g(t) - x_7 \,,\end{aligned} \tag{3.81d}$$

$$\dot{x}_7 = L_g^{-1}\left[v_g(t) - \bar{\gamma}_0\, x_{52}(t)\, x_8\right] \,, \tag{3.81e}$$

$$\dot{x}_8 = C_{dc}^{-1}\left[\bar{\gamma}_0\, x_{52}(t)\, x_7 - R_{dc}^{-1}\, x_8\right] \,, \tag{3.81f}$$

where

$$x_{52}(t) = \frac{d(t)}{\bar{\sigma}_0} \,, \tag{3.82a}$$

$$\begin{aligned}d(t) = {} & V_{\text{ref}}^{-1}\Big\{v_g(t)[1 - k_{pi}k_{pv}(p_0x_1 + p_1x_2 + k_nV_{\text{ref}} - k_nx_8) - k_{pi}k_{iv}x_3] \\ & - k_{ii}x_4 + k_{pi}x_7\Big\}.\end{aligned} \tag{3.82b}$$

Following this procedure, two out of the eight ODEs from (3.17) are neglected

and two algebraic equations are added. In (3.82), the variable $\hat{x}_{62}(t)$, representing the governing equation of x_6, is not included. If needed, it can be found from (3.65a) and computed as a function of x_{52}.

To assess the validity of the reduction, solutions of the system (3.81) have been compared to solutions of the full system (3.17) in both time domain and Fourier coefficients. First, (3.81) has been solved by MATLAB ode45 and those results have been compared with the corresponding time-domain solution of the full system. This comparison is plotted in Figure 3.8., while the error between full and reduced time-domain solutions is shown in Figure 3.9: the error amplitude on i_g is the 1.29% of the current amplitude, while the error amplitude on v_{dc} is equal to the 0.01% of the reference value for v_{dc} and the 0.47% of its ripple. The relative error on v_{dc} is much smaller than that on i_g due to the nature of their steady-state behaviours: i_g is a sinusoid, while v_dc is the sum of a constant of the order of 100 V and a sinusoidal ripple. The error amplitude on the voltage, then, is more significant compared to the amplitude of the voltage ripple.

After this, the reduced time-domain solution has been sampled and analysed by MATLAB fft, analogously to the procedure applied to compute the full solution Fourier coefficients. A comparison between full and reduced model Fourier coefficients is depicted in Figure 3.10.

In both time domain simulations and Fourier coefficients, a good agreement is observable between the behaviour of the full and the reduced model.

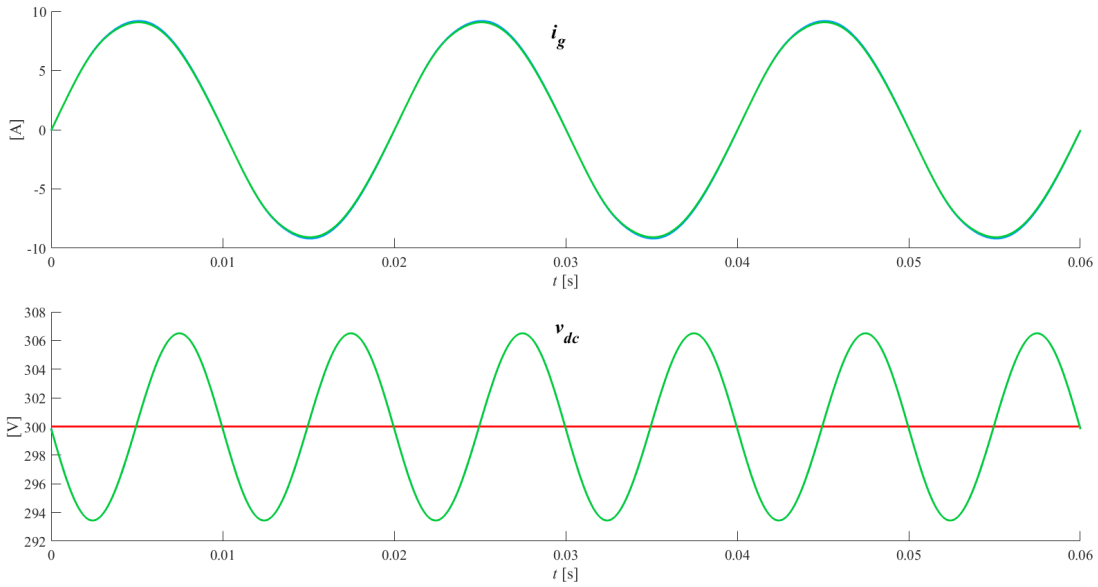

Figure 3.8: Comparison in time-domain between exact solution (blue) and reduced solution (green)

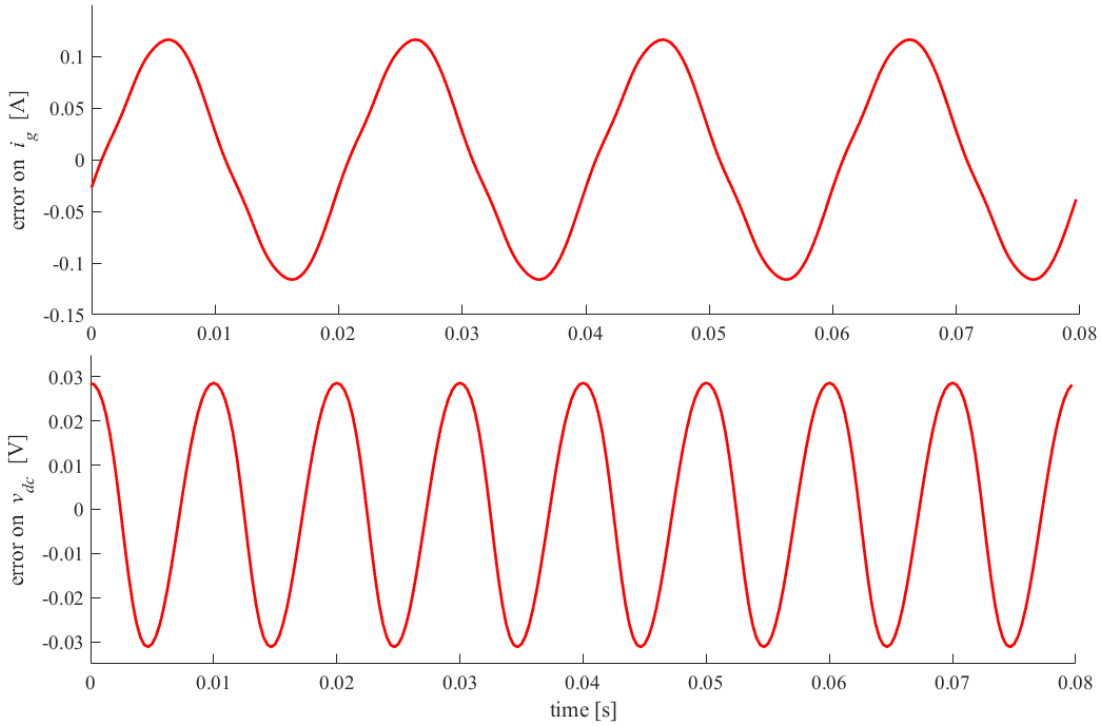

Figure 3.9: Errors between the full system time domain simulations and the 6-equation model

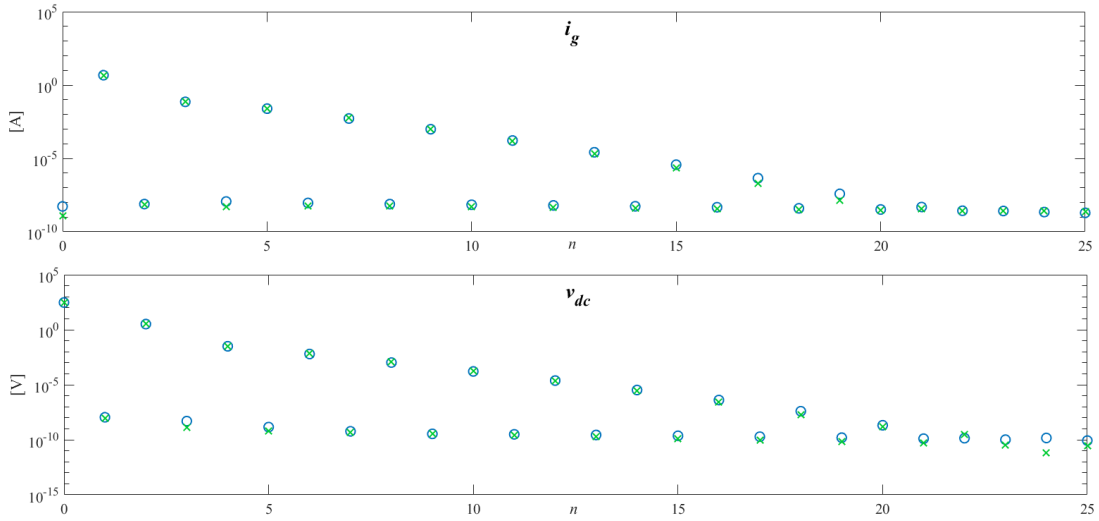

Figure 3.10: Absolute values of the Fourier coefficients computed for i_g and v_{dc}: exact solution (blue circles) and reduced solution (green crosses)

3.3.3.2 Approximated Steady-State Calculation for the Reduced Model

To obtain the steady state of the 6-equation reduced model, engineering approximations have been applied to the system, analogously to §3.3.2.2.

Since, in §3.3.2.3, (3.40) and (3.55) have been shown to be good approximations of the steady state of i_g and v_{dc}, respectively, the same expressions have been considered for the corresponding 6-equation steady states. (3.81e) and (3.81f), indeed, describe the behaviour of the grid current and DC-link voltage, respectively; if the reduced model approximates the full one well enough, there will not be big discrepancies between corresponding steady-states.

As x_5 and x_6 do not appear in the reduced model (3.81), their steady states do not need to be computed.

The steady states for the first four variables, instead, can be found by writing each as a (truncated) Fourier series and equating coefficients of the Fourier components $e^{jn\omega_g t}$.

3.3.3.3 5-Equation Reduced Model

To reduce the system by a further equation, $\alpha = 1$, while $\beta = \epsilon^{-1}$. Then, $\hat{L}_g$ is of $\mathcal{O}(\epsilon)$ and $\hat{q}_0$ of $\mathcal{O}(1)$. Let the hats drop from the notation. Proceeding analogously to §3.3.3.1 (i.e. substituting leading-order terms and neglecting $\mathcal{O}(\epsilon)$ terms or smaller) leads to

$$\dot{x}_1 = x_2 \,, \tag{3.83a}$$

$$\dot{x}_2 = -q_0\, x_1 - q_1\, x_2 + V_{\text{ref}} - x_8 \,, \tag{3.83b}$$

$$\dot{x}_3 = p_0\, x_1 + p_1\, x_2 + k_n(V_{\text{ref}} - x_8) \,, \tag{3.83c}$$

$$\begin{aligned}\dot{x}_4 = {} & k_{iv}\, v_g(t)\, x_3 + k_{pv}\, p_0\, v_g(t)\, x_1 + k_{pv}\, p_1\, v_g(t)\, x_2 \\ & + k_{pv}\, k_n(V_{\text{ref}} - x_8) v_g(t) - x_7(t) \,,\end{aligned} \tag{3.83d}$$

$$\dot{x}_8 = C_{dc}^{-1}\left[\bar{\gamma}_0\, x_{52}(t)\, x_7(t) - R_{dc}^{-1}\, x_8\right] , \tag{3.83e}$$

where

$$\begin{aligned}x_7(t) = {} & k_{pi}^{-1}\left\{ v_g(t)\left[\frac{V_{\text{ref}}\bar{\sigma}_0}{x_8\bar{\gamma}_0} - 1 + k_{pi}k_{pv}\left(p_0x_1 + p_1x_2 + k_nV_{\text{ref}} - k_nx_8\right)\right.\right. \\ & \left.\left. + k_{pi}k_{iv}x_3\right] + k_{ii}x_4\right\} ,\end{aligned} \tag{3.84a}$$

$$d(t) = \frac{\bar{\sigma}_0\, v_g(t)}{\bar{\gamma}_0\, x_8} \,, \tag{3.84b}$$

$$x_{52}(t) = \frac{d(t)}{\bar{\sigma}_0}. \tag{3.84c}$$

Proceeding in this way, three degrees of freedom from (3.17) have been eliminated.

Time domain simulations have been run to validate the reduced system, as plotted in Figure 3.11. The differences between the full system and the 5-equation reduced model in time domain, computed for i_g and v_{dc}, are plotted in Figure 3.12.

The 5-equation model seems to agree well with the full model voltage, but the approximation for the current displayed in (3.84) has a different shape and shows a greater contribution of the third harmonic. In particular, the error amplitude

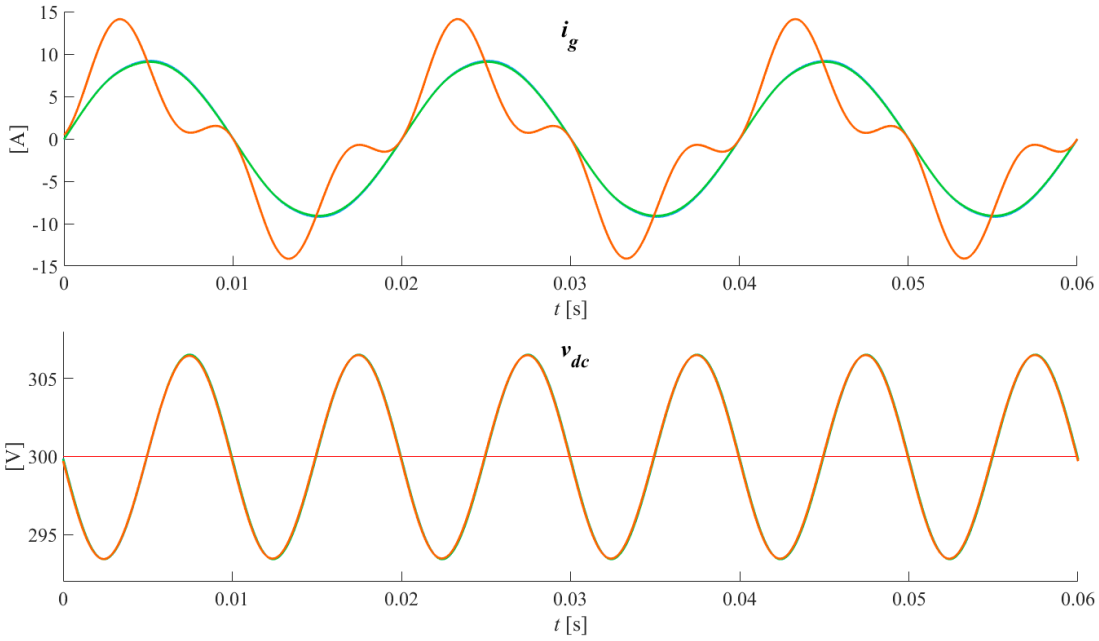

Figure 3.11: Comparison in time-domain between exact solution (blue), 6-equations reduced solution (green) and 5 equations reduced solution (orange)

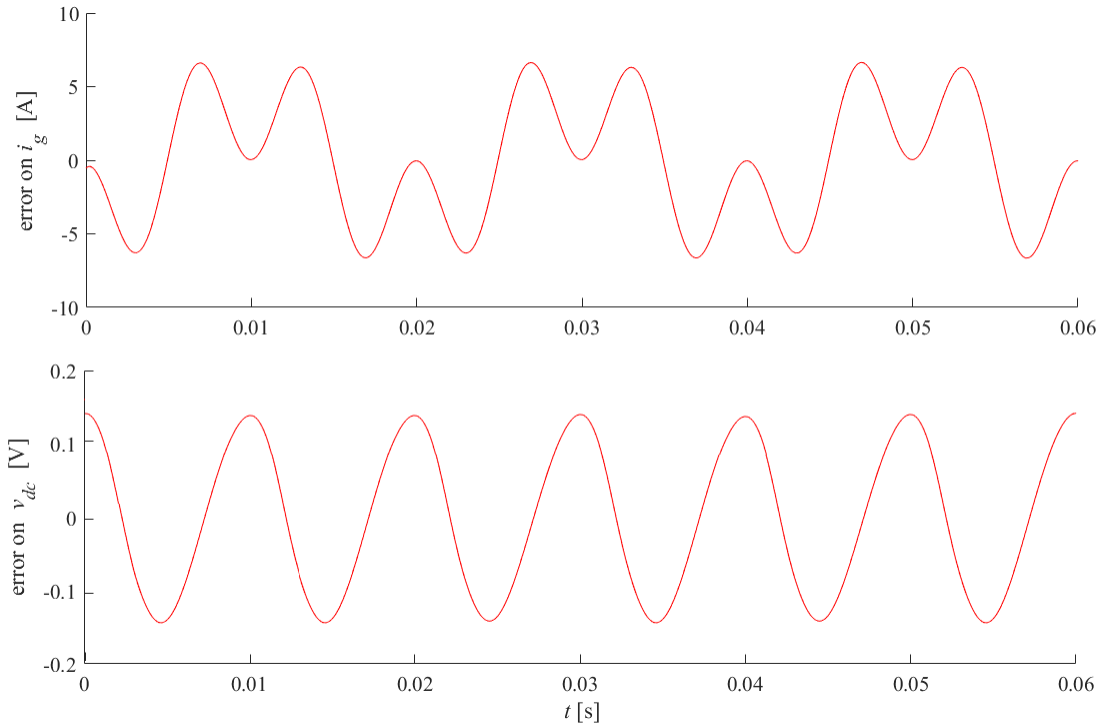

Figure 3.12: Error between the time-domain solutions computed for i_g and v_{dc}: full system simulations - 5-equations-reduced model

for i_g is of the same order as its amplitude, while the error amplitude for the voltage is equal to about the 2% of the ripple amplitude on v_{dc}.

This may be caused by the absence of the seventh ODE of the full system (3.17) from the 5-equation reduced system. In this model, as shown in (3.84a),

the value of x_7, corresponding to the current i_g, is not computed by solving an ODE, but algebraically.

The system (3.83) is characterised by a high influence of nonlinearities: equation (3.83e), modelling the behaviour of the DC-link voltage, contains the product of $d(t)$ and $x_7(t)$, both computed algebraically from the state variable values. Thus, in this case, the computation of its corresponding linearised system and LTP stability analysis would be challenging (in particular in writing the LTP system matrices). Therefore, the 5-equation reduced system analysis will be performed only by observing the system behaviour in time domain for different values of the controller parameters, as explained in §3.3.4. This makes the computation of the steady-state expressions not necessary.

3.3.3.4 4-Equation Reduced Model

Here, α has been considered equal to ϵ^{-1}, while β to 1. Then, $\hat{L}_g$ is of $\mathcal{O}(1)$ and $\hat{q}_0$ of $\mathcal{O}(\epsilon^{-1})$. Therefore, selecting the leading order terms and neglecting the terms of $\mathcal{O}(\epsilon)$ and $\mathcal{O}(\epsilon^2)$ lead to

$$\dot{x}_3 = k_n(V_{\text{ref}} - x_8) \,, \tag{3.85a}$$

$$\dot{x}_4 = k_{iv}\, v_g(t)\, x_3 + k_{pv}\, k_n(V_{\text{ref}} - x_8) v_g(t) - x_7(t) \,, \tag{3.85b}$$

$$\dot{x}_7 = L_g^{-1} \left[v_g(t) - \bar{\gamma}_0\, x_{52}(t) x_8 \right] \,, \tag{3.85c}$$

$$\dot{x}_8 = C_{dc}^{-1} \left[\bar{\gamma}_0\, x_{52}(t)\, x_7(t) - R_{dc}^{-1}\, x_8 \right] \,, \tag{3.85d}$$

where

$$\begin{aligned} d(t) = V_{\text{ref}}^{-1} \left[v_g\,(t) - k_{pi} k_{iv} v_g\,(t)\, x_3 - k_{ii} x_4 \right. \\ \left. + k_{pi} x_7 - k_n k_{pi} k_{pv} v_g\,(t)\,(V_{\text{ref}} - x_8) \right] \,, \end{aligned} \tag{3.86a}$$

and

$$x_{52}(t) = \frac{d(t)}{\bar{\sigma}_0} \,. \tag{3.87}$$

Therefore, four degrees of freedom of the full system have been eliminated.

Figure 3.13 shows a time-domain simulation of the system. In this case, both i_g and v_{dc} show distortions. The first two ODEs of (3.17), here neglected, represent the action of the notch filter on the system. Removing the filter from the system behaviour leads to significant errors in the solutions. The error between the 4-equation reduced model and the full system in time domain is depicted in Figure 3.14. In this case, the error amplitude on i_g is close to the current amplitude, while the error amplitude on v_{dc} is of the same order of the ripple on v_{dc}.

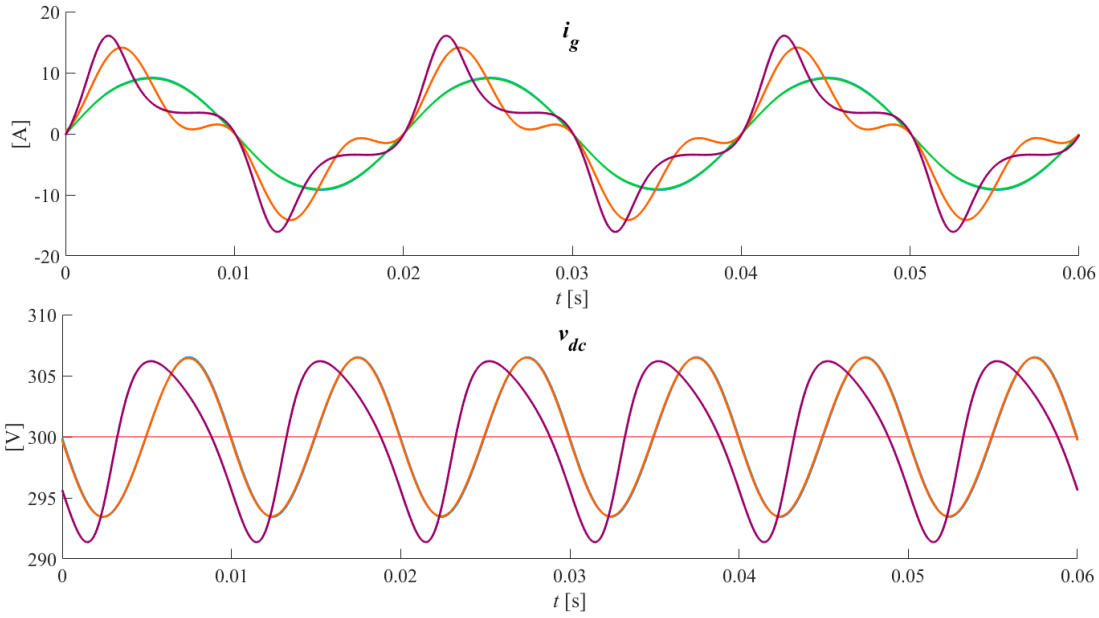

Figure 3.13: Comparison in time-domain between exact solution (blue), 6-equation reduced solution (green), 5-equation reduced solution (orange) and 4-equation reduced solution (purple)

The 4-equation time domain solutions computed by ode45 have then been sampled and analysed by fft, as previously performed on the full system and on the 6-equation reduced model, in order to obtain the Fourier coefficients of the steady-state solution. As depicted in Figure 3.15, some discrepancies can be observed between the Fourier coefficients of the full model and the corresponding coefficients of the 4-equation reduced model.

Therefore, this reduction cannot be considered to be a good approximation of the behaviour of the system in time domain.

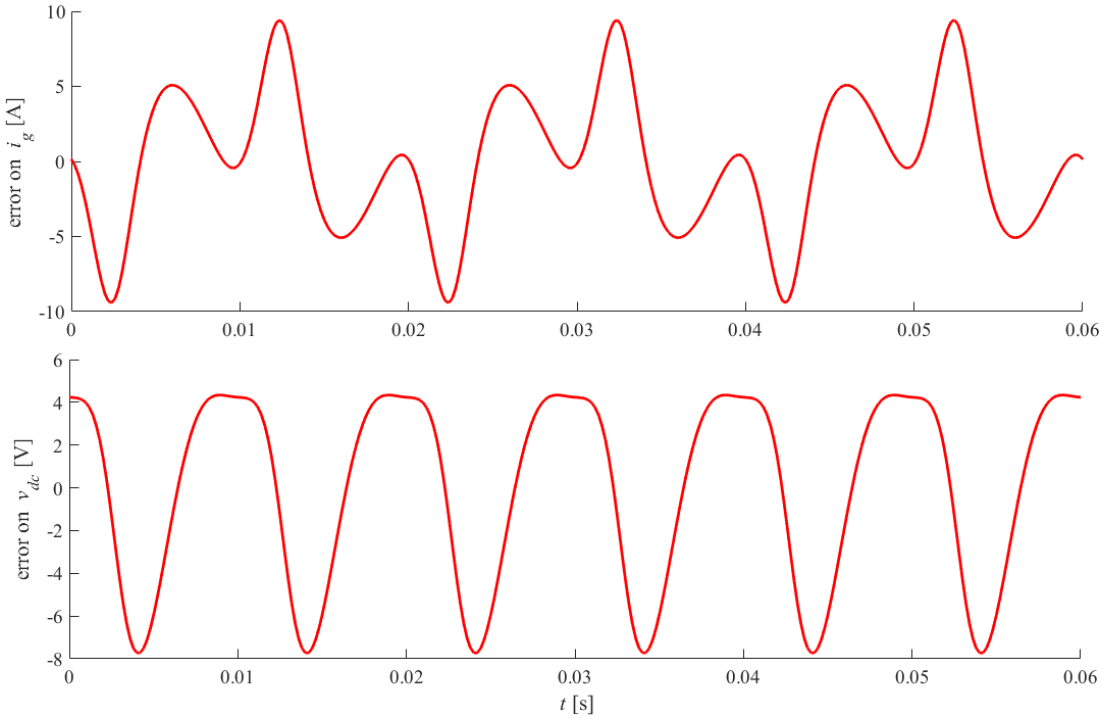

Figure 3.14: Error between the time-domain solutions computed for i_g and v_{dc}: full system simulations - 4-equation reduced model

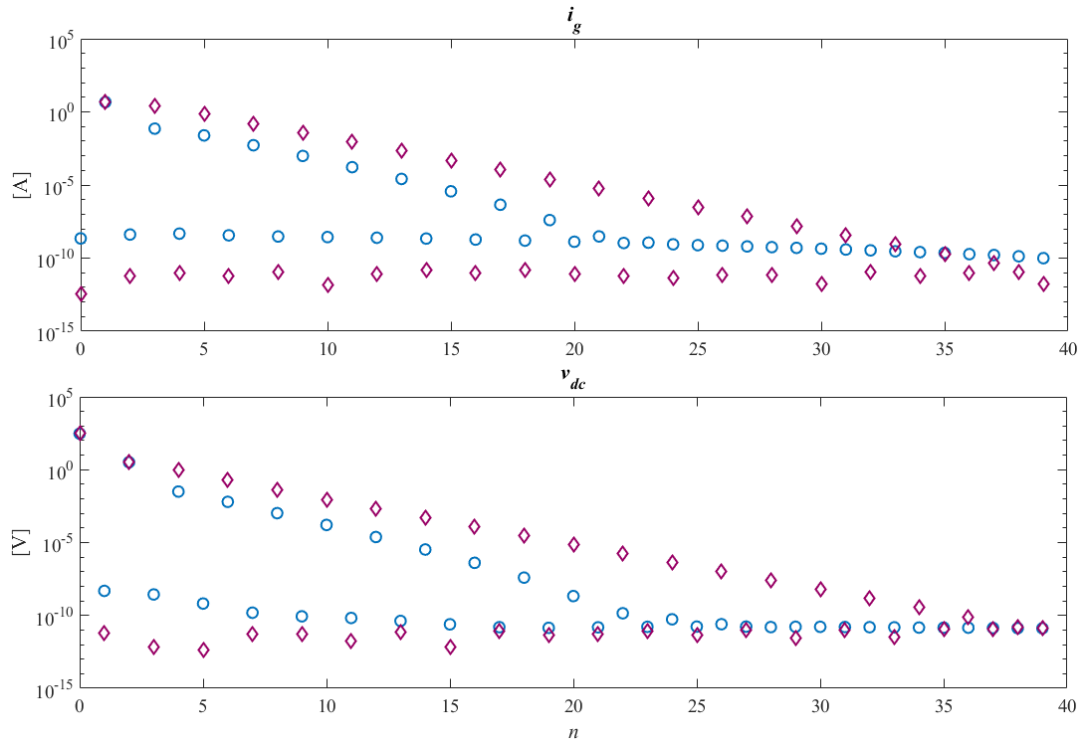

Figure 3.15: Fourier coefficients: full model (blue circles) and 4-equation reduced model (purple diamonds).

3.3.4 SP-AFE Eigenvalues and Stability Analysis

Applying linearisation to full and reduced systems and exploiting LTP theory, a plot of the system eigenvalues can be obtained, as depicted in Figure 3.16 for the full and 6-equations reduced models. Bifurcations that are visible at the ends of the eigenvalue columns are artefacts due to the truncation of the infinite matrices of the LTP system, and are, then, not significant.

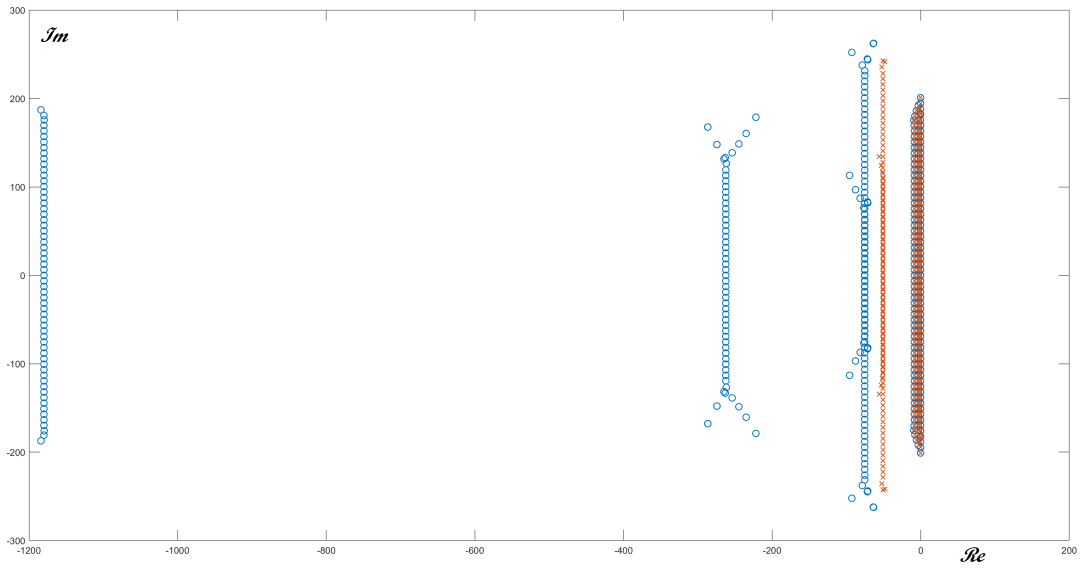

Figure 3.16: Full system eigenvalues (blue) and 6-equation reduced system eigenvalues (red), plotted in the complex plane

The eigenvalue columns far from the imaginary axes show some mismatch between the full and 6-equation reduced system (the two furthest are even missing), but the closer ones, more significant for the stability assessment, show a better agreement, as observable in Figure 3.17.

The same stability analysis has been repeated for different voltage PI parameters, corresponding to different control bandwidths, in order to find a stability threshold for the voltage PI control BW. A consistency in both time domain simulations and stability analysis has been found for voltage PI BWs varying from 10 to 260 Hz. It can be observed that the real part of the eigenvalue column on the extreme right (i.e., the first to make the system unstable) computed for the reduced model differs by an error of order 10^{-4} or less from the equivalent eigenvalue real part computed for the full model.

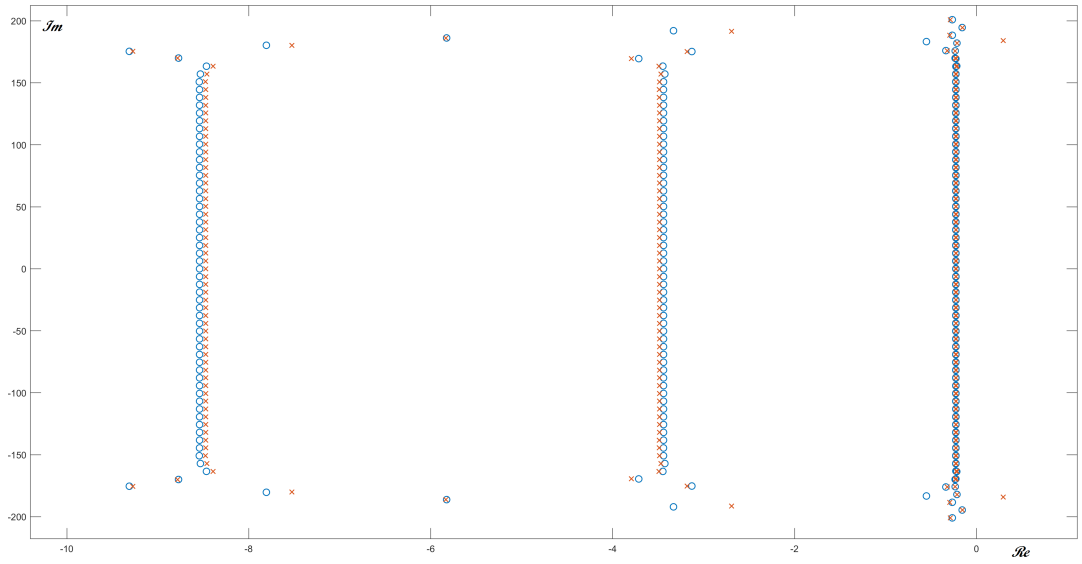

Figure 3.17: Zoom on the eigenvalues which are closest to the imaginary axis: full system (blue) and 6-equation reduced system (red) comparison

In the full model stability analysis, a voltage design BW equal to 255.6 Hz has been found as a threshold for stability. For the reduced model, the equivalent threshold is equal to 256.1 Hz. The relative error is then equal to 0.2%. This can be considered a very good agreement, as in practical applications a control BW would never be set exactly equal or extremely close to the stability threshold due to the nonlinear nature of the real system, and possible inaccuracies on parameter values or other uncertainties.

The same procedure could be applied to the 5-equations reduced model, which, however, due to the high presence of nonlinearities would lead to difficulties in computing the LTP matrices and lead to more significant errors, as explained in §3.3.3.3. Then, additional time-domain simulations with increasing BWs have been run, in order to find empirically the stability threshold. In this case, the threshold is found at 265 Hz, with a relative error equal to 3.5% with respect to the full-system threshold.

Concerning the 4-equation reduced system, both time-domain simulations and LTP stability analysis have been performed. However, as displayed in Figure 3.18 and 3.19 for a $BW = 260Hz$, the closest eigenvalue column to the imaginary axis is not present for the reduced model, making s stability assessment qualitatively incorrect.

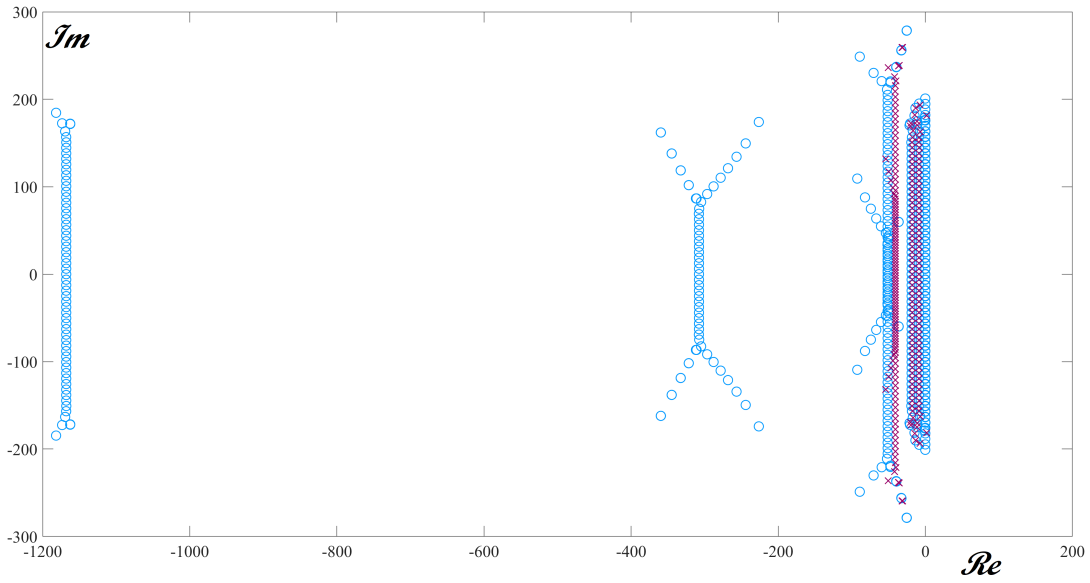

Figure 3.18: Full system eigenvalues (blue) and 4-equation reduced system eigenvalues (purple), plotted in the complex plane. ($BW = 260\,Hz$)

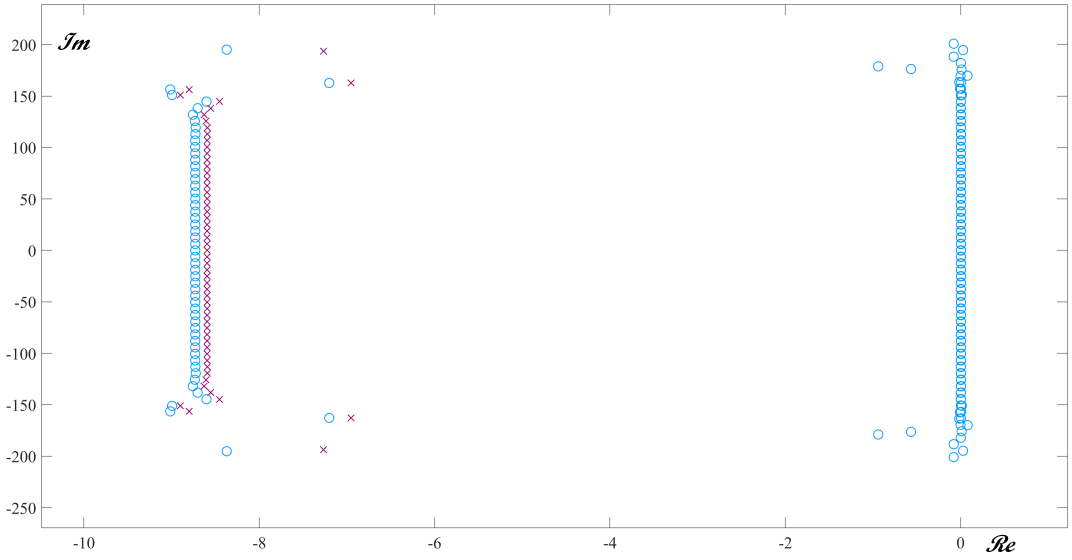

Figure 3.19: Zoom on the eigenvalues which are closest to the imaginary axis: full system (blue) and 4-equation reduced system (purple) comparison

3.3.5 Conclusions

In this work, a system reduction through nondimensionalisation, identification of a small dimensionless parameter, then retention of only leading-order terms has been presented and applied to a SP-AFE.

It can be observed that a moderate reduction in the size of the model (reduc-

tion from 8 to 6 in the number of variables and ODEs) can be achieved through a rational reduction strategy based on identifying a small dimensionless parameter. This reduced model performs well and agrees with the full model in both time domain simulations and stability analysis.

A more ambitious reduction leading to 5 or 4 degrees of freedon does not, in this case, perform so well. Since only the leading-order terms have been taken into account, those results may be improved by including further terms in an expansion of some of the variables. However, the system describes some physical processes which sometimes cannot be neglected without affecting the model reliability. In general, drastic approximations of those phenomena are unlikely to be effective.

Similar procedures may be attempted to perform model reductions of more complex systems, characterised by more both physical and control variables, as, for example, three-phase controllers in unbalanced systems, or in systems where the contribution of harmonics of second or higher order cannot be neglected. In such cases, it is not possible to apply a Park DQ0 transform, and the state-space systems describing their behaviours are inherently LTP or, more often, NLTP. Their stability analysis can therefore be computationally challenging, and model reductions might be beneficial for both stability assessment and control design purposes.

Chapter 4

AC Microgrids: Theory and Literature Review

This chapter and the two following concern the work which was performed about AC microgrids. In particular, the present chapter regards the theoretical aspects of AC microgrids and gives a general overview about the related literature. The current project is about the application of mathematical methods to power electronic systems, in order to model them effectively, and eventually achieve a deeper understanding about their operation, through a systematic reduction in the size of their associated mathematical model using perturbation methods.
This chapter will help a reader without a strong technical background in Electrical Engineering achieve an easier understanding of §5-6, while guiding engineers through the main aspects which have concerned our work.

4.1 Introduction to AC microgrids

Because of environmental concerns, in the last decades the production of electrical energy has been gradually shifting towards renewable sources. Hence, the shape of the electrical grid has changed from a traditional model, where few big power stations (mostly fuelled by fossil or nuclear fuels) produce high voltage (HV) energy, to a distributed generation system, where many small generation plants inject electrical energy into the grid, mostly in low voltage (LV) [25], [26]. Due to the large number of generators involved, it is harder to control the voltage amplitude and frequency of the system in every point; for the same reason, assess-

ing the stability of electrical grids is a problem that is now growing in complexity. A microgrid is a small autonomous system based on distributed generation, formed by a group of interconnected loads and distributed energy sources within clearly defined electrical boundaries. Microgrids act as single controllable entities with respect to the main grid, from which they can connect and disconnect, being able to operate in both grid-connected or island mode. Distributed generation sources are generally interfaced to the grid by power electronic converters [25], [26]. When not in island mode, microgrids can be controlled in ways that force them to behave similarly to synchronous generators, following transients due to mechanical rotating inertiae and synchronous generators exciting circuits; this technique is known as "grid supporting", and allows the microgrid's converters to influence the network frequency and voltage amplitude. When, instead, microgrids are demanded to provide power to the network without interfering with its governing dynamics, a phase-locked loop (PLL) is added to the controller, in order to passively follow the grid frequency and phase; this is possible thanks to the converters time constants, which tend to be negligible compared to synchronous generators time constants, and make converters controls "fast".

Due to the electromechanical properties of synchronous generators, when the power load changes, traditional grids naturally vary their voltage amplitude and frequency until a new equilibrium is reached. In microgrids, however, this does not happen, and controllers included in microgrids need additional controllers to achieve a similar self-regulatory behaviour, which is generally needed when in island or "grid supporting" mode [27], [26], [25]. Moreover, while in a thermal power station it is in general possible to choose the amount of produced power (typically, by varying the amount of input fuel), power provided by renewable sources cannot be controlled and is by nature intermittent.

The controller of a converter in an AC microgrid, thus, generally includes nested loops: traditional and widespread proportional-integral (PI) controllers which act directly on the values of currents and voltages, and some more controllers that modify the references for the PIs [28].

4.2 Model Reduction of AC Microgrids

When grids formed by a large number (at least 10) of converters are taken into account, the usual approach in engineering practice is to neglect the effect that a grid-connected converter has on the grid voltage and frequency. Those parameters are usually considered as constant and to be uninfluenced by the action of any single device. However, when smaller grids are considered (e.g. a microgrid in island mode), this approximation cannot be valid and the mutual interactions between the converters cannot be neglected. For this reason, when a microgrid is modelled, all the variables from each power electronic converter must be taken into account, leading to large systems of equations. In our case, a state-space system has a dimension that is 15 times the number of converters involved; similar system sizes can be found in the engineering literature [29], [30], [31], [28], [32]. Moreover, island mode microgrids are more prone to instability than larger grids, but the size of their models can make evaluating their stability quite challenging [25], [26].

Several attempts have been performed in order to reduce the size of state-space models of microgrids, mostly in order to achieve reliable stability analyses with a smaller computational effort and requiring fewer variables. In traditional grids, dominated by synchronous generators, stability is easier to obtain thanks to the nature of such generators: they are rotating machines with big inertiae, and their spinning frequency cannot vary instantly, but need instead to go through a transient phase. Power electronic converters, instead, generate sinusoidal voltage through filtered high-frequency switching. They are then able to change phase and frequency of the voltage almost instantly (the switching period of converters is in general negligible compared with the other time constants of the electrical grids). These behaviours make the stability of microgrids heavily dependent on the good functioning of the controllers. Preliminary stability analyses are hence particularly critical before running physical models of microgrids, and reliable reduced models are very desirable for this purpose.

Several approaches can be found in the literature regarding the model reduc-

tion of AC microgrids. Most of them are based on singular perturbation.

In [33], singular perturbation is explicitly mentioned, and boundaries are set for some parameters to provide stability. Small parameters ϵ, with the dimension of time, are chosen by comparing combinations of parameters found in the state-space ODEs.

A similar approach can be found in [34], where the variables are subsequently divided into "fast" and "slow" to allow simulations of both fast transients and quasi-stable behaviour. The separation is achieved by grouping the eigenvalues of the Jacobian matrix of the system into those that are "near" and "far" from the imaginary axis.

A method based on fast and slow variables is also presented in [30], which presents an analogous eigenvalue-based technique.

Ref. [35], instead, combines a Kron reduction (a method generally employed for power systems, based on combinations of electrical parameters) with a subsequent reduction based on singular perturbation theory. In [29], a model reduction based on singular perturbation is first performed. Then, observing how the system behaves in simulations, additional variables are removed from the reduced model.

Copious examples of similar results can be found in the engineering literature. A common feature of those articles is that they keep the systems dimensional. This choice often limits the comparability of the linearised system's eigenvalues, while preventing a full identification of the negligible terms. This is sometimes compensated by the practical knowledge obtained by researchers through experimental practice: in a chosen system, some variables will naturally tend to be slow and some others fast. However, these hindsight-based procedures may lead to inaccuracies, especially when the system parameters vary.

In the following chapters, perturbation theory is applied to dimensionless systems, hoping to compute a more systematic procedure for the model reduction of AC microgrid systems, that could be applied to a wide variety of engineering systems with a similar structure.

Chapter 5

Analysis of a Single Inverter Controlled as an AC Microgrid Converter

5.1 Introduction and Chapter Summary

As a preliminary stage, attention is focused on a system formed by a single inverter, whose controller, however, acts analogously to controllers of general AC microgrids including more devices. For the present study, the microgrid is assumed to behave in island mode. The state-space model of such system is derived in §5.2.

In practice, a microgrid is not likely to be composed of only one device, but this preliminary step allowed us to familiarise ourselves with the controller and its operation. The purpose of this first model is obtaining a general understanding the structure of the controllers, knowing better their way of operation, and identifying the variables and parameters that are more significant for the model reduction, in the expectation that this identification will be applicable even when a system with more devices is taken into account.

After the state-space model of the system is computed, its ODEs are simulated and the results compared with the behaviour of a second system where the same controller is applied to some pre-built MATLAB switching elements. Since the average model agrees with the average of the switching system, the work proceeds with the reduction of the model, as illustrated in §5.3.

First, the system is nondimensionalised, then some small parameters are identified, and finally the system ODEs are reduced according to singular perturbation theory. In the reduction process, each parameter is given an estimated "size",

defined as a power of a small dimensionless parameter ϵ. For some of the parameters, this choice is not unequivocal and different reduced models can reasonably be obtained by different choices. In §5.3.2.9, the different reduced models are listed and some results obtained through simulations are shown. Simulations were run in parallel to compare the behaviour of the reduced systems with the full model. Good agreement was found between the full model and the reduced models where 4 or more state-space variables are kept and defined by ODEs, while the others are neglected or modelled by algebraic equations.

5.2 Single inverter model

This section is about the model and the operation of an AC microgrid formed by one inverter and one resistive load. This system has been analysed as a preliminary step before working with bigger grids, as converters forming microgrids necessitate complex nested controllers. §5.2.1 describes the physical system and derives the average state-space ODEs of its variables, §5.2.2 analyses the controller, considering its components one by one, §5.2.3 shows the overall state-space model of the system. The model reduction relevant to this model is performed in §5.3.

5.2.1 Physical Variable Behaviours

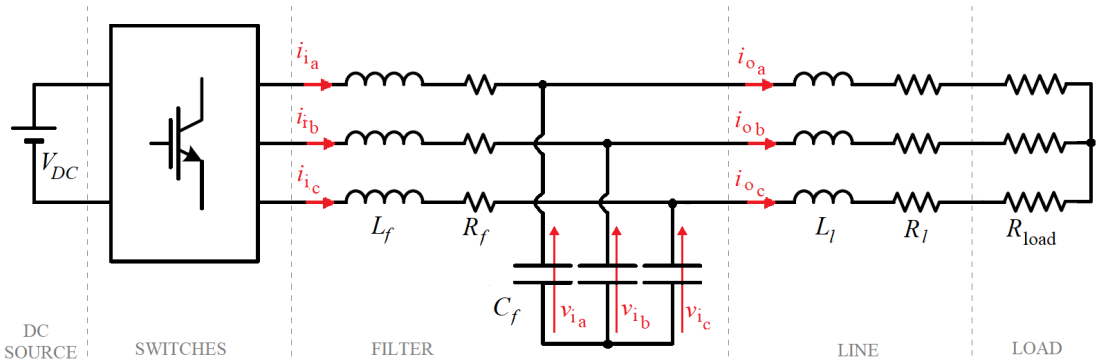

Figure 5.1: Overall scheme of the system

In Figure 5.1, a scheme of a three-phase voltage-source inverter, its load and

the line connecting them is shown. The system is assumed to be symmetric; the corresponding parameters are assumed to be identical in each phase. Therefore, the sum of three corresponding currents or voltages is always equal to zero (e.g. $i_{\mathrm{i_a}}(t) + i_{\mathrm{i_b}}(t) + i_{\mathrm{i_c}}(t) = 0$) and the centres of three-phase Y-connections are assumed to have zero voltage even if not grounded. This voltage is found to be small in experimental practice and assuming it to be equal to zero allows the DQ0 transform to be applied to the system.

Notation: in this work, vectors expressed as $\boldsymbol{x}_{\mathrm{abc}}(t)$ denote the three-phase $[x_{\mathrm{a}}(t)\ x_{\mathrm{b}}(t)\ x_{\mathrm{c}}(t)]^{\mathrm{T}}$, while $\boldsymbol{x}_{\mathrm{dq}}(t)$ is the equivalent of $\boldsymbol{x}_{\mathrm{abc}}(t)$ expressed in the DQ0 reference frame.

$$\boldsymbol{x}_{\mathrm{dq}}(t) = \boldsymbol{T}(\theta)\, \boldsymbol{x}_{\mathrm{abc}}(t)\,, \tag{5.1}$$

where θ is the phase angle of the electrical phase A and $\boldsymbol{T}(\theta)$ is the Park transformation matrix computed for θ [11]-[12].

As depicted in Figure 1, V_{DC} is the input DC voltage source of the inverter and is assumed to be constant. Six switches, included in the switching block in the picture, are controlled by Pulse-Width Modulation (PWM) signals, which in turn depend on the output of the controller. In this analysis, the switching behaviour of the system is neglected and only average equations are computed. This simplification is allowed by the switching period being much smaller than the other time constants of the system. Simulations have been run in MATLAB Simulink to demonstrate the effectiveness of these simplifications, comparing the average system behaviour with a switching system having the same controller, but whose physical variables have been modelled by Simulink pre-built electrical components (including a switching three-phase inverter). The simulations show good agreement in both steady state and transients between switching and average models: the average system variables behave like the average of the switching variables and the ripple amplitude caused by the switching is small compared with the sinusoid amplitude of the average system.

After the switching block, an LC filter is present, whose inductance, capacitance and parasitic resistance are represented by the parameters L_f, C_f and R_f, respectively. The average currents flowing out of the switches through the filter inductors are represented by $\boldsymbol{i}_{\mathrm{i_{abc}}}(t)$, the voltages on the filter capacitors by $\boldsymbol{v}_{\mathrm{i_{abc}}}(t)$.

After the filter, a three-phase line connects the inverter to the load. The line impedance is modelled by a series of a resistor and an inductor, whose resistance and inductance are given, respectively, by R_l and L_l. The load is assumed to be a single, balanced, three-phase resistor; its resistance is denoted by R_{load}. Currents $\boldsymbol{i}_{\text{o}_{\text{abc}}}(t)$ denote the three-phase current flowing through the line and the load.

5.2.1.1 ABC reference frame, physical variable behaviours

The presence of the inductors and the capacitors leads to the following set of ODEs describing the behaviour of the physical variables of the system:

$$\frac{\mathrm{d}\boldsymbol{i}_{\text{i}_{\text{abc}}}(t)}{\mathrm{d}t} = \frac{V_{DC}}{2\,L_f}\boldsymbol{m}_{\text{abc}}(t) \;-\; \frac{R_f}{L_f}\boldsymbol{i}_{\text{i}_{\text{abc}}}(t) \;-\; \frac{\boldsymbol{v}_{\text{i}_{\text{abc}}}(t)}{L_f}\,, \tag{5.2a}$$

$$\frac{\mathrm{d}\boldsymbol{v}_{\text{i}_{\text{abc}}}(t)}{\mathrm{d}t} = \frac{\boldsymbol{i}_{\text{i}_{\text{abc}}}(t)}{C_f} \;-\; \frac{\boldsymbol{i}_{\text{o}_{\text{abc}}}(t)}{C_f}\,, \tag{5.2b}$$

$$\frac{\mathrm{d}\boldsymbol{i}_{\text{o}_{\text{abc}}}(t)}{\mathrm{d}t} = \frac{\boldsymbol{v}_{\text{i}_{\text{abc}}}(t)}{L_l} \;-\; \frac{R_l + R_{\text{load}}}{L_l}\boldsymbol{i}_{\text{o}_{\text{abc}}}(t)\,, \tag{5.2c}$$

where $\boldsymbol{m}_{\text{abc}}(t)$ is the vector of the modulation indices. Modulation indices are dimensionless signals which are the output of the controller and the input of the PWM; they can vary continuously from -1 to 1. Ideally, the output voltage after the switches would be a three-phase sinewave. In practice, the voltage oscillates between its maximum and its minimum value (in this case, $+V_{DC}/2$ or $-V_{DC}/2$), according to the switches' configuration. At each switching period, the fraction of time spent at V_{MAX} or V_{MIN} is determined by the modulation index corresponding to the considered phase. Since the switching period is much smaller than the grid period, additional low-pass filters can be placed after the converter, in order to reduce the amplitude of the ripple and provide voltage waves close to the sinusoidal reference. In this work, the high-frequency switching is neglected and only the average behaviour is analysed. Since the maximum voltage difference is the DC source voltage V_{DC}. Thus, the voltages after the switching block are considered equal to the product of half of the DC source and the corresponding modulation indices.

5.2.1.2 DQ0 reference frame, physical variable behaviours

Applying the Park transformation to (5.2) leads to

$$\frac{\mathrm{d}i_{\mathrm{i_d}}(t)}{\mathrm{d}t} = \frac{V_{DC}}{2\,L_f} m_{\mathrm{d}}(t) - \frac{R_f}{L_f} i_{\mathrm{i_d}}(t) - \frac{v_{\mathrm{i_d}}(t)}{L_f} + \omega(t)\, i_{\mathrm{i_q}}(t)\,, \tag{5.3a}$$

$$\frac{\mathrm{d}i_{\mathrm{i_q}}(t)}{\mathrm{d}t} = \frac{V_{DC}}{2\,L_f} m_{\mathrm{q}}(t) - \frac{R_f}{L_f} i_{\mathrm{i_q}}(t) - \frac{v_{\mathrm{i_q}}(t)}{L_f} - \omega(t)\, i_{\mathrm{i_d}}(t)\,, \tag{5.3b}$$

$$\frac{\mathrm{d}v_{\mathrm{i_d}}(t)}{\mathrm{d}t} = \frac{i_{\mathrm{i_d}}(t)}{C_f} - \frac{i_{\mathrm{o_d}}(t)}{C_f} + \omega(t)\, v_{\mathrm{i_q}}(t)\,, \tag{5.3c}$$

$$\frac{\mathrm{d}v_{\mathrm{i_q}}(t)}{\mathrm{d}t} = \frac{i_{\mathrm{i_q}}(t)}{C_f} - \frac{i_{\mathrm{o_q}}(t)}{C_f} - \omega(t)\, v_{\mathrm{i_d}}(t)\,, \tag{5.3d}$$

$$\frac{\mathrm{d}i_{\mathrm{o_d}}(t)}{\mathrm{d}t} = \frac{v_{\mathrm{i_d}}(t)}{L_l} - \frac{R_l + R_{\mathrm{load}}}{L_l} i_{\mathrm{o_d}}(t) + \omega(t)\, i_{\mathrm{o_q}}(t)\,, \tag{5.3e}$$

$$\frac{\mathrm{d}i_{\mathrm{o_q}}(t)}{\mathrm{d}t} = \frac{v_{\mathrm{i_q}}(t)}{L_l} - \frac{R_l + R_{\mathrm{load}}}{L_l} i_{\mathrm{o_q}}(t) - \omega(t)\, i_{\mathrm{o_d}}(t)\,, \tag{5.3f}$$

where $\omega(t)$ is the fundamental frequency of the AC average variables and its value is one of the two outputs of the droop controller, as explained in §5.2.2.1.
The six equations listed in (5.3) model the physical behaviour of the average system. However, the value of the modulation indices has not yet been specified. For the system to be self-consistent, further ODEs describing the controller action (and hence the modulation indices) must be added to it.

5.2.2 Controller

This subsection describes the controller that is applied to the inverter. It is formed of a droop control, a virtual inductance, a proportional-integral (PI) controller for the voltage, and a PI controller for the current. A subsubsection is dedicated to each.

5.2.2.1 Droop Control

The aim of the droop control is to force an inverter to behave like a synchronous generator. Since power electronic converters have in general a small physical inertia, they are more prone to instability than rotating generators. Increasing the output frequency of a rotating generator, for example, involves accelerating its spinning mass; this has physical limits due to mechanical inertia and large inductance of the generator. A change in the output frequency or voltage amplitude of a rotating generator can be performed with time constants of order 0.1 s-1 s. A power-electronic converter, instead, could change its switching frequency almost instantaneously, in the switching period next to the actual one, after 10^{-5} s - 10^{-6} s. Sudden changes in the grid voltage of frequency are likely to cause instability, especially if the grid is small.

Moreover, because of electromagnetic and mechanical phenomena, synchronous generators tend naturally to modify their spinning frequency and voltage amplitude depending on the amount of active and reactive power which are drawn from them, tending to a natural equilibrium point. Power electronic converters need to be properly controlled to achieve their operating steady states. If the controller is not implemented properly, the system becomes unstable.

Droop controllers were first implemented by engineers that tried to make power electronic converters mimic the behaviour of rotating generators. This process involves a certain degree of approximation from the engineering custom, but is widely used in practical application and is known to work well enough for controlling grid-connected inverters [25, Chapter 3.3.3] [26, Chapter 5.3].

The general derivation of droop controllers is reported below: it starts with the description of the behaviour of a grid-connected rotating generator, proceeds with an approximated computation of how phase difference and voltage amplitude difference influence the power exchange between the generator and the grid, and provides a description of how the droop controller is normally implemented.

5.2.2.1.1 Single-phase approximated generator and grid model

This section describes the behaviour of a system formed of one monophase generator, a connecting line and one phase of the main grid. The grid voltage amplitude

and frequency are assumed to be constant.

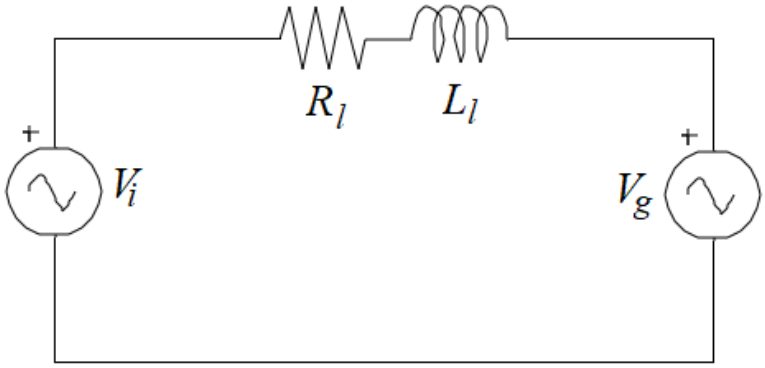

Figure 5.2: Approximated model of one phase

Figure 5.2 depicts an approximated model of one phase. The AC source denoted by V_i represents a synchronous generator, while V_g represents the grid AC voltage. Between them, a RL impedance models the connecting line. If the phase difference between generator and grid is zero and they have the same voltage amplitude, there is no power exchange between them, since the instantaneous voltage at the opposite ends of the RL impedance is always the same and, hence, no current flows in the impedance.

Neglecting eventual variations in the grid voltage amplitude and frequency, v_g can be expressed as

$$v_g(t) = V_g \sin(\omega t), \tag{5.4}$$

where V_g is the amplitude of v_g.

Regarding the inverter voltage, in steady state its voltage is also given by a sinusoid,

$$v_i(t) = \bar{V}_i \sin(\omega t + \bar{\delta}), \tag{5.5}$$

where $\bar{V}_i$ is the steady state of the inverter voltage amplitude and $\bar{\delta}$ is the steady-state phase difference between the generator and the grid. In steady state, v_g and v_i have exactly the same frequency ω, while V_g and V_i can differ slightly (by about 10% of their value in practice). If $V_g = V_i$ and $\delta = 0$, there is no power exchange between the generator and the grid. Active and reactive power transmitted to the grid depend on V_i and δ, as explained below. While the voltage amplitude V_i can be varied by the system controller, in general the phase difference between the

generator and the grid cannot be modified directly, as synchronous generators are rotating machines that cannot move instantaneously from one angle to another. During transients, (small) variations are allowed in the generator frequency in order to change δ. Given the large mechanical inertia of synchronous generators, their frequency usually varies according to time constants that are much bigger than all the other inherent time constants of the system.

5.2.2.1.2 Power computation for the approximated model

In order to understand the theoretical bases for droop controllers, the steady-state power exchanges between the generator and the grid are computed; then, perturbations on the generator voltage amplitude and phase difference are applied to the steady state equations.

From Figure 5.2, the following differential equation can be derived:

$$L_l \frac{\mathrm{d}i(t)}{\mathrm{d}t} + R_l i(t) = v_i(t) - v_g(t)\,, \tag{5.6}$$

where $i(t)$ is the current flowing between the inverter and the grid through the line. Voltages v_g and v_i can also be expressed as the imaginary part of complex exponential, as follows.

$$v_g(t) = \Im\left\{V_g(t)\mathrm{e}^{\mathrm{j}\omega t}\right\}\,, \tag{5.7}$$

$$v_i(t) = \Im\left\{\bar{V}_i\mathrm{e}^{\mathrm{j}\left(\omega t+\bar{\delta}\right)}\right\}\,. \tag{5.8}$$

Hence, the complex solution of the problem will be evaluated, and successively the imaginary part will be selected as the expression for the line current.

Since (5.6) is linear, its complex solution can be expressed as

$$i_c(t) = I(t)\mathrm{e}^{\mathrm{j}\omega t}\,. \tag{5.9}$$

Its time derivative, therefore, can be computed by differentiating (5.9) to give

$$\frac{\mathrm{d}i_c(t)}{\mathrm{d}t} = \left(\frac{\mathrm{d}I(t)}{\mathrm{d}t} + \mathrm{j}\,\omega\, I(t)\right)\mathrm{e}^{\mathrm{j}\,\omega\, t}. \tag{5.10}$$

Substituting (5.10) into (5.6) leads to

$$L_l \frac{\mathrm{d}I(t)}{\mathrm{d}t} + (\mathrm{j}\,\omega\,L_l + R_l)\,I(t) = \bar{V}_i \mathrm{e}^{\mathrm{j}\,\bar{\delta}} - V_g. \tag{5.11}$$

Considering a quasi-steady-state condition where the current amplitude does not vary significantly leads to neglect the first term of the equation, based on the following assumption:

$$\left| L_l \frac{\mathrm{d}I(t)}{\mathrm{d}t} \right| \ll \left| (\mathrm{j}\,\omega\,L_l + R_l)\,I(t) \right|. \tag{5.12}$$

Applying the approximation stated in (5.12), $I(t)$ can be computed as

$$I(t) \sim \frac{\bar{V}_i \mathrm{e}^{\mathrm{j}\bar{\delta}} - V_g}{\mathrm{j}\,\omega\,L_l + R_l}. \tag{5.13}$$

Therefore, the current flowing in the system can be approximated by

$$i(t) = \Im\left\{ I(t)\,\mathrm{e}^{\mathrm{j}\omega t} \right\} \sim \Im\left\{ \frac{\bar{V}_i \mathrm{e}^{\mathrm{j}\bar{\delta}} - V_g}{\mathrm{j}\,\omega\,L_l + R_l} \mathrm{e}^{\mathrm{j}\omega t} \right\}. \tag{5.14}$$

From (5.14), it can be noticed that $I(t)$ is equal to the phasor $\boldsymbol{I}(t)$ for $i(t)$. Proceeding further with (5.13) leads to

$$\begin{aligned} \boldsymbol{I}(t) = I(t) &= \frac{\bar{V}_i \mathrm{e}^{\mathrm{j}\bar{\delta}} - V_g}{R_l + \mathrm{j}\omega L_l} \\ &= \frac{\bar{V}_i \omega L_l \sin(\bar{\delta}) + R_l[\bar{V}_i \cos(\bar{\delta}) - V_g]}{R_l^2 + \omega^2 L_l^2} \\ &\qquad + \mathrm{j}\frac{\omega L_l[-\bar{V}_i \cos(\bar{\delta}) + V_g] + R_l \bar{V}_i \sin(\bar{\delta})}{R_l^2 + \omega^2 L_l^2} \end{aligned} \tag{5.15}$$

Assuming that the system is purely sinusoidal, the apparent exchanged power is given by

$$\boldsymbol{S}(t) = P(t) + \mathrm{j}Q(t) = \frac{\boldsymbol{V}_g(t)\,\boldsymbol{I}^*(t)}{2}, \tag{5.16}$$

where $\boldsymbol{S}$ is the apparent power, P is the real power, Q is the reactive power, $\boldsymbol{V}_g$ is the phasor corresponding to v_g, $\boldsymbol{I}^*$ is the complex conjugate of the current phasor $\boldsymbol{I}$.

Therefore, from (5.15) and (5.16), the power flowing into the grid can be computed as

$$\boldsymbol{S}(t) = V_g \frac{\bar{V}_i \omega L_l \sin(\bar{\delta}) + R_l[\bar{V}_i \cos(\bar{\delta}) - V_g]}{2(R_l^2 + \omega^2 L_l^2)} + \mathrm{j} V_g \frac{\omega L_l[\bar{V}_i \cos(\bar{\delta}) - V_g] - R_l \bar{V}_i \sin(\bar{\delta})}{2(R_l^2 + \omega^2 L_l^2)} . \quad (5.17)$$

From (5.17), the active and reactive powers of the system are expressed, respectively, as

$$P(t) = \Re\{\boldsymbol{S}(t)\} = \frac{V_g\{\bar{V}_i \omega L_l \sin(\bar{\delta}) + R_l[\bar{V}_i \cos(\bar{\delta}) - V_g]\}}{2(R_l^2 + \omega^2 L_l^2)} , \quad (5.18)$$

$$Q(t) = \Im\{\boldsymbol{S}(t)\} = \frac{V_g\{\omega L_l[\bar{V}_i \cos(\bar{\delta}) - V_g] - R_l \bar{V}_i \sin(\bar{\delta})\}}{2(R_l^2 + \omega^2 L_l^2)} . \quad (5.19)$$

Since the angle δ is small in practical applications , the following approximations are valid:

$$\sin(\delta) \approx \delta , \quad \cos(\delta) \approx 1 . \quad (5.20)$$

Using (5.20) into (5.18) and (5.19) leads to

$$P(t) \approx \frac{V_g\{\bar{V}_i \omega L_l \bar{\delta} + R_l[\bar{V}_i - V_g]\}}{2(R_l^2 + \omega^2 L_l^2)} , \quad (5.21)$$

$$Q(t) \approx \frac{V_g\{\omega L_l[\bar{V}_i - V_g] - R_l \bar{V}_i \bar{\delta}\}}{2(R_l^2 + \omega^2 L_l^2)} . \quad (5.22)$$

In medium and high voltage the line resistance is negligible compared with the line reactance. Since synchronous generators are usually connected to the MV or HV grid, the following approximation can be considered valid.

$$R_l \ll \omega L . \quad (5.23)$$

Therefore, the expressions for the current phasor, active and reactive power can be approximated, respectively, as follows:

$$\boldsymbol{I}(t) \approx \frac{\bar{V}_i \, \bar{\delta}}{\omega \, L_l} + \mathrm{j} \frac{[-\bar{V}_i + V_g]}{\omega \, L_l} , \quad (5.24)$$

$$P(t) \approx \frac{\bar{V}_i V_g \bar{\delta}}{2\omega L_l}, \tag{5.25}$$

$$Q(t) \approx \frac{V_g[\bar{V}_i - V_g]}{2\omega L_l}, \tag{5.26}$$

Equations (5.25) and (5.26) approximate the steady-state values of active and reactive powers, respectively. In order to design the droop controller correctly, equations (5.25)-(5.26) are linearised to obtain the equation governing small perturbations of the system. In the notation adopted, $\bar{x}$ is the steady-state value of x, while $\tilde{x}$ is the variable modelling its perturbed behaviour. Linearising the steady-state equations listed above and considering small variations of δ and V_i leads to

$$\tilde{P}(t) \approx \frac{\bar{V}_i V_g}{2\omega L_l}\tilde{\delta}(t) + \frac{V_g \bar{\delta}}{2\omega L_l}\tilde{V}_i(t), \tag{5.27}$$

and

$$\tilde{Q}(t) \approx \frac{V_g \tilde{V}_i(t)}{2\omega L_l}. \tag{5.28}$$

Therefore, a change in the phase leads to a change in the active power only, while a variation in V_i influences both active and reactive power. Equations (5.27) and (5.28) are the bases for the implementation of droop controllers, as reported in the next section.

5.2.2.1.3 Droop control implementation

The actual implementation of droop controllers, based on (5.27) and (5.28), is adapted to the limits and requirements of the physical device and the operating functioning of controllers. This process can be split into the elements listed below.

1) Inverse implementation need

Since the aim of the droop control is to force the inverter to behave like a synchronous generator, theoretically good results could be achieved by imposing on the inverter that it produces P and Q according to (5.27) and (5.28). However, in practical applications, an accurate measurement of the frequency is in general harder to perform than the power measurement. Measuring the frequency typically requires the presence of a Phase-Locked Loop (PLL), which would make the controller more complicated. Therefore, an inverse control is usually preferred: a

reference value is set for P and Q, and δ and V_i vary.

2) Approximation: neglect of cross-coupling terms

In order to keep the controller simple, the term in (5.27) depending on the perturbation of the voltage amplitude is in general not considered. This makes the power control physically less accurate, but in the literature there is some evidence demonstrating the effectiveness of this ad hoc approximation in laboratory practice [36] [37].

3) Frequency-based implementation

In this section, the actual form of the droop controller used in practice is obtained, starting from (5.25)-(5.26). An ideal droop controller is depicted in Figure 5.3, while some manipulations to the block diagram are performed in the following pictures to guide the reader towards the formulation of the droop control that is used in practice. In Figure 5.3 and following, the Laplace domain notation is used for feedback loop diagrams.

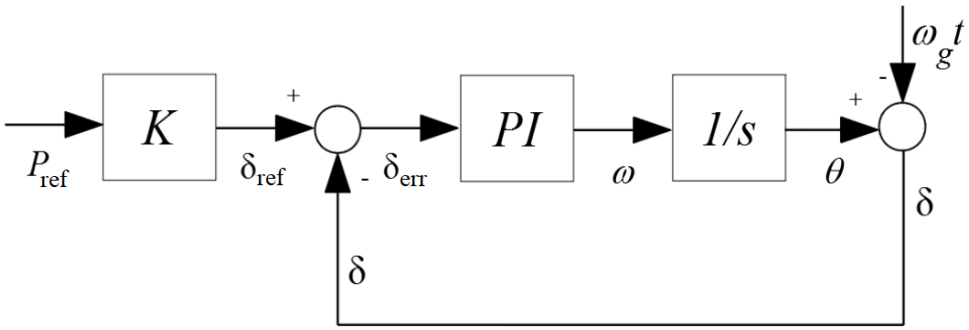

Figure 5.3: Ideal droop control scheme, Laplace domain

Ideally, a droop controller would be implemented as depicted in Figure 5.3: δ is the phase difference between the generator and the grid; the reference for the phase difference, in the picture denoted as δ_{ref}, is computed proportionally (with coefficient K) to the reference P_{ref} for the active power. The phase error δ_{err} enters a proportional-integral (PI) controller that sets the frequency ω of the system. The generator phase θ is found by integrating ω, and the phase difference δ by subtracting the grid phase, given by $\omega_g t$, from θ. In case the generator is

constituted of a grid-connected inverter, ω is the modulation frequency used by the PWM, while the phase θ is needed for the Park transforms operated by the controller.

The scheme of Figure 5.3 can be modified by moving the proportional gain K inside the loop, as shown in Figure 5.4. In this case, the error is computed on the active power P instead of the phase difference. P is computed by multiplying δ by the inverse of K, previously used to pass from power reference to phase difference reference. The coefficients of the new PI controller, denoted by PI_2, can be simply obtained by multiplying the original PI's coefficients by K. Moreover, the phase difference can be substituted by the frequency difference, computed before the integrator, given a correct setting of the initial condition of the integral block. Hence, the phase difference δ is now the output of the integrator.

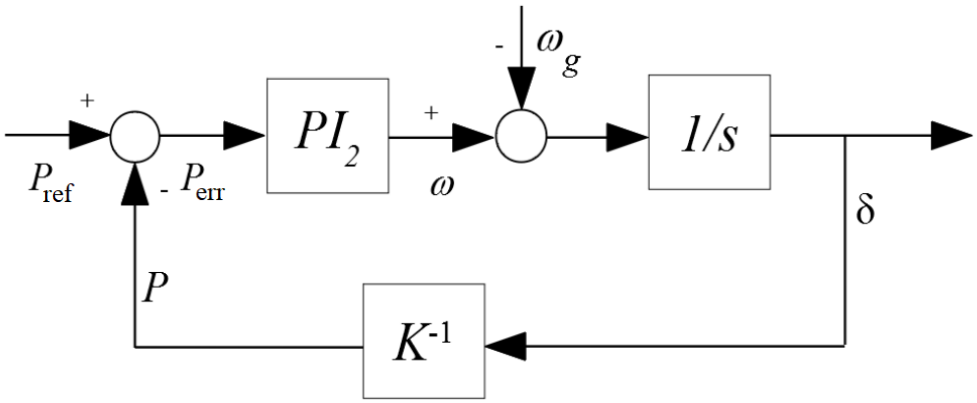

Figure 5.4: Modified droop control scheme with the error computed on the active power, Laplace domain.

A PI controller in general gives a null steady-state error. In this case, however, a steady-state error is preferable to an inverter frequency that differs too much from the grid frequency, as this could cause issues to the appliances that are fed by the grid. Thus, the PI controller is replaced by the proportional constant K_p only.

Figure 5.5 depicts the droop control scheme as usually implemented in the engineering literature. The red proportional block represents the physical generator system.

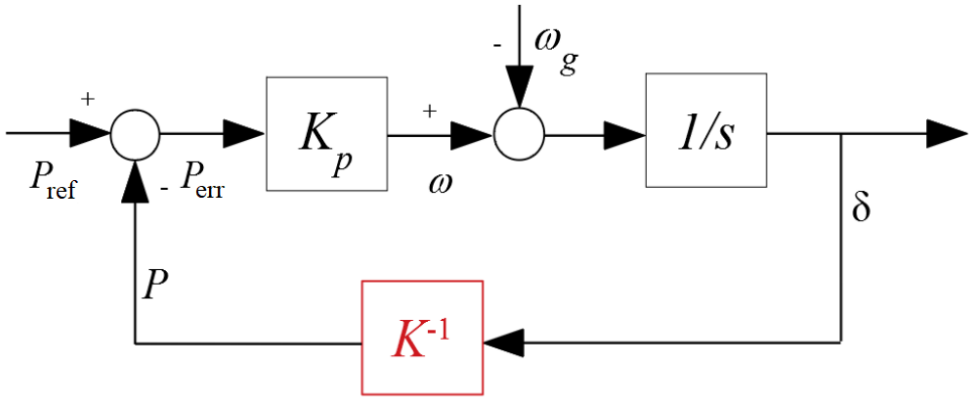

Figure 5.5: Proportional droop control scheme

5.2.2.1.4 Droop control equations

Considering both active and reactive power, the overall action of the droop controller is given by

$$\omega(t) \;=\; \omega_n \;+\; K_{dp}\,(P_{\text{ref}} \;-\; P(t))\,, \tag{5.29a}$$

$$V_{d_{\text{ref}}}(t) \;=\; V_{d_n} \;+\; K_{dq}\,(Q_{\text{ref}} \;-\; Q(t))\,, \tag{5.29b}$$

where P_{ref} and Q_{ref} are the reference values for P and Q, respectively, ω_n and V_{d_n} are the nominal values for the angular frequency and the d-component of the inverter output voltage, K_{dp} and K_{dq} are the control proportional constants used by the droop controller. In particular, K_{dp} corresponds to K_p of Figure 5.5.

5.2.2.1.5 Low-pass filter

Generally, P and Q are low-pass filtered to avoid excessive oscillations of ω and $V_{d_{\text{ref}}}$ during transients.

Therefore, two ODEs are added to the system:

$$\frac{\mathrm{d}P_{lp}(t)}{\mathrm{d}t} \;=\; \omega_{cd}[P(t) \;-\; P_{lp}(t)] \;=\; \omega_{cd}[v_{\mathrm{i_d}}(t)\,i_{\mathrm{o_d}}(t) \;+\; v_{\mathrm{i_q}}(t)\,i_{\mathrm{o_q}}(t) \;-\; P_{lp}(t)]\,, \tag{5.30a}$$

$$\frac{\mathrm{d}Q_{lp}(t)}{\mathrm{d}t} \;=\; \omega_{cd}[Q(t) \;-\; Q_{lp}(t)] \;=\; \omega_{cd}[v_{\mathrm{i_d}}(t)\,i_{\mathrm{o_q}}(t) \;-\; v_{\mathrm{i_q}}(t)\,i_{\mathrm{o_d}}(t) \;-\; Q_{lp}(t)]\,, \tag{5.30b}$$

where $P_{lp}(t)$ and $Q_{lp}(t)$ are the variables expressing the low-passed value of active

and reactive power, respectively, ω_{cd} is the cut-off frequency of the low-pass filter and its value must be chosen to be small if compared with the cut-off frequency of the voltage PI (§5.2.2.3).

Substituting $P(t)$ and $Q(t)$ with $P_{lp}(t)$ and $Q_{lp}(t)$ in (5.29) leads to

$$\omega(t) = \omega_n + K_{dp}\left(P_{\text{ref}} - P_{lp}(t)\right), \tag{5.31a}$$

$$V_{d_{\text{ref}}}(t) = V_{d_n} + K_{dq}\left(Q_{\text{ref}} - Q_{lp}(t)\right). \tag{5.31b}$$

The phase of $v_{\text{i}_\text{a}}(t)$, $\theta(t)$, is estimated by integrating $\omega(t)$, adding a further ODE to the system:

$$\frac{\mathrm{d}\theta}{\mathrm{d}t} = \omega(t) = \omega_n + K_{dp}\left(P_{\text{ref}} - P_{lp}(t)\right). \tag{5.32}$$

The angle θ must be computed explicitly because it is needed to perform the Park transformations. Currents and voltages are measured and transformed to the DQ0 reference frame. The controller computes the modulation indices as DQ0 variables first, but their values must be transformed into ABC reference before being sent to the PWM.

5.2.2.2 Virtual Inductance

The power computation performed in §5.2.2.1, analysing the theoretical bases for the droop controller, includes the assumption of the resistive component of the connecting line being small compared with the reactance. This is generally true for high voltage (HV) and medium voltage (MV) systems, but in low voltage (LV) this assumption does not hold. The droop controller is hence prevented from operating properly, and a further controller component is added to compensate for this behaviour.

The virtual inductance method enhances the stability of the system through the introduction of an auxiliary variable, computed as the voltage drop on an inductance L_v. The inductance L_v, however, is not real, but is a parameter of the controller having the dimension of an inductance.

The next paragraph describes what happens when a droop controller is applied

to a LV system, without a virtual inductance; in the following, the action of a virtual inductance is added, its effects on the power control are analysed and its implementation is described.

5.2.2.2.1 Low voltage systems without virtual inductance

In low voltage, the line reactance is negligible compared with the line resistance:

$$\omega L_l \ll R_l. \tag{5.33}$$

This is actually the opposite of what was assumed in (5.23); thus, the power computations performed from (5.24) onwards are not valid in the present case. The approximated steady-state current, active and reactive power can be computed by applying (5.33) to the equations (5.15), (5.21)-(5.22), that are here reported for the sake of clarity.

$$\begin{aligned} \boldsymbol{I}(t) \approx & \frac{\bar{V}_i \omega L_l \sin(\bar{\delta}) + R_l[\bar{V}_i \cos(\bar{\delta}) - V_g]}{R_l^2 + \omega^2 L_l^2} \\ & + \mathrm{j}\frac{\omega L_l[-\bar{V}_i \cos(\bar{\delta}) + V_g] + R_l \bar{V}_i \sin(\bar{\delta})}{R_l^2 + \omega^2 L_l^2} \end{aligned} \tag{5.34}$$

$$P(t) \approx \frac{V_g\{\bar{V}_i \omega L_l \bar{\delta} + R_l[\bar{V}_i - V_g]\}}{2(R_l^2 + \omega^2 L_l^2)}, \tag{5.35}$$

$$Q(t) \approx \frac{V_g\{\omega L_l[\bar{V}_i - V_g] - R_l \bar{V}_i \bar{\delta}\}}{2(R_l^2 + \omega^2 L_l^2)}. \tag{5.36}$$

Considering (5.33), the reactive component of the line impedance can be neglected. Applying this approximation, together with the small-δ approximation in (5.20), leads to the following steady-state expressions for the line current and active and reactive powers:

$$\bar{\boldsymbol{I}} \approx \frac{\bar{V}_i - V_g}{R_l} + \mathrm{j}\frac{\bar{V}_i \bar{\delta}}{R_l}, \tag{5.37}$$

$$\bar{P} \approx \frac{V_g[\bar{V}_i - V_g]}{2\,R_l}, \tag{5.38}$$

$$\bar{Q} \approx \frac{\bar{V}_i\, V_g\, \bar{\delta}}{2\,R_l}. \tag{5.39}$$

The same notation applied to the droop controller equations is used here to denote steady-state values and perturbed variables.

Thus, linearising (5.38)-(5.39) and considering small perturbations about the equilibrium point, the perturbed expressions for the powers in this case are given by

$$\tilde{P}(t) \approx \frac{V_g \tilde{V}_i(t)}{2\,R_l}\,, \tag{5.40}$$

$$\tilde{Q}(t) \approx \frac{\bar{V}_i\,V_g}{2\,R_l}\,\tilde{\delta}(t) + \frac{V_g\,\bar{\delta}}{2\,R_l}\tilde{V}_i(t)\,. \tag{5.41}$$

From (5.40) and (5.41), it can be noticed that nature of the dependence of $\tilde{P}$ and $\tilde{Q}$ on $\tilde{V}_i$ and $\tilde{\delta}$ is swapped if compared with (5.27) and (5.41).

5.2.2.2.2 Low voltage systems with virtual inductance

In this section, a virtual inductance is added to the controller and the powers are recomputed according to the new system.

Assuming that the output voltage of the inverter is instantaneously equal to the droop output (5.31b) gives

$$\boldsymbol{v}_{\mathrm{i_{dq}}}(t) = \begin{bmatrix} V_d(t) \\ 0 \end{bmatrix}\,, \tag{5.42}$$

where V_d is the amplitude of the droop voltage and the q component of the voltage is set to 0.

Adding a virtual inductance means modifying the reference voltage by subtracting a voltage drop on a fictitious inductor, as follows:

$$\boldsymbol{v}_{\mathrm{i_{dq}}}(t) = \begin{bmatrix} V_d(t) \\ 0 \end{bmatrix} - \mathrm{j}\omega\,L_v\,\boldsymbol{I}(t)\,, \tag{5.43}$$

where L_v has the dimensions of an inductance and its value is chosen so that

$$R_l \ll \omega L_v. \tag{5.44}$$

The current phasor $\boldsymbol{I}$ can be computed substituting (5.43) into (5.34) and ne-

glecting the inductive component of the impedance, leading to

$$\boldsymbol{I}(t) \approx \frac{\boldsymbol{v}_{\mathrm{i_{dq}}}(t) - V_g + \mathrm{j}V_g\delta(t)}{R_l} = \frac{V_d(t) - \mathrm{j}\omega L_v \boldsymbol{I}(t) - V_g + \mathrm{j}V_g\delta(t)}{R_l}. \quad (5.45)$$

Isolating $\boldsymbol{I}$ in (5.45) leads to

$$\boldsymbol{I}(t) \sim \frac{V_d(t) - V_g + \mathrm{j}V_g\delta(t)}{R_l + \mathrm{j}\,\omega L_v}. \quad (5.46)$$

Using (5.44) in (5.46) allows a further approximation to be performed:

$$\boldsymbol{I}(t) \sim \frac{V_g\,\delta(t)}{\omega L_v} - \mathrm{j}\frac{V_d(t) - V_g}{\omega L_v}. \quad (5.47)$$

Using (5.47) and (5.43) to compute the apparent power leads to

$$\begin{aligned}
\boldsymbol{S}(t) \sim & \frac{(V_d(t) - \mathrm{j}\,\omega L_v\,\boldsymbol{I}(t))\,\boldsymbol{I(t)}^*}{2} \\
= & \frac{V_d(t)\boldsymbol{I}(t)^* - \mathrm{j}\,\omega L_v|\boldsymbol{I}(t)|^2}{2} \\
= & \frac{V_g\,\delta(t)\,V_d(t)}{2\omega L_v} + \mathrm{j}\frac{V_d(t)\,[V_d(t) - V_g] - V_g^2\,(\delta(t))^2 - [V_d(t) - V_g]^2}{2\omega L_v} \\
= & \frac{V_g\,\delta(t)\,V_d(t)}{2\omega L_v} + \mathrm{j}\frac{V_g\,V_d(t) - V_g^2 - V_g^2(\delta(t))^2}{2\omega L_v}.
\end{aligned} \quad (5.48)$$

Let $\bar{V}_d$ be the steady-state value for $V_d(t)$. Therefore, the steady-state expressions for P and Q, depending on V_d and δ, in this case can be approximated by

$$\bar{P} \approx \frac{V_g\,\bar{\delta}\,\bar{V}_d}{2\omega L_v}, \quad (5.49)$$

$$\bar{Q} \approx \frac{V_g\,\bar{V}_d - V_g^2 - V_g^2\bar{\delta}^2}{2\omega L_v}. \quad (5.50)$$

Since $\bar{\delta}$ is small,

$$V_g^2\,\bar{\delta}^2 \ll V_g\,\bar{V}_d, \quad (5.51a)$$

$$V_g^2\,\bar{\delta}^2 \ll V_g^2. \quad (5.51b)$$

Hence, (5.50) can be approximated as

$$\bar{Q} \sim \frac{V_g \bar{V}_d - V_g^2}{2\omega L_v} . \tag{5.52}$$

Equations (5.49) and (5.52) are the steady-state equations for active and reactive power, respectively. If (5.49)- (5.52) are linearised, their behaviours for small perturbations become

$$\tilde{P}(t) \approx \frac{V_g \bar{\delta}}{2\omega L_v} \tilde{V}_d(t) + \frac{V_g \bar{V}_d}{2\omega L_v} \tilde{\delta}(t) , \tag{5.53}$$

$$\tilde{Q}(t) \approx \frac{V_g}{2\omega L_v} \tilde{V}_d(t) . \tag{5.54}$$

The relationships stated in (5.53) and (5.54) between active and reactive powers, voltage amplitude and phase have the same structure observable in (5.27) and (5.28). This allows the droop controller to be applied effectively to the system.

5.2.2.2.2 Low-pass filter

In the examined case, a second low-pass filter is added to the measure of the current $\boldsymbol{i}_{\mathrm{o_{dq}}}$ to avoid excessive oscillations. This adds two more variables and ODEs to the system.

The filtered DQ currents are defined by

$$\frac{\mathrm{d}i_{\mathrm{lp_d}}(t)}{\mathrm{d}t} = \omega_{ci}[i_{\mathrm{o_d}}(t) - i_{\mathrm{lp_d}}(t)] , \tag{5.55a}$$

$$\frac{\mathrm{d}i_{\mathrm{lp_q}}(t)}{\mathrm{d}t} = \omega_{ci}[i_{\mathrm{o_q}}(t) - i_{\mathrm{lp_q}}(t)] . \tag{5.55b}$$

5.2.2.2.3 Joint action of droop control and virtual inductance

The droop controller, or the joint presence of the droop controller and the virtual inductance, determines how the output frequency and voltage of the converter change. In particular, a change in the voltage computed by the droop does not have a direct effect, but it represents a reference for the PI voltage controller, described in the next subsubsection.

The voltage references computed by applying a droop controller and a virtual

reference are given by

$$v_{\mathrm{ref_d}}(t) = V_{\mathrm{d_n}} + K_{dq}(Q_{\mathrm{ref}} - Q_{\mathrm{lp}}(t)) + L_v\{[\omega_n + K_{dp}(P_{\mathrm{ref}} - P_{\mathrm{lp}}(t))]i_{\mathrm{lp_q}}(t) + \omega_{ci}(i_{\mathrm{lp_d}}(t) - i_{\mathrm{o_d}}(t))\}, \tag{5.56a}$$

$$v_{\mathrm{ref_q}}(t) = V_{\mathrm{q_n}} + L_v\{-[\omega_n + K_{dp}(P_{\mathrm{ref}} - P_{\mathrm{lp}}(t))]i_{\mathrm{lp_d}}(t) + \omega_{ci}(i_{\mathrm{lp_q}}(t) - i_{\mathrm{o_q}}(t))\}. \tag{5.56b}$$

Equations (5.56) are the final expressions for the output voltage references: they combine the action of droop controller and virtual inductance, and constitute the input of the voltage proportional-integral controller, which is analysed in the next section.

5.2.2.3 Voltage Proportional-Integral Control

The voltage PI receives the angular frequency $\omega(t)$ from the droop controller and the voltage references $\boldsymbol{v}_{\mathrm{ref_{dq}(t)}}$ from the virtual inductance block, as stated in (5.56).
Its output is the DQ0 reference for the currents $\boldsymbol{i}_{\mathrm{i_{dq}(t)}}$:

$$i_{\mathrm{ref_d}}(t) = K_{vp}[v_{\mathrm{ref_d}}(t) - v_{\mathrm{i_d}}(t)] + K_{vi}\, x_{\mathrm{int,v_d}}(t) - \omega(t)\, C_f\, v_{\mathrm{i_q}}(t), \tag{5.57a}$$

$$i_{\mathrm{ref_q}}(t) = K_{vp}[v_{\mathrm{ref_q}}(t) - v_{\mathrm{i_q}}(t)] + K_{vi}\, x_{\mathrm{int,v_q}}(t) + \omega(t)\, C_f\, v_{\mathrm{i_d}}(t)\,, \tag{5.57b}$$

where K_{vp} and K_{vi} are the proportional and the integral coefficients of the voltage PI, $\boldsymbol{x}_{\mathrm{int,v_{dq}}}(t)$ are the integral variables for the voltage error and are defined by

$$\frac{\mathrm{d}\boldsymbol{x}_{\mathrm{int,v_{dq}}}(t)}{\mathrm{d}t} = \boldsymbol{v}_{\mathrm{ref_{dq}}}(t) - \boldsymbol{v}_{\mathrm{i_{dq}}}(t)\,. \tag{5.58}$$

5.2.2.4 Current Proportional-Integral Control

The current PI receives as inputs the angular frequency $\omega(t)$ from the droop controller and the current references $\boldsymbol{i}_{\mathrm{ref_{dq}(t)}}$ from the voltage PI, computed as (5.57).

Its output is the DQ0 vector of the modulation indices, scaled by $V_{DC}/2$.

$$m_{\mathrm{d}}(t) \;=\; \Big\{K_{ip}[i_{rmref_d}(t) \;-\; i_{\mathrm{i_d}}(t)] \;+\; K_{ii}\, x_{\mathrm{int,i_d}}(t) \;-\; \omega(t)\, L_f\, i_{\mathrm{i_q}}(t)\Big\}\frac{2}{V_{DC}}\,, \tag{5.59a}$$

$$m_{\mathrm{q}}(t) \;=\; \Big\{K_{ip}[i_{\mathrm{ref_q}}(t) \;-\; i_{\mathrm{i_q}}(t)] \;+\; K_{ii}\, x_{\mathrm{int,i_q}}(t) \;+\; \omega(t)\, L_f\, i_{\mathrm{i_d}}(t)\Big\}\frac{2}{V_{DC}}\,, \tag{5.59b}$$

where K_{ip} and K_{ii} are the proportional and the integral coefficients of the current PI, $\boldsymbol{x}_{\mathrm{int,i_{dq}}}(t)$ are the integral variables for the current error and are defined by

$$\frac{\mathrm{d}\boldsymbol{x}_{\mathrm{int,i_{dq}}}(t)}{\mathrm{d}t} \;=\; \boldsymbol{i}_{\mathrm{ref_{dq}}}(t) \;-\; \boldsymbol{i}_{\mathrm{i_{dq}}}(t)\,. \tag{5.60}$$

5.2.3 Complete State-Space Model

As explained in §5.2.1, the average behaviour of the system physical variables can be modelled by six ODEs. In order to model also the controller action, another nine ODEs must be added: two for the power low-pass filter, two for the current low-pass filter, one for the phase, two for the voltage integral variables, and two for the current integral variables.

The complete state-space model of the system is given by (5.61), where the system variables are listed in Table 5.1 and the system parameters in Table 5.2.

$\boldsymbol{i}_{\mathrm{i_{abc}}}$	Average currents entering the LC filter, ABC reference frame
$\boldsymbol{i}_{\mathrm{i_{dq}}}$	Average currents entering the LC filter, DQ0 reference frame
$\boldsymbol{v}_{\mathrm{i_{abc}}}$	Average voltages on the filter capacitors, ABC reference frame
$\boldsymbol{v}_{\mathrm{i_{dq}}}$	Average voltages on the filter capacitors, DQ0 reference frame
$\boldsymbol{i}_{\mathrm{o_{abc}}}$	Average currents entering the transmission line, ABC reference frame
$\boldsymbol{i}_{\mathrm{o_{dq}}}$	Average currents entering the transmission line, DQ0 reference frame
$\boldsymbol{m}_{\mathrm{abc}}$	Inverter modulation indices, ABC reference frame
$\boldsymbol{m}_{\mathrm{dq}}$	Inverter modulation indices, DQ0 reference frame
P_{lp}	Low-pass-filtered active power
Q_{lp}	Low-pass-filtered reactive power
$\boldsymbol{i}_{\mathrm{lp_{dq}}}$	Low-pass filter on $\boldsymbol{i}_{\mathrm{o_{dq}}}$
$\boldsymbol{x}_{\mathrm{int,v_{dq}}}$	Integral variable of the error on $\boldsymbol{v}_{\mathrm{i_{dq}}}$
$\boldsymbol{x}_{\mathrm{int,i_{dq}}}$	Integral variable of the error on $\boldsymbol{i}_{\mathrm{i_{dq}}}$
θ	Phase angle of $v_{\mathrm{i_a}}$, used in the Park transformation matrices

Table 5.1: AC microgrids, single inverter - List of the system variables

ω_{cd}	Power low-pass filter cut-off angular frequency	$10 \cdot 2\pi$ rad/s
ω_{ci}	Current low-pass filter cut-off angular frequency	$20 \cdot 2\pi$ rad/s
V_g	Grid nominal peak voltage	$\sqrt{2} \cdot 230$ V
f_g	Grid nominal frequency	50 Hz
T_g	Grid nominal period	0.020 s
ω_n	Grid nominal angular frequency	$50 \cdot 2\pi$ rad/s
K_{dp}	Droop control active power coefficient	$2.0 \cdot 10^{-4}$ rad/J
K_{dq}	Droop control reactive power coefficient	$2.5 \cdot 10^{-3}$ V/VAR
P_{ref}	Active power reference for droop control	5202.7 W
Q_{ref}	Reactive power reference for droop control	2439.3 VAR
V_{d_n}	Reference for v_{i_d} without droop control and virtual inductance	398.79 V
V_{q_n}	Reference for v_{i_q} without droop control and virtual inductance	41.03 V
L_v	Virtual inductance	0.010 H
K_{vp}	Voltage PI proportional coefficient	0.1257 $(\Omega)^{-1}$
K_{vi}	Voltage PI integral coefficient	78.9568 $(\Omega\text{s})^{-1}$
K_{ip}	Current PI proportional coefficient	16.8646 Ω
K_{ii}	Current PI integral coefficient	$5.3296 \cdot 10^4$ Ω/s
L_f	Filter inductance	$1.35 \cdot 10^{-3}$ H
R_f	Filter resistance	0.1 Ω
C_f	Filter capacitance	$50 \cdot 10^{-6}$ F
L_l	Line inductance	$1.0 \cdot 10^{-3}$ H
R_l	Line resistance	0.5 Ω
R_{load}	Load resistance	30 Ω
V_{DC}	DC source voltage	800 V

Table 5.2: AC microgrids, single inverter - System parameters: symbol, description, value.

$$\frac{\mathrm{d}P_{\mathrm{lp}}(t)}{\mathrm{d}t} = \omega_{cd}[v_{\mathrm{i_d}}(t)\, i_{\mathrm{o_d}}(t) + v_{\mathrm{i_q}}(t)\, i_{\mathrm{o_q}}(t) - P_{\mathrm{lp}}(t)]\,, \tag{5.61a}$$

$$\frac{\mathrm{d}Q_{\mathrm{lp}}(t)}{\mathrm{d}t} = \omega_{cd}[v_{\mathrm{i_d}}(t)\, i_{\mathrm{o_q}}(t) - v_{\mathrm{i_q}}(t)\, i_{\mathrm{o_d}}(t) - Q_{\mathrm{lp}}(t)]\,, \tag{5.61b}$$

$$\frac{\mathrm{d}\theta(t)}{\mathrm{d}t} = \omega(t)\,, \tag{5.61c}$$

$$\frac{\mathrm{d}i_{lp_d}(t)}{\mathrm{d}t} = \omega_{ci}[i_{\mathrm{o_d}}(t) - i_{\mathrm{lp_d}}(t)]\,, \tag{5.61d}$$

$$\frac{\mathrm{d}i_{\mathrm{lp_q}}(t)}{\mathrm{d}t} = \omega_{ci}[i_{\mathrm{o_q}}(t) - i_{\mathrm{lp_q}}(t)]\,, \tag{5.61e}$$

$$\frac{\mathrm{d}x_{\mathrm{int,v_d}}(t)}{\mathrm{d}t} = v_{\mathrm{ref_d}}(t) - v_{\mathrm{i_d}}(t)\,, \tag{5.61f}$$

$$\frac{\mathrm{d}x_{\mathrm{int,v_q}}(t)}{\mathrm{d}t} = v_{\mathrm{ref_q}}(t) - v_{\mathrm{i_q}}(t)\,, \tag{5.61g}$$

$$\frac{\mathrm{d}x_{\mathrm{int,i_d}}(t)}{\mathrm{d}t} = i_{\mathrm{ref_d}}(t) - i_{\mathrm{i_d}}(t)\,, \tag{5.61h}$$

$$\frac{\mathrm{d}x_{\mathrm{int,i_q}}(t)}{\mathrm{d}t} = i_{\mathrm{ref_q}}(t) - i_{\mathrm{i_q}}(t) \tag{5.61i}$$

$$\frac{\mathrm{d}i_{\mathrm{i_d}}(t)}{\mathrm{d}t} = \frac{V_{DC}}{2\,L_f} m_{\mathrm{d}}(t) - \frac{R_f}{L_f} i_{\mathrm{i_d}}(t) - \frac{v_{\mathrm{i_d}}(t)}{L_f} + \omega(t)\, i_{\mathrm{i_q}}(t)\,, \tag{5.61j}$$

$$\frac{\mathrm{d}i_{\mathrm{i_q}}(t)}{\mathrm{d}t} = \frac{V_{DC}}{2\,L_f} m_{\mathrm{q}}(t) - \frac{R_f}{L_f} i_{\mathrm{i_q}}(t) - \frac{v_{\mathrm{i_q}}(t)}{L_f} - \omega(t)\, i_{\mathrm{i_d}}(t)\,, \tag{5.61k}$$

$$\frac{\mathrm{d}v_{\mathrm{i_d}}(t)}{\mathrm{d}t} = \frac{i_{\mathrm{i_d}}(t)}{C_f} - \frac{i_{\mathrm{o_d}}(t)}{C_f} + \omega(t)\, v_{\mathrm{i_q}}(t)\,, \tag{5.61l}$$

$$\frac{\mathrm{d}v_{\mathrm{i_q}}(t)}{\mathrm{d}t} = \frac{i_{\mathrm{i_q}}(t)}{C_f} - \frac{i_{\mathrm{o_q}}(t)}{C_f} - \omega(t)\, v_{\mathrm{i_d}}(t)\,, \tag{5.61m}$$

$$\frac{\mathrm{d}i_{\mathrm{o_d}}(t)}{\mathrm{d}t} = \frac{v_{\mathrm{i_d}}(t)}{L_l} - \frac{R_l + R_{\mathrm{load}}}{L_l} i_{\mathrm{o_d}}(t) + \omega(t)\, i_{\mathrm{o_q}}(t)\,, \tag{5.61n}$$

$$\frac{\mathrm{d}i_{\mathrm{o_q}}(t)}{\mathrm{d}t} = \frac{v_{\mathrm{i_q}}(t)}{L_l} - \frac{R_l + R_{\mathrm{load}}}{L_l} i_{\mathrm{o_q}}(t) - \omega(t)\, i_{\mathrm{o_d}}(t)\,, \tag{5.61o}$$

where $\omega(t)$, $\boldsymbol{v}_{\mathrm{ref_{dq}}}(t)$, $\boldsymbol{v}_{\mathrm{i_{dq}}}(t)$, $\boldsymbol{i}_{\mathrm{ref_{dq}}}(t)$, $\boldsymbol{m}_{\mathrm{dq}}(t)$ are given by the following algebraic equations:

$$\omega(t) \;=\; \omega_n \;+\; K_{dp}\,(P_{\text{ref}} \;-\; P_{\text{lp}}(t))\,, \tag{5.62a}$$

$$\begin{aligned} v_{\text{ref}_\text{d}}(t) = V_{\text{d}_\text{n}} + K_{dq}(Q_{\text{ref}} - Q_{\text{lp}}(t)) \\ + L_v\{[\omega_n + K_{dp}(P_{\text{ref}} - P_{rmlp}(t))]i_{\text{lp}_\text{q}}(t) + \omega_{ci}(i_{\text{lp}_\text{d}}(t) - i_{\text{o}_\text{d}}(t))\}, \end{aligned} \tag{5.62b}$$

$$\begin{aligned} v_{\text{ref}_\text{q}}(t) = V_{\text{q}_\text{n}} + L_v\{ - [\omega_n + K_{dp}(P_{\text{ref}} - P_{\text{lp}}(t))]i_{\text{lp}_\text{d}}(t) \\ + \omega_{ci}(i_{\text{lp}_\text{q}}(t) - i_{\text{o}_\text{q}}(t))\}, \end{aligned} \tag{5.62c}$$

$$i_{\text{ref}_\text{d}}(t) \;=\; K_{vp}[v_{\text{ref}_\text{d}}(t) \;-\; v_{\text{i}_\text{d}}(t)] \;+\; K_{vi}\,x_{\text{int,v}_\text{d}}(t) \;-\; \omega(t)\,C_f\,v_{\text{i}_\text{q}}(t), \tag{5.62d}$$

$$i_{\text{ref}_\text{q}}(t) \;=\; K_{vp}[v_{\text{ref}_\text{q}}(t) \;-\; v_{\text{i}_\text{q}}(t)] \;+\; K_{vi}\,x_{\text{int,v}_\text{q}}(t) \;+\; \omega(t)\,C_f\,v_{\text{i}_\text{d}}(t)\,, \tag{5.62e}$$

$$m_{\text{d}}(t) \;=\; \Big\{K_{ip}[i_{\text{ref}_\text{d}}(t) \;-\; i_{\text{i}_\text{d}}(t)] \;+\; K_{ii}\,x_{\text{int,i}_\text{d}}(t) \;-\; \omega(t)\,L_f\,i_{\text{i}_\text{q}}(t)\Big\}\frac{2}{V_{DC}}\,, \tag{5.62f}$$

$$m_{\text{q}}(t) \;=\; \Big\{K_{ip}[i_{\text{ref}_\text{q}}(t) \;-\; i_{\text{i}_\text{q}}(t)] \;+\; K_{ii}\,x_{\text{int,i}_\text{q}}(t) \;+\; \omega(t)\,L_f\,i_{\text{i}_\text{d}}(t)\Big\}\frac{2}{V_{DC}}\,. \tag{5.62g}$$

5.3 Single Inverter Model Reduction

5.3.1 Nondimensionalisation

In order to proceed with the reduction of the model described in §5.2, all the parameters listed in Table 3.1 have been nondimensionalised. Parameters T_b, R_b and V_b have been chosen as base values for time, resistance and voltage, respectively, and their values are given by

$$T_b = 0.25 \text{ s}, \tag{5.63a}$$

$$V_b = \sqrt{1.5} V_g = \sqrt{3} \cdot 230 \text{ V}, \tag{5.63b}$$

$$R_b = 30 \ \Omega. \tag{5.63c}$$

The base value for the time is bigger than the grid nominal period (0.02 s) because the droop control action is in general slow, with time constants of order 1 s or 0.1 s. The base value for the voltage is equal to the nominal value of the grid voltage in the DQ reference frame; it corresponds to an amplitude of $\sqrt{2}\,230$ V. The resistance base value is the resistance of the load.
Using (5.63) to nondimensionalise the system, the variables of Table 5.3 and the parameters of Table 5.4 can be obtained. In this section, $\hat{x}$ is used to denote the dimensionless parameter/variable corresponding to the dimensional variable x. In Table 5.3, the modulation indices and the phase angle are reported without modifications, as they are already dimensionless. To each nondimensionalised parameter, a magnitude order is attributed in terms of powers of a small dimensionless parameter ϵ.

$\hat{\boldsymbol{i}}_{\mathrm{i_{abc}}}(\hat{t}) = \boldsymbol{i}_{\mathrm{i_{abc}}}(t)\, V_b^{-1} R_b$	Average currents entering the LC filter, ABC reference frame
$\hat{\boldsymbol{i}}_{\mathrm{i_{dq}}}(\hat{t}) = \boldsymbol{i}_{\mathrm{i_{dq}}}(t)\, V_b^{-1} R_b$	Average currents entering the LC filter, DQ0 reference frame
$\hat{\boldsymbol{v}}_{\mathrm{i_{abc}}}(\hat{t}) = \boldsymbol{v}_{\mathrm{i_{abc}}}(t)\, V_b^{-1}$	Average voltages on the filter capacitors, ABC reference frame
$\hat{\boldsymbol{v}}_{\mathrm{i_{abc}}}(\hat{t}) = \boldsymbol{v}_{\mathrm{i_{dq}}}(t)\, V_b^{-1}$	Average voltages on the filter capacitors, DQ0 reference frame
$\hat{\boldsymbol{i}}_{\mathrm{o_{abc}}}(\hat{t}) = \boldsymbol{i}_{\mathrm{o_{abc}}}(t)\, V_b^{-1} R_b$	Average currents entering the transmission line, ABC reference frame
$\hat{\boldsymbol{i}}_{\mathrm{o_{dq}}}(\hat{t}) = \boldsymbol{i}_{\mathrm{o_{dq}}}(t)\, V_b^{-1} R_b$	Average currents entering the transmission line, DQ0 reference frame
$\boldsymbol{m}_{\mathrm{abc}}(\hat{t})$	Inverter modulation indices, ABC reference frame
$\boldsymbol{m}_{\mathrm{dq}}(\hat{t})$	Inverter modulation indices, DQ0 reference frame
$\hat{P}_{\mathrm{lp}}(\hat{t}) = P_{\mathrm{lp}}(t) V_b^{-2} R_b$	Low-pass-filtered active power
$\hat{Q}_{\mathrm{lp}}(\hat{t}) = Q_{\mathrm{lp}}(t) V_b^{-2} R_b$	Low-pass-filtered reactive power
$\hat{\boldsymbol{i}}_{\mathrm{i_{lp}}}(\hat{t}) = \boldsymbol{i}_{\mathrm{i_{lp}}}(t)\, V_b^{-1} R_b$	Low-pass filter on $\hat{\boldsymbol{i}}_{\mathrm{o_{dq}}}(\hat{t})$
$\hat{\boldsymbol{x}}_{\mathrm{int,v_{dq}}}(\hat{t}) = \boldsymbol{x}_{\mathrm{int,v_{dq}}}(t)\, V_b^{-1} T_b^{-1}$	Integral variable of the error on $\hat{\boldsymbol{v}}_{\mathrm{i_{dq}}}(\hat{t})$
$\hat{\boldsymbol{x}}_{\mathrm{int,i_{dq}}}(\hat{t}) = \boldsymbol{x}_{\mathrm{int,i_{dq}}}(t)\, V_b^{-1} T_b^{-1}$	Integral variable of the error on $\hat{\boldsymbol{i}}_{\mathrm{i_{dq}}}(t)$
$\theta(\hat{t})$	Phase angle of $\hat{v}_{i_a}$, used in the Park transformation matrices
$\hat{t} = t T_b^{-1}$	Time

Table 5.3: AC microgrids, single inverter - System dimensionless variables

The overall nondimensionalised system is thus

$$\frac{\mathrm{d}\hat{P}_{\mathrm{lp}}(\hat{t})}{\mathrm{d}\hat{t}} = \hat{\omega}_{cd}[\hat{v}_{\mathrm{i_d}}(\hat{t})\,\hat{i}_{\mathrm{o_d}}(\hat{t}) + \hat{v}_{\mathrm{i_q}}(\hat{t})\,\hat{i}_{\mathrm{o_q}}(\hat{t}) - \hat{P}_{\mathrm{lp}}(\hat{t})]\,, \tag{5.64a}$$

$$\frac{\mathrm{d}\hat{Q}_{\mathrm{lp}}(\hat{t})}{\mathrm{d}\hat{t}} = \hat{\omega}_{cd}[\hat{v}_{\mathrm{i_d}}(\hat{t})\,\hat{i}_{\mathrm{o_q}}(\hat{t}) - \hat{v}_{\mathrm{i_q}}(\hat{t})\,\hat{i}_{\mathrm{o_d}}(\hat{t}) - \hat{Q}_{\mathrm{lp}}(\hat{t})]\,, \tag{5.64b}$$

$$\frac{\mathrm{d}\theta(\hat{t})}{\mathrm{d}\hat{t}} = \hat{\omega}_n + \hat{K}_{dp}[\hat{P}_{\mathrm{ref}} - \hat{P}_{\mathrm{lp}}(t)]\,, \tag{5.64c}$$

$$\frac{\mathrm{d}\hat{i}_{\mathrm{lp_d}}(\hat{t})}{\mathrm{d}\hat{t}} = \hat{\omega}_{ci}[\hat{i}_{\mathrm{o_d}}(\hat{t}) - \hat{i}_{\mathrm{lp_d}}(\hat{t})]\,, \tag{5.64d}$$

$$\frac{\mathrm{d}\hat{i}_{\mathrm{lp_q}}(\hat{t})}{\mathrm{d}\hat{t}} = \hat{\omega}_{ci}[\hat{i}_{\mathrm{o_q}}(\hat{t}) - \hat{i}_{\mathrm{lp_q}}(\hat{t})]\,, \tag{5.64e}$$

$$\frac{\mathrm{d}\hat{x}_{\mathrm{int,v_d}}(\hat{t})}{\mathrm{d}\hat{t}} = \hat{v}_{\mathrm{ref_d}}(\hat{t}) - \hat{v}_{\mathrm{i_d}}(\hat{t})\,, \tag{5.64f}$$

$$\frac{\mathrm{d}\hat{x}_{\mathrm{int,v_q}}(\hat{t})}{\mathrm{d}\hat{t}} = \hat{v}_{\mathrm{ref_q}}(\hat{t}) - \hat{v}_{\mathrm{i_q}}(\hat{t})\,, \tag{5.64g}$$

$$\frac{\mathrm{d}\hat{x}_{\mathrm{int,i_d}}(\hat{t})}{\mathrm{d}\hat{t}} = \hat{i}_{\mathrm{ref_d}}(\hat{t}) - \hat{i}_{\mathrm{i_d}}(\hat{t})\,, \tag{5.64h}$$

$$\frac{\mathrm{d}\hat{x}_{\mathrm{int,i_q}}(\hat{t})}{\mathrm{d}\hat{t}} = \hat{i}_{\mathrm{ref_q}}(\hat{t}) - \hat{i}_{\mathrm{i_q}}(\hat{t}) \tag{5.64i}$$

$$\frac{\mathrm{d}\hat{i}_{\mathrm{i_d}}(\hat{t})}{\mathrm{d}\hat{t}} = \frac{\hat{V}_{DC}}{2\,\hat{L}_f} m_{\mathrm{d}}(\hat{t}) - \frac{\hat{R}_f}{\hat{L}_f}\hat{i}_{\mathrm{i_d}}(\hat{t}) - \frac{\hat{v}_{\mathrm{i_d}}(\hat{t})}{\hat{L}_f} + \hat{\omega}(\hat{t})\,\hat{i}_{\mathrm{i_q}}(\hat{t})\,, \tag{5.64j}$$

$$\frac{\mathrm{d}\hat{i}_{\mathrm{i_q}}(\hat{t})}{\mathrm{d}\hat{t}} = \frac{\hat{V}_{DC}}{2\,\hat{L}_f} m_{\mathrm{q}}(\hat{t}) - \frac{\hat{R}_f}{\hat{L}_f}\hat{i}_{\mathrm{i_q}}(\hat{t}) - \frac{\hat{v}_{\mathrm{i_q}}(t)}{\hat{L}_f} - \hat{\omega}(\hat{t})\,\hat{i}_{\mathrm{i_d}}(\hat{t})\,, \tag{5.64k}$$

$$\frac{\mathrm{d}\hat{v}_{\mathrm{i_d}}(\hat{t})}{\mathrm{d}\hat{t}} = \frac{\hat{i}_{\mathrm{i_d}}(\hat{t})}{\hat{C}_f} - \frac{\hat{i}_{\mathrm{o_d}}(\hat{t})}{\hat{C}_f} + \hat{\omega}(\hat{t})\,\hat{v}_{\mathrm{i_q}}(\hat{t})\,, \tag{5.64l}$$

$$\frac{\mathrm{d}\hat{v}_{\mathrm{i_q}}(\hat{t})}{\mathrm{d}\hat{t}} = \frac{\hat{i}_{\mathrm{i_q}}(\hat{t})}{\hat{C}_f} - \frac{\hat{i}_{\mathrm{o_q}}(\hat{t})}{\hat{C}_f} - \hat{\omega}(\hat{t})\,\hat{v}_{\mathrm{i_d}}(\hat{t})\,, \tag{5.64m}$$

$$\frac{\mathrm{d}\hat{i}_{\mathrm{o_d}}(\hat{t})}{\mathrm{d}\hat{t}} = \frac{\hat{v}_{\mathrm{i_d}}(\hat{t})}{\hat{L}_l} - \frac{\hat{R}_l + \hat{R}_{\mathrm{load}}}{\hat{L}_l}\hat{i}_{\mathrm{o_d}}(\hat{t}) + \hat{\omega}(\hat{t})\,\hat{i}_{\mathrm{o_q}}(\hat{t})\,, \tag{5.64n}$$

$$\frac{\mathrm{d}\hat{i}_{\mathrm{o_q}}(\hat{t})}{\mathrm{d}\hat{t}} = \frac{\hat{v}_{\mathrm{i_q}}(\hat{t})}{\hat{L}_l} - \frac{\hat{R}_l + \hat{R}_{\mathrm{load}}}{\hat{L}_l}\hat{i}_{\mathrm{o_q}}(\hat{t}) - \hat{\omega}(\hat{t})\,\hat{i}_{\mathrm{o_d}}(\hat{t})\,, \tag{5.64o}$$

where

$$\hat{\omega}(\hat{t}) = \hat{\omega}_n + \hat{K}_{dp}\left(\hat{P}_{\mathrm{ref}} - \hat{P}_{\mathrm{lp}}(\hat{t})\right), \tag{5.65a}$$

$$\hat{v}_{\mathrm{ref_d}}(\hat{t}) = \hat{V}_{\mathrm{d_n}} + \hat{K}_{dq}(\hat{Q}_{\mathrm{ref}} - \hat{Q}_{\mathrm{lp}}(\hat{t})) + \hat{L}_v\{[\hat{\omega}_n + \hat{K}_{dp}(\hat{P}_{\mathrm{ref}} - \hat{P}_{\mathrm{lp}}(\hat{t}))]\hat{\imath}_{\mathrm{lp_q}}(\hat{t}) + \hat{\omega}_{ci}(\hat{\imath}_{\mathrm{lp_d}}(\hat{t}) - \hat{\imath}_{\mathrm{o_d}}(\hat{t}))\}, \quad (5.65b)$$

$$v_{\mathrm{ref_q}}(t) = V_{\mathrm{q_n}} + L_v\{-[\omega_n + K_{dp}(P_{\mathrm{ref}} - P_{\mathrm{lp}}(t))]i_{\mathrm{lp_d}}(t) + \omega_{ci}(i_{\mathrm{lp_q}}(t) - i_{\mathrm{o_q}}(t))\}, \quad (5.65c)$$

$$\hat{\imath}_{\mathrm{ref_d}}(\hat{t}) = \hat{K}_{vp}[\hat{v}_{\mathrm{ref_d}}(\hat{t}) - \hat{v}_{\mathrm{i_d}}(\hat{t})] + \hat{K}_{vi}\,\hat{x}_{\mathrm{int,v_d}}(\hat{t}) - \hat{\omega}(\hat{t})\,\hat{C}_f\,\hat{v}_{\mathrm{i_q}}(\hat{t}), \quad (5.65d)$$

$$\hat{\imath}_{\mathrm{ref_q}}(\hat{t}) = \hat{K}_{vp}[\hat{v}_{\mathrm{ref_q}}(\hat{t}) - \hat{v}_{\mathrm{i_q}}(\hat{t})] + \hat{K}_{vi}\,\hat{x}_{\mathrm{int,v_q}}(\hat{t}) + \hat{\omega}(\hat{t})\,\hat{C}_f\,\hat{v}_{\mathrm{i_d}}(\hat{t}), \quad (5.65e)$$

$$m_{\mathrm{d}}(\hat{t}) = \left\{\hat{K}_{ip}[\hat{\imath}_{\mathrm{ref_d}}(\hat{t}) - \hat{\imath}_{\mathrm{i_d}}(\hat{t})] + \hat{K}_{ii}\,\hat{x}_{\mathrm{int,i_d}}(\hat{t}) - \hat{\omega}(\hat{t})\,\hat{L}_f\,\hat{\imath}_{\mathrm{i_q}}(\hat{t})\right\}\frac{2}{\hat{V}_{DC}}, \quad (5.65f)$$

$$m_{\mathrm{q}}(\hat{t}) = \left\{\hat{K}_{ip}[\hat{\imath}_{\mathrm{ref_q}}(\hat{t}) - \hat{\imath}_{\mathrm{i_q}}(\hat{t})] + \hat{K}_{ii}\,\hat{x}_{\mathrm{int,i_q}}(\hat{t}) + \hat{\omega}(\hat{t})\,\hat{L}_f\,\hat{\imath}_{\mathrm{i_d}}(\hat{t})\right\}\frac{2}{\hat{V}_{DC}}. \quad (5.65g)$$

Power low-pass filter cut-off angular frequency	$\hat{\omega}_{cd} = \omega_{cd} T_b = 2\pi\, 2.50 \approx 15.7080$	$\mathcal{O}(1)$
Current low-pass filter cut-off angular frequency	$\hat{\omega}_{ci} = \omega_{cd} T_b = 2\pi\, 10.0 \approx 62.8319$	$\mathcal{O}(1)$ or $\mathcal{O}(\epsilon^{-1})$
Grid nominal peak voltage	$\hat{V}_g = V_g V_b^{-1} = \sqrt{2/3} \approx 0.8165$	$\mathcal{O}(1)$
Grid nominal frequency	$\hat{f}_g = f_g T_b = 12.50$	$\mathcal{O}(1)$
Grid nominal period	$\hat{T}_g = T_g T_b^{-1} = 0.0800$	$\mathcal{O}(1)$
Grid nominal angular frequency	$\hat{\omega}_n = \omega_n\, T_b = 2\pi\, 12.5 \approx 78.5398$	$\mathcal{O}(\epsilon^{-1})$
Droop control active power coefficient	$\hat{K}_{dp} = K_{dp} R_b\, V_b^2\, T_b \approx 0.2645$	$\mathcal{O}(1)$
Droop control reactive power coefficient	$\hat{K}_{dq} = K_{dq} V_b R_b^{-1} \approx 0.0332$	$\mathcal{O}(1)$
Active power reference for droop control	$\hat{P}_{\text{ref}} = P_{\text{ref}} V_b^{-2} R_b \approx 0.9835$	$\mathcal{O}(1)$
Reactive power reference for droop control	$\hat{Q}_{\text{ref}} = Q_{\text{ref}} V_b^{-2} R_b \approx 0.4611$	$\mathcal{O}(1)$
Reference for $\hat{v}_{i_d}$ entering the virtual inductance	$\hat{V}_{d_n} = V_{d_n} V_b^{-1} \approx 1.0011$	$\mathcal{O}(1)$
Reference for $\hat{v}_{i_q}$ entering the virtual inductance	$\hat{V}_{q_n} = V_{q_n} V_b^{-1} \approx 0.1030$	$\mathcal{O}(1)$
Virtual inductance	$\hat{L}_v = L_v R_b^{-1} T_b^{-1} \approx 1.333 \cdot 10^{-3}$	$\mathcal{O}(\bullet)$
Voltage PI proportional coefficient	$\hat{K}_{vp} = K_{vp}\, R_b \approx 3.7699$	$\mathcal{O}(1)$
Voltage PI integral coefficient	$\hat{K}_{vi} = K_{vi}\, R_b\, T_b \approx 592.1763$	$\mathcal{O}(\epsilon^{-1})$
Current PI proportional coefficient	$\hat{K}_{ip} = K_{ip}\, R_b^{-1} \approx 0.5622$	$\mathcal{O}(1)$
Current PI integral coefficient	$\hat{K}_{ii} = K_{ii}\, R_b^{-1}\, T_b \approx 444.1322$	$\mathcal{O}(\epsilon^{-1})$
Filter inductance	$\hat{L}_f = L_f R_b^{-1} T_b^{-1} = 1.8000 \cdot 10^{-4}$	$\mathcal{O}(\epsilon)$
Filter resistance	$\hat{R}_f = R_f R_b^{-1} \approx 3.3333 \cdot 10^{-3}$	$\mathcal{O}(\epsilon)$
Filter capacitance	$\hat{C}_f = C_f R_b T_b^{-1} = 6.0 \cdot 10^{-3}$	$\mathcal{O}(\epsilon)$
Line inductance	$\hat{L}_l = L_l R_b^{-1} T_b^{-1} = 1.3333 \cdot 10^{-4}$	$\mathcal{O}(\epsilon)$
Line resistance	$\hat{R}_l = R_l R_b^{-1} \approx 1.6667 \cdot 10^{-2}$	$\mathcal{O}(1)$
Load resistance	$\hat{R}_{\text{load}} = R_{\text{load}}\, R_b^{-1} = 1$	$\mathcal{O}(1)$
DC source voltage	$\hat{V}_{DC} = V_{DC}\, V_b^{-1} \approx 2.0082$	$\mathcal{O}(1)$

Table 5.4: AC microgrids - System nondimensionalised parameters: description, dimensionless value, "size"

5.3.2 Model reduction

In this work, the system is reduced by using perturbation theory and retaining the leading-order terms of each equation. In order to proceed with this, a single small dimensionless parameter ϵ is introduced. The choice of the value of ϵ, together with the attribution of the system parameters to powers of ϵ involves a certain degree of judgement about the importance of some aspects of the model. The attribution of a parameter to a power of ϵ may, in fact, lead one to ignore some physical processes and to retain only fewer aspects in the reduced model. Some informed judgements about the nature of the system and its working conditions are needed and the process involves some trial-and-error. In the present case, ϵ is assumed to be equal to 10^{-3}. Assigning particular powers of ϵ to quantities has been performed. In this section, ϵ is assumed to be of order 10^{-3}.
For the remainder of this section, the hats will be dropped from the notation of dimensionless variables. Since everything has been nondimensionalised before, this will not cause any ambiguity, but aid clarity of notation.
Before the system (5.64) is considered for reduction, performed in the following subsections, §5.3.2.1 gives a brief overview of the singular perturbation principles that are used later on in the section, to both help the reader understand the theoretical bases which have been applied while reducing the system, and describe the followed procedure in a more symbolic and compact way.

5.3.2.1 Introduction to Singular Perturbation Systems

In general, a system is singularly perturbed system if it can be modelled in the form

$$\frac{\mathrm{d}\boldsymbol{x}}{\mathrm{d}t} = \boldsymbol{f}(t,\, \boldsymbol{x},\, \boldsymbol{z},\, \epsilon), \tag{5.66a}$$

$$\epsilon\frac{\mathrm{d}\boldsymbol{z}}{\mathrm{d}t} = \boldsymbol{g}(t,\, \boldsymbol{x},\, \boldsymbol{z},\, \epsilon), \tag{5.66b}$$

where $\boldsymbol{x} \in \mathbb{R}^n$ and $\boldsymbol{z} \in \mathbb{R}^m$ are vectors of state-space variables and ϵ is a "small" dimensionless parameter. System (5.66) highlights the presence of a double option for the time scaling: variables grouped in $\boldsymbol{x}$ are "slow", while variables grouped

in $\boldsymbol{z}$ are "fast".

Letting $\epsilon \to 0$ turns the ODEs (5.66b) into the algebraic or transcendental equation

$$0 = \boldsymbol{g}(t, \boldsymbol{x}, \boldsymbol{z}, 0). \tag{5.67}$$

A system is said to be in standard form if (5.67) has at least one real root

$$\boldsymbol{z} = \boldsymbol{h}(t, \boldsymbol{x}). \tag{5.68}$$

Substituting (5.68) into (5.66a) and assuming $\epsilon \to 0$ leads to the reduced system

$$\frac{\mathrm{d}\boldsymbol{x}}{\mathrm{d}t} = \boldsymbol{f}(t, \boldsymbol{x}, \boldsymbol{h}(t, \boldsymbol{x}), \epsilon), \tag{5.69}$$

of dimension n [10].

The behaviour of the fast variables is more precisely modelled by ODEs, but in (5.69) is approximated by algebraic equations (5.68). In general, the approximation holds when bigger time scales/slow processes are considered, while some discrepancies occur during transients and observing faster phenomena. During transients, the algebraic or transcendental equations are not likely to model the system behaviour effectively, and the original ODEs are needed to provide an accurate determination of this transient behaviour.

Application of this approach to the microgrid systems defined in the previous sections is described next.

5.3.2.2 Constant frequency

Assuming that $\omega_n = \mathcal{O}(\epsilon^{-1})$, an auxiliary variable $\bar{\omega}_n = \mathcal{O}(1)$ can be defined by

$$\bar{\omega}_n = \epsilon\, \omega_n\,. \tag{5.70}$$

Substituting (5.70) into (5.64c) leads to

$$\omega(t) = \epsilon^{-1}\bar{\omega}_n + K_{dp}[P_{ref} - P_{lp}(t)]\,. \tag{5.71}$$

Since, according to the simulations, P is $\mathcal{O}(1)$, to avoid imbalance in (5.71) $\omega(t)$

must be $\mathcal{O}(\epsilon^{-1})$. A new $\mathcal{O}(1)$ variable can therefore be defined by

$$\bar{\omega}(t) \;=\; \epsilon\,\omega(t) \;=\; \bar{\omega}_n \;+\; \epsilon\,K_{dp}[P_{\text{ref}} \;-\; P_{\text{lp}}(t)]\,. \tag{5.72}$$

Hence, $\bar{\omega}(t)$ can be approximated by

$$\bar{\omega}(t) \;\sim\; \bar{\omega}_n \;+\; \mathcal{O}(\epsilon)\,. \tag{5.73}$$

Considering ω to constant and equal to ω_n leads to a reduction of the system (5.64) by one ODE and one state-space variable. The system is then given by

$$\frac{\mathrm{d}P_{\text{lp}}(t)}{\mathrm{d}t} \;=\; \omega_{cd}[v_{\text{i}_\text{d}}(t)\,i_{\text{o}_\text{d}}(t) \;-\; v_{\text{i}_\text{q}}(t)\,i_{\text{o}_\text{q}}(t) \;-\; P_{\text{lp}}(t)]\,, \tag{5.74a}$$

$$\frac{\mathrm{d}Q_{\text{lp}}(t)}{\mathrm{d}t} \;=\; \omega_{cd}[v_{\text{i}_\text{d}}(t)\,i_{\text{o}_\text{q}}(t) \;-\; v_{\text{i}_\text{q}}(t)\,i_{\text{o}_\text{d}}(t) \;-\; Q_{\text{lp}}(t)]\,, \tag{5.74b}$$

$$\frac{\mathrm{d}i_{\text{lp}_\text{d}}(t)}{\mathrm{d}t} \;=\; \omega_{ci}[i_{\text{o}_\text{d}}t) \;-\; i_{\text{lp}_\text{d}}(t)]\,, \tag{5.74c}$$

$$\frac{\mathrm{d}i_{\text{lp}_\text{q}}(t)}{\mathrm{d}t} \;=\; \omega_{ci}[i_{\text{o}_\text{q}}(t) \;-\; i_{\text{lp}_\text{q}}(t)]\,, \tag{5.74d}$$

$$\frac{\mathrm{d}x_{\text{int,v}_\text{d}}(t)}{\mathrm{d}\hat{t}} \;=\; v_{\text{ref}_\text{d}}(t) \;-\; v_{\text{i}_\text{d}}(t)\,, \tag{5.74e}$$

$$\frac{\mathrm{d}x_{\text{int,v}_\text{q}}(t)}{\mathrm{d}t} \;=\; v_{\text{ref}_\text{q}}(t) \;-\; v_{\text{i}_\text{q}}(t)\,, \tag{5.74f}$$

$$\frac{\mathrm{d}x_{\text{int,i}_\text{d}}(t)}{\mathrm{d}t} \;=\; i_{\text{ref}_\text{d}}(\hat{t}) \;-\; i_{\text{i}_\text{d}}(\hat{t})\,, \tag{5.74g}$$

$$\frac{\mathrm{d}x_{\text{int,i}_\text{q}}(t)}{\mathrm{d}t} \;=\; i_{\text{ref}_\text{q}}(t) \;-\; i_{\text{i}_\text{q}}(t) \tag{5.74h}$$

$$\frac{\mathrm{d}i_{\text{i}_\text{d}}(t)}{\mathrm{d}t} \;=\; \frac{V_{DC}}{2\,L_f}m_{\text{d}}(t) \;-\; \frac{R_f}{L_f}i_{\text{i}_\text{d}}(t) \;-\; \frac{v_{\text{i}_\text{d}}(t)}{L_f} \;+\; \omega_n\,i_{\text{i}_\text{q}}(t)\,, \tag{5.74i}$$

$$\frac{\mathrm{d}i_{\text{i}_\text{q}}(t)}{\mathrm{d}t} \;=\; \frac{V_{DC}}{2\,L_f}m_{\text{q}}(t) \;-\; \frac{R_f}{L_f}i_{\text{i}_\text{q}}(\hat{t}) \;-\; \frac{v_{\text{i}_\text{q}}(t)}{L_f} \;-\; \omega_n\,i_{\text{i}_\text{d}}(t)\,, \tag{5.74j}$$

$$\frac{\mathrm{d}v_{\text{i}_\text{d}}(t)}{\mathrm{d}t} \;=\; \frac{i_{\text{i}_\text{d}}(t)}{C_f} \;-\; \frac{i_{\text{o}_\text{d}}(t)}{C_f} \;+\; \omega_n\,v_{\text{i}_\text{q}}(t)\,, \tag{5.74k}$$

$$\frac{\mathrm{d}v_{\text{i}_\text{q}}(t)}{\mathrm{d}t} \;=\; \frac{i_{\text{i}_\text{q}}(t)}{C_f} \;-\; \frac{i_{\text{o}_\text{q}}(t)}{C_f} \;-\; \omega_n(t)\,v_{\text{i}_\text{d}}(t)\,, \tag{5.74l}$$

$$\frac{\mathrm{d}i_{\text{o}_\text{d}}(t)}{\mathrm{d}t} \;=\; \frac{v_{\text{i}_\text{d}}(t)}{L_l} \;-\; \frac{R_l + R_{\text{load}}}{L_l}i_{\text{o}_\text{d}}(t) \;+\; \omega_n\,i_{\text{o}_\text{q}}(t)\,, \tag{5.74m}$$

$$\frac{\mathrm{d}i_{\mathrm{o_q}}(t)}{\mathrm{d}t} \;=\; \frac{v_{\mathrm{i_q}}(t)}{L_l} \;-\; \frac{R_l + R_{\mathrm{load}}}{L_l} i_{\mathrm{o_q}}(t) \;-\; \omega_n \, i_{\mathrm{o_d}}(t)\,, \tag{5.74n}$$

where

$$v_{\mathrm{ref_d}}(t) = V_{\mathrm{d_n}} + K_{dq}(Q_{\mathrm{ref}} - Q_{\mathrm{lp}}(t)) + \tag{5.75a}$$
$$L_v\{[\omega_n + K_{dp}(P_{\mathrm{ref}} - P_{\mathrm{lp}}(t))] i_{\mathrm{lp_q}}(t) + \omega_{ci}(i_{\mathrm{lp_d}}(t) - i_{\mathrm{o_d}}(t))\},$$

$$v_{\mathrm{ref_q}}(t) = V_{\mathrm{q_n}} + L_v\{ - [\omega_n + K_{dp}(P_{\mathrm{ref}} - P_{\mathrm{lp}}(t))] i_{\mathrm{lp_d}}(t) + \omega_{ci}(i_{\mathrm{lp_q}}(t) - i_{\mathrm{o_q}}(t))\}, \tag{5.75b}$$

$$i_{\mathrm{ref_d}}(t) \;=\; K_{vp}[v_{\mathrm{ref_d}}(t) \;-\; v_{\mathrm{i_d}}(t)] \;+\; K_{vi}\, x_{\mathrm{int,v_d}}(t) \;-\; \omega_n \, C_f \, v_{\mathrm{i_q}}(t), \tag{5.75c}$$

$$i_{\mathrm{ref_q}}(t) \;=\; K_{vp}[v_{\mathrm{ref_q}}(t) \;-\; v_{\mathrm{i_q}}(t)] \;+\; K_{vi}\, x_{\mathrm{int,v_q}}(t) \;+\; \omega_n \, C_f \, v_{\mathrm{i_d}}(t)\,, \tag{5.75d}$$

$$m_{\mathrm{d}}(t) \;=\; \Big\{K_{ip}[i_{\mathrm{ref_d}}(t) \;-\; i_{\mathrm{i_d}}(t)] \;+\; K_{ii}\, x_{\mathrm{int,i_d}}(t) \;-\; \omega_n \, L_f \, i_{\mathrm{i_q}}(t)\Big\}\frac{2}{V_{DC}}\,, \tag{5.75e}$$

$$m_{\mathrm{q}}(t) \;=\; \Big\{K_{ip}[i_{\mathrm{ref_q}}(t) \;-\; i_{\mathrm{i_q}}(t)] \;+\; K_{ii}\, x_{\mathrm{int,i_q}}(t) \;+\; \omega_n \, L_f \, i_{\mathrm{i_d}}(t)\Big\}\frac{2}{V_{DC}}\,. \tag{5.75f}$$

The system obtained through this approximation has been simulated in parallel with the full system. In order to observe the systems' agreement during transients, an instantaneous change in the load resistance R_{load} is introduced at $t = 0.5$s (in particular, the resistance is halved.). In Figure 5.6, the behaviour of $i_{\mathrm{i_d}}$ is depicted. The full and reduced system show a good agreement in both steady state and transients: in the picture, they are overlapped. The error between them is shown in Figure 5.7. Due to the large size of the system, only one variable is shown in the pictures as an example. Considering all the variables of the system, the maximum dimensionless error is order 10^{-5}.

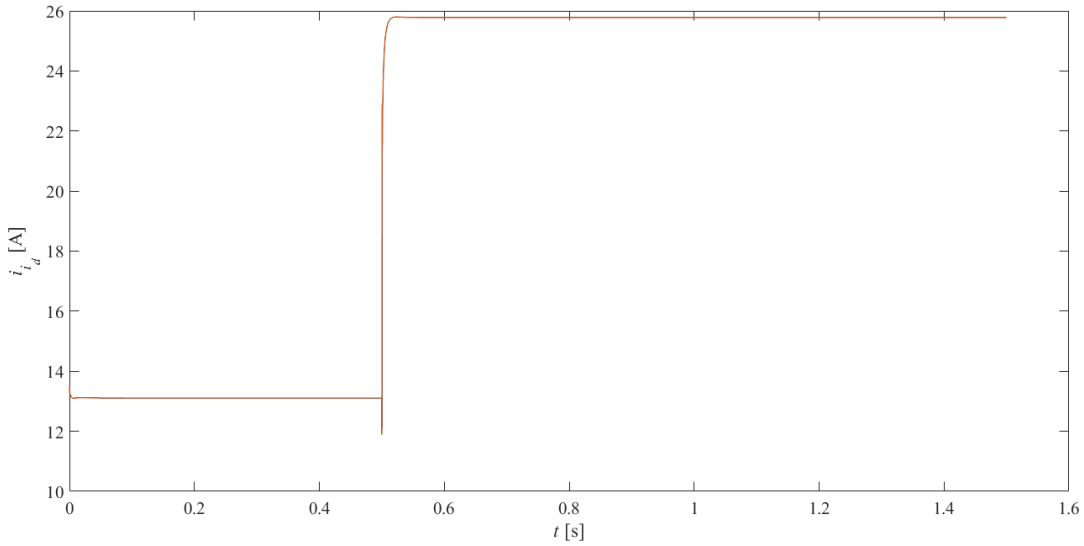

Figure 5.6: Single inverter - Behaviour of $i_{\mathrm{i_d}}$: full system (blue) and reduced system (red), at a sudden halving of R_{load}.

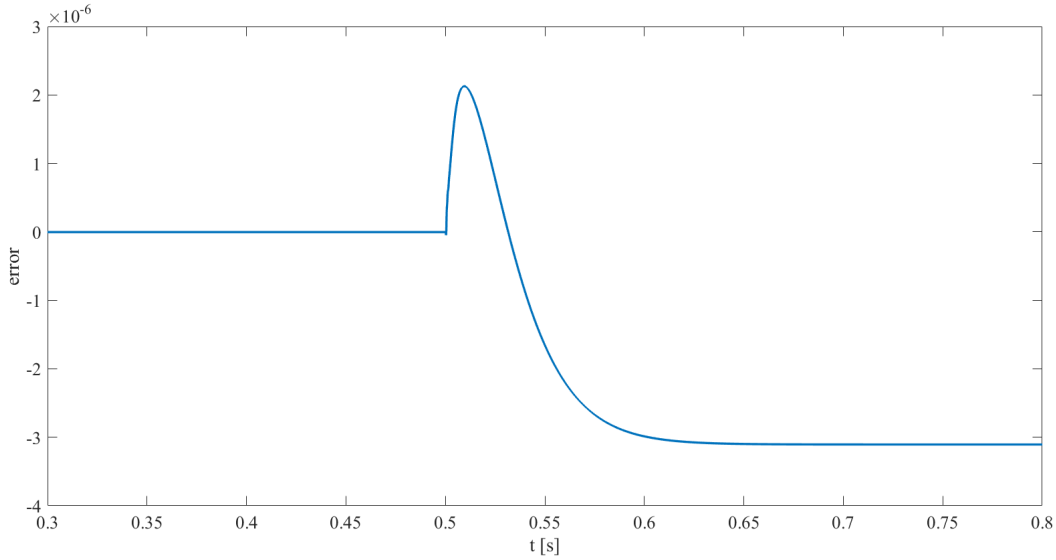

Figure 5.7: Dimensionless error on $i_{\mathrm{i_d}}$, computed between the full system and the first reduced system.

5.3.2.3 Small line inductance

The second approximation is based on the assumption that the line inductance L_l is "small". Therefore, inductive behaviours on the electrical lines connecting the inverter to the load are neglected, and there are reasonable expactations that the two ODEs describing the inductance behaviour will be substituted by algebraic equations.

If L_l is $\mathcal{O}(\epsilon)$ another auxiliary variable $\bar{L}_l$ can be introduced, given by

$$\bar{L}_l \;=\; \epsilon^{-1} L_l \,. \tag{5.76}$$

Then, equations (5.64n)-(5.64o) become

$$\frac{\mathrm{d}i_{\mathrm{o_d}}(t)}{\mathrm{d}t} = \frac{v_{\mathrm{i_d}}(t)}{\epsilon\bar{L}_l} - \frac{R_l + R_{\mathrm{load}}}{\epsilon\bar{L}_l} i_{\mathrm{o_d}}(t) + \epsilon^{-1}\bar{\omega}_n\, i_{\mathrm{o_q}}(t)\,, \tag{5.77a}$$

$$\frac{\mathrm{d}i_{\mathrm{o_q}}(t)}{\mathrm{d}t} = \frac{v_{\mathrm{i_q}}(t)}{\epsilon\bar{L}_l} - \frac{R_l + R_{\mathrm{load}}}{\epsilon\bar{L}_l} i_{\mathrm{o_q}}(t) - \epsilon^{-1}\bar{\omega}_n\, i_{\mathrm{o_d}}(t)\,, \tag{5.77b}$$

where the approximation (5.73) is used for ω. Multiplying (5.77) by ϵ and keeping only the leading-order terms leads to

$$0 = \frac{v_{i_d}(t)}{\bar{L}_l} - \frac{R_l + R_{load}}{\bar{L}_l} i_{o_d}(t) + \bar{\omega}_n\, i_{o_q}(t) + \mathcal{O}(\epsilon)\,, \tag{5.78a}$$

$$0 = \frac{v_{i_q}(t)}{\bar{L}_l} - \frac{R_l + R_{load}}{\bar{L}_l} i_{o_q}(t) - \bar{\omega}_n\, i_{o_d}(t) + \mathcal{O}(\epsilon)\,. \tag{5.78b}$$

Therefore, $i_{\mathrm{o_d}}$ and $i_{\mathrm{o_q}}$ can be considered among the fast variables and (5.78) correspond to (5.67). Algebraic expressions for $i_{\mathrm{o_d}}$ and $i_{\mathrm{o_q}}$ can be found by solving (5.78) for $i_{\mathrm{o_d}}$ and $i_{\mathrm{o_q}}$, leading to

$$i_{\mathrm{o_d}}(t) \sim \frac{(R_l + R_{\mathrm{load}})\, v_{\mathrm{i_d}}(t) + \bar{\omega}_n \bar{L}_l v_{\mathrm{i_q}}(t)}{\left(\bar{\omega}_n \bar{L}_l\right)^2 + \left(R_l + R_{\mathrm{load}}\right)^2}\,, \tag{5.79a}$$

$$i_{\mathrm{o_q}}(t) \sim \frac{(R_l + R_{\mathrm{load}})\, v_{\mathrm{i_q}}(t) - \bar{\omega}_n \bar{L}_l v_{\mathrm{i_d}}(t)}{\left(\bar{\omega}_n \bar{L}_l\right)^2 + \left(R_l + R_{\mathrm{load}}\right)^2}\,. \tag{5.79b}$$

Again, equations (5.79) correspond to (5.68). Using the algebraic equations (5.79) instead of the ODEs (5.64n)-(5.64o) allows a reduction of the system by two further ODEs and two corresponding state-space variables. This corresponds to

assuming that $i_{\mathrm{o_d}}$ and $i_{\mathrm{o_q}}$ constitute the "fast" variable vector $\boldsymbol{z}$, whose behaviour is approximated by algebraic equations. All the other variables belong to the "slow" variable vector $\boldsymbol{x}$. In particular, ω is slow and quasi-constant.

$$\frac{\mathrm{d}P_{\mathrm{lp}}(t)}{\mathrm{d}t} = \omega_{cd}[v_{\mathrm{i_d}}(t)\, i_{\mathrm{o_d}}(t) - v_{\mathrm{i_q}}(t)\, i_{\mathrm{o_q}}(t) - P_{\mathrm{lp}}(t)]\,, \tag{5.80a}$$

$$\frac{\mathrm{d}Q_{\mathrm{lp}}(t)}{\mathrm{d}t} = \omega_{cd}[v_{\mathrm{i_d}}(t)\, i_{\mathrm{o_q}}(t) - v_{\mathrm{i_q}}(t)\, i_{\mathrm{o_d}}(t) - Q_{\mathrm{lp}}(t)]\,, \tag{5.80b}$$

$$\frac{\mathrm{d}i_{\mathrm{lp_d}}(t)}{\mathrm{d}t} = \omega_{ci}[i_{\mathrm{o_d}}t) - i_{\mathrm{lp_d}}(t)]\,, \tag{5.80c}$$

$$\frac{\mathrm{d}i_{\mathrm{lp_q}}(t)}{\mathrm{d}t} = \omega_{ci}[i_{\mathrm{o_q}}(t) - i_{\mathrm{lp_q}}(t)]\,, \tag{5.80d}$$

$$\frac{\mathrm{d}x_{\mathrm{int,v_d}}(t)}{\mathrm{d}t} = v_{\mathrm{ref_d}}(t) - v_{\mathrm{i_d}}(t)\,, \tag{5.80e}$$

$$\frac{\mathrm{d}x_{\mathrm{int,v_q}}(t)}{\mathrm{d}t} = v_{\mathrm{ref_q}}(t) - v_{\mathrm{i_q}}(t)\,, \tag{5.80f}$$

$$\frac{\mathrm{d}x_{\mathrm{int,i_d}}(t)}{\mathrm{d}t} = i_{\mathrm{ref_d}}(\hat{t}) - i_{\mathrm{i_d}}(\hat{t})\,, \tag{5.80g}$$

$$\frac{\mathrm{d}x_{\mathrm{int,i_q}}(t)}{\mathrm{d}t} = i_{\mathrm{ref_q}}(t) - i_{\mathrm{i_q}}(t) \tag{5.80h}$$

$$\frac{\mathrm{d}i_{\mathrm{i_d}}(t)}{\mathrm{d}t} = \frac{V_{DC}}{2\,L_f} m_{\mathrm{d}}(t) - \frac{R_f}{L_f} i_{\mathrm{i_d}}(t) - \frac{v_{\mathrm{i_d}}(t)}{L_f} + \omega_n\, i_{\mathrm{i_q}}(t)\,, \tag{5.80i}$$

$$\frac{\mathrm{d}i_{\mathrm{i_q}}(t)}{\mathrm{d}t} = \frac{V_{DC}}{2\,L_f} m_{\mathrm{q}}(t) - \frac{R_f}{L_f} i_{\mathrm{i_q}}(\hat{t}) - \frac{v_{\mathrm{i_q}}(t)}{L_f} - \omega_n\, i_{\mathrm{i_d}}(t)\,, \tag{5.80j}$$

$$\frac{\mathrm{d}v_{\mathrm{i_d}}(t)}{\mathrm{d}t} = \frac{i_{\mathrm{i_d}}(t)}{C_f} - \frac{i_{\mathrm{o_d}}(t)}{C_f} + \omega_n\, v_{\mathrm{i_q}}(t)\,, \tag{5.80k}$$

$$\frac{\mathrm{d}v_{\mathrm{i_q}}(t)}{\mathrm{d}t} = \frac{i_{\mathrm{i_q}}(t)}{C_f} - \frac{i_{\mathrm{o_q}}(t)}{C_f} - \omega_n\, v_{\mathrm{i_d}}(t)\,, \tag{5.80l}$$

and $i_{\mathrm{o_d}}$ and $i_{\mathrm{o_q}}$ are given by (5.79).

The system (5.80) has been simulated in parallel with the full system. The same instantaneous change in the load resistance R_{load} is introduced at $t = 0.5$s and the behaviour of $i_{\mathrm{i_d}}$ is depicted in Figure 5.8. The full and reduced system show a good agreement in steady state, with dimensionless errors of order 10^{-4}. As observable in Figure 5.9, in this case errors during transients can reach order 10^{-1} (it must be noted that this kind of sudden, step-like change in the load resistance can be considered a worst-case scenario for the system, while slower changes would cause better transient agreements). Similar error plots are obtained from

the remaining system variables.

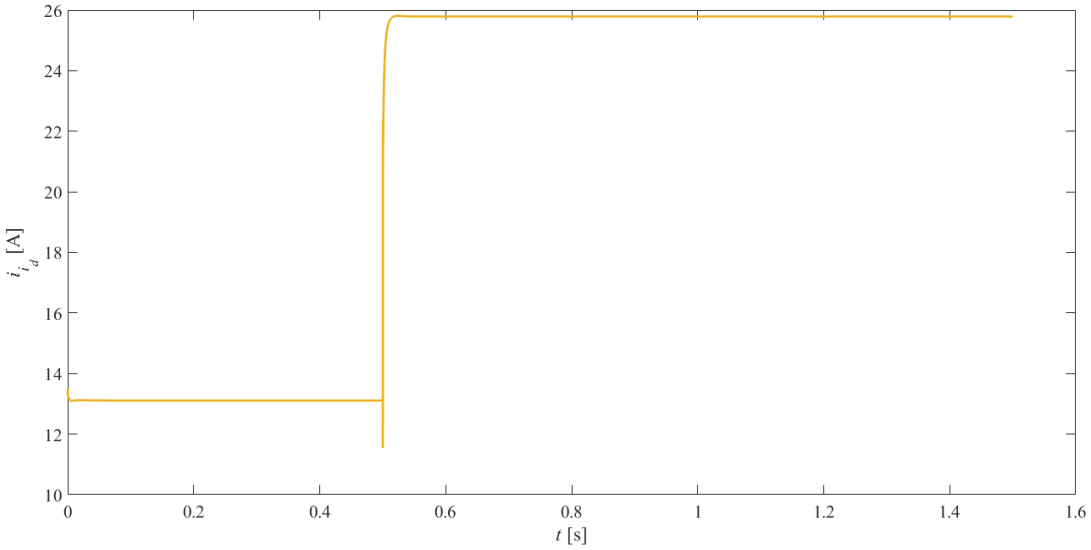

Figure 5.8: Single inverter - Behaviour of $i_{\mathrm{i_d}}$: full system (blue) and 12-equation-reduced system (orange); sudden halving of R_{load}.

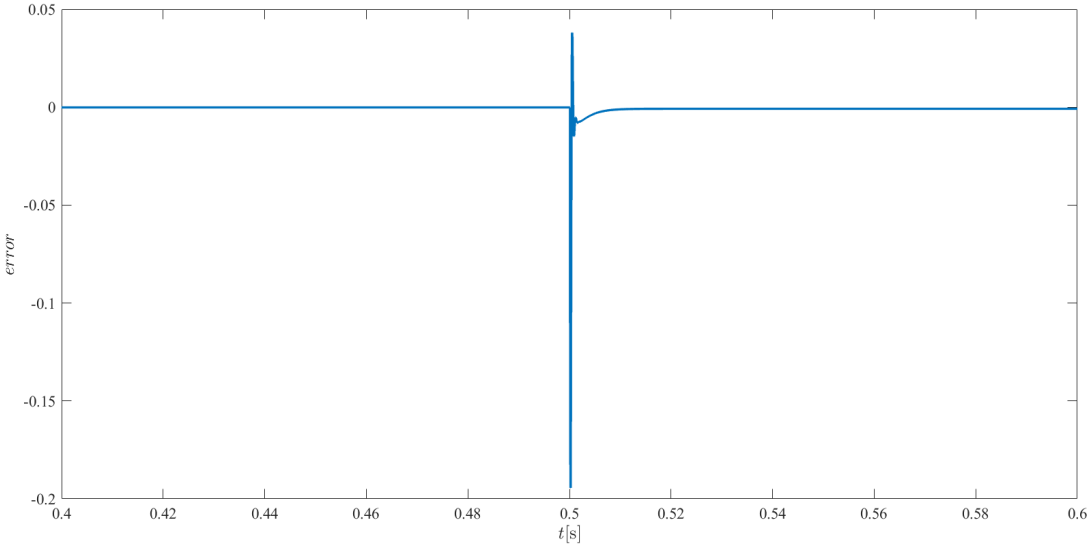

Figure 5.9: SIngle inverter - Dimensionless error on $i_{\mathrm{i_d}}$, computed between the full system and the second reduced system.

5.3.2.4 Small filter inductance

A further approximation is considering the filter inductance L_f and the filter resistance R_f "small". Neglecting the inductance corresponds, in practice, to eliminate from the system the two ODEs that describe the behaviour of voltages across the inductors. It is expected that such ODEs will be approximated by algebraic equations.
Defining

$$\bar{L}_f = \epsilon^{-1} L_f = \mathcal{O}(1), \tag{5.81a}$$

$$\bar{R}_f = \epsilon^{-1} R_f = \mathcal{O}(1), \tag{5.81b}$$

a procedure similar to that explained in §5.3.2.3 can be applied to (5.64j) and (5.64k), leading to

$$\frac{\mathrm{d}i_{\mathrm{i_d}}(t)}{\mathrm{d}t} \sim \frac{V_{DC}\, m_{\mathrm{d}}(t)}{2\epsilon\bar{L}_f} - \frac{\bar{R}_f}{\bar{L}_f} i_{\mathrm{i_d}}(t) - \frac{v_{\mathrm{i_d}}(t)}{\epsilon\bar{L}_f} i_{\mathrm{i_d}}(t) + \epsilon^{-1}\bar{\omega}_n\, i_{\mathrm{o_q}}(t)\,, \tag{5.82a}$$

$$\frac{\mathrm{d}i_{\mathrm{i_q}}(t)}{\mathrm{d}t} \sim \frac{V_{DC}\, m_{\mathrm{q}}(t)}{2\epsilon\bar{L}_f} - \frac{\bar{R}_f}{\bar{L}_f} i_{\mathrm{i_q}}(t) - \frac{v_{\mathrm{i_q}}(t)}{\epsilon\bar{L}_f} i_{\mathrm{i_q}}(t) - \epsilon^{-1}\bar{\omega}_n\, i_{\mathrm{o_d}}(t)\,, \tag{5.82b}$$

Two more algebraic equations can be obtained by retaining the leading-order terms only in (5.82):

$$v_{\mathrm{i_d}}(t) - \bar{L}_f\bar{\omega}_n i_{\mathrm{i_q}}(t) \sim \frac{V_{DC}}{2} m_{\mathrm{d}}(t)\,, \tag{5.83a}$$

$$v_{\mathrm{i_q}}(t) - \bar{L}_f\bar{\omega}_n i_{\mathrm{i_d}}(t) \sim \frac{V_{DC}}{2} m_{\mathrm{q}}(t), \tag{5.83b}$$

where the RHSs of (5.83), according to (5.59), are given by

$$\begin{aligned} \frac{V_{DC}}{2} m_{\mathrm{d}}(t) &= K_{ip}[i_{\mathrm{ref_d}}(t) - i_{\mathrm{i_d}}(t)] + K_{ii}\, x_{\mathrm{int,i_d}}(t) - \omega(t)\, L_f\, i_{\mathrm{i_q}}(t) \\ &\sim K_{ip}[i_{\mathrm{ref_d}}(t) - i_{\mathrm{i_d}}(t)] + K_{ii}\, x_{\mathrm{int,i_d}}(t) - \bar{\omega}_n\, \bar{L}_f\, i_{\mathrm{i_q}}(t), \end{aligned} \tag{5.84a}$$

$$\begin{aligned} \frac{V_{DC}}{2} m_{\mathrm{q}}(t) &= K_{ip}[i_{\mathrm{ref_q}}(t) - i_{\mathrm{i_q}}(t)] + K_{ii}\, x_{\mathrm{int,i_q}}(t) + \omega(t)\, L_f\, i_{\mathrm{i_d}}(t) \\ &\sim K_{ip}[i_{\mathrm{ref_q}}(t) - i_{\mathrm{i_q}}(t)] + K_{ii}\, x_{\mathrm{int,i_d}}(t) - \bar{\omega}_n\, \bar{L}_f\, i_{\mathrm{i_q}}(t). \end{aligned} \tag{5.84b}$$

Substituting (5.84) into (5.83) leads to

$$v_{\mathrm{i_d}}(t) \sim K_{ip}[i_{\mathrm{ref_d}}(t) - i_{\mathrm{i_d}}(t)] + K_{ii}\, x_{\mathrm{int,i_d}}(t)\,, \tag{5.85a}$$

$$v_{\mathrm{i_q}}(t) \sim K_{ip}[i_{\mathrm{ref_q}}(t) - i_{\mathrm{i_q}}(t)] + K_{ii}\, x_{\mathrm{int,i_q}}(t)\,. \tag{5.85b}$$

Algebraic expressions for the internal currents can therefore be found by solving (5.85) for $i_{\mathrm{i_d}}$ and $i_{\mathrm{i_q}}$, leading to

$$i_{\mathrm{i_d}}(t) \sim i_{\mathrm{ref_d}}(t) + \frac{K_{ii}\, x_{\mathrm{int,i_d}} - v_{\mathrm{i_d}}(t)}{K_{ip}}\,, \tag{5.86a}$$

$$i_{\mathrm{i_q}}(t) \sim i_{\mathrm{ref_q}}(t) + \frac{K_{ii}\, x_{\mathrm{int,i_q}} - v_{\mathrm{i_q}}(t)}{K_{ip}}\,. \tag{5.86b}$$

Hence, considering the filter inductance and resistance to be "small" allows reduction of the system by two ODEs and elimination of the corresponding state-space variables.

In this case, the "fast" variable vector $\boldsymbol{z}$ is defined by

$$\boldsymbol{z}(t) = \begin{bmatrix} i_{\mathrm{i_d}}(t) \\ i_{\mathrm{i_q}}(t) \\ i_{\mathrm{o_d}}(t) \\ i_{\mathrm{o_q}}(t), \end{bmatrix} \tag{5.87}$$

and the angular frequency ω is quasi-constant and assumed to be equal to its nominal value ω_n. All the other state-space variables belong to the "slow" variable vector $\boldsymbol{x}$.

5.3.2.5 Neglect of integral error on the currents

After assuming that the internal currents are "fast", and eliminating their corresponding ODEs from the system, it is quite natural to assume that the two state-space variables describing the behaviour of the integral errors on the internal currents are "fast" as well. This will allow a further reduction of the system by two ODEs.

A more rigorous explanation of this choices is given below.

Since $V_{DC} = \mathcal{O}(1)$ and $m_{\mathrm{d}}(t)$ can vary between -1 and 1, the LHS of (5.84) is $\mathcal{O}(1)$. K_{ip}, $i_{\mathrm{ref_d}}(t)$ and $i_{\mathrm{i_d}}(t)$ are $\mathcal{O}(1)$, but $K_{ii} = \mathcal{O}(\epsilon^{-1})$. To avoid imbalance, $x_{\mathrm{int,i_d}}(t)$ must be $\mathcal{O}(\epsilon)$. Let the auxiliary parameter $\bar{K}_{ii}$ and the auxiliary variable $\bar{x}_{\mathrm{int,i_d}}(t)$ be defined, respectively, by

$$\bar{K}_{ii} = \epsilon\, K_{ii}\,, \tag{5.88}$$

$$\bar{x}_{\mathrm{int,i_d}}(t) = \epsilon^{-1}\, x_{\mathrm{int,i_d}}(t)\,. \tag{5.89}$$

Substituting (5.88) and (5.89) into (5.85) leads to

$$i_{\mathrm{i_d}}(t) - i_{\mathrm{ref_d}}(t) \sim \frac{\bar{K}_{ii}\,\bar{x}_{\mathrm{int,i_d}} - v_{\mathrm{i_d}}(t)}{K_{ip}}\,, \tag{5.90a}$$

$$i_{\mathrm{i_q}}(t) - i_{\mathrm{ref_q}}(t) \sim \frac{\bar{K}_{ii}\,\bar{x}_{\mathrm{int,i_q}} - v_{\mathrm{i_q}}(t)}{K_{ip}}\,. \tag{5.90b}$$

Substituting (5.89) into (5.64h) gives

$$\epsilon\frac{\mathrm{d}\bar{x}_{\mathrm{int,i_d}}(t)}{\mathrm{d}t} = i_{\mathrm{ref_d}}(t) - i_{\mathrm{i_d}}(t)\,, \tag{5.91a}$$

$$\epsilon\frac{\mathrm{d}\bar{x}_{\mathrm{int,i_q}}(t)}{\mathrm{d}t} = i_{\mathrm{ref_q}}(t) - i_{\mathrm{i_q}}(t)\,, \tag{5.91b}$$

where results from simulations support the assumption that $i_{\mathrm{ref_d}}(t)$, $i_{\mathrm{i_d}}(t)$, $i_{\mathrm{ref_q}}(t)$, $i_{\mathrm{i_q}}(t)$ are all $\mathcal{O}(1)$. Therefore, the following approximation can be adopted:

$$i_{\mathrm{i_d}}(t) \sim i_{\mathrm{ref_d}}(t)\,, \tag{5.92a}$$

$$i_{\mathrm{i_q}}(t) \sim i_{\mathrm{ref_q}}(t)\,. \tag{5.92b}$$

This approach reduces the system by two further ODEs and state-space variables, corresponding to the integral errors on the internal currents. Adopting this reduction eliminates the variables $x_{\mathrm{int,i_d}}$ and $x_{\mathrm{int,i_q}}$ from the state-space system. In case one would need to compute their approximate values, they can be obtained algebraically from (5.90); considering the LHSs to be $\mathcal{O}(\epsilon)$ and then solving for

$\bar{x}_{int,i_d}$ and $\bar{x}_{int,i_q}$ allow one to the following approximation:

$$\bar{x}_{\mathrm{int,i_d}}(t) \sim \frac{v_{\mathrm{i_d}}(t)}{\bar{K}_{ii}}\,, \tag{5.93a}$$

$$\bar{x}_{\mathrm{int,i_q}}(t) \sim \frac{v_{\mathrm{i_q}}(t)}{\bar{K}_{ii}}\,. \tag{5.93b}$$

This approximated system corresponds to assuming that the "fast" and "slow" variables are grouped as

$$\boldsymbol{z}(t) = \begin{bmatrix} x_{\mathrm{int,i_d}}(t) & x_{\mathrm{int,i_q}}(t) & i_{\mathrm{i_d}}(t) & i_{\mathrm{i_q}}(t) & i_{\mathrm{o_d}}(t) & i_{\mathrm{o_q}}(t) \end{bmatrix}^{\mathrm{T}}, \tag{5.94a}$$

$$\boldsymbol{x}(t) = \begin{bmatrix} P_{\mathrm{lp}}(t) & Q_{\mathrm{lp}}(t) & i_{\mathrm{lp_d}}(t) & i_{\mathrm{lp_q}}(t) & x_{\mathrm{int,v_d}}(t) & x_{\mathrm{int,v_q}}(t) & v_{\mathrm{i_d}}(t) & v_{\mathrm{i_q}}(t) \end{bmatrix}^{\mathrm{T}}. \tag{5.94b}$$

One state-space variable of the original full system, ω, is approximated by its nominal value ω_n.

At this point, 8 ODEs are left in the state-space model of the system, leading to

$$\frac{\mathrm{d}P_{\mathrm{lp}}(t)}{\mathrm{d}t} = \omega_{cd}[v_{\mathrm{i_d}}(t)\, i_{\mathrm{o_d}}(t) - v_{\mathrm{i_q}}(t)\, i_{\mathrm{o_q}}(t) - P_{\mathrm{lp}}(t)]\,, \tag{5.95a}$$

$$\frac{\mathrm{d}Q_{\mathrm{lp}}(t)}{\mathrm{d}t} = \omega_{cd}[v_{\mathrm{i_d}}(t)\, i_{\mathrm{o_q}}(t) - v_{\mathrm{i_q}}(t)\, i_{\mathrm{o_d}}(t) - Q_{\mathrm{lp}}(t)]\,, \tag{5.95b}$$

$$\frac{\mathrm{d}i_{\mathrm{lp_d}}(t)}{\mathrm{d}t} = \omega_{ci}[i_{\mathrm{o_d}}t) - i_{\mathrm{lp_d}}(t)]\,, \tag{5.95c}$$

$$\frac{\mathrm{d}i_{\mathrm{lp_q}}(t)}{\mathrm{d}t} = \omega_{ci}[i_{\mathrm{o_q}}(t) - i_{\mathrm{lp_q}}(t)]\,, \tag{5.95d}$$

$$\frac{\mathrm{d}x_{\mathrm{int,v_d}}(t)}{\mathrm{d}t} = v_{\mathrm{ref_d}}(t) - v_{\mathrm{i_d}}(t)\,, \tag{5.95e}$$

$$\frac{\mathrm{d}x_{\mathrm{int,v_q}}(t)}{\mathrm{d}t} = v_{\mathrm{ref_q}}(t) - v_{\mathrm{i_q}}(t)\,, \tag{5.95f}$$

$$\frac{\mathrm{d}v_{\mathrm{i_d}}(\hat{t})}{\mathrm{d}t} = \frac{i_{\mathrm{i_d}}(t)}{C_f} - \frac{i_{\mathrm{o_d}}(t)}{C_f} + \omega_n\, v_{\mathrm{i_q}}(t)\,, \tag{5.95g}$$

$$\frac{\mathrm{d}v_{\mathrm{i_q}}(t)}{\mathrm{d}t} = \frac{i_{\mathrm{i_q}}(t)}{\hat{C}_f} - \frac{i_{\mathrm{o_q}}(t)}{C_f} - \omega_n\, v_{\mathrm{i_d}}(t)\,, \tag{5.95h}$$

where $i_{\mathrm{i_d}}$ and $i_{\mathrm{i_q}}$ are given by (6.49), while $i_{\mathrm{o_d}}$ and $i_{\mathrm{o_q}}$ by (5.79).

Figure 5.10 has been obtained by simulating the system (5.95) in parallel with

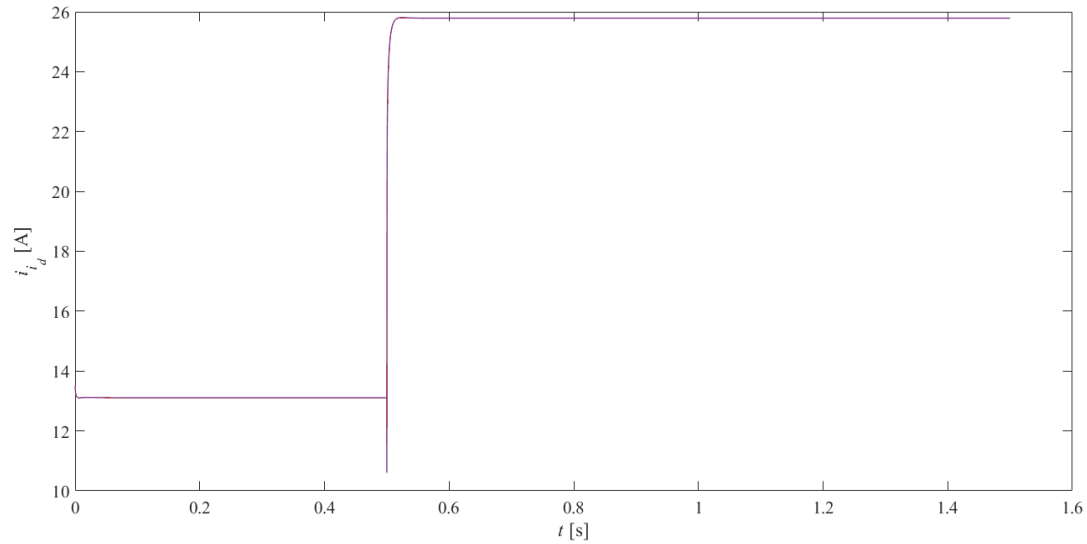

Figure 5.10: Behaviour of i_{i_d}: full system (blue) and reduced system (purple).

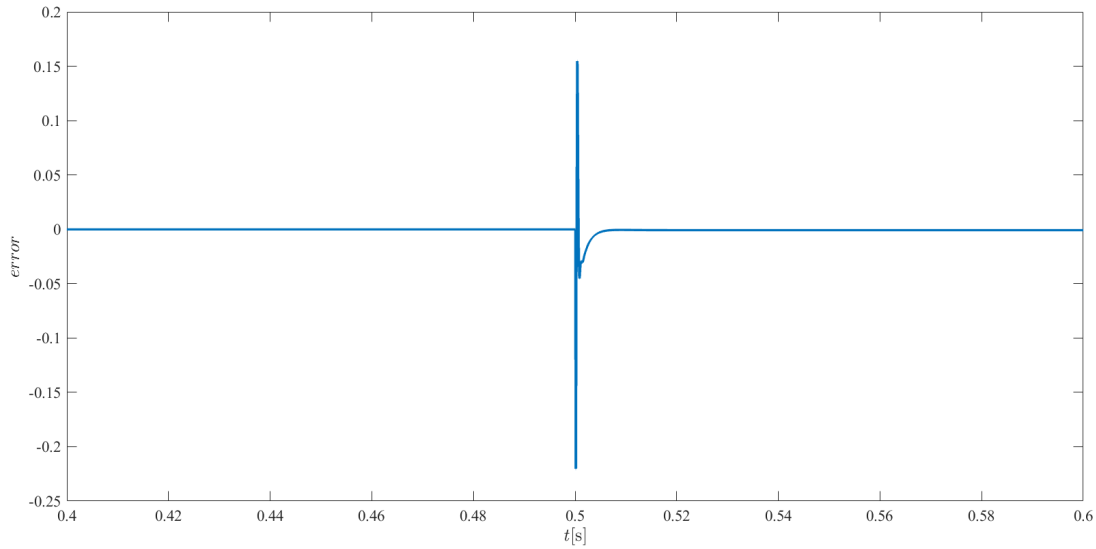

Figure 5.11: Dimensionless error on i_{i_d}, computed between the full system and the third reduced system.

the full system. In steady state, the maximum dimensionless error among the system variables is order 10^{-3}. As shown in Figure 5.11, during transients it can reach order 10^{-1}.

5.3.2.6 Small filter capacitance

Now, the filter inductance Cf is assumed to be "small". If so, the current behaviours caused by the presence of the capacitors are neglected, and two more ODEs might be eliminated from the system.
Considering the dimensionless parameter C_f to be $\mathcal{O}(\epsilon)$, an $\mathcal{O}(1)$ variable $\bar{C}_f$ can be defined by

$$\bar{C}_f \;=\; \epsilon^{-1}\, C_f\,. \tag{5.96}$$

Substituting (5.96) and (5.72) into (5.64l)-(5.64m) leads to

$$\frac{\mathrm{d}v_{\mathrm{i_d}}(t)}{\mathrm{d}t} \sim \frac{i_{\mathrm{i_d}}(t)}{\epsilon\,\bar{C}_f} - \frac{i_{\mathrm{o_d}}(t)}{\epsilon\bar{C}_f} + \epsilon^{-1}\bar{\omega}_n\, v_{\mathrm{i_q}}(t)\,, \tag{5.97a}$$

$$\frac{\mathrm{d}v_{\mathrm{i_q}}(t)}{\mathrm{d}t} \sim \frac{i_{\mathrm{i_q}}(t)}{\epsilon\,\bar{C}_f} - \frac{i_{\mathrm{o_q}}(t)}{\epsilon\bar{C}_f} - \epsilon^{-1}\bar{\omega}_n\, v_{\mathrm{i_d}}(t)\,. \tag{5.97b}$$

Multiplying (5.97) by ϵ and retaining only the $\mathcal{O}(1)$ terms leads to

$$i_{\mathrm{i_d}}(t) \sim i_{\mathrm{o_d}}(t) - \bar{\omega}_n\,\bar{C}_f\, v_{\mathrm{i_q}}(t)\,, \tag{5.98a}$$

$$i_{\mathrm{i_q}}(t) \sim i_{\mathrm{o_q}}(t) + \bar{\omega}_n\,\bar{C}_f\, v_{\mathrm{i_d}}(t)\,, \tag{5.98b}$$

where $i_{\mathrm{i_d}}$ and $i_{\mathrm{i_q}}$ are given by (6.49), $i_{\mathrm{o_d}}$ and $i_{\mathrm{o_q}}$ by (5.79). Substituting 6.49) and (5.79) into (5.98) and solving for $v_{\mathrm{i_d}}$ and $v_{\mathrm{i_q}}$ leads to the algebraic expressions of the voltages, while their two corresponding ODEs can be eliminated from the so-reduced system. Before proceeding with the computation of the state-space system based on this approximations, attention focuses on the variables modelling the behaviour of the integral errors on the voltages. Since the voltages are now assumed to be "fast" variables, so should be their integral errors. This is explained more in details in the next section.

5.3.2.7 Neglect of voltage integral errors

In this section, the system is reduced by two more ODEs, according to the assumption that the variables modelling the behaviour of the integral errors on the voltages are "fast". This assumption is based on the computations shown below.

The reference currents $i_{\mathrm{ref_d}}(t)$ and $i_{\mathrm{ref_q}}(t)$, according to (5.57), are computed as

$$i_{\mathrm{ref_d}}(t) \sim K_{vp}[v_{\mathrm{ref_d}}(t) - v_{\mathrm{i_d}}(t)] + K_{vi}\, x_{\mathrm{int,v_d}}(t) - \bar{\omega}_n \bar{C}_f\, v_{\mathrm{i_q}}(t)\,, \tag{5.99a}$$

$$i_{\mathrm{ref_q}}(t) \sim K_{vp}[v_{\mathrm{ref_q}}(t) - v_{\mathrm{i_q}}(t)] + K_{vi}\, x_{\mathrm{int,v_q}}(t) + \bar{\omega}_n \bar{C}_f\, v_{\mathrm{i_d}}(t)\,, \tag{5.99b}$$

where (5.72) is used for ω.

Employing the same procedure for (5.84), since K_{vi} is $\mathcal{O}(\epsilon^{-1})$, while all the other terms in the equation are $\mathcal{O}(1)$ or smaller, $x_{\mathrm{int,v_d}}(t)$ must be $\mathcal{O}(\epsilon)$ to avoid imbalance, leading to

$$i_{\mathrm{ref_d}}(t) \sim K_{vp}[v_{\mathrm{ref_d}}(t) - v_{\mathrm{i_d}}(t)] + \bar{K}_{vi}\, \bar{x}_{\mathrm{int,v_d}}(t) - \bar{\omega}_n \bar{C}_f\, v_{\mathrm{i_q}}(t)\,, \tag{5.100a}$$

$$i_{\mathrm{ref_q}}(t) \sim K_{vp}[v_{\mathrm{ref_q}}(t) - v_{\mathrm{i_q}}(t)] + \bar{K}_{vi}\, \bar{x}_{\mathrm{int,v_q}}(t) + \bar{\omega}_n \bar{C}_f\, v_{\mathrm{i_d}}(t)\,, \tag{5.100b}$$

where

$$\bar{K}_{iv} = \epsilon\, K_{iv}, \tag{5.101}$$

and

$$\bar{x}_{\mathrm{int,v_d}}(t) = \epsilon^{-1}\, x_{\mathrm{int,v_d}}(t)\,, \tag{5.102a}$$

$$\bar{x}_{\mathrm{int,v_q}}(t) = \epsilon^{-1}\, x_{\mathrm{int,v_q}}(t)\,. \tag{5.102b}$$

Analogously to (5.91), the ODEs (5.64f)-(5.64g) become

$$\epsilon \frac{\mathrm{d}\bar{x}_{\mathrm{int,v_d}}(t)}{\mathrm{d}t} = v_{\mathrm{ref_d}}(t) - v_{\mathrm{i_d}}(t)\,, \tag{5.103a}$$

$$\epsilon \frac{\mathrm{d}\bar{x}_{\mathrm{int,v_q}}(t)}{\mathrm{d}t} = v_{\mathrm{ref_q}}(t) - v_{\mathrm{i_q}}(t)\,, \tag{5.103b}$$

where $v_{\mathrm{ref_d}}(t)$, $v_{\mathrm{i_d}}(t)$, $v_{\mathrm{ref_q}}(t)$ and $v_{\mathrm{i_q}}(t)$ are $\mathcal{O}(1)$. Therefore, considering leading orders only leads to

$$v_{\mathrm{i_d}}(t) \sim v_{rmref_d}(t)\,, \tag{5.104a}$$

$$v_{Rmi_q}(t) \sim v_{rmref_q}(t)\,, \tag{5.104b}$$

Following the definition (5.56) of $v_{rmref_d}(t)$ and substituting (5.72) gives

$$\begin{aligned} v_{\mathrm{ref_d}}(t) = \; & V_{\mathrm{d_n}} + K_{dq}[Q_{\mathrm{ref}} - Q_{\mathrm{lp}}(t)] \\ & + L_v\{[\epsilon^{-1}\bar{\omega}_n + K_{dp}(P_{\mathrm{ref}} - P_{\mathrm{lp}}(t))]i_{\mathrm{lp_q}}(t) + \omega_{ci}(i_{\mathrm{lp_d}}(t) - i_{\mathrm{o_d}}(t))\}, \end{aligned} \tag{5.105}$$

where, according to Table 5.4, $L_v \sim \epsilon$. A further parameter $\bar{L}_v = \mathcal{O}(1)$ can thus be defined by

$$\bar{L}_v \; = \; \epsilon^{-1}\, L_v. \tag{5.106}$$

Substituting (5.106) into (5.105) leads to

$$\begin{aligned} v_{\mathrm{ref_d}}(t) = \; & V_{\mathrm{d_n}} + K_{dq}[Q_{\mathrm{ref}} - Q_{\mathrm{lp}}(t)] + \epsilon\bar{L}_v\{[\epsilon^{-1}\bar{\omega}_n + K_{dp}(P_{\mathrm{ref}} - P_{\mathrm{lp}}(t))]i_{\mathrm{lp_q}}(t) \\ & + \omega_{ci}(i_{\mathrm{lp_d}}(t) - i_{\mathrm{o_d}}(t))\} \\ \sim \; & V_{\mathrm{d_n}} + K_{dq}[Q_{\mathrm{ref}} - Q_{\mathrm{lp}}(t)] + \bar{L}_v\,\bar{\omega}_n\, i_{\mathrm{lp_q}}(t)\,. \end{aligned} \tag{5.107}$$

Analogously, for $v_{\mathrm{ref_q}}(t)$,

$$v_{\mathrm{ref_q}}(t) \; \sim \; V_{\mathrm{q_n}} \; - \; \bar{L}_v\,\bar{\omega}_n\, i_{\mathrm{lp_d}}(t)\,. \tag{5.108}$$

Equating the RHS of (5.107)-(5.108) and (5.104) leads to

$$v_{\mathrm{i_d}}(t) \sim V_{\mathrm{d_n}} + K_{dq}[Q_{\mathrm{ref}} - Q_{\mathrm{lp}}(t)] + \bar{L}_v\,\bar{\omega}_n\, i_{\mathrm{lp_q}}(t)\,, \tag{5.109a}$$

$$v_{\mathrm{i_q}}(t) \sim V_{\mathrm{q_n}} - \bar{L}_v\,\bar{\omega}_n\, i_{\mathrm{lp_d}}(t)\,. \tag{5.109b}$$

Thus, this approximation leads to a further reduction by two ODEs and variables, leading to the fourth reduced state-space system (5.111). In this case, the "slow" variable vector is defined by

$$\boldsymbol{x}(t) \; = \; \begin{bmatrix} P_{\mathrm{lp}}(t) & Q_{\mathrm{lp}}(t) & i_{\mathrm{lp_d}}(t) & i_{\mathrm{lp_q}}(t) \end{bmatrix}^{\mathrm{T}}, \tag{5.110}$$

while the angular frequency ω is assumed to be constantly equal to its reference $\bar{\omega}_n$, and all the remaining variables belong to the "fast" variable vector $\boldsymbol{z}$. The behaviour of the elements of $\boldsymbol{z}$ is approximated by algebraic equations depending

on the state of $\boldsymbol{x}$. The reduced state-space system is then given by

$$\frac{\mathrm{d}P_{\mathrm{lp}}(t)}{\mathrm{d}t} = \omega_{cd}[v_{\mathrm{i_d}}(t)\, i_{\mathrm{i_d}}(t) - v_{\mathrm{i_q}}(t)\, i_{\mathrm{i_q}}(t) - P_{\mathrm{lp}}(t)]\,, \tag{5.111a}$$

$$\frac{\mathrm{d}Q_{\mathrm{lp}}(t)}{\mathrm{d}t} = \omega_{cd}[v_{\mathrm{i_d}}(t)\, i_{\mathrm{i_q}}(t) - v_{\mathrm{i_q}}(t)\, i_{\mathrm{i_d}}(t) - Q_{\mathrm{lp}}(t)]\,, \tag{5.111b}$$

$$\frac{\mathrm{d}i_{\mathrm{lp_d}}(t)}{\mathrm{d}t} = \omega_{ci}[i_{\mathrm{o_d}}t) - i_{\mathrm{lp_d}}(t)]\,, \tag{5.111c}$$

$$\frac{\mathrm{d}i_{\mathrm{lp_q}}(t)}{\mathrm{d}t} = \omega_{ci}[i_{\mathrm{o_q}}(t) - i_{\mathrm{lp_q}}(t)]\,. \tag{5.111d}$$

The external and internal currents, in this case, can be computed from (5.79) and (5.98), respectively, while $v_{\mathrm{i_d}}$ and $v_{\mathrm{i_q}}$ from (5.109).

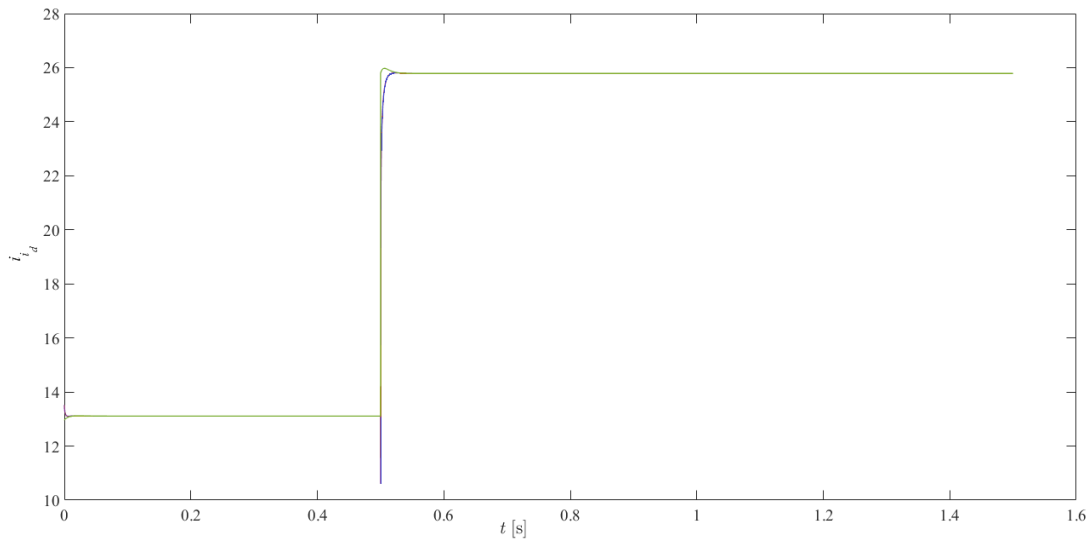

Figure 5.12: SIngle inverter - Behaviour of $i_{\mathrm{i_d}}$: full system (blue) and reduced system with four ODEs (green), during a sudden change in the value of R_{load}.

As depicted in Figure 5.12, this reduced system does not agree very well with the full one during transients (their dimensionless errors are of order 1), but the steady-state behaviour show errors of order 10^{-3}. This is valid also for the rest of the state-space variables, whose picture are not included in this documents in order to avoid repetition.

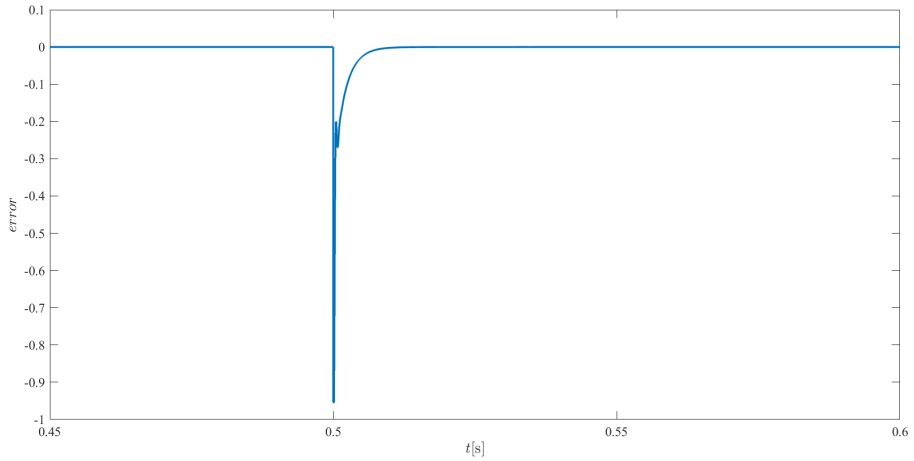

Figure 5.13: Dimensionless error on $i_{\mathrm{i_d}}$, computed between the full system and the reduced system characterised by four ODEs.

5.3.2.8 Neglect of Low-Pass Filter on the Current

The last approximation that is considered is assuming that the frequency ω_{ci} of the low-pass filter on the external currents is "big". This corresponds to assuming that the low-pass-filtered currents are "fast". Given the presence of a low-pass filter, this might seem counter-intuitive, but, in general, the cut-off frequency required to implement a virtual inductance is relatively high.
If the cut-off frequency ω_{ci}, used to low-pass filter the external currents, is $\mathcal{O}(\epsilon^{-1})$, an auxiliary variable $\bar{\omega}_{ci}$ can be defined using

$$\bar{\omega}_{ci} \;=\; \epsilon\,\omega_{ci}. \tag{5.112}$$

Substitution of (5.112) into (5.64d)-(5.64e) leads to

$$\frac{\mathrm{d}i_{\mathrm{lp_d}}(t)}{\mathrm{d}t} = \epsilon^{-1}\bar{\omega}_{ci}[i_{\mathrm{o_d}}(t) \;-\; i_{\mathrm{lp_d}}(t)]\,, \tag{5.113a}$$

$$\frac{\mathrm{d}i_{\mathrm{lp_q}}(t)}{\mathrm{d}t} = \epsilon^{-1}\bar{\omega}_{ci}[i_{\mathrm{o_q}}(t) \;-\; i_{\mathrm{lp_d}}(t)]\,. \tag{5.113b}$$

Algebraic expressions for $i_{\mathrm{lp_d}}$ and $i_{\mathrm{lp_q}}$ can be found by retaining the leading-order terms of (5.113):

$$i_{\mathrm{lp_d}}(t) \sim\; i_{\mathrm{o_d}}(t), \tag{5.114a}$$

$$i_{\mathrm{lp_q}}(t) \sim i_{\mathrm{o_q}}(t). \tag{5.114b}$$

Using (5.114) and (5.79) in (5.109) and solving for $v_{\mathrm{i_d}}$ and $v_{\mathrm{i_q}}$ lead to

$$v_{\mathrm{i_d}}(t) \sim \alpha \left[V_{\mathrm{d_n}} + \frac{\bar{\omega}_n \bar{L}_v}{R_{\mathrm{load}} + R_l} V_{\mathrm{q_n}} + K_{dq}(Q_{\mathrm{ref}} - Q_{\mathrm{lp}}(t)) \right], \tag{5.115a}$$

$$v_{\mathrm{i_q}}(t) \sim V_{\mathrm{q_n}} - \beta \left[V_{\mathrm{d_n}} + \frac{\bar{\omega}_n \bar{L}_v}{R_{\mathrm{load}} + R_l} V_{\mathrm{q_n}} + K_{dq}(Q_{\mathrm{ref}} - Q_{\mathrm{lp}}(t)) \right], \tag{5.115b}$$

$$\tag{5.115c}$$

where

$$\alpha = \frac{(R_{\mathrm{load}} + R_l)^2}{(R_{\mathrm{load}} + R_l)^2 + (\bar{\omega}_n \bar{L}_v)^2}, \tag{5.116a}$$

$$\beta = \frac{(R_{\mathrm{load}} + R_l)\bar{\omega}_n \bar{L}_v}{(R_{\mathrm{load}} + R_l)^2 + (\bar{\omega}_n \bar{L}_v)^2}. \tag{5.116b}$$

The final reduced state-space model comprises two equations only. In fact, the "slow" vector $\boldsymbol{x}$ is formed of P_{lp} and Q_{lp} only, while all the other variables belong to the "fast" vector $\boldsymbol{z}$ and are modelled by algebraic equations.

The state-space system is given by

$$\frac{\mathrm{d}P_{\mathrm{lp}}(t)}{\mathrm{d}t} = \omega_{cd}[v_{\mathrm{i_d}}(t)\, i_{\mathrm{i_d}}(t) - v_{\mathrm{i_q}}(t)\, i_{\mathrm{i_q}}(t) - P_{\mathrm{lp}}(t)], \tag{5.117a}$$

$$\frac{\mathrm{d}Q_{\mathrm{lp}}(t)}{\mathrm{d}t} = \omega_{cd}[v_{\mathrm{i_d}}(t)\, i_{\mathrm{i_q}}(t) - v_{\mathrm{i_q}}(t)\, i_{\mathrm{i_d}}(t) - Q_{\mathrm{lp}}(t)], \tag{5.117b}$$

where voltages and currents are given by (5.109) and (5.98), respectively.

This system, however, leads to some discrepancies in both transients and the steady state, with dimensionless errors order 10^{-1} also in steady state, as depicted in Figures 5.14 and 5.15. The accuracy is not considered to be good enough for analysing phenomena of the system.

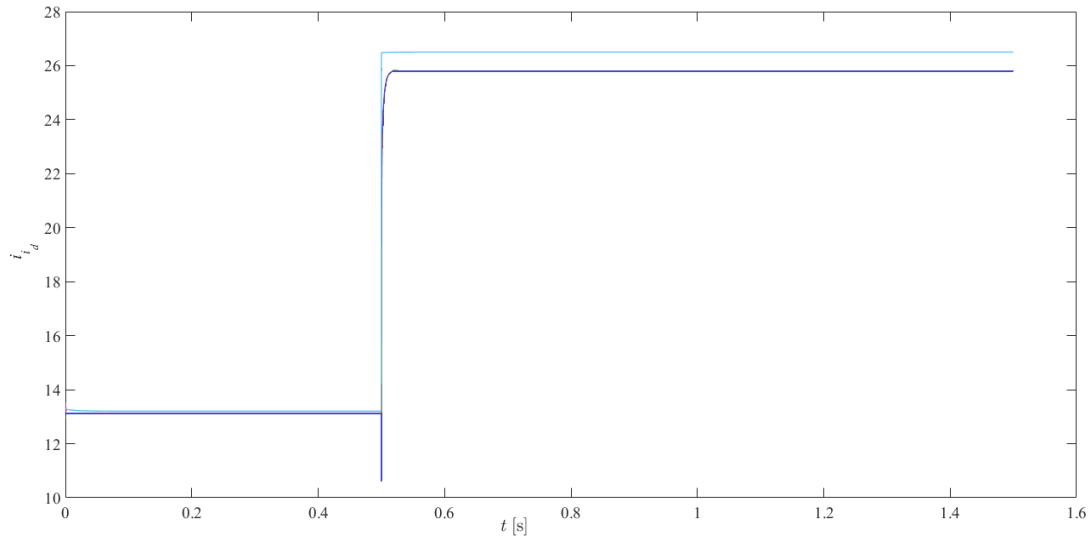

Figure 5.14: Behaviour of i_{i_d}: full system (dark blue) and reduced system (light blue).

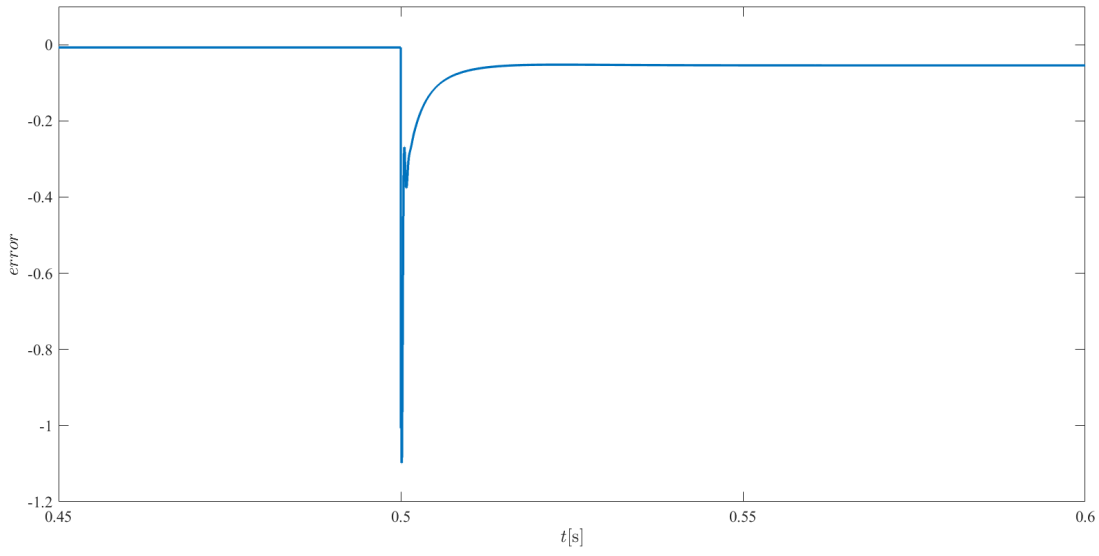

Figure 5.15: Dimensionless error on i_{i_d}, computed between the full system and the fifth reduced system.

5.3.2.9 Reduction Summary

The system reduction described in earlier sections has been tested through simulations, gradually adding the approximations presented in this subsection.

***CASE* 1** : $\omega(t) \sim \omega_n$

"Slow" variables: P_{lp}, Q_{lp}, $i_{\mathrm{lp_d}}$, $i_{\mathrm{lp_q}}$, $x_{\mathrm{int,v_d}}$, $x_{\mathrm{int,v_q}}$, $x_{\mathrm{int,i_d}}$, $x_{\mathrm{int,i_q}}$, $i_{\mathrm{i_d}}$, $i_{\mathrm{i_q}}$, $v_{\mathrm{i_d}}$, $v_{\mathrm{i_q}}$, $i_{\mathrm{o_d}}$, $i_{\mathrm{o_q}}$.

Constant variable: ω.

The system has 14 ODEs, given by

$$\frac{\mathrm{d}P_{\mathrm{lp}}(t)}{\mathrm{d}t} = \omega_{cd}[v_{\mathrm{i_d}}(t)\, i_{\mathrm{o_d}}(t) + v_{\mathrm{i_q}}(t)\, i_{\mathrm{o_q}}(t) - P_{\mathrm{lp}}(t)]\,, \tag{5.118a}$$

$$\frac{\mathrm{d}Q_{\mathrm{lp}}(t)}{\mathrm{d}t} = \omega_{cd}[v_{\mathrm{i_d}}(t)\, i_{\mathrm{o_q}}(t) - v_{\mathrm{i_q}}(t)\, i_{\mathrm{o_d}}(t) - Q_{\mathrm{lp}}(t)]\,, \tag{5.118b}$$

$$\frac{\mathrm{d}i_{\mathrm{lp_d}}(t)}{\mathrm{d}t} = \omega_{ci}[i_{\mathrm{o_d}}(t) - i_{\mathrm{lp_d}}(t)]\,, \tag{5.118c}$$

$$\frac{\mathrm{d}i_{\mathrm{lp_q}}(t)}{\mathrm{d}t} = \omega_{ci}[i_{\mathrm{o_q}}(t) - i_{\mathrm{lp_q}}(t)]\,, \tag{5.118d}$$

$$\frac{\mathrm{d}x_{\mathrm{int,v_d}}(t)}{\mathrm{d}t} = v_{\mathrm{ref_d}}(t) - v_{\mathrm{i_d}}(t)\,, \tag{5.118e}$$

$$\frac{\mathrm{d}x_{\mathrm{int,v_q}}(t)}{\mathrm{d}t} = v_{\mathrm{ref_q}}(t) - v_{\mathrm{i_q}}(t)\,, \tag{5.118f}$$

$$\frac{\mathrm{d}x_{\mathrm{int,i_d}}(t)}{\mathrm{d}t} = i_{\mathrm{ref_d}}(t) - i_{\mathrm{i_d}}(t)\,, \tag{5.118g}$$

$$\frac{\mathrm{d}x_{\mathrm{int,i_q}}(t)}{\mathrm{d}t} = i_{\mathrm{ref_q}}(t) - i_{\mathrm{i_q}}(t) \tag{5.118h}$$

$$\frac{\mathrm{d}i_{\mathrm{i_d}}(t)}{\mathrm{d}t} = \frac{V_{DC}}{2\,L_f} m_{\mathrm{d}}(t) - \frac{R_f}{L_f} i_{\mathrm{i_d}}(t) - \frac{v_{\mathrm{i_d}}(t)}{L_f} + \omega_n\, i_{\mathrm{i_q}}(t)\,, \tag{5.118i}$$

$$\frac{\mathrm{d}i_{\mathrm{i_q}}(t)}{\mathrm{d}t} = \frac{V_{DC}}{2\,L_f} m_{\mathrm{q}}(t) - \frac{R_f}{L_f} i_{\mathrm{i_q}}(t) - \frac{v_{\mathrm{i_q}}(t)}{L_f} - \omega_n\, i_{\mathrm{i_d}}(t)\,, \tag{5.118j}$$

$$\frac{\mathrm{d}v_{\mathrm{i_d}}(t)}{\mathrm{d}t} = \frac{i_{\mathrm{i_d}}(t)}{C_f} - \frac{i_{\mathrm{o_d}}(t)}{C_f} + \omega_n\, v_{\mathrm{i_q}}(t)\,, \tag{5.118k}$$

$$\frac{\mathrm{dv}_{\mathrm{i_q}}(t)}{\mathrm{d}t} = \frac{i_{\mathrm{i_q}}(t)}{C_f} - \frac{i_{\mathrm{o_q}}(t)}{C_f} - \omega_n\, v_{\mathrm{i_d}}(t)\,, \tag{5.118l}$$

$$\frac{\mathrm{d}i_{\mathrm{o_d}}(t)}{\mathrm{d}t} = \frac{v_{\mathrm{i_d}}(t)}{L_l} - \frac{R_l + R_{\mathrm{load}}}{L_l} i_{\mathrm{o_d}}(t) + \omega_n\, i_{\mathrm{o_q}}(t)\,, \tag{5.118m}$$

$$\frac{\mathrm{d}i_{\mathrm{o_q}}(t)}{\mathrm{d}t} \;=\; \frac{v_{\mathrm{i_q}}(t)}{L_l} \;-\; \frac{R_l + R_{\mathrm{load}}}{L_l} i_{\mathrm{o_q}}(t) \;-\; \omega_n \, i_{\mathrm{o_d}}(t), \tag{5.118n}$$

where

$$v_{\mathrm{ref_d}}(t) = V_{\mathrm{d_n}} + K_{dq}(Q_{\mathrm{ref}} - Q_{\mathrm{lp}}(t)) + L_v\{[\omega_n + K_{dp}(P_{\mathrm{ref}} - P_{\mathrm{lp}}(t))] i_{\mathrm{lp_q}}(t) \tag{5.119a}$$

$$+ \omega_{ci}(i_{\mathrm{lp_d}}(t) - i_{\mathrm{o_d}}(t))\},$$

$$v_{\mathrm{ref_q}}(t) = V_{\mathrm{q_n}} + L_v\{ - [\omega_n + K_{dp}(P_{\mathrm{ref}} - P_{\mathrm{lp}}(t))] i_{\mathrm{lp_d}}(t) + \omega_{ci}(i_{\mathrm{lp_q}}(t) - i_{\mathrm{o_q}}(t))\}, \tag{5.119b}$$

$$i_{\mathrm{ref_d}}(t) = \; K_{vp}[v_{\mathrm{ref_d}}(t) \;-\; v_{\mathrm{i_d}}(t)] \;+\; K_{vi}\, x_{\mathrm{int,v_d}}(t) \;-\; \omega(t)\, C_f \, v_{\mathrm{i_q}}(t), \tag{5.119c}$$

$$i_{\mathrm{ref_q}}(t) = \; K_{vp}[v_{\mathrm{ref_q}}(t) \;-\; v_{\mathrm{i_q}}(t)] \;+\; K_{vi}\, x_{\mathrm{int,v_q}}(t) \;+\; \omega(t)\, C_f \, v_{\mathrm{i_d}}(t)\,, \tag{5.119d}$$

$$m_{\mathrm{d}}(t) \;=\; \Big\{K_{ip}[i_{\mathrm{ref_d}}(t) \;-\; i_{\mathrm{i_d}}(t)] \;+\; K_{ii}\, x_{\mathrm{int,i_d}}(t) \;-\; \omega_n \, L_f \, i_{\mathrm{i_q}}(t)\Big\}\frac{2}{V_{DC}}\,, \tag{5.119e}$$

$$m_{\mathrm{q}}(t) \;=\; \Big\{K_{ip}[i_{\mathrm{ref_q}}(t) \;-\; i_{\mathrm{i_q}}(t)] \;+\; K_{ii}\, x_{\mathrm{int,i_q}}(t) \;+\; \omega_n \, L_f \, i_{\mathrm{i_d}}(t)\Big\}\frac{2}{V_{DC}}\,. \tag{5.119f}$$

If the full and the above systems are simulated in parallel, the dimensionless steady-state errors are of order $10^{-6} - 10^{-5}$ and can therefore be considered negligible.

CASE 2 : $\omega(t) \sim \omega_n$, algebraic external currents

"Slow" variables: P_{lp}, Q_{lp}, $i_{\mathrm{lp_d}}$, $i_{\mathrm{lp_q}}$, $x_{\mathrm{int,v_d}}$, $x_{\mathrm{int,v_q}}$, $x_{\mathrm{int,i_d}}$, $x_{\mathrm{int,i_q}}$, $i_{\mathrm{i_d}}$, $i_{\mathrm{i_q}}$, $v_{\mathrm{i_d}}$, $v_{\mathrm{i_q}}$.

"Fast" variables: $i_{\mathrm{o_d}}$, $i_{\mathrm{o_q}}$.

Constant variable: ω.

The system has 12 ODEs:

$$\frac{\mathrm{d}P_{\mathrm{lp}}(t)}{\mathrm{d}t} \;=\; \omega_{cd}[v_{\mathrm{i_d}}(t)\, i_{\mathrm{o_d}}(t) \;+\; v_{\mathrm{i_q}}(t)\, i_{\mathrm{o_q}}(t) \;-\; P_{\mathrm{lp}}(t)]\,, \tag{5.120a}$$

$$\frac{\mathrm{d}Q_{\mathrm{lp}}(t)}{\mathrm{d}t} \;=\; \omega_{cd}[v_{\mathrm{i_d}}(t)\, i_{\mathrm{o_q}}(t) \;-\; v_{\mathrm{i_q}}(t)\, i_{\mathrm{o_d}}(t) \;-\; Q_{\mathrm{lp}}(t)]\,, \tag{5.120b}$$

$$\frac{\mathrm{d}i_{\mathrm{lp_d}}(t)}{\mathrm{d}t} \;=\; \omega_{ci}[i_{\mathrm{o_d}}(t) \;-\; i_{\mathrm{lp_d}}(t)]\,, \tag{5.120c}$$

$$\frac{\mathrm{d}i_{\mathrm{lp_q}}(t)}{\mathrm{d}t} = \omega_{ci}[i_{\mathrm{o_q}}(t) - i_{\mathrm{lp_q}}(t)]\,, \tag{5.120d}$$

$$\frac{\mathrm{d}x_{\mathrm{int,v_d}}(t)}{\mathrm{d}t} = v_{\mathrm{ref_d}}(t) - v_{\mathrm{i_d}}(t)\,, \tag{5.120e}$$

$$\frac{\mathrm{d}x_{\mathrm{int,v_q}}(t)}{\mathrm{d}t} = v_{\mathrm{ref_q}}(t) - v_{\mathrm{i_q}}(t)\,, \tag{5.120f}$$

$$\frac{\mathrm{d}x_{\mathrm{int,i_d}}(t)}{\mathrm{d}t} = i_{\mathrm{ref_d}}(t) - i_{\mathrm{i_d}}(t)\,, \tag{5.120g}$$

$$\frac{\mathrm{d}x_{\mathrm{int,i_q}}(t)}{\mathrm{d}t} = i_{\mathrm{ref_q}}(t) - i_{\mathrm{i_q}}(t) \tag{5.120h}$$

$$\frac{\mathrm{d}i_{\mathrm{i_d}}(t)}{\mathrm{d}t} = \frac{V_{DC}}{2\,L_f}m_{\mathrm{d}}(t) - \frac{R_f}{L_f}i_{\mathrm{i_d}}(t) - \frac{v_{\mathrm{i_d}}(t)}{L_f} + \omega_n\, i_{\mathrm{i_q}}(t)\,, \tag{5.120i}$$

$$\frac{\mathrm{d}i_{\mathrm{i_q}}(t)}{\mathrm{d}t} = \frac{V_{DC}}{2\,L_f}m_{\mathrm{q}}(t) - \frac{R_f}{L_f}i_{\mathrm{i_q}}(t) - \frac{v_{\mathrm{i_q}}(t)}{L_f} - \omega_n\, i_{\mathrm{i_d}}(t)\,, \tag{5.120j}$$

$$\frac{\mathrm{d}v_{\mathrm{i_d}}(t)}{\mathrm{d}t} = \frac{i_{\mathrm{i_d}}(t)}{C_f} - \frac{i_{\mathrm{o_d}}(t)}{C_f} + \omega_n\, v_{\mathrm{i_q}}(t)\,, \tag{5.120k}$$

$$\frac{\mathrm{d}v_{\mathrm{i_q}}(t)}{\mathrm{d}t} = \frac{i_{\mathrm{i_q}}(t)}{C_f} - \frac{i_{\mathrm{o_q}}(t)}{C_f} - \omega_n\, v_{\mathrm{i_d}}(t)\,, \tag{5.120l}$$

where $v_{\mathrm{ref_d}}$, $v_{\mathrm{ref_q}}$, $i_{\mathrm{ref_d}}$, $i_{\mathrm{ref_q}}$, m_{d} and m_{q} are defined in (5.119), while $i_{\mathrm{o_d}}$ and $i_{\mathrm{o_q}}$ are given by

$$i_{\mathrm{o_d}}(t) \sim \frac{v_{\mathrm{i_d}}(t)}{R_l + R_{\mathrm{load}}} + \frac{\bar{\omega}_n \bar{L}_l v_{\mathrm{i_q}}(t)}{(R_l + R_{\mathrm{load}})^2}\,, \tag{5.121a}$$

$$i_{\mathrm{o_d}}(t) \sim \frac{v_{\mathrm{i_q}}(t)}{R_l + R_{\mathrm{load}}} - \frac{\bar{\omega}_n \bar{L}_l v_{\mathrm{i_d}}(t)}{(R_l + R_{\mathrm{load}})^2}\,. \tag{5.121b}$$

Comparing the simulations of system (5.120) with the simulations of the full system, the dimensionless recorded steady-state errors are of order 10^{-4} or smaller.

CASE 3 : $\omega(t) \sim \omega_n$, algebraic external currents, no current PI

"Slow" variables: P_{lp}, Q_{lp}, $i_{\mathrm{lp_d}}$, $i_{\mathrm{lp_q}}$, $x_{\mathrm{int,v_d}}$, $x_{\mathrm{int,v_q}}$, $v_{\mathrm{i_d}}$, $v_{\mathrm{i_q}}$.

"Fast" variables: $i_{\mathrm{i_d}}$, $i_{\mathrm{i_q}}$, $x_{\mathrm{int,i_d}}$, $x_{\mathrm{int,i_q}}$, $i_{\mathrm{o_d}}$, $i_{\mathrm{o_q}}$.

Constant variable: ω.

The system has 8 ODEs:

$$\frac{\mathrm{d}P_{\mathrm{lp}}(t)}{\mathrm{d}t} = \omega_{cd}[v_{\mathrm{i_d}}(t)\, i_{\mathrm{o_d}}(t) + v_{\mathrm{i_q}}(t)\, i_{\mathrm{o_q}}(t) - P_{\mathrm{lp}}(t)]\,, \tag{5.122a}$$

$$\frac{\mathrm{d}Q_{\mathrm{lp}}(t)}{\mathrm{d}t} = \omega_{cd}[v_{\mathrm{i_d}}(t)\, i_{\mathrm{o_q}}(t) - v_{\mathrm{i_q}}(t)\, i_{\mathrm{o_d}}(t) - Q_{\mathrm{lp}}(t)]\,, \tag{5.122b}$$

$$\frac{\mathrm{d}i_{\mathrm{lp_d}}(t)}{\mathrm{d}t} = \omega_{ci}[i_{\mathrm{o_d}}(t) - i_{\mathrm{lp_d}}(t)]\,, \tag{5.122c}$$

$$\frac{\mathrm{d}i_{\mathrm{lp_q}}(t)}{\mathrm{d}t} = \omega_{ci}[i_{\mathrm{o_q}}(t) - i_{\mathrm{lp_q}}(t)]\,, \tag{5.122d}$$

$$\frac{\mathrm{d}x_{\mathrm{int,v_d}}(t)}{\mathrm{d}t} = v_{\mathrm{ref_d}}(t) - v_{\mathrm{i_d}}(t)\,, \tag{5.122e}$$

$$\frac{\mathrm{d}x_{\mathrm{int,v_q}}(t)}{\mathrm{d}t} = v_{\mathrm{ref_q}}(t) - v_{\mathrm{i_q}}(t)\,, \tag{5.122f}$$

$$\frac{\mathrm{dv}_{\mathrm{i_d}}(t)}{\mathrm{d}t} = \frac{i_{\mathrm{i_d}}(t)}{C_f} - \frac{i_{\mathrm{o_d}}(t)}{C_f} + \omega_n\, v_{\mathrm{i_q}}(t)\,, \tag{5.122g}$$

$$\frac{\mathrm{d}v_{\mathrm{i_q}}(t)}{\mathrm{d}t} = \frac{i_{\mathrm{i_q}}(t)}{C_f} - \frac{i_{\mathrm{o_q}}(t)}{C_f} - \omega_n\, v_{\mathrm{i_d}}(t)\,, \tag{5.122h}$$

where the references for the voltages are defined in (5.119), while $i_{\mathrm{o_d}}$-$i_{\mathrm{o_q}}$ and $i_{\mathrm{i_d}}$-$i_{\mathrm{i_q}}$ are given, respectively, by

$$i_{\mathrm{o_d}}(t) \sim \frac{v_{\mathrm{i_d}}(t)}{R_l + R_{\mathrm{load}}} + \frac{\bar{\omega}_n \bar{L}_l v_{\mathrm{i_q}}(t)}{(R_l + R_{\mathrm{load}})^2}\,, \tag{5.123a}$$

$$i_{\mathrm{o_q}}(t) \sim \frac{v_{\mathrm{i_q}}(t)}{R_l + R_{\mathrm{load}}} - \frac{\bar{\omega}_n \bar{L}_l v_{\mathrm{i_d}}(t)}{(R_l + R_{\mathrm{load}})^2}\,, \tag{5.123b}$$

and

$$i_{\mathrm{i_d}}(t) \sim i_{\mathrm{o_d}}(t) - \bar{\omega}_n\, \bar{C}_f\, v_{\mathrm{i_q}}(t)\,, \tag{5.124a}$$

$$i_{\mathrm{i_q}}(t) \sim i_{\mathrm{o_q}}(t) + \bar{\omega}_n\, \bar{C}_f\, v_{\mathrm{i_d}}(t)\,. \tag{5.124b}$$

Simulations show a steady-state error of order 10^{-4} or smaller, for every variable.

***CASE* 4** : $\omega(t) \sim \omega_n$, algebraic currents and voltages

"Slow" variables: P_{lp}, Q_{lp}, $i_{\mathrm{lp_d}}$, $i_{\mathrm{lp_q}}$.

"Fast" variables: $x_{\mathrm{int,v_d}}$, $x_{\mathrm{int,v_q}}$, $x_{\mathrm{int,i_d}}$, $x_{\mathrm{int,i_q}}$, $i_{\mathrm{i_d}}$, $i_{\mathrm{i_q}}$, $v_{\mathrm{i_d}}$, $v_{\mathrm{i_q}}$, $i_{\mathrm{o_d}}$, $i_{\mathrm{o_q}}$.

Constant variable: ω.

The system has 4 ODEs:

$$\frac{\mathrm{d}P_{\mathrm{lp}}(t)}{\mathrm{d}t} = \omega_{cd}[v_{\mathrm{i_d}}(t)\, i_{\mathrm{o_d}}(t) + v_{\mathrm{i_q}}(t)\, i_{\mathrm{o_q}}(t) - P_{\mathrm{lp}}(t)]\,, \tag{5.125a}$$

$$\frac{\mathrm{d}Q_{\mathrm{lp}}(t)}{\mathrm{d}t} = \omega_{cd}[v_{\mathrm{i_d}}(t)\, i_{\mathrm{o_q}}(t) - v_{\mathrm{i_q}}(t)\, i_{\mathrm{o_d}}(t) - Q_{\mathrm{lp}}(t)]\,, \tag{5.125b}$$

$$\frac{\mathrm{d}i_{\mathrm{lp_d}}(t)}{\mathrm{d}t} = \omega_{ci}[i_{\mathrm{o_d}}(t) - i_{\mathrm{lp_d}}(t)]\,, \tag{5.125c}$$

$$\frac{\mathrm{d}i_{\mathrm{lp_q}}(t)}{\mathrm{d}t} = \omega_{ci}[i_{\mathrm{o_q}}(t) - i_{\mathrm{lp_q}}(t)]\,,\,, \tag{5.125d}$$

where $v_{\mathrm{i_d}}$-$v_{\mathrm{i_q}}$ and $i_{\mathrm{o_d}}$-$i_{\mathrm{o_q}}$ are given, respectively, by

$$v_{\mathrm{i_d}}(t) \sim V_{\mathrm{d_n}} + K_{dq}[Q_{\mathrm{ref}} - Q_{\mathrm{lp}}(t)] + \bar{L}_v\, \bar{\omega}_n\, i_{\mathrm{lp_q}}(t)\,, \tag{5.126a}$$

$$v_{\mathrm{i_q}}(t) \sim V_{\mathrm{q_n}} - \bar{L}_v\, \bar{\omega}_n\, i_{\mathrm{lp_d}}(t)\,. \tag{5.126b}$$

and

$$i_{\mathrm{o_d}}(t) \sim \frac{v_{\mathrm{i_d}}(t)}{R_l + R_{\mathrm{load}}} + \frac{\bar{\omega}_n \bar{L}_l v_{\mathrm{i_q}}(t)}{(R_l + R_{\mathrm{load}})^2}\,, \tag{5.127a}$$

$$i_{\mathrm{o_d}}(t) \sim \frac{v_{\mathrm{i_q}}(t)}{R_l + R_{\mathrm{load}}} - \frac{\bar{\omega}_n \bar{L}_l v_{\mathrm{i_d}}(t)}{(R_l + R_{\mathrm{load}})^2}\,. \tag{5.127b}$$

If the internal currents $i_{\mathrm{i_d}}$-$i_{\mathrm{i_q}}$ need to be known, they can be computed as

$$i_{\mathrm{i_d}}(t) \sim i_{\mathrm{o_d}}(t) - \bar{\omega}_n\, \bar{C}_f\, v_{\mathrm{i_q}}(t)\,, \tag{5.128a}$$

$$i_{\mathrm{i_q}}(t) \sim i_{\mathrm{o_q}}(t) + \bar{\omega}_n\, \bar{C}_f\, v_{\mathrm{i_d}}(t)\,. \tag{5.128b}$$

Simulations show a steady-state error of order 10^{-4} or smaller, for every variable.

***CASE* 5** : $\omega(t) \sim \omega_n$, algebraic equations for currents and voltages, no low-pass filter on the external currents

"Slow" variables: P_{lp}, Q_{lp}.

"Fast" variables: $i_{\mathrm{lp_d}}$, $i_{\mathrm{lp_q}}$, $x_{\mathrm{int,v_d}}$, $x_{\mathrm{int,v_q}}$, $x_{\mathrm{int,i_d}}$, $x_{\mathrm{int,i_q}}$, $i_{\mathrm{i_d}}$, $i_{\mathrm{i_q}}$, $v_{\mathrm{i_d}}$, $v_{\mathrm{i_q}}$, $i_{\mathrm{o_d}}$, $i_{\mathrm{o_q}}$.

Constant variable: ω.

The system has 2 ODEs:

$$\frac{\mathrm{d}P_{\mathrm{lp}}(t)}{\mathrm{d}t} = \omega_{cd}[v_{\mathrm{i_d}}(t)\, i_{\mathrm{o_d}}(t) + v_{\mathrm{i_q}}(t)\, i_{\mathrm{o_q}}(t) - P_{\mathrm{lp}}(t)]\,, \tag{5.129a}$$

$$\frac{\mathrm{d}Q_{\mathrm{lp}}(t)}{\mathrm{d}t} = \omega_{cd}[v_{\mathrm{i_d}}(t)\, i_{\mathrm{o_q}}(t) - v_{\mathrm{i_q}}(t)\, i_{\mathrm{o_d}}(t) - Q_{\mathrm{lp}}(t)]\,, \tag{5.129b}$$

where

$$v_{\mathrm{i_d}}(t) \sim \alpha[V_{\mathrm{d_n}} + \frac{\bar{\omega}_n \bar{L}_v}{R_{\mathrm{load}} + R_l} V_{\mathrm{q_n}} + K_{dq}(Q_{\mathrm{ref}} - Q_{\mathrm{lp}}(t))]\,, \tag{5.130a}$$

$$v_{\mathrm{i_q}}(t) \sim V_{\mathrm{q_n}} - \beta[V_{\mathrm{d_n}} + \frac{\bar{\omega}_n \bar{L}_v}{R_{\mathrm{load}} + R_l} V_{\mathrm{q_n}} + K_{dq}(Q_{\mathrm{ref}} - Q_{\mathrm{lp}}(t))]\,, \tag{5.130b}$$

$$\tag{5.130c}$$

$$\alpha = \frac{(R_{\mathrm{load}} + R_l)^2}{(R_{\mathrm{load}} + R_l)^2 + (\bar{\omega}_n \bar{L}_v)^2}, \tag{5.131a}$$

$$\beta = \frac{(R_{\mathrm{load}} + R_l)\bar{\omega}_n \bar{L}_v}{(R_{\mathrm{load}} + R_l)^2 + (\bar{\omega}_n \bar{L}_v)^2}, \tag{5.131b}$$

and

$$i_{\mathrm{o_d}}(t) \sim \frac{v_{\mathrm{i_d}}(t)}{R_l + R_{\mathrm{load}}} + \frac{\bar{\omega}_n \bar{L}_l v_{\mathrm{i_q}}(t)}{(R_l + R_{\mathrm{load}})^2}\,, \tag{5.132a}$$

$$i_{\mathrm{o_d}}(t) \sim \frac{v_{\mathrm{i_q}}(t)}{R_l + R_{\mathrm{load}}} - \frac{\bar{\omega}_n \bar{L}_l v_{\mathrm{i_d}}(t)}{(R_l + R_{\mathrm{load}})^2}\,. \tag{5.132b}$$

The internal currents can eventually be computed as

$$i_{\mathrm{i_d}}(t) \sim i_{\mathrm{o_d}}(t) - \bar{\omega}_n\, \bar{C}_f\, v_{\mathrm{i_q}}(t)\,, \tag{5.133a}$$

$$i_{\mathrm{i_q}}(t) \sim i_{\mathrm{o_q}}(t) + \bar{\omega}_n\, \bar{C}_f\, v_{\mathrm{i_d}}(t)\,. \tag{5.133b}$$

Simulations of this system run in parallel with the full system show errors of order 10^{-1}, which is not considered good enough for using the reduced system as a faithful representation of the full model's behaviour.

5.4 Chapter Summary

In this chapter, a three-phase inverter controlled as an islanded AC microgrid converter is considered.

First, the physical variables are described and listed, and an approximate explanation of the inverter way of operating is given in §5.2.

In the second part of the section, the controller structure is described, and the state-space ODEs describing the behaviour of the control variables are derived.

In §5.3, a model reduction based on singular perturbation is performed on the system. The model is nondimensionalised, and a gradual reduction is applied according to assumptions on the "size" of some systems parameters. The variables are then split into "fast" and "slow", and the ODEs of the "fast" variables are approximated by algebraic equations. The reduction is validated at each stage through simulations comparing the behaviour of the full and of the reduced model, and computing the relative error between them.

Good results are found for reduced model with as few as four ODEs (the full system has fifteen). The smaller reduced model, having two ODEs only, does not perform so well in simulations, and hence should not be used to approximate the system's behaviour.

If droop controllers are added to multiple converters belonging to the same microgrid, their reciprocal interactions might cause instabilities in the system. These phenomena are not observable in the single-inverter system analysed in the present chapter. In the following sections, a larger AC microgrid composed by two inverters is analysed, and a similar model reduction is applied to the system.

Chapter 6

Two-Inverter AC Microgrid

6.1 Introduction and Work Summary

In this chapter, a two-inverter AC microgrid, working in island mode, is analysed. The system is composed of two inverters and one resistive load. The controllers of the two inverters and the LC filters through which they are interfaced to the line are identical, but the three-phase lines that connect the inverters to the load have different lengths, and, thus, different impedance values. The state-space model of the system is computed as explained in §6.2; subsequently, the equilibrium values of the variables is found (most of them, analytically, some, numerically).Then, the system is linearised about its the steady-state point and stability is analysed by computing the eigenvalues of the linearised system. When plotting the eigenvalues on the complex plane, some of them appear to be grouped relatively far away from the imaginary axis. These are interpreted as representing the fast phenomena of the system, whose ODEs are more likely to be neglected or turned into algebraic equations in the reduction process. The eigenvalues are computed for different values of the controller parameters and some parameters have been identified as being more significant for the system stability.

A model reduction similar to that performed on the single inverter is applied to the two inverter system, as explained in §6.3. As in the single-inverter case, a gradual reduction is performed, as four different reduced models are considered, corresponding to different degrees of reduction. The equilibrium points and corresponding linearised models are computed for each reduced system. The effectiveness of each reduction was tested by MATLAB simulation and eigenvalue

comparison. The full state-space model is formed of 30 ODEs; good agreement in the steady-state behaviour can be achieved by reduced models with 10 or more ODEs. However, the 10-ODE reduced model behaves quite differently during transients and there is a discrepancy regarding the models' prediction of stability: in the case where the controller parameters are modified in a way that makes the full system unstable, the stability of the reduced model is not affected. Therefore, for stability analysis purposes, reduced systems with 14 or more ODEs should be used.
Comparing the so-obtained results with other reductions performed on similar systems in the engineering literature, some analogies and some differences are observed regarding which variables need to be kept in the reduced models in order to achieve effective stability analyses.

6.2 Two-Inverter Model

6.2.1 Physical Variable Behaviours

In this case, a system composed of two inverters and a resistive load is considered. While the DC-source value, the filter and the controller parameters are assumed to be the same in both inverters, the line impedances are, in general, different. In the following simulations, values used are

$$L_{l2} = 3L_{l1} = 3.0 \cdot 10^{-3}\,\mathrm{H}, \tag{6.1a}$$

$$R_{l2} = 3R_{l1} = 1.50\,\Omega\,, \tag{6.1b}$$

where L_{l1} and R_{l1} have the same values, respectively, of L_l and R_l used for the case of the single inverter, as listed in Table 3.1.
The average state-space system of the model is therefore given by

$$\frac{\mathrm{d}\boldsymbol{i}_{\boldsymbol{i_{abc1}}}(t)}{\mathrm{d}t} = \frac{V_{DC}}{2\,L_f}\boldsymbol{m_{abc1}}(t) - \frac{R_f}{L_f}\boldsymbol{i}_{\boldsymbol{i_{abc1}}}(t) - \frac{\boldsymbol{v}_{\boldsymbol{i_{abc1}}}(t)}{L_f}\,, \tag{6.2a}$$

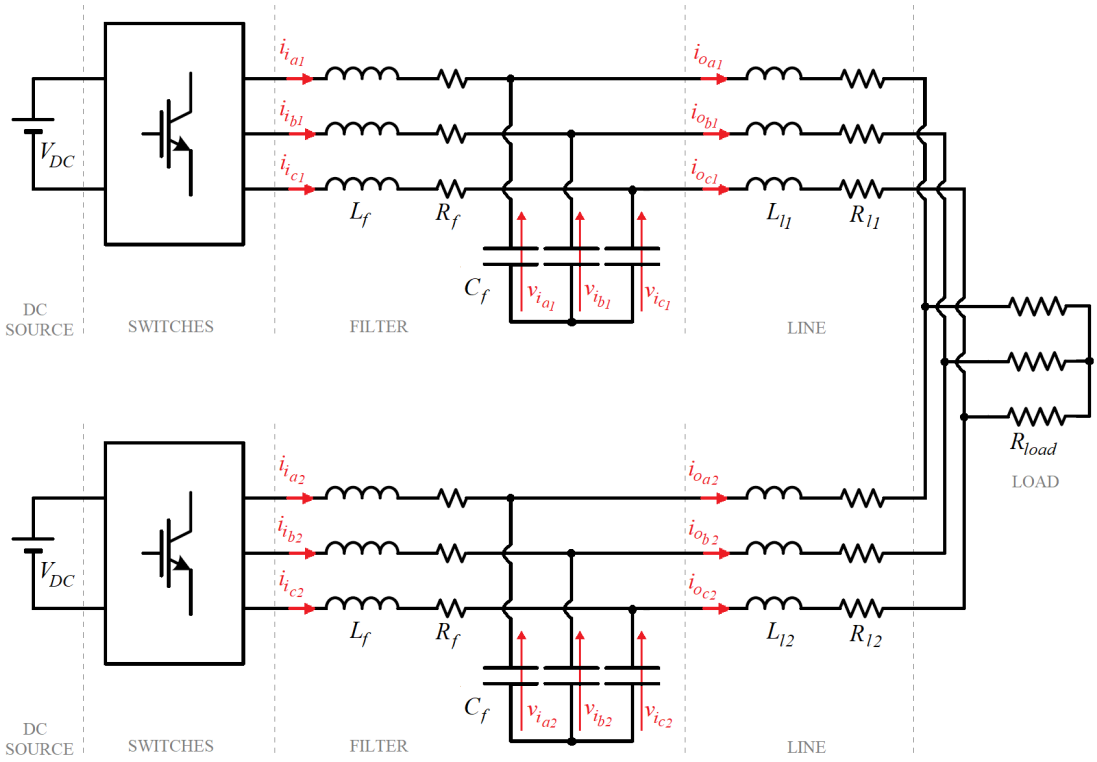

Figure 6.1: Overall scheme of the two-inverter system

$$\frac{\mathrm{d}\boldsymbol{v}_{\boldsymbol{i}_{\boldsymbol{abc1}}}(t)}{\mathrm{d}t} = \frac{\boldsymbol{i}_{\boldsymbol{i}_{\boldsymbol{abc1}}}(t)}{C_f} - \frac{\boldsymbol{i}_{\boldsymbol{o}_{\boldsymbol{abc1}}}(t)}{C_f}\,, \tag{6.2b}$$

$$\frac{\mathrm{d}\boldsymbol{i}_{\boldsymbol{o}_{\boldsymbol{abc1}}}(t)}{\mathrm{d}t} = \frac{\boldsymbol{v}_{\boldsymbol{i}_{\boldsymbol{abc1}}}(t)}{L_{l1}} - \frac{R_l}{L_{l1}}\boldsymbol{i}_{\boldsymbol{o}_{\boldsymbol{abc1}}}(t) - \frac{R_{load}}{L_{l1}}\left[\boldsymbol{i}_{\boldsymbol{o}_{\boldsymbol{abc1}}}(t) + \boldsymbol{i}_{\boldsymbol{o}_{\boldsymbol{abc2}}}(t)\right] \tag{6.2c}$$

$$\frac{\mathrm{d}\boldsymbol{i}_{\boldsymbol{i}_{\boldsymbol{abc2}}}(t)}{\mathrm{d}t} = \frac{V_{DC}}{2\,L_f}\boldsymbol{m}_{\boldsymbol{abc2}}(t) - \frac{R_f}{L_f}\boldsymbol{i}_{\boldsymbol{i}_{\boldsymbol{abc2}}}(t) - \frac{\boldsymbol{v}_{\boldsymbol{i}_{\boldsymbol{abc2}}}(t)}{L_f}\,, \tag{6.2d}$$

$$\frac{\mathrm{d}\boldsymbol{v}_{\boldsymbol{i}_{\boldsymbol{abc2}}}(t)}{\mathrm{d}t} = \frac{\boldsymbol{i}_{\boldsymbol{i}_{\boldsymbol{abc2}}}(t)}{C_f} - \frac{\boldsymbol{i}_{\boldsymbol{o}_{\boldsymbol{abc2}}}(t)}{C_f}\,, \tag{6.2e}$$

$$\frac{\mathrm{d}\boldsymbol{i}_{\boldsymbol{o}_{\boldsymbol{abc2}}}(t)}{\mathrm{d}t} = \frac{\boldsymbol{v}_{\boldsymbol{i}_{\boldsymbol{abc2}}}(t)}{L_{l1}} - \frac{R_l}{L_{l2}}\boldsymbol{i}_{\boldsymbol{o}_{\boldsymbol{abc2}}}(t) - \frac{R_{load}}{L_{l2}}\left[\boldsymbol{i}_{\boldsymbol{o}_{\boldsymbol{abc1}}}(t) + \boldsymbol{i}_{\boldsymbol{o}_{\boldsymbol{abc2}}}(t)\right]\,. \tag{6.2f}$$

When transforming (6.2) into the DQ0 reference frame, two different phases must be taken into account: each phase depends only on the controller of the relative inverter.

A phase difference α_2 can thus be defined as

$$\alpha_2(t) = \theta_2(t) - \theta_1(t)\,, \tag{6.3}$$

where θ_1 and θ_2 are the phases of $v_{i_{a1}}$ and $v_{i_{a2}}$, respectively.

Therefore, (6.2a)-(6.2c) are transformed by applying the Park matrix $T(\theta_1)$, while (6.2d)-(6.2f) by applying $T(\theta_2)$. Hence, the DQ0 average state-space system of the model is given by

$$\frac{\mathrm{d}i_{i_{d1}}(t)}{\mathrm{d}t} = \frac{V_{DC}}{2\,L_f} m_{d1}(t) - \frac{R_f}{L_f} i_{i_{d1}}(t) - \frac{v_{i_{d1}}(t)}{L_f} + \omega_1(t)\, i_{i_{q1}}(t)\,, \tag{6.4a}$$

$$\frac{\mathrm{d}i_{i_{q1}}(t)}{\mathrm{d}t} = \frac{V_{DC}}{2\,L_f} m_{q1}(t) - \frac{R_f}{L_f} i_{i_{q1}}(t) - \frac{v_{i_{q1}}(t)}{L_f} - \omega_1(t)\, i_{i_{d1}}(t)\,, \tag{6.4b}$$

$$\frac{\mathrm{d}v_{i_{d1}}(t)}{\mathrm{d}t} = \frac{i_{i_{d1}}(t)}{C_f} - \frac{i_{o_{d1}}(t)}{C_f} + \omega_1(t)\, v_{i_{q1}}(t)\,, \tag{6.4c}$$

$$\frac{\mathrm{d}v_{i_{q1}}(t)}{\mathrm{d}t} = \frac{i_{i_{q1}}(t)}{C_f} - \frac{i_{o_{q1}}(t)}{C_f} - \omega_1(t)\, v_{i_{d1}}(t)\,, \tag{6.4d}$$

$$\frac{\mathrm{d}i_{o_{d1}}(t)}{\mathrm{d}t} = \frac{v_{i_{d1}}(t)}{L_{l1}} - \frac{R_{l1}}{L_{l1}} i_{o_{d1}}(t) - \frac{R_{load}}{L_{l1}} \left[i_{o_{d1}}(t) + i_{o_{d21}}(t)\right] + \omega_1(t)\, i_{o_{q1}}(t)\,, \tag{6.4e}$$

$$\frac{\mathrm{d}i_{o_{q1}}(t)}{\mathrm{d}t} = \frac{v_{i_{q1}}(t)}{L_{l1}} - \frac{R_{l1}}{L_{l1}} i_{o_{q1}}(t) - \frac{R_{load}}{L_{l1}} \left[i_{o_{q1}}(t) + i_{o_{q21}}(t)\right] - \omega_1(t)\, i_{o_{d1}}(t)\,, \tag{6.4f}$$

$$\frac{\mathrm{d}i_{i_{d2}}(t)}{\mathrm{d}t} = \frac{V_{DC}}{2\,L_f} m_{d2}(t) - \frac{R_f}{L_f} i_{i_{d2}}(t) - \frac{v_{i_{d2}}(t)}{L_f} + \omega_2(t)\, i_{i_{q2}}(t)\,, \tag{6.4g}$$

$$\frac{\mathrm{d}i_{i_{q2}}(t)}{\mathrm{d}t} = \frac{V_{DC}}{2\,L_f} m_{q2}(t) - \frac{R_f}{L_f} i_{i_{q2}}(t) - \frac{v_{i_{q2}}(t)}{L_f} - \omega_2(t)\, i_{i_{d2}}(t)\,, \tag{6.4h}$$

$$\frac{\mathrm{d}v_{i_{d2}}(t)}{\mathrm{d}t} = \frac{i_{i_{d2}}(t)}{C_f} - \frac{i_{o_{d2}}(t)}{C_f} + \omega_2(t)\, v_{i_{q2}}(t)\,, \tag{6.4i}$$

$$\frac{\mathrm{d}v_{i_{q2}}(t)}{\mathrm{d}t} = \frac{i_{i_{q2}}(t)}{C_f} - \frac{i_{o_{q2}}(t)}{C_f} - \omega_2(t)\, v_{i_{d2}}(t)\,, \tag{6.4j}$$

$$\frac{\mathrm{d}i_{o_{d2}}(t)}{\mathrm{d}t} = \frac{v_{i_{d2}}(t)}{L_{l2}} - \frac{R_{l2}}{L_{l2}} i_{o_{d2}}(t) - \frac{R_{load}}{L_{l2}} \left[i_{o_{d2}}(t) + i_{o_{d12}}(t)\right] + \omega_2(t)\, i_{o_{q2}}(t)\,, \tag{6.4k}$$

$$\frac{\mathrm{d}i_{o_{q2}}(t)}{\mathrm{d}t} = \frac{v_{i_{q2}}(t)}{L_{l2}} - \frac{R_{l2}}{L_{l2}} i_{o_{q2}}(t) - \frac{R_{load}}{L_{l2}} \left[i_{o_{q2}}(t) + i_{o_{q12}}(t)\right] - \omega_2(t)\, i_{o_{d2}}(t)\,, \tag{6.4l}$$

where $i_{o_{d12}}$ and $i_{o_{q12}}$ are the corresponding of $i_{o_{d1}}$ and $i_{o_{q1}}$, respectively, transformed in the θ_2 DQ0 reference frame, while $i_{o_{d21}}$ and $i_{o_{q21}}$ are the corresponding

of $i_{o_{d2}}$ and $i_{o_{q2}}$, respectively, transformed in the θ_1 DQ0 reference frame.

$$i_{o_{d12}}(t) = +\cos\alpha_2(t)\, i_{o_{d1}}(t) + \sin\alpha_2(t)\, i_{o_{q1}}(t)\,, \tag{6.5a}$$

$$i_{o_{q12}}(t) = -\sin\alpha_2(t)\, i_{o_{d1}}(t) + \cos\alpha_2(t)\, i_{o_{q1}}(t)\,, \tag{6.5b}$$

$$i_{o_{d21}}(t) = +\cos\alpha_2(t)\, i_{o_{d2}}(t) - \sin\alpha_2(t)\, i_{o_{q2}}(t)\,, \tag{6.5c}$$

$$i_{o_{q21}}(t) = +\sin\alpha_2(t)\, i_{o_{d2}}(t) + \cos\alpha_2(t)\, i_{o_{q2}}(t)\,, \tag{6.5d}$$

where α_2 has been defined in (6.3).

6.2.2 Controllers

For both inverters, the same controller as described in §5.2.2 has been used. The parameters are the same and their values are as listed in Table 3.1. The phase of the first inverter, θ_1, has been chosen to be a reference for the system. Therefore, α_2 will be present in the state-space system instead of θ_2. The other control variables depend on the variables of their corresponding inverter only and there is no explicit coupling in their ODEs.

6.2.3 Overall Average State-Space System

The complete system of equations can be computed by adding eighteen ODEs modelling the controller actions (nine for each inverter) to the system (6.4) describing the physical variable behaviours. As observable in (6.4), among the physical variables only the equations modelling the behaviour of $\boldsymbol{i_{o_{dq1}}}$ and $\boldsymbol{i_{o_{dq2}}}$ have an explicit presence of variables from the other inverter. The ODE relative to the phase difference α_2 is the only other equation containing variables from both inverters.
The overall state-space model of the system is then given by

$$\frac{\mathrm{d}P_{lp1}(t)}{\mathrm{d}t} = \omega_{cd}[v_{i_{d1}}(t)\, i_{i_{d1}}(t) + v_{i_{q1}}(t)\, i_{i_{q1}}(t) - P_{lp1}(t)]\,, \tag{6.6a}$$

$$\frac{\mathrm{d}Q_{lp1}(t)}{\mathrm{d}t} = \omega_{cd}[v_{i_{d1}}(t)\, i_{i_{q1}}(t) - v_{i_{q1}}(t)\, i_{i_{d1}}(t) - Q_{lp1}(t)]\,, \tag{6.6b}$$

$$\frac{\mathrm{d}\theta_1(t)}{\mathrm{d}t} = \omega_n + K_{dp}[P_{ref1} - P_{lp1}(t)]\,, \tag{6.6c}$$

$$\frac{\mathrm{d}i_{lp_{d1}}(t)}{\mathrm{d}t} = \omega_{ci}[i_{o_{d1}}(t) - i_{lp_{d1}}(t)]\,, \tag{6.6d}$$

$$\frac{\mathrm{d}i_{lp_{q1}}(t)}{\mathrm{d}t} = \omega_{ci}[i_{o_{q1}}(t) - i_{lp_{q1}}(t)]\,, \tag{6.6e}$$

$$\frac{\mathrm{d}x_{int,v_{d1}}(t)}{\mathrm{d}t} = v_{ref_{d1}}(t) - v_{i_{d1}}(t)\,, \tag{6.6f}$$

$$\frac{\mathrm{d}x_{int,v_{q1}}(t)}{\mathrm{d}t} = v_{ref_{q1}}(t) - v_{i_{q1}}(t)\,, \tag{6.6g}$$

$$\frac{\mathrm{d}x_{int,i_{d1}}(t)}{\mathrm{d}t} = i_{ref_{d1}}(t) - i_{i_{d1}}(t)\,, \tag{6.6h}$$

$$\frac{\mathrm{d}x_{int,i_{q1}}(t)}{\mathrm{d}t} = i_{ref_{q1}}(t) - i_{i_{q1}}(t) \tag{6.6i}$$

$$\frac{\mathrm{d}i_{i_{d1}}(t)}{\mathrm{d}t} = \frac{V_{DC}}{2\,L_f}m_{d1}(t) - \frac{R_f}{L_f}i_{i_{d1}}(t) - \frac{v_{i_{d1}}(t)}{L_f} + \omega_1(t)\,i_{i_{q1}}(t)\,, \tag{6.6j}$$

$$\frac{\mathrm{d}i_{i_{q1}}(t)}{\mathrm{d}t} = \frac{V_{DC}}{2\,L_f}m_{q1}(t) - \frac{R_f}{L_f}i_{i_{q1}}(t) - \frac{v_{i_{q1}}(t)}{L_f} - \omega_1(t)\,i_{i_{d1}}(t)\,, \tag{6.6k}$$

$$\frac{\mathrm{d}v_{i_{d1}}(t)}{\mathrm{d}t} = \frac{i_{i_{d1}}(t)}{C_f} - \frac{i_{o_{d1}}(t)}{C_f} + \omega_1(t)\,v_{i_{q1}}(t)\,, \tag{6.6l}$$

$$\frac{\mathrm{d}v_{i_{q1}}(t)}{\mathrm{d}t} = \frac{i_{i_{q1}}(t)}{C_f} - \frac{i_{o_{q1}}(t)}{C_f} - \omega_1(t)\,v_{i_{d1}}(t)\,, \tag{6.6m}$$

$$\frac{\mathrm{d}i_{o_{d1}}(t)}{\mathrm{d}t} = \frac{v_{i_{d1}}(t)}{L_{l1}} - \frac{R_{l1}}{L_{l1}}i_{o_{d1}}(t) - \frac{R_{load}}{L_{l1}}\left[i_{o_{d1}}(t) + i_{o_{d21}}(t)\right] + \omega_1(t)\,i_{o_{q1}}(t)\,, \tag{6.6n}$$

$$\frac{\mathrm{d}i_{o_{q1}}(t)}{\mathrm{d}t} = \frac{v_{i_{q1}}(t)}{L_{l1}} - \frac{R_{l1}}{L_{l1}}i_{o_{q1}}(t) - \frac{R_{load}}{L_{l1}}\left[i_{o_{q1}}(t) + i_{o_{q21}}(t)\right] - \omega_1(t)\,i_{o_{d1}}(t)\,, \tag{6.6o}$$

$$\frac{\mathrm{d}P_{lp2}(t)}{\mathrm{d}t} = \omega_{cd}[v_{i_{d2}}(t)\,i_{i_{d2}}(t) + v_{i_{q2}}(t)\,i_{i_{q2}}(t) - P_{lp2}(t)]\,, \tag{6.7a}$$

$$\frac{\mathrm{d}Q_{lp2}(t)}{\mathrm{d}t} = \omega_{cd}[v_{i_{d2}}(t)\,i_{i_{q2}}(t) - v_{i_{q2}}(t)\,i_{i_{d2}}(t) - Q_{lp2}(t)]\,, \tag{6.7b}$$

$$\frac{\mathrm{d}\alpha_2(t)}{\mathrm{d}t} = K_{dp}[P_{ref2} - P_{ref1} - P_{lp2}(t) + P_{lp1}(t)]\,, \tag{6.7c}$$

$$\frac{\mathrm{d}i_{lp_{d2}}(t)}{\mathrm{d}t} = \omega_{ci}[i_{o_{d2}}(t) - i_{lp_{d2}}(t)]\,, \tag{6.7d}$$

$$\frac{\mathrm{d}i_{lp_{q2}}(t)}{\mathrm{d}t} = \omega_{ci}[i_{o_{q2}}(t) - i_{lp_{q2}}(t)]\,, \tag{6.7e}$$

$$\frac{\mathrm{d}x_{int,v_{d2}}(t)}{\mathrm{d}t} = v_{ref_{d2}}(t) - v_{i_{d2}}(t)\,, \tag{6.7f}$$

$$\frac{\mathrm{d}x_{int,v_{q2}}(t)}{\mathrm{d}t} = v_{ref_{q2}}(t) - v_{i_{q2}}(t)\,, \tag{6.7g}$$

$$\frac{\mathrm{d}x_{int,i_{d2}}(t)}{\mathrm{d}t} = i_{ref_{d2}}(t) - i_{i_{d2}}(t)\,, \tag{6.7h}$$

$$\frac{\mathrm{d}x_{int,i_{q2}}(t)}{\mathrm{d}t} = i_{ref_{q2}}(t) - i_{i_{q2}}(t) \tag{6.7i}$$

$$\frac{\mathrm{d}i_{i_{d2}}(t)}{\mathrm{d}t} = \frac{V_{DC}}{2\,L_f}m_{d2}(t) - \frac{R_f}{L_f}i_{i_{d2}}(t) - \frac{v_{i_{d2}}(t)}{L_f} + \omega_2(t)\,i_{i_{q2}}(t)\,, \tag{6.7j}$$

$$\frac{\mathrm{d}i_{i_{q2}}(t)}{\mathrm{d}t} = \frac{V_{DC}}{2\,L_f}m_{q2}(t) - \frac{R_f}{L_f}i_{i_{q2}}(t) - \frac{v_{i_{q2}}(t)}{L_f} - \omega_2(t)\,i_{i_{d2}}(t)\,, \tag{6.7k}$$

$$\frac{\mathrm{d}v_{i_{d2}}(t)}{\mathrm{d}t} = \frac{i_{i_{d2}}(t)}{C_f} - \frac{i_{o_{d2}}(t)}{C_f} + \omega_2(t)\,v_{i_{q2}}(t)\,, \tag{6.7l}$$

$$\frac{\mathrm{d}v_{i_{q2}}(t)}{\mathrm{d}t} = \frac{i_{i_{q2}}(t)}{C_f} - \frac{i_{o_{q2}}(t)}{C_f} - \omega_2(t)\,v_{i_{d2}}(t)\,, \tag{6.7m}$$

$$\frac{\mathrm{d}i_{o_{d2}}(t)}{\mathrm{d}t} = \frac{v_{i_{d2}}(t)}{L_{l2}} - \frac{R_{l2}}{L_{l2}}i_{o_{d2}}(t) - \frac{R_{load}}{L_{l2}}\left[i_{o_{d2}}(t) + i_{o_{d12}}(t)\right] + \omega_2(t)\,i_{o_{q2}}(t)\,, \tag{6.7n}$$

$$\frac{\mathrm{d}i_{o_{q2}}(t)}{\mathrm{d}t} = \frac{v_{i_{q2}}(t)}{L_{l2}} - \frac{R_{l2}}{L_{l2}}i_{o_{q2}}(t) - \frac{R_{load}}{L_{l2}}\left[i_{o_{q2}}(t) + i_{o_{q12}}(t)\right] - \omega_2(t)\,i_{o_{d2}}(t)\,, \tag{6.7o}$$

where

$$\omega_{1,2}(t) = \omega_n + K_{dp}\left(P_{ref} - P_{lp1,2}(t)\right), \tag{6.8a}$$

$$\begin{aligned} v_{ref_d}1,2(t) = {} & V_{d_n} + K_{dq}(Q_{ref} - Q_{lp1,2}(t)) \\ & + L_v\{[\omega_n + K_{dp}(P_{ref} - P_{lp1,2}(t))]i_{lp_q}1,2(t) + \omega_{ci}(i_{lp_d}1,2(t) - i_{o_d}1,2(t))\}, \end{aligned} \tag{6.8b}$$

$$v_{ref_q}1,2(t) = V_{q_n} + L_v\{-[\omega_n + K_{dp}(P_{ref} - P_{lp1,2}(t))]i_{lp_d}1,2(t) + \omega_{ci}(i_{lp_q}1,2(t) - i_{o_q}1,2(t))\}. \tag{6.8c}$$

$$i_{ref_d}1,2(t) = K_{vp}[v_{ref_d}1,2(t) - v_{id}1,2(t)] + K_{vi}\,x_{int,v_d}1,2(t) - \omega_{1,2}(t)\,C_f\,v_{iq}1,2(t), \tag{6.8d}$$

$$i_{ref_q 1,2}(t) = K_{vp}[v_{ref_q 1,2}(t) - v_{i_q 1,2}(t)] + K_{vi}\, x_{int,v_q 1,2}(t) + \omega_{1,2}(t)\, C_f\, v_{i_d 1,2}(t)\,, \tag{6.8e}$$

$$m_{d1,2}(t) = \left\{K_{ip}[i_{ref_d 1,2}(t) - i_{i_d 1,2}(t)] + K_{ii}\, x_{int,i_d 1,2}(t) - \omega_{1,2}(t)\, L_f\, i_{i_q 1,2}(t)\right\}\frac{2}{V_{DC}}\,, \tag{6.8f}$$

$$m_{q1,2}(t) = \left\{K_{ip}[i_{ref_q 1,2}(t) - i_{i_q 1,2}(t)] + K_{ii}\, x_{int,i_q 1,2}(t) + \omega_{1,2}(t)\, L_f\, i_{i_d 1,2}(t)\right\}\frac{2}{V_{DC}}\,. \tag{6.8g}$$

In particular, (6.6) describe the behaviour of the first inverter variables, while (6.7) of the second inverter variables. The algebraic terms are computed according to (6.8): the index 1 is used for variables of the first inverter, index 2 for the second inverter. Even though θ_1 does not appear anywhere in the ODE system, its value is used in practice for the Park transforms: the voltages and currents are measured in *abc* reference frame, then brought to *dq*0 to perform the control. The modulation indices are then transformed back to the *abc* reference frame before being sent to the switches.

6.2.4 Equilibrium point

In order to analyse the system stability, the equilibrium points of the ODE system formed by (6.6) and (6.7) must be computed. Subsequently, the system is linearised about its steady state operating point. The equilibrium points are found by setting the RHS of all the ODEs equal to 0, excepting (6.6c). In a steady-state condition, the system phase would in fact not be constant, but it would instead keep increasing with constant speed $\bar{\omega}$, given by

$$\bar{\omega} = \omega_n + K_{dp}\left(P_{ref1} - \bar{P}_{lp1}\right)\,. \tag{6.9}$$

The equilibrium frequency is the same for both inverters. In an AC system, where the generators are synchronous machines or droop-regulated inverters, in steady state all the generators work with the same frequency $\bar{\omega}$. Hence, in this case $\bar{\omega}$ is the equilibrium frequency for both inverters and the phase difference α_2 in steady

state is constant. Setting the RHS of (6.7c) equal to 0 leads to

$$P_{ref2} - \bar{P}_{lp2} = P_{ref1} - \bar{P}_{lp1}\,. \tag{6.10}$$

In both inverters, the steady state of the low-filtered powers is given by setting their corresponding derivatives (6.6a), (6.6b), (6.7a) and (6.7b) equal to zero:

$$\bar{P}_{lp1} = \bar{v}_{i_{d1}}\bar{i}_{i_{d1}} + \bar{v}_{i_{q1}}\bar{i}_{i_{q1}}, \tag{6.11a}$$

$$\bar{Q}_{lp1} = \bar{v}_{i_{d1}}\bar{i}_{i_{q1}} - \bar{v}_{i_{q1}}\bar{i}_{i_{d1}}, \tag{6.11b}$$

$$\bar{P}_{lp2} = \bar{v}_{i_{d2}}\bar{i}_{i_{d2}} + \bar{v}_{i_{q2}}\bar{i}_{i_{q2}}, \tag{6.11c}$$

$$\bar{Q}_{lp2} = \bar{v}_{i_{d2}}\bar{i}_{i_{q2}} - \bar{v}_{i_{q2}}\bar{i}_{i_{d2}}. \tag{6.11d}$$

Substituting (6.11) into (6.9) and (6.10) leads to

$$\bar{\omega} = \omega_n + K_{dp}\left(P_{ref1} - \bar{v}_{i_{d1}}\bar{i}_{i_{d1}} - \bar{v}_{i_{q1}}\bar{i}_{i_{q1}}\right), \tag{6.12}$$

$$P_{ref2} - P_{ref1} - \bar{v}_{i_{d2}}\bar{i}_{i_{d2}} - \bar{v}_{i_{q2}}\bar{i}_{i_{q2}} + \bar{v}_{i_{d1}}\bar{i}_{i_{d1}} + \bar{v}_{i_{q1}}\bar{i}_{i_{q1}} = 0\,. \tag{6.13}$$

Proceeding analogously with (6.6d), (6.6e), (6.7d) and (6.7e), the steady-state low-pass-filtered currents are given by

$$\bar{i}_{lp_{d1}} = \bar{i}_{o_{d1}}, \tag{6.14a}$$

$$\bar{i}_{lp_{q1}} = \bar{i}_{o_{q1}}, \tag{6.14b}$$

$$\bar{i}_{lp_{d2}} = \bar{i}_{o_{d2}}, \tag{6.14c}$$

$$\bar{i}_{lp_{q2}} = \bar{i}_{o_{q2}}. \tag{6.14d}$$

Substituting the explicit expressions for $\boldsymbol{i_{ref_{dq}}}$ and $\boldsymbol{m_{dq}}$ into (6.6h)-(6.6k), (6.7h)-(6.7k) and setting them equal to zero leads to

$$\bar{x}_{int,v_{d1}} = \frac{\bar{i}_{i_{d1}} + \bar{\omega}\,C_f\,\bar{v}_{i_{q1}}}{K_{vi}}\,, \tag{6.15a}$$

$$\bar{x}_{int,v_{q1}} = \frac{\bar{i}_{i_{q1}} - \bar{\omega}\,C_f\,\bar{v}_{i_{d1}}}{K_{vi}}\,, \tag{6.15b}$$

$$\bar{x}_{int,i_{d1}} = \frac{R_f\,\bar{i}_{i_{d1}} + \bar{v}_{i_{d1}}}{K_{ii}}\,, \tag{6.15c}$$

$$\bar{x}_{int,i_{q1}} = \frac{R_f\,\bar{i}_{i_{q1}} + \bar{v}_{i_{q1}}}{K_{ii}}\,, \tag{6.15d}$$

$$\bar{x}_{int,v_{d2}} = \frac{\bar{i}_{i_{d2}} + \bar{\omega}\,C_f\,\bar{v}_{i_{q2}}}{K_{vi}}\,, \tag{6.15e}$$

$$\bar{x}_{int,v_{q2}} = \frac{\bar{i}_{i_{q2}} - \bar{\omega}\,C_f\,\bar{v}_{i_{d2}}}{K_{vi}}\,, \tag{6.15f}$$

$$\bar{x}_{int,i_{d2}} = \frac{R_f\,\bar{i}_{i_{d2}} + \bar{v}_{i_{d2}}}{K_{ii}}\,, \tag{6.15g}$$

$$\bar{x}_{int,i_{q2}} = \frac{R_f\,\bar{i}_{i_{q2}} + \bar{v}_{i_{q2}}}{K_{ii}}\,. \tag{6.15h}$$

Therefore, apart from $\bar{\alpha}_2$, the steady-state values of the control variables depend only on the physical variables of the corresponding inverter. The controllers are hence not directly coupled.

Applying equilibrium conditions to (6.6f)-(6.6g) and (6.7f)-(6.7g) leads to

$$0 = -\bar{v}_{i_{d1}} + V_{d_{n1}} + K_{dq}(Q_{ref,1} - \bar{v}_{i_{d1}}\,\bar{i}_{i_{q1}} + \bar{v}_{i_{q1}}\,\bar{i}_{i_{d1}}) + L_v\,\bar{\omega}\,\bar{i}_{o_{q1}}\,, \tag{6.16a}$$

$$0 = -\bar{v}_{i_{q1}} + V_{q_{n1}} - L_v\,\bar{\omega}\,\bar{i}_{o_{d1}}\,, \tag{6.16b}$$

$$0 = -\bar{v}_{i_{d2}} + V_{d_{n2}} + K_{dq}(Q_{ref,2} - \bar{v}_{i_{d2}}\,\bar{i}_{i_{q2}} + \bar{v}_{i_{q2}}\,\bar{i}_{i_{d2}}) + L_v\,\bar{\omega}\,\bar{i}_{o_{q2}}\,, \tag{6.16c}$$

$$0 = -\bar{v}_{i_{q2}} + V_{q_{n2}} - L_v\,\bar{\omega}\,\bar{i}_{o_{d2}}\,. \tag{6.16d}$$

The relationship between $\bar{\boldsymbol{i}}_{\boldsymbol{i_{dq}}}$ and $\bar{\boldsymbol{i}}_{\boldsymbol{o_{dq}}}$ can be derived from the equilibrium conditions on (6.6l)-(6.6m) and (6.7l)-(6.7m), as follows.

$$\bar{i}_{i_{d1}} = +\bar{i}_{o_{d1}} - C_f\,\bar{\omega}\,\bar{v}_{i_{q1}}, \tag{6.17a}$$

$$\bar{i}_{i_{q1}} = +\bar{i}_{o_{q1}} + C_f\,\bar{\omega}\,\bar{v}_{i_{d1}}, \tag{6.17b}$$

$$\bar{i}_{i_{d2}} = +\bar{i}_{o_{d2}} - C_f\,\bar{\omega}\,\bar{v}_{i_{q2}}, \tag{6.17c}$$

$$\bar{i}_{i_{q2}} = +\bar{i}_{o_{q2}} + C_f\,\bar{\omega}\,\bar{v}_{i_{d2}}. \tag{6.17d}$$

Coupling between the steady states of the two inverters is described by setting

the RHS of (6.6n)-(6.6o) and (6.7n)-(6.7n) equal to zero:

$$0 = \bar{v}_{i_{d1}} - (R_{l1} + R_{load})\bar{\imath}_{o_{d1}} + \bar{\omega}\, L_{l1}\bar{\imath}_{o_{q1}} - R_{load}\left[\cos(\bar{\alpha}_2)\bar{\imath}_{o_{d2}} - \sin(\bar{\alpha}_2)\bar{\imath}_{o_{q2}}\right], \tag{6.18a}$$

$$0 = \bar{v}_{i_{q1}} - (R_{l1} + R_{load})\bar{\imath}_{o_{q1}} + \bar{\omega}\, L_{l1}\bar{\imath}_{o_{d1}} - R_{load}\left[\sin(\bar{\alpha}_2)\bar{\imath}_{o_{d2}} + \cos(\bar{\alpha}_2)\bar{\imath}_{o_{q2}}\right], \tag{6.18b}$$

$$0 = \bar{v}_{i_{d2}} - (R_{l2} + R_{load})\bar{\imath}_{o_{d2}} + \bar{\omega}\, L_{l2}\bar{\imath}_{o_{q2}} - R_{load}\left[\cos(\bar{\alpha}_2)\bar{\imath}_{o_{d1}} + \sin(\bar{\alpha}_2)\bar{\imath}_{o_{q1}}\right], \tag{6.18c}$$

$$0 = \bar{v}_{i_{q2}} - (R_{l2} + R_{load})\bar{\imath}_{o_{q2}} + \bar{\omega}\, L_{l2}\bar{\imath}_{o_{d2}} - R_{load}\left[-\sin(\bar{\alpha}_2)\bar{\imath}_{o_{d1}} + \cos(\bar{\alpha}_2)\bar{\imath}_{o_{q1}}\right]. \tag{6.18d}$$

The interactions between the output currents of both inverters and the nonlinearities due to the steady state expression (6.12) for $\bar{\omega}$ make the analytical expressions for $\bar{\boldsymbol{\imath}}_{\boldsymbol{i_{dq}}}$, $\bar{\boldsymbol{v}}_{\boldsymbol{i_{dq}}}$, $\bar{\boldsymbol{\imath}}_{\boldsymbol{o_{dq}}}$ and $\bar{\alpha}_2$ complicated and inconvenient for practical purposes. A numerical solution has therefore been used in this work. (6.12) has been substituted into (6.16), (6.17) and (6.18). The so-obtained twelve equations and (6.13) form a nonlinear system of thirteen equations for the thirteen unknowns $\bar{\alpha}_2$, $\bar{\imath}_{i_{d1}}$, $\bar{\imath}_{i_{q1}}$, $\bar{v}_{i_{d1}}$, $\bar{v}_{i_{q1}}$, $\bar{\imath}_{o_{d1}}$, $\bar{\imath}_{o_{q1}}$, $\bar{\imath}_{i_{d2}}$, $\bar{\imath}_{i_{q2}}$, $\bar{v}_{i_{d2}}$, $\bar{v}_{i_{q2}}$, $\bar{\imath}_{o_{d2}}$, $\bar{\imath}_{o_{q2}}$. The system has been solved by the MATLAB function fsolve and its solutions have been substituted into (6.12), (6.11), (6.14) and (6.15) to compute the remaining seventeen steady states.

6.2.5 Linearised System

Since the system formed by (6.6) and (6.7) is nonlinear, in order to evaluate its steady-state stability it must first be linearised about equilibrium.

Let $\boldsymbol{x_1}(t)$ and $\boldsymbol{x_2}(t)$ be the variable vectors for the first and the second inverter, respectively. Let $\bar{\boldsymbol{x}}_{\boldsymbol{1}}(t)$ and $\bar{\boldsymbol{x}}_{\boldsymbol{2}}(t)$ be their corresponding steady states and $\tilde{\boldsymbol{x}}_{\boldsymbol{1}}(t)$ and $\tilde{\boldsymbol{x}}_{\boldsymbol{2}}(t)$ the corresponding perturbations.

Therefore, the linearised system is given by

$$\begin{bmatrix} \dfrac{\mathrm{d}\tilde{\boldsymbol{x}}_{\boldsymbol{1}}(t)}{\mathrm{d}t} \\ \dfrac{\mathrm{d}\tilde{\boldsymbol{x}}_{\boldsymbol{2}}(t)}{\mathrm{d}t} \end{bmatrix} = \begin{bmatrix} \boldsymbol{A_{11}} & \boldsymbol{A_{12}} \\ \boldsymbol{A_{21}} & \boldsymbol{A_{22}} \end{bmatrix} \begin{bmatrix} \tilde{\boldsymbol{x}}_{\boldsymbol{1}}(t) \\ \tilde{\boldsymbol{x}}_{\boldsymbol{2}}(t) \end{bmatrix}, \tag{6.19}$$

where

$$\boldsymbol{A_{11}} = \begin{bmatrix}
-\omega_{cd} & 0 & 0 & 0 & 0 & 0 & 0 & \cdots \\
0 & -\omega_{cd} & 0 & 0 & 0 & 0 & 0 & \cdots \\
K_{dp} & 0 & 0 & 0 & 0 & 0 & 0 & \cdots \\
0 & 0 & 0 & -\omega_{ci} & 0 & 0 & 0 & \cdots \\
0 & 0 & 0 & 0 & -\omega_{ci} & 0 & 0 & \cdots \\
-K_{dp}\, L_v\, \bar{\imath}_{lp_{q1}} & -K_{dq} & 0 & L_v\omega_{ci} & L_v\bar{\omega} & 0 & 0 & \cdots \\
K_{dp}\, L_v\, \bar{\imath}_{lp_{d1}} & 0 & 0 & -L_v\bar{\omega} & L_v\omega_{ci} & 0 & 0 & \cdots \\
K_{dp}(C_f\bar{v}_{i_{q1}} - K_{vp}L_v\bar{\imath}_{o_{q1}}) & -K_{dq}K_{vp} & 0 & K_{vp}L_v\omega_{ci} & L_v\bar{\omega}K_{vp} & K_{vi} & 0 & \cdots \\
K_{dp}(L_vK_{vp}\bar{\imath}_{o_{d1}} - \bar{v}_{i_{d1}}C_f) & 0 & 0 & -K_{vp}L_v\bar{\omega} & L_v\omega_{ci}K_{vp} & 0 & K_{vi} & \cdots \\
\dfrac{K_{dp}K_{ip}}{L_f}(C_f\bar{v}_{i_{q1}} - K_{vp}L_v\bar{\imath}_{o_{q1}}) & -\dfrac{K_{dq}K_{vp}K_{ip}}{L_f} & 0 & \dfrac{K_{ip}K_{vp}L_v\omega_{ci}}{L_f} & \dfrac{L_v\bar{\omega}K_{vp}K_{ip}}{L_f} & \dfrac{K_{vi}K_{ip}}{L_f} & 0 & \cdots \\
\dfrac{K_{dp}K_{ip}}{L_f}(L_vK_{vp}\bar{\imath}_{o_{d1}} - \bar{v}_{i_{d1}}C_f) & 0 & 0 & -\dfrac{K_{ip}K_{vp}L_v\bar{\omega}}{L_f} & \dfrac{K_{ip}L_v\omega_{ci}K_{vp}}{L_f} & 0 & \dfrac{K_{vi}K_{ip}}{L_f} & \cdots \\
-\bar{v}_{i_{q1}}K_{dp} & 0 & 0 & 0 & 0 & 0 & 0 & \cdots \\
\bar{v}_{i_{d1}}K_{dp} & 0 & 0 & 0 & 0 & 0 & 0 & \cdots \\
-\bar{\imath}_{o_{q1}}K_{dp} & 0 & 0 & 0 & 0 & 0 & 0 & \cdots \\
\bar{\imath}_{o_{d1}}K_{dp} & 0 & 0 & 0 & 0 & 0 & 0 & \cdots
\end{bmatrix}$$

$$\begin{bmatrix}
\cdots & 0 & 0 & \bar{v}_{i_{d1}}\,\omega_{cd} & \bar{v}_{i_{q1}}\,\omega_{cd} & \bar{\imath}_{i_{d1}}\,\omega_{cd} & \bar{\imath}_{i_{q1}}\,\omega_{cd} & 0 & 0 \\
\cdots & 0 & 0 & -\bar{v}_{i_{q1}}\,\omega_{cd} & \bar{v}_{i_{d1}}\,\omega_{cd} & \bar{\imath}_{i_{q1}}\,\omega_{cd} & -\bar{\imath}_{i_{d1}}\,\omega_{cd} & 0 & 0 \\
\cdots & 0 & 0 & 0 & 0 & 0 & 0 & 0 & 0 \\
\cdots & 0 & 0 & 0 & 0 & 0 & 0 & \omega_{ci} & 0 \\
\cdots & 0 & 0 & 0 & 0 & 0 & 0 & 0 & \omega_{ci} \\
\cdots & 0 & 0 & 0 & 0 & -1 & 0 & -L_v\omega_{ci} & 0 \\
\cdots & 0 & 0 & 0 & 0 & 0 & -1 & 0 & -L_v\omega_{ci} \\
\cdots & 0 & 0 & -1 & 0 & -K_{vp} & -\bar{\omega}C_f & -K_{vp}L_v\omega_{ci} & 0 \\
\cdots & 0 & 0 & 0 & -1 & \bar{\omega}C_f & -K_{vp} & 0 & -K_{vp}L_v\omega_{ci} \\
\cdots & \dfrac{K_{ii}}{L_f} & 0 & -\dfrac{K_{ip}+R_f}{L_f} & 0 & -\dfrac{K_{vp}K_{ip}+1}{L_f} & -\dfrac{\bar{\omega}C_fK_{ip}}{L_f} & -\dfrac{K_{vp}L_v\omega_{ci}K_{ip}}{L_f} & 0 \\
\cdots & 0 & \dfrac{K_{ii}}{L_f} & 0 & -\dfrac{K_{ip}+R_f}{L_f} & \bar{\omega}C_fK_{ip}L_f & -\dfrac{K_{vp}K_{ip}+1}{L_f} & 0 & -\dfrac{K_{vp}L_v\omega_{ci}K_{ip}}{L_f} \\
\cdots & 0 & 0 & C_f^{-1} & 0 & 0 & \bar{\omega} & -C_f^{-1} & 0 \\
\cdots & 0 & 0 & 0 & C_f^{-1} & -\bar{\omega} & 0 & 0 & -C_f^{-1} \\
\cdots & 0 & 0 & 0 & 0 & L_{l1}^{-1} & 0 & -\dfrac{R_{load}+R_{l1}}{L_{l1}} & \bar{\omega} \\
\cdots & 0 & 0 & 0 & 0 & 0 & L_{l1}^{-1} & -\bar{\omega} & -\dfrac{R_{load}+R_{l1}}{L_{l1}}
\end{bmatrix}, \tag{6.20}$$

$$
\boldsymbol{A_{12}} = \begin{bmatrix}
0 & 0 & 0 & 0 & 0 & 0 & 0 & 0 & 0 & 0 & 0 & 0 & 0 & 0 & 0 \\
0 & 0 & 0 & 0 & 0 & 0 & 0 & 0 & 0 & 0 & 0 & 0 & 0 & 0 & 0 \\
0 & 0 & 0 & 0 & 0 & 0 & 0 & 0 & 0 & 0 & 0 & 0 & 0 & 0 & 0 \\
0 & 0 & 0 & 0 & 0 & 0 & 0 & 0 & 0 & 0 & 0 & 0 & 0 & 0 & 0 \\
0 & 0 & 0 & 0 & 0 & 0 & 0 & 0 & 0 & 0 & 0 & 0 & 0 & 0 & 0 \\
0 & 0 & 0 & 0 & 0 & 0 & 0 & 0 & 0 & 0 & 0 & 0 & 0 & 0 & 0 \\
0 & 0 & 0 & 0 & 0 & 0 & 0 & 0 & 0 & 0 & 0 & 0 & 0 & 0 & 0 \\
0 & 0 & 0 & 0 & 0 & 0 & 0 & 0 & 0 & 0 & 0 & 0 & 0 & 0 & 0 \\
0 & 0 & 0 & 0 & 0 & 0 & 0 & 0 & 0 & 0 & 0 & 0 & 0 & 0 & 0 \\
0 & 0 & 0 & 0 & 0 & 0 & 0 & 0 & 0 & 0 & 0 & 0 & 0 & 0 & 0 \\
0 & 0 & 0 & 0 & 0 & 0 & 0 & 0 & 0 & 0 & 0 & 0 & 0 & 0 & 0 \\
0 & 0 & 0 & 0 & 0 & 0 & 0 & 0 & 0 & 0 & 0 & 0 & 0 & 0 & 0 \\
0 & 0 & 0 & 0 & 0 & 0 & 0 & 0 & 0 & 0 & 0 & 0 & 0 & 0 & 0 \\
0 & 0 & \frac{R_{load}\,\bar{\imath}_{o_{q21}}}{L_{l1}} & 0 & 0 & 0 & 0 & 0 & 0 & 0 & 0 & 0 & 0 & -\frac{R_{load}\cos(\bar{\alpha}_2)}{L_{l1}} & \frac{R_{load}\sin(\bar{\alpha}_2)}{L_{l1}} \\
0 & 0 & -\frac{R_{load}\,\bar{\imath}_{o_{d21}}}{L_{l1}} & 0 & 0 & 0 & 0 & 0 & 0 & 0 & 0 & 0 & 0 & -\frac{R_{load}\sin(\bar{\alpha}_2)}{L_{l1}} & -\frac{R_{load}\cos(\bar{\alpha}_2)}{L_{l1}}
\end{bmatrix}, \tag{6.21}
$$

$$
\boldsymbol{A_{21}} = \begin{bmatrix}
0 & 0 & 0 & 0 & 0 & 0 & 0 & 0 & 0 & 0 & 0 & 0 & 0 & 0 & 0 \\
0 & 0 & 0 & 0 & 0 & 0 & 0 & 0 & 0 & 0 & 0 & 0 & 0 & 0 & 0 \\
K_{dp} & 0 & 0 & 0 & 0 & 0 & 0 & 0 & 0 & 0 & 0 & 0 & 0 & 0 & 0 \\
0 & 0 & 0 & 0 & 0 & 0 & 0 & 0 & 0 & 0 & 0 & 0 & 0 & 0 & 0 \\
0 & 0 & 0 & 0 & 0 & 0 & 0 & 0 & 0 & 0 & 0 & 0 & 0 & 0 & 0 \\
0 & 0 & 0 & 0 & 0 & 0 & 0 & 0 & 0 & 0 & 0 & 0 & 0 & 0 & 0 \\
0 & 0 & 0 & 0 & 0 & 0 & 0 & 0 & 0 & 0 & 0 & 0 & 0 & 0 & 0 \\
0 & 0 & 0 & 0 & 0 & 0 & 0 & 0 & 0 & 0 & 0 & 0 & 0 & 0 & 0 \\
0 & 0 & 0 & 0 & 0 & 0 & 0 & 0 & 0 & 0 & 0 & 0 & 0 & 0 & 0 \\
0 & 0 & 0 & 0 & 0 & 0 & 0 & 0 & 0 & 0 & 0 & 0 & 0 & 0 & 0 \\
0 & 0 & 0 & 0 & 0 & 0 & 0 & 0 & 0 & 0 & 0 & 0 & 0 & 0 & 0 \\
0 & 0 & 0 & 0 & 0 & 0 & 0 & 0 & 0 & 0 & 0 & 0 & 0 & 0 & 0 \\
0 & 0 & 0 & 0 & 0 & 0 & 0 & 0 & 0 & 0 & 0 & 0 & 0 & 0 & 0 \\
0 & 0 & 0 & 0 & 0 & 0 & 0 & 0 & 0 & 0 & 0 & 0 & 0 & -\frac{R_{load}\cos(\bar{\alpha}_2)}{L_{l2}} & -\frac{R_{load}\sin(\bar{\alpha}_2)}{L_{l2}} \\
0 & 0 & 0 & 0 & 0 & 0 & 0 & 0 & 0 & 0 & 0 & 0 & 0 & \frac{R_{load}\sin(\bar{\alpha}_2)}{L_{l2}} & -\frac{R_{load}\cos(\bar{\alpha}_2)}{L_{l2}}
\end{bmatrix}, \tag{6.22}
$$

$$
\boldsymbol{A_{22}}=\begin{bmatrix}
-\omega_{cd} & 0 & 0 & 0 & 0 & 0 & 0 & \cdots \\
0 & -\omega_{cd} & 0 & 0 & 0 & 0 & 0 & \cdots \\
-K_{dp} & 0 & 0 & 0 & 0 & 0 & 0 & \cdots \\
0 & 0 & 0 & -\omega_{ci} & 0 & 0 & 0 & \cdots \\
0 & 0 & 0 & 0 & -\omega_{ci} & 0 & 0 & \cdots \\
-K_{dp}\,L_v\,\bar{\imath}_{lp_{q2}} & -K_{dq} & 0 & L_v\omega_{ci} & L_v\bar{\omega} & 0 & 0 & \cdots \\
K_{dp}\,L_v\,\bar{\imath}_{lp_{d2}} & 0 & 0 & -L_v\bar{\omega} & L_v\omega_{ci} & 0 & 0 & \cdots \\
K_{dp}(C_f\bar{v}_{i_{q2}}-K_{vp}L_v\bar{\imath}_{o_{q2}}) & -K_{dq}K_{vp} & 0 & K_{vp}L_v\omega_{ci} & L_v\bar{\omega}K_{vp} & K_{vi} & 0 & \cdots \\
K_{dp}(L_vK_{vp}\bar{\imath}_{o_{d2}}-\bar{v}_{i_{d2}}C_f) & 0 & 0 & -K_{vp}L_v\bar{\omega} & L_v\omega_{ci}K_{vp} & 0 & K_{vi} & \cdots \\
\frac{K_{dp}K_{ip}}{L_f}(C_f\bar{v}_{i_{q2}}-K_{vp}L_v\bar{\imath}_{o_{q2}}) & -\frac{K_{dq}K_{vp}K_{ip}}{L_f} & 0 & \frac{K_{ip}K_{vp}L_v\omega_{ci}}{L_f} & \frac{L_v\bar{\omega}K_{vp}K_{ip}}{L_f} & \frac{K_{vi}K_{ip}}{L_f} & 0 & \cdots \\
\frac{K_{dp}K_{ip}}{L_f}(L_vK_{vp}\bar{\imath}_{o_{d2}}-\bar{v}_{i_{d2}}C_f) & 0 & 0 & -\frac{K_{ip}K_{vp}L_v\bar{\omega}}{L_f} & \frac{K_{ip}L_v\omega_{ci}K_{vp}}{L_f} & 0 & \frac{K_{vi}K_{ip}}{L_f} & \cdots \\
-\bar{v}_{i_{q2}}K_{dp} & 0 & 0 & 0 & 0 & 0 & 0 & \cdots \\
\bar{v}_{i_{d2}}K_{dp} & 0 & 0 & 0 & 0 & 0 & 0 & \cdots \\
-\bar{\imath}_{o_{q2}}K_{dp} & 0 & -\frac{R_{load}\bar{\imath}_{o_{q12}}}{L_{l2}} & 0 & 0 & 0 & 0 & \cdots \\
\bar{\imath}_{o_{d2}}K_{dp} & 0 & \frac{R_{load}\bar{\imath}_{o_{d12}}}{L_{l2}} & 0 & 0 & 0 & 0 & \cdots
\end{bmatrix}
$$

$$
\begin{bmatrix}
\cdots & 0 & 0 & \bar{v}_{i_{d2}}\,\omega_{cd} & \bar{v}_{i_{q2}}\,\omega_{cd} & \bar{\imath}_{i_{d2}}\,\omega_{cd} & \bar{\imath}_{i_{q2}}\,\omega_{cd} & 0 & 0 \\
\cdots & 0 & 0 & -\bar{v}_{i_{q2}}\,\omega_{cd} & \bar{v}_{i_{d2}}\,\omega_{cd} & \bar{\imath}_{i_{q2}}\,\omega_{cd} & -\bar{\imath}_{i_{d2}}\,\omega_{cd} & 0 & 0 \\
\cdots & 0 & 0 & 0 & 0 & 0 & 0 & 0 & 0 \\
\cdots & 0 & 0 & 0 & 0 & 0 & 0 & \omega_{ci} & 0 \\
\cdots & 0 & 0 & 0 & 0 & 0 & 0 & 0 & \omega_{ci} \\
\cdots & 0 & 0 & 0 & 0 & -1 & 0 & -L_v\omega_{ci} & 0 \\
\cdots & 0 & 0 & 0 & 0 & 0 & -1 & 0 & -L_v\omega_{ci} \\
\cdots & 0 & 0 & -1 & 0 & -K_{vp} & -\bar{\omega}C_f & -K_{vp}L_v\omega_{ci} & 0 \\
\cdots & 0 & 0 & 0 & -1 & \bar{\omega}C_f & -K_{vp} & 0 & -K_{vp}L_v\omega_{ci} \\
\cdots & \frac{K_{ii}}{L_f} & 0 & -\frac{K_{ip}+R_f}{L_f} & 0 & -\frac{K_{vp}K_{ip}+1}{L_f} & -\frac{\bar{\omega}C_fK_{ip}}{L_f} & -\frac{K_{vp}L_v\omega_{ci}K_{ip}}{L_f} & 0 \\
\cdots & 0 & \frac{K_{ii}}{L_f} & 0 & -\frac{K_{ip}+R_f}{L_f} & \bar{\omega}C_fK_{ip}L_f & -\frac{K_{vp}K_{ip}+1}{L_f} & 0 & -\frac{K_{vp}L_v\omega_{ci}K_{ip}}{L_f} \\
\cdots & 0 & 0 & C_f^{-1} & 0 & 0 & \bar{\omega} & -C_f^{-1} & 0 \\
\cdots & 0 & 0 & 0 & C_f^{-1} & -\bar{\omega} & 0 & 0 & -C_f^{-1} \\
\cdots & 0 & 0 & 0 & 0 & L_{l1}^{-1} & 0 & -\frac{R_{load}+R_{l1}}{L_{l1}} & \bar{\omega} \\
\cdots & 0 & 0 & 0 & 0 & 0 & L_{l1}^{-1} & -\bar{\omega} & -\frac{R_{load}+R_{l1}}{L_{l1}}
\end{bmatrix}, \tag{6.23}
$$

where

$$
\bar{\imath}_{o_{d12}} = +\cos(\bar{\alpha}_2)\bar{\imath}_{o_{d1}} + \sin(\bar{\alpha}_2)\bar{\imath}_{o_{q1}}\,, \tag{6.24a}
$$

$$
\bar{\imath}_{o_{q12}} = -\sin(\bar{\alpha}_2)\bar{\imath}_{o_{d1}} + \cos(\bar{\alpha}_2)\bar{\imath}_{o_{q1}}\,, \tag{6.24b}
$$

$$
\bar{\imath}_{o_{d21}} = +\cos(\bar{\alpha}_2)\bar{\imath}_{o_{d2}} - \sin(\bar{\alpha}_2)\bar{\imath}_{o_{q2}}\,, \tag{6.24c}
$$

$$\bar{\imath}_{o_{q21}} = +\sin(\bar{\alpha}_2)\bar{\imath}_{o_{d2}} + \cos(\bar{\alpha}_2)\bar{\imath}_{o_{q2}}\,. \tag{6.24d}$$

Despite the fact that the mutual actions of the inverters are symmetrical, A_{21} and A_{12} are not identical because the first inverter is chosen as a reference for the phase: the third ODE of the inverter 1 describes the behaviour of θ_1, while the third variable of the inverter 2 describes the behaviour of α_2, corresponding to the phase difference between the two devices. α_2 is used to transform the output currents between dq0 reference frames having different phases.

6.3 Two-Inverter Model Reduction

In this section, a model reduction analogous to that performed in §5.3 is applied to the system described in §6.2. The ODE system (6.6)-(6.7) is nondimensionalised; the dimensionless parameters are assigned to a "class" according to the closest power of a small parameter ϵ; small parameters are identified; the leading-order terms are retained. Similarly to the case of single-inverter reduction, some ODEs are turned into algebraic equations and their corresponding state-space variables become terms which are dependent on the other variables. Again, as for some parameters the attribution to a certain power of ϵ is not unequivocal, a gradual model reduction is performed. Each step of the reduction is then validated through time-domain simulations and stability analysis.

6.3.1 Nondimensionalisation

Analogously to the single-inverter model reduction, the two-inverter model is nondimensionalised before proceeding with the model reduction.
Since the same base values as in §5.3 are used for nondimensionalisation here, the dimensionless parameters for both inverters are the same as in Table 5.4, with the exception of the line resistances and inductances. According to (6.1), the line impedance of the second inverter is three times the impedance of the first inverter. Hence, R_{l1} and L_{l1} have the same values reported in Table 5.4, while for the second inverter the following parameters are computed:

$$\hat{R}_{l2} = 3\hat{R}_{l1} = 5.0 \times 10^{-2}\,, \tag{6.25a}$$

$$\hat{L}_{l2} = 3\hat{L}_{l1} = 4.0 \times 10^{-4}\,. \tag{6.25b}$$

Regarding the attribution of the power of ϵ, R_{l2} is considered $\mathcal{O}(1)$, while L_{12} is assumed to be $\mathcal{O}(\epsilon)$.

The full nondimensionalised state-space system is therefore given by

$$\frac{\mathrm{d}\hat{P}_{lp1}(\hat{t})}{\mathrm{d}\hat{t}} = \hat{\omega}_{cd}[\hat{v}_{i_d1}(\hat{t})\,\hat{i}_{o_d1}(\hat{t}) + \hat{v}_{i_q1}(\hat{t})\,\hat{i}_{o_q1}(\hat{t}) - \hat{P}_{lp1}(\hat{t})]\,, \tag{6.26a}$$

$$\frac{\mathrm{d}\hat{Q}_{lp1}(\hat{t})}{\mathrm{d}\hat{t}} = \hat{\omega}_{cd}[\hat{v}_{i_d1}(\hat{t})\,\hat{i}_{o_q1}(\hat{t}) - \hat{v}_{i_q1}(\hat{t})\,\hat{i}_{o_d1}(\hat{t}) - \hat{Q}_{lp1}(\hat{t})]\,, \tag{6.26b}$$

$$\frac{\mathrm{d}\theta(\hat{t})}{\mathrm{d}\hat{t}} = \hat{\omega}_n + \hat{K}_{dp}[\hat{P}_{ref} - \hat{P}_{lp1}(t)]\,, \tag{6.26c}$$

$$\frac{\mathrm{d}\hat{i}_{lp_{d}1}(\hat{t})}{\mathrm{d}\hat{t}} = \hat{\omega}_{ci}[\hat{i}_{o_d1}(\hat{t}) - \hat{i}_{lp_{d}1}(\hat{t})]\,, \tag{6.26d}$$

$$\frac{\mathrm{d}\hat{i}_{lp_{q}1}(\hat{t})}{\mathrm{d}\hat{t}} = \hat{\omega}_{ci}[\hat{i}_{o_q1}(\hat{t}) - \hat{i}_{lp_{q}1}(\hat{t})]\,, \tag{6.26e}$$

$$\frac{\mathrm{d}\hat{x}_{int,v_{d1}}(\hat{t})}{\mathrm{d}\hat{t}} = \hat{v}_{ref_{d1}}(\hat{t}) - \hat{v}_{i_{d1}}(\hat{t})\,, \tag{6.26f}$$

$$\frac{\mathrm{d}\hat{x}_{int,v_{q1}}(\hat{t})}{\mathrm{d}\hat{t}} = \hat{v}_{ref_{q1}}(\hat{t}) - \hat{v}_{i_{q1}}(\hat{t})\,, \tag{6.26g}$$

$$\frac{\mathrm{d}\hat{x}_{int,i_{d1}}(\hat{t})}{\mathrm{d}\hat{t}} = \hat{i}_{ref_{d1}}(\hat{t}) - \hat{i}_{i_{d1}}(\hat{t})\,, \tag{6.26h}$$

$$\frac{\mathrm{d}\hat{x}_{int,i_{q1}}(\hat{t})}{\mathrm{d}\hat{t}} = \hat{i}_{ref_{q1}}(\hat{t}) - \hat{i}_{i_{q1}}(\hat{t}) \tag{6.26i}$$

$$\frac{\mathrm{d}\hat{i}_{i_{d1}}(\hat{t})}{\mathrm{d}\hat{t}} = \frac{\hat{V}_{DC}}{2\,\hat{L}_f} m_{d1}(\hat{t}) - \frac{\hat{R}_f}{\hat{L}_f}\hat{i}_{i_{d1}}(\hat{t}) - \frac{\hat{v}_{i_{d1}}(\hat{t})}{\hat{L}_f} + \hat{\omega_1}(\hat{t})\,\hat{i}_{i_{q1}}(\hat{t})\,, \tag{6.26j}$$

$$\frac{\mathrm{d}\hat{i}_{i_{q1}}(\hat{t})}{\mathrm{d}\hat{t}} = \frac{\hat{V}_{DC}}{2\,\hat{L}_f} m_{q1}(\hat{t}) - \frac{\hat{R}_f}{\hat{L}_f}\hat{i}_{i_{q1}}(\hat{t}) - \frac{\hat{v}_{i_{q1}}(t)}{\hat{L}_f} - \hat{\omega_1}(\hat{t})\,\hat{i}_{i_{d1}}(\hat{t})\,, \tag{6.26k}$$

$$\frac{\mathrm{d}\hat{v}_{i_{d1}}(\hat{t})}{\mathrm{d}\hat{t}} = \frac{\hat{i}_{i_{d1}}(\hat{t})}{\hat{C}_f} - \frac{\hat{i}_{o_{d1}}(\hat{t})}{\hat{C}_f} + \hat{\omega}_1(\hat{t})\,\hat{v}_{i_q1}(\hat{t})\,, \tag{6.26l}$$

$$\frac{\mathrm{d}\hat{v}_{i_{q1}}(\hat{t})}{\mathrm{d}\hat{t}} = \frac{\hat{i}_{i_{q1}}(\hat{t})}{\hat{C}_f} - \frac{\hat{i}_{o_{q1}}(\hat{t})}{\hat{C}_f} - \hat{\omega}_1(\hat{t})\,\hat{v}_{i_d1}(\hat{t})\,, \tag{6.26m}$$

$$\frac{\mathrm{d}\hat{i}_{o_{d1}}(\hat{t})}{\mathrm{d}\hat{t}} = \frac{\hat{v}_{i_{d1}}(\hat{t})}{\hat{L}_{l1}} - \frac{\hat{R}_{l1}}{\hat{L}_{l1}}\hat{i}_{o_{d1}}(\hat{t}) - \frac{\hat{R}_{load}}{\hat{L}_{l1}}[\hat{i}_{o_{d1}}(\hat{t}) + \hat{i}_{o_{d21}}(\hat{t})] + \hat{\omega}_1(\hat{t})\,\hat{i}_{o_q1}(\hat{t})\,, \tag{6.26n}$$

$$\frac{\mathrm{d}\hat{i}_{o_{q1}}(\hat{t})}{\mathrm{d}\hat{t}} = \frac{\hat{v}_{i_{q1}}(\hat{t})}{\hat{L}_{l1}} - \frac{\hat{R}_{l1}}{\hat{L}_{l1}}\hat{i}_{o_{q1}}(\hat{t}) - \frac{\hat{R}_{load}}{\hat{L}_{l1}}[\hat{i}_{o_{q1}}(\hat{t}) + \hat{i}_{o_{q21}}(\hat{t})] - \hat{\omega}_1(\hat{t})\,\hat{i}_{o_d1}(\hat{t})\,, \tag{6.26o}$$

$$\frac{\mathrm{d}\hat{P}_{lp2}(\hat{t})}{\mathrm{d}\hat{t}} = \hat{\omega}_{cd}[\hat{v}_{i_d2}(\hat{t})\,\hat{i}_{i_d2}(\hat{t}) + \hat{v}_{i_q2}(\hat{t})\,\hat{i}_{i_q2}(\hat{t}) - \hat{P}_{lp2}(\hat{t})]\,, \tag{6.27a}$$

$$\frac{\mathrm{d}\hat{Q}_{lp2}(\hat{t})}{\mathrm{d}\hat{t}} = \hat{\omega}_{cd}[\hat{v}_{i_d2}(\hat{t})\,\hat{i}_{i_q2}(\hat{t}) - \hat{v}_{i_q2}(\hat{t})\,\hat{i}_{i_d2}(\hat{t}) - \hat{Q}_{lp2}(\hat{t})]\,, \tag{6.27b}$$

$$\frac{\mathrm{d}\alpha_2(\hat{t})}{\mathrm{d}\hat{t}} = +\hat{K}_{dp}[\hat{P}_{ref2} - \hat{P}_{ref1} - \hat{P}_{lp2}(t) + -\hat{P}_{lp1}(t)]\,, \tag{6.27c}$$

$$\frac{\mathrm{d}\hat{i}_{lp_d2}(\hat{t})}{\mathrm{d}\hat{t}} = \hat{\omega}_{ci}[\hat{i}_{o_d2}(\hat{t}) - \hat{i}_{lp_d2}(\hat{t})]\,, \tag{6.27d}$$

$$\frac{\mathrm{d}\hat{i}_{lp_q2}(\hat{t})}{\mathrm{d}\hat{t}} = \hat{\omega}_{ci}[\hat{i}_{o_q2}(\hat{t}) - \hat{i}_{lp_q2}(\hat{t})]\,, \tag{6.27e}$$

$$\frac{\mathrm{d}\hat{x}_{int,v_{d2}}(\hat{t})}{\mathrm{d}\hat{t}} = \hat{v}_{ref_{d2}}(\hat{t}) - \hat{v}_{i_{d2}}(\hat{t})\,, \tag{6.27f}$$

$$\frac{\mathrm{d}\hat{x}_{int,v_{q2}}(\hat{t})}{\mathrm{d}\hat{t}} = \hat{v}_{ref_{q2}}(\hat{t}) - \hat{v}_{i_{q2}}(\hat{t})\,, \tag{6.27g}$$

$$\frac{\mathrm{d}\hat{x}_{int,i_{d2}}(\hat{t})}{\mathrm{d}\hat{t}} = \hat{i}_{ref_{d2}}(\hat{t}) - \hat{i}_{i_{d2}}(\hat{t})\,, \tag{6.27h}$$

$$\frac{\mathrm{d}\hat{x}_{int,i_{q2}}(\hat{t})}{\mathrm{d}\hat{t}} = \hat{i}_{ref_{q2}}(\hat{t}) - \hat{i}_{i_{q2}}(\hat{t}) \tag{6.27i}$$

$$\frac{\mathrm{d}\hat{i}_{i_{d2}}(\hat{t})}{\mathrm{d}\hat{t}} = \frac{\hat{V}_{DC}}{2\,\hat{L}_f} m_{d2}(\hat{t}) - \frac{\hat{R}_f}{\hat{L}_f}\hat{i}_{i_{d2}}(\hat{t}) - \frac{\hat{v}_{i_{d2}}(\hat{t})}{\hat{L}_f} + \hat{\omega_2}(\hat{t})\,\hat{i}_{i_q2}(\hat{t})\,, \tag{6.27j}$$

$$\frac{\mathrm{d}\hat{i}_{i_{q2}}(\hat{t})}{\mathrm{d}\hat{t}} = \frac{\hat{V}_{DC}}{2\,\hat{L}_f} m_{q2}(\hat{t}) - \frac{\hat{R}_f}{\hat{L}_f}\hat{i}_{i_{q2}}(\hat{t}) - \frac{\hat{v}_{i_{q2}}(t)}{\hat{L}_f} - \hat{\omega_2}(\hat{t})\,\hat{i}_{i_d2}(\hat{t})\,, \tag{6.27k}$$

$$\frac{\mathrm{d}\hat{v}_{i_{d2}}(\hat{t})}{\mathrm{d}\hat{t}} = \frac{\hat{i}_{i_{d2}}(\hat{t})}{\hat{C}_f} - \frac{\hat{i}_{o_{d2}}(\hat{t})}{\hat{C}_f} + \hat{\omega}_2(\hat{t})\,\hat{v}_{i_q2}(\hat{t})\,, \tag{6.27l}$$

$$\frac{\mathrm{d}\hat{v}_{i_{q2}}(\hat{t})}{\mathrm{d}\hat{t}} = \frac{\hat{i}_{i_{q2}}(\hat{t})}{\hat{C}_f} - \frac{\hat{i}_{o_{q2}}(\hat{t})}{\hat{C}_f} - \hat{\omega}_2(\hat{t})\,\hat{v}_{i_d2}(\hat{t})\,, \tag{6.27m}$$

$$\frac{\mathrm{d}\hat{i}_{o_{d2}}(\hat{t})}{\mathrm{d}\hat{t}} = \frac{\hat{v}_{i_{d2}}(\hat{t})}{\hat{L}_{l2}} - \frac{\hat{R}_{l2}}{\hat{L}_{l2}}\hat{i}_{o_{d2}}(\hat{t}) - \frac{\hat{R}_{load}}{\hat{L}_{l2}}[\hat{i}_{o_{d2}}(\hat{t}) + \hat{i}_{o_{d12}}(\hat{t})] + \hat{\omega}_2(\hat{t})\,\hat{i}_{o_q1}(\hat{t})\,, \tag{6.27n}$$

$$\frac{\mathrm{d}\hat{i}_{o_{q2}}(\hat{t})}{\mathrm{d}\hat{t}} = \frac{\hat{v}_{i_{q2}}(\hat{t})}{\hat{L}_{l2}} - \frac{\hat{R}_{l2}}{\hat{L}_{l2}}\hat{i}_{o_{q2}}(\hat{t}) - \frac{\hat{R}_{load}}{\hat{L}_{l2}}[\hat{i}_{o_{q2}}(\hat{t}) + \hat{i}_{o_{q12}}(\hat{t})] - \hat{\omega}_2(\hat{t})\,\hat{i}_{o_d2}(\hat{t})\,, \tag{6.27o}$$

where

$$\hat{\omega}_{1,2}(\hat{t}) = \hat{\omega}_n + \hat{K}_{dp}\left(\hat{P}_{ref} - \hat{P}_{lp1,2}(\hat{t})\right), \tag{6.28a}$$

$$\hat{v}_{ref_d1,2}(\hat{t}) = \hat{V}_{d_n} + \hat{K}_{dq}(\hat{Q}_{ref} - \hat{Q}_{lp1,2}(\hat{t})) \tag{6.28b}$$
$$+ \hat{L}_v\{[\hat{\omega}_n + \hat{K}_{dp}(\hat{P}_{ref} - \hat{P}_{lp1,2}(\hat{t}))]\hat{i}_{lp_q}1,2(\hat{t}) + \hat{\omega}_{ci}(\hat{i}_{lp_d}1,2(\hat{t}) - \hat{i}_{o_d}1,2(\hat{t}))\},$$

$$v_{ref_q1,2}(t) = V_{q_n} + L_v\{-[\omega_n + K_{dp}(P_{ref} - P_{lp1,2}(t))]i_{lp_d}1,2(t) \tag{6.28c}$$

$$+\,\omega_{ci}(i_{lp_q1,2}(t) - i_{o_q1,2}(t))\},$$

$$\hat{i}_{ref_d1,2}(\hat{t}) = \hat{K}_{vp}[\hat{v}_{ref_d1,2}(\hat{t}) - \hat{v}_{i_d1,2}(\hat{t})] + \hat{K}_{vi}\,\hat{x}_{int,v_d1,2}(\hat{t}) - \hat{\omega}_{1,2}(\hat{t})\,\hat{C}_f\,\hat{v}_{i_q1,2}(\hat{t}), \tag{6.28d}$$

$$\hat{i}_{ref_q1,2}(\hat{t}) = \hat{K}_{vp}[\hat{v}_{ref_q1,2}(\hat{t}) - \hat{v}_{i_q1,2}(\hat{t})] + \hat{K}_{vi1,2}\,\hat{x}_{int,v_q1,2}(\hat{t}) + \hat{\omega}_{1,2}(\hat{t})\,\hat{C}_f\,\hat{v}_{i_d1,2}(\hat{t})\,, \tag{6.28e}$$

$$m_{d1,2}(\hat{t}) = \left\{\hat{K}_{ip}[\hat{i}_{ref_d1,2}(\hat{t}) - \hat{i}_{i_d1,2}(\hat{t})] + \hat{K}_{ii}\,\hat{x}_{int,i_d1,2}(\hat{t}) - \hat{\omega}_{1,2}(\hat{t})\,\hat{L}_f\,\hat{i}_{i_q1,2}(\hat{t})\right\}\frac{2}{\hat{V}_{DC}}\,, \tag{6.28f}$$

$$m_{q1,2}(\hat{t}) = \left\{\hat{K}_{ip}[\hat{i}_{ref_q1,2}(\hat{t}) - \hat{i}_{i_q1,2}(\hat{t})] + \hat{K}_{ii}\,\hat{x}_{int,i_q1,2}(\hat{t}) + \hat{\omega}_{1,2}(\hat{t})\,\hat{L}_f\,\hat{i}_{i_d1,2}(\hat{t})\right\}\frac{2}{\hat{V}_{DC}}\,. \tag{6.28g}$$

The system formed of (6.26), (6.27) and (6.28) is reduced gradually in the following sections.

For the sake of clarity, the hats will be dropped from the notation from now on.

6.3.1.1 Constant frequency

Given the good approximation obtained by considering $\omega_n = \mathcal{O}(\epsilon^{-1})$ in the case of a single inverter, the analogous procedure is replicated here for the two-inverter model. Again, an auxiliary variable $\bar{\omega}_n = \mathcal{O}(1)$ is defined as

$$\bar{\omega}_n = \epsilon\,\omega\,. \tag{6.29}$$

Substituting (6.29) into the equations for the angular frequencies leads to

$$\omega_{1,2}(t) = \epsilon^{-1}\bar{\omega}_n + K_{dp}[P_{ref} - P_{lp1,2}(t)]\,. \tag{6.30}$$

As, $P_{lp1,2}$ is $\mathcal{O}(1)$ (data available from simulations), $\omega_{1,2}(t)$ must be $\mathcal{O}(\epsilon^{-1})$. Hence, two new $\mathcal{O}(1)$ variables are defined as

$$\bar{\omega}_{1,2}(t) = \epsilon\,\omega_{1,2}(t) = \bar{\omega}_n + \epsilon\,K_{dp}[P_{ref} - P_{lp1,2}(t)]\,. \tag{6.31}$$

Thus, $\bar{\omega}_{1,2}(t)$ can be approximated by

$$\bar{\omega}_{1,2}(t) \sim \bar{\omega}_n + \mathcal{O}(\epsilon)\,. \tag{6.32}$$

This approximation, besides reducing slightly the size of the system (by 1 ODE and its respective state-space variable), eliminates some of the nonlinearities due to the $dq0$ coupling terms (e.g. $\omega_1(t)\, i_{i_q}1(t)$, $\omega_1(t)\, v_{i_d}2(t)$,...). In steady state, ω_1 will always be equal to ω_2, because of physical laws of electrical systems. In transients, however, the two frequencies might differ slightly to allow their phase difference α_2 to change value. The errors due to these inaccuracies are usually negligible, as shown later in simulations.
The overall reduced system is then given by

$$\frac{\mathrm{d}P_{lp1,2}(t)}{\mathrm{d}t} = \omega_{cd}[v_{i_d}1,2(t)\, i_{o_d}1,2(t) - v_{i_q}1,2(t)\, i_{o_q}1,2(t) - P_{lp1,2}(t)]\,, \tag{6.33a}$$

$$\frac{\mathrm{d}Q_{lp1,2}(t)}{\mathrm{d}t} = \omega_{cd}[v_{i_d}1,2(t)\, i_{o_q}1,2(t) - v_{i_q}1,2(t)\, i_{o_d}1,2(t) - Q_{lp1,2}(t)]\,, \tag{6.33b}$$

$$\frac{\mathrm{d}\alpha_2(t)}{\mathrm{d}t} = K_{dp}[P_{ref2} - P_{ref1} - P_{lp2}(t) + P_{lp1}(t)]\,, \tag{6.33c}$$

$$\frac{\mathrm{d}i_{lp_d}1,2(t)}{\mathrm{d}t} = \omega_{ci}[i_{o_d}1,2t) - i_{lp_d}1,2(t)]\,, \tag{6.33d}$$

$$\frac{\mathrm{d}i_{lp_q}1,2(t)}{\mathrm{d}t} = \omega_{ci}[i_{o_q}1,2(t) - i_{lp_q}1,2(t)]\,, \tag{6.33e}$$

$$\frac{\mathrm{d}x_{int,v_{d1,2}}(t)}{\mathrm{d}t} = v_{ref_{d1,2}}(t) - v_{i_{d1,2}}(t)\,, \tag{6.33f}$$

$$\frac{\mathrm{d}x_{int,v_{q1,2}}(t)}{\mathrm{d}t} = v_{ref_{q1,2}}(t) - v_{i_{q1,2}}(t)\,, \tag{6.33g}$$

$$\frac{\mathrm{d}x_{int,i_{d1,2}}(t)}{\mathrm{d}t} = i_{ref_{d1,2}}(\hat{t}) - i_{i_{d1,2}}(\hat{t})\,, \tag{6.33h}$$

$$\frac{\mathrm{d}x_{int,i_{q1,2}}(t)}{\mathrm{d}t} = i_{ref_{q1,2}}(t) - i_{i_{q1,2}}(t)\,, \tag{6.33i}$$

$$\frac{\mathrm{d}i_{i_{d1,2}}(t)}{\mathrm{d}t} = \frac{V_{DC}}{2\,L_f} m_{d1,2}(t) - \frac{R_f}{L_f} i_{i_{d1,2}}(t) - \frac{v_{i_{d1,2}}(t)}{L_f} + \omega_n\, i_{i_q}1,2(t)\,, \tag{6.33j}$$

$$\frac{\mathrm{d}i_{i_{q1,2}}(t)}{\mathrm{d}t} = \frac{V_{DC}}{2\,L_f} m_{q1,2}(t) - \frac{R_f}{L_f} i_{i_{q1,2}}(\hat{t}) - \frac{v_{i_{q1,2}}(t)}{L_f} - \omega_n\, i_{i_d}1,2(t)\,, \tag{6.33k}$$

$$\frac{\mathrm{d}v_{i_{d1,2}}(t)}{\mathrm{d}t} = \frac{i_{i_{d1,2}}(t)}{C_f} - \frac{i_{o_{d1,2}}(t)}{C_f} + \omega_n\, v_{i_q}1,2(t)\,, \tag{6.33l}$$

$$\frac{\mathrm{d}v_{i_{q1,2}}(t)}{\mathrm{d}t} = \frac{i_{i_{q1,2}}(t)}{C_f} - \frac{i_{o_{q1,2}}(t)}{C_f} - \omega_n(t)\, v_{i_d}1,2(t)\,, \tag{6.33m}$$

$$\frac{\mathrm{d}i_{o_{d1}}(t)}{\mathrm{d}t} = \frac{v_{i_{d1}}(t)}{L_{l1}} - \frac{R_{l1}}{L_{l1}} i_{o_{d1}}(t) - \frac{R_{load}}{L_{l1}}\left[i_{o_{d1}}(t) + i_{o_{d21}}(t)\right] + \omega_n\, i_{o_{q1}}(t)\,, \tag{6.33n}$$

$$\frac{\mathrm{d}i_{o_{q1}}(t)}{\mathrm{d}t} = \frac{v_{i_{q1}}(t)}{L_{l1}} - \frac{R_{l1}}{L_{l1}} i_{o_{q1}}(t) - \frac{R_{load}}{L_{l1}}\left[i_{o_{q1}}(t) + i_{o_{q21}}(t)\right] - \omega_n\, i_{o_{d1}}(t)\,, \tag{6.33o}$$

$$\frac{\mathrm{d}i_{o_{d2}}(t)}{\mathrm{d}t} = \frac{v_{i_{d2}}(t)}{L_{l2}} - \frac{R_{l2}}{L_{l2}} i_{o_{d2}}(t) - \frac{R_{load}}{L_{l2}}\left[i_{o_{d2}}(t) + i_{o_{d12}}(t)\right] + \omega_n\, i_{o_{q2}}(t)\,, \tag{6.33p}$$

$$\frac{\mathrm{d}i_{o_{q2}}(t)}{\mathrm{d}t} = \frac{v_{i_{q2}}(t)}{L_{l2}} - \frac{R_{l2}}{L_{l2}} i_{o_{q2}}(t) - \frac{R_{load}}{L_{l2}}\left[i_{o_{q12}}(t) + i_{o_{q12}}(t)\right] - \omega_n\, i_{o_{d2}}(t)\,, \tag{6.33q}$$

where

$$\begin{aligned} v_{ref_d}1,2(t) &= V_{d_n} + K_{dq}(Q_{ref} - Q_{lp1,2}(t)) \\ &\quad + L_v\{[\omega_n + K_{dp}(P_{ref} - P_{lp1,2}(t))]i_{lp_q}1,2(t) + \omega_{ci}(i_{lp_d}1,2(t) - i_{o_d}1,2(t))\}, \end{aligned} \tag{6.34a}$$

$$\begin{aligned} v_{ref_q}1,2(t) &= V_{q_n} + L_v\{-[\omega_n + K_{dp}(P_{ref} - P_{lp1,2}(t))]i_{lp_d}1,2(t) \\ &\quad + \omega_{ci}(i_{lp_q}1,2(t) - i_{o_q}1,2(t))\}, \end{aligned} \tag{6.34b}$$

$$i_{ref_d}1,2(t) = K_{vp}[v_{ref_d}1,2(t) - v_{i_d}1,2(t)] + K_{vi}\, x_{int,v_d}1,2(t) - \omega_n\, C_f\, v_{i_q}1,2(t), \tag{6.34c}$$

$$i_{ref_q}1,2(t) = K_{vp}[v_{ref_q}1,2(t) - v_{i_q}1,2(t)] + K_{vi}\, x_{int,v_q}1,2(t) + \omega_n\, C_f\, v_{i_d}1,2(t)\,, \tag{6.34d}$$

$$m_{d1,2}(t) = \left\{K_{ip}[i_{ref_d}1,2(t) - i_{i_d}1,2(t)] + K_{ii}\, x_{int,i_d}1,2(t) - \omega_n\, L_f\, i_{i_q}1,2(t)\right\}\frac{2}{V_{DC}}\,, \tag{6.34e}$$

$$m_{q1,2}(t) = \left\{K_{ip}[i_{ref_q}1,2(t) - i_{i_q}1,2(t)] + K_{ii}\, x_{int,i_q}1,2(t) + \omega_n\, L_f\, i_{i_d}1,2(t)\right\}\frac{2}{V_{DC}}\,, \tag{6.34f}$$

$$i_{o_{d12}}(t) = +\cos\alpha_2(t)\, i_{o_{d1}}(t) + \sin\alpha_2(t)\, i_{o_{q1}}(t)\,, \tag{6.35a}$$

$$i_{o_{q12}}(t) = -\sin\alpha_2(t)\, i_{o_{d1}}(t) + \cos\alpha_2(t)\, i_{o_{q1}}(t)\,, \tag{6.35b}$$

$$i_{o_{d21}}(t) = +\cos\alpha_2(t)\, i_{o_{d2}}(t) - \sin\alpha_2(t)\, i_{o_{q2}}(t)\,, \tag{6.35c}$$

$$i_{o_{q21}}(t) = +\sin\alpha_2(t)\, i_{o_{d2}}(t) + \cos\alpha_2(t)\, i_{o_{q2}}(t)\,. \tag{6.35d}$$

The system obtained through this approximation is simulated in parallel with the full system. The system behaviour is observed in both steady state and transients. In particular, Figure 6.2 depicts the dimensionless error on the system variable i_{i_d1}; the transient is caused by an instantaneous change in the load resistance (R_{load} is instantaneously halved). In the picture, an oscillating behaviour due to the mutual interactions of the two inverters is observable. The maximum dimensionless steady-state error is order 10^{-4}, but it increases to order 10^{-3} during transients.

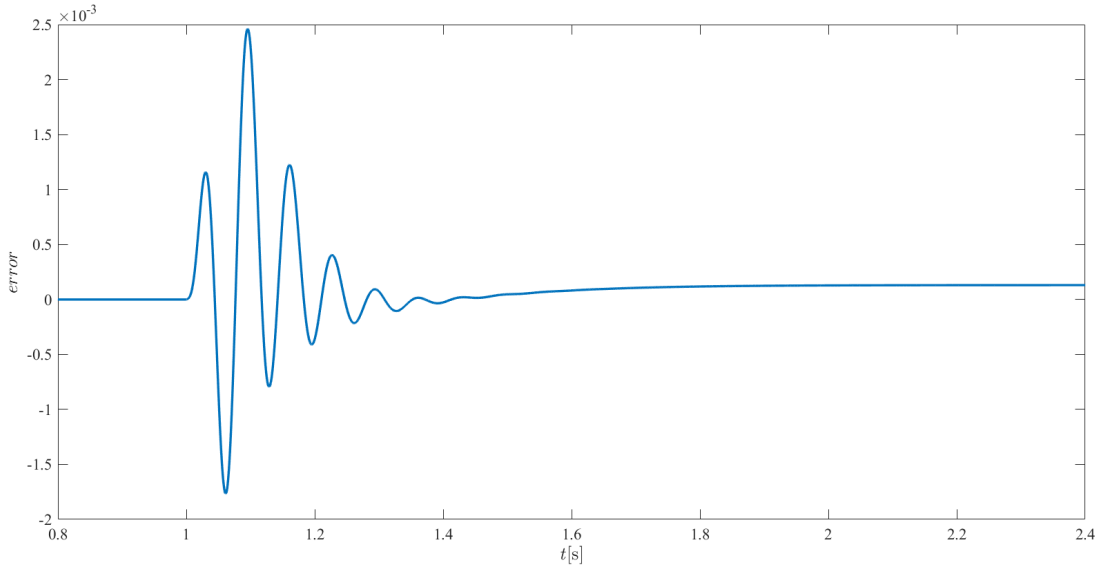

Figure 6.2: Dimensionless error on i_{i_d1}, computed between the full system and the first reduced system.

EQUILIBRIUM POINT

Before analysing the system stability, the equilibrium points of the ODE system are found and the system is linearised about its steady state point. In this case, given the good agreement between the full-system and the reduced-system simu-

lations, the steady-state values are assumed to be equal.

LINEARISED SYSTEM

Given the nonlinearities present in (6.33), the system is linearised before proceeding with the stability analysis.

Considering the submatrix division

$$\begin{bmatrix} \dfrac{\mathrm{d}\tilde{\boldsymbol{x}}_{\mathbf{1}}(t)}{\mathrm{d}t} \\ \dfrac{\mathrm{d}\tilde{\boldsymbol{x}}_{\mathbf{2}}(t)}{\mathrm{d}t} \end{bmatrix} = \begin{bmatrix} \boldsymbol{A_{11}} & \boldsymbol{A_{12}} \\ \boldsymbol{A_{21}} & \boldsymbol{A_{22}} \end{bmatrix} \begin{bmatrix} \tilde{\boldsymbol{x}}_{\mathbf{1}}(t) \\ \tilde{\boldsymbol{x}}_{\mathbf{2}}(t) \end{bmatrix}, \tag{6.36}$$

the linearised system is given by

$$\boldsymbol{A_{11}} = \begin{bmatrix} -\omega_{cd} & 0 & 0 & 0 & 0 & 0 & \cdots \\ 0 & -\omega_{cd} & 0 & 0 & 0 & 0 & \cdots \\ 0 & 0 & 0 & -\omega_{ci} & 0 & 0 & \cdots \\ 0 & 0 & 0 & 0 & -\omega_{ci} & 0 & \cdots \\ -K_{dp}\, L_v\, \bar{\imath}_{lp_{q1}} & -K_{dq} & L_v\omega_{ci} & L_v\bar{\omega} & 0 & 0 & \cdots \\ K_{dp}\, L_v\, \bar{\imath}_{lp_{d1}} & 0 & -L_v\omega_n & L_v\omega_{ci} & 0 & 0 & \cdots \\ K_{dp}(C_f\bar{v}_{i_{q1}} - K_{vp}L_v\bar{\imath}_{o_{q1}}) & -K_{dq}K_{vp} & K_{vp}L_v\omega_{ci} & L_v\omega_n K_{vp} & K_{vi} & 0 & \cdots \\ K_{dp}(L_v K_{vp}\bar{\imath}_{o_{d1}} - \bar{v}_{i_{d1}}C_f) & 0 & -K_{vp}L_v\omega_n & L_v\omega_{ci}K_{vp} & 0 & K_{vi} & \cdots \\ \dfrac{K_{dp}K_{ip}}{L_f}(C_f\bar{v}_{i_{q1}} - K_{vp}L_v\bar{\imath}_{o_{q1}}) & -\dfrac{K_{dq}K_{vp}K_{ip}}{L_f} & \dfrac{K_{ip}K_{vp}L_v\omega_{ci}}{L_f} & \dfrac{L_v\omega_n K_{vp}K_{ip}}{L_f} & \dfrac{K_{vi}K_{ip}}{L_f} & 0 & \cdots \\ \dfrac{K_{dp}K_{ip}}{L_f}(L_v K_{vp}\bar{\imath}_{o_{d1}} - \bar{v}_{i_{d1}}C_f) & 0 & -\dfrac{K_{ip}K_{vp}L_v\omega_n}{L_f} & \dfrac{K_{ip}L_v\omega_{ci}K_{vp}}{L_f} & 0 & \dfrac{K_{vi}K_{ip}}{L_f} & \cdots \\ -\bar{v}_{i_{q1}}K_{dp} & 0 & 0 & 0 & 0 & 0 & \cdots \\ \bar{v}_{i_{d1}}K_{dp} & 0 & 0 & 0 & 0 & 0 & \cdots \\ -\bar{\imath}_{o_{q1}}K_{dp} & 0 & 0 & 0 & 0 & 0 & \cdots \\ \bar{\imath}_{o_{d1}}K_{dp} & 0 & 0 & 0 & 0 & 0 & \cdots \end{bmatrix}$$

$$
\begin{matrix}
\cdots & 0 & 0 & \bar{v}_{i_{d1}}\,\omega_{cd} & \bar{v}_{i_{q1}}\,\omega_{cd} & \bar{\imath}_{i_{d1}}\,\omega_{cd} & \bar{\imath}_{i_{q1}}\,\omega_{cd} & 0 & 0 \\
\cdots & 0 & 0 & -\bar{v}_{i_{q1}}\,\omega_{cd} & \bar{v}_{i_{d1}}\,\omega_{cd} & \bar{\imath}_{i_{q1}}\,\omega_{cd} & -\bar{\imath}_{i_{d1}}\,\omega_{cd} & 0 & 0 \\
\cdots & 0 & 0 & 0 & 0 & 0 & 0 & \omega_{ci} & 0 \\
\cdots & 0 & 0 & 0 & 0 & 0 & 0 & 0 & \omega_{ci} \\
\cdots & 0 & 0 & 0 & 0 & -1 & 0 & -L_v\omega_{ci} & 0 \\
\cdots & 0 & 0 & 0 & 0 & 0 & -1 & 0 & -L_v\omega_{ci} \\
\cdots & 0 & 0 & -1 & 0 & -K_{vp} & -\omega_n C_f & -K_{vp}L_v\omega_{ci} & 0 \\
\cdots & 0 & 0 & 0 & -1 & \omega_n C_f & -K_{vp} & 0 & -K_{vp}L_v\omega_{ci} \\
\cdots & \dfrac{K_{ii}}{L_f} & 0 & -\dfrac{K_{ip}+R_f}{L_f} & 0 & -\dfrac{K_{vp}K_{ip}+1}{L_f} & -\dfrac{\omega_n C_f K_{ip}}{L_f} & -\dfrac{K_{vp}L_v\omega_{ci}K_{ip}}{L_f} & 0 \\
\cdots & 0 & \dfrac{K_{ii}}{L_f} & 0 & -\dfrac{K_{ip}+R_f}{L_f} & \omega_n C_f K_{ip} L_f & -\dfrac{K_{vp}K_{ip}+1}{L_f} & 0 & -\dfrac{K_{vp}L_v\omega_{ci}K_{ip}}{L_f} \\
\cdots & 0 & 0 & C_f^{-1} & 0 & 0 & \omega_n & -C_f^{-1} & 0 \\
\cdots & 0 & 0 & 0 & C_f^{-1} & -\omega_n & 0 & 0 & -C_f^{-1} \\
\cdots & 0 & 0 & 0 & 0 & L_{l1}^{-1} & 0 & -\dfrac{R_{load}+R_{l1}}{L_{l1}} & \omega_n \\
\cdots & 0 & 0 & 0 & 0 & 0 & L_{l1}^{-1} & -\omega_n & -\dfrac{R_{load}+R_{l1}}{L_{l1}}
\end{matrix}
\Bigg],
\tag{6.37}
$$

$$
\boldsymbol{A_{12}} =
\begin{bmatrix}
0 & 0 & 0 & 0 & 0 & 0 & 0 & 0 & 0 & 0 & 0 & 0 & 0 & 0 & 0 \\
0 & 0 & 0 & 0 & 0 & 0 & 0 & 0 & 0 & 0 & 0 & 0 & 0 & 0 & 0 \\
0 & 0 & 0 & 0 & 0 & 0 & 0 & 0 & 0 & 0 & 0 & 0 & 0 & 0 & 0 \\
0 & 0 & 0 & 0 & 0 & 0 & 0 & 0 & 0 & 0 & 0 & 0 & 0 & 0 & 0 \\
0 & 0 & 0 & 0 & 0 & 0 & 0 & 0 & 0 & 0 & 0 & 0 & 0 & 0 & 0 \\
0 & 0 & 0 & 0 & 0 & 0 & 0 & 0 & 0 & 0 & 0 & 0 & 0 & 0 & 0 \\
0 & 0 & 0 & 0 & 0 & 0 & 0 & 0 & 0 & 0 & 0 & 0 & 0 & 0 & 0 \\
0 & 0 & 0 & 0 & 0 & 0 & 0 & 0 & 0 & 0 & 0 & 0 & 0 & 0 & 0 \\
0 & 0 & 0 & 0 & 0 & 0 & 0 & 0 & 0 & 0 & 0 & 0 & 0 & 0 & 0 \\
0 & 0 & 0 & 0 & 0 & 0 & 0 & 0 & 0 & 0 & 0 & 0 & 0 & 0 & 0 \\
0 & 0 & 0 & 0 & 0 & 0 & 0 & 0 & 0 & 0 & 0 & 0 & 0 & 0 & 0 \\
0 & 0 & 0 & 0 & 0 & 0 & 0 & 0 & 0 & 0 & 0 & 0 & 0 & 0 & 0 \\
0 & 0 & \dfrac{R_{load}\,\bar{\imath}_{o_{q21}}}{L_{l1}} & 0 & 0 & 0 & 0 & 0 & 0 & 0 & 0 & 0 & 0 & -\dfrac{R_{load}\cos(\bar{\alpha}_2)}{L_{l1}} & \dfrac{R_{load}\sin(\bar{\alpha}_2)}{L_{l1}} \\
0 & 0 & -\dfrac{R_{load}\,\bar{\imath}_{o_{d21}}}{L_{l1}} & 0 & 0 & 0 & 0 & 0 & 0 & 0 & 0 & 0 & 0 & -\dfrac{R_{load}\sin(\bar{\alpha}_2)}{L_{l1}} & -\dfrac{R_{load}\cos(\bar{\alpha}_2)}{L_{l1}}
\end{bmatrix},
\tag{6.38}
$$

$$
\boldsymbol{A_{21}} = \begin{bmatrix}
0 & 0 & 0 & 0 & 0 & 0 & 0 & 0 & 0 & 0 & 0 & 0 & 0 & 0 \\
0 & 0 & 0 & 0 & 0 & 0 & 0 & 0 & 0 & 0 & 0 & 0 & 0 & 0 \\
K_{dp} & 0 & 0 & 0 & 0 & 0 & 0 & 0 & 0 & 0 & 0 & 0 & 0 & 0 \\
0 & 0 & 0 & 0 & 0 & 0 & 0 & 0 & 0 & 0 & 0 & 0 & 0 & 0 \\
0 & 0 & 0 & 0 & 0 & 0 & 0 & 0 & 0 & 0 & 0 & 0 & 0 & 0 \\
0 & 0 & 0 & 0 & 0 & 0 & 0 & 0 & 0 & 0 & 0 & 0 & 0 & 0 \\
0 & 0 & 0 & 0 & 0 & 0 & 0 & 0 & 0 & 0 & 0 & 0 & 0 & 0 \\
0 & 0 & 0 & 0 & 0 & 0 & 0 & 0 & 0 & 0 & 0 & 0 & 0 & 0 \\
0 & 0 & 0 & 0 & 0 & 0 & 0 & 0 & 0 & 0 & 0 & 0 & 0 & 0 \\
0 & 0 & 0 & 0 & 0 & 0 & 0 & 0 & 0 & 0 & 0 & 0 & 0 & 0 \\
0 & 0 & 0 & 0 & 0 & 0 & 0 & 0 & 0 & 0 & 0 & 0 & 0 & 0 \\
0 & 0 & 0 & 0 & 0 & 0 & 0 & 0 & 0 & 0 & 0 & 0 & 0 & 0 \\
0 & 0 & 0 & 0 & 0 & 0 & 0 & 0 & 0 & 0 & 0 & 0 & 0 & 0 \\
0 & 0 & 0 & 0 & 0 & 0 & 0 & 0 & 0 & 0 & 0 & 0 & -\frac{R_{load}\cos(\bar{\alpha}_2)}{L_{l2}} & -\frac{R_{load}\sin(\bar{\alpha}_2)}{L_{l2}} \\
0 & 0 & 0 & 0 & 0 & 0 & 0 & 0 & 0 & 0 & 0 & 0 & \frac{R_{load}\sin(\bar{\alpha}_2)}{L_{l2}} & -\frac{R_{load}\cos(\bar{\alpha}_2)}{L_{l2}}
\end{bmatrix}, \tag{6.39}
$$

$$
\boldsymbol{A_{22}} = \begin{bmatrix}
-\omega_{cd} & 0 & 0 & 0 & 0 & 0 & 0 & \cdots \\
0 & -\omega_{cd} & 0 & 0 & 0 & 0 & 0 & \cdots \\
-K_{dp} & 0 & 0 & 0 & 0 & 0 & 0 & \cdots \\
0 & 0 & 0 & -\omega_{ci} & 0 & 0 & 0 & \cdots \\
0 & 0 & 0 & 0 & -\omega_{ci} & 0 & 0 & \cdots \\
-K_{dp}\,L_v\,\bar{\imath}_{lp_{q2}} & -K_{dq} & 0 & L_v\omega_{ci} & L_v\omega_n & 0 & 0 & \cdots \\
K_{dp}\,L_v\,\bar{\imath}_{lp_{d2}} & 0 & 0 & -L_v\omega_n & L_v\omega_{ci} & 0 & 0 & \cdots \\
K_{dp}(C_f\bar{v}_{i_{q2}} - K_{vp}L_v\bar{\imath}_{o_{q2}}) & -K_{dq}K_{vp} & 0 & K_{vp}L_v\omega_{ci} & L_v\omega_n K_{vp} & K_{vi} & 0 & \cdots \\
K_{dp}(L_vK_{vp}\bar{\imath}_{o_{d2}} - \bar{v}_{i_{d2}}C_f) & 0 & 0 & -K_{vp}L_v\omega_n & L_v\omega_{ci}K_{vp} & 0 & K_{vi} & \cdots \\
\frac{K_{dp}K_{ip}}{L_f}(C_f\bar{v}_{i_{q2}} - K_{vp}L_v\bar{\imath}_{o_{q2}}) & -\frac{K_{dq}K_{vp}K_{ip}}{L_f} & 0 & \frac{K_{ip}K_{vp}L_v\omega_{ci}}{L_f} & \frac{L_v\omega_nK_{vp}K_{ip}}{L_f} & \frac{K_{vi}K_{ip}}{L_f} & 0 & \cdots \\
\frac{K_{dp}K_{ip}}{L_f}(L_vK_{vp}\bar{\imath}_{o_{d2}} - \bar{v}_{i_{d2}}C_f) & 0 & 0 & -\frac{K_{ip}K_{vp}L_v\omega_n}{L_f} & \frac{K_{ip}L_v\omega_{ci}K_{vp}}{L_f} & 0 & \frac{K_{vi}K_{ip}}{L_f} & \cdots \\
-\bar{v}_{i_{q2}}K_{dp} & 0 & 0 & 0 & 0 & 0 & 0 & \cdots \\
\bar{v}_{i_{d2}}K_{dp} & 0 & 0 & 0 & 0 & 0 & 0 & \cdots \\
-\bar{\imath}_{o_{q2}}K_{dp} & 0 & -\frac{R_{load}\bar{\imath}_{o_{q12}}}{L_{l2}} & 0 & 0 & 0 & 0 & \cdots \\
\bar{\imath}_{o_{d2}}K_{dp} & 0 & \frac{R_{load}\bar{\imath}_{o_{d12}}}{L_{l2}} & 0 & 0 & 0 & 0 & \cdots
\end{bmatrix}
$$

$$
\begin{bmatrix}
\cdots & 0 & 0 & \bar{v}_{i_{d2}}\,\omega_{cd} & \bar{v}_{i_{q2}}\,\omega_{cd} & \bar{\imath}_{i_{d2}}\,\omega_{cd} & \bar{\imath}_{i_{q2}}\,\omega_{cd} & 0 & 0 \\
\cdots & 0 & 0 & -\bar{v}_{i_{q2}}\,\omega_{cd} & \bar{v}_{i_{d2}}\,\omega_{cd} & \bar{\imath}_{i_{q2}}\,\omega_{cd} & -\bar{\imath}_{i_{d2}}\,\omega_{cd} & 0 & 0 \\
\cdots & 0 & 0 & 0 & 0 & 0 & 0 & 0 & 0 \\
\cdots & 0 & 0 & 0 & 0 & 0 & 0 & \omega_{ci} & 0 \\
\cdots & 0 & 0 & 0 & 0 & 0 & 0 & 0 & \omega_{ci} \\
\cdots & 0 & 0 & 0 & 0 & -1 & 0 & -L_v\omega_{ci} & 0 \\
\cdots & 0 & 0 & 0 & 0 & 0 & -1 & 0 & -L_v\omega_{ci} \\
\cdots & 0 & 0 & -1 & 0 & -K_{vp} & -\omega_n C_f & -K_{vp}L_v\omega_{ci} & 0 \\
\cdots & 0 & 0 & 0 & -1 & \omega_n C_f & -K_{vp} & 0 & -K_{vp}L_v\omega_{ci} \\
\cdots & \frac{K_{ii}}{L_f} & 0 & -\frac{K_{ip}+R_f}{L_f} & 0 & -\frac{K_{vp}K_{ip}+1}{L_f} & -\frac{\omega_n C_f K_{ip}}{L_f} & -\frac{K_{vp}L_v\omega_{ci}K_{ip}}{L_f} & 0 \\
\cdots & 0 & \frac{K_{ii}}{L_f} & 0 & -\frac{K_{ip}+R_f}{L_f} & \omega_n C_f K_{ip} L_f & -\frac{K_{vp}K_{ip}+1}{L_f} & 0 & -\frac{K_{vp}L_v\omega_{ci}K_{ip}}{L_f} \\
\cdots & 0 & 0 & C_f^{-1} & 0 & 0 & \omega_n & -C_f^{-1} & 0 \\
\cdots & 0 & 0 & 0 & C_f^{-1} & -\omega_n & 0 & 0 & -C_f^{-1} \\
\cdots & 0 & 0 & 0 & 0 & L_{l1}^{-1} & 0 & -\frac{R_{load}+R_{l1}}{L_{l1}} & \omega_n \\
\cdots & 0 & 0 & 0 & 0 & 0 & L_{l1}^{-1} & -\omega_n & -\frac{R_{load}+R_{l1}}{L_{l1}}
\end{bmatrix}, \tag{6.40}
$$

STABILITY ANALYSIS

If a linear system is stable, all its eigenvalues must be in the LHS of the complex plane.

The eigenvalues of the linearised matrix of the full system are plotted together with the eigenvalues of the reduced system linearised matrix. The comparison is shown in Figure 6.3, where they are plotted in the complex plane.

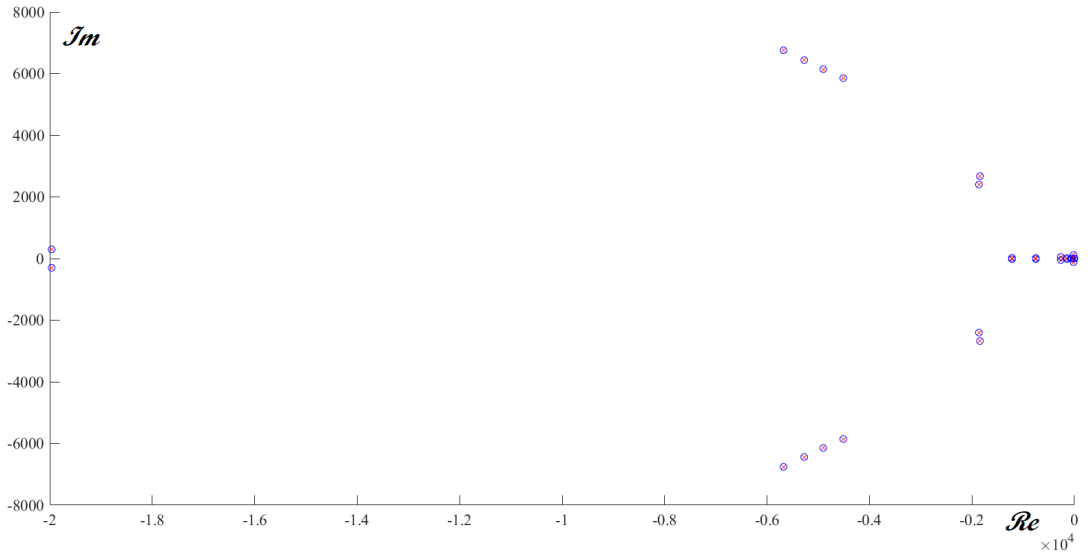

Figure 6.3: Full system eigenvalues (red crosses) and reduced system eigenvalues (blu dots), plotted on the complex plane.

The agreement between the two stability analyses is good also near the imaginary axis, as observable in the zoom of Figure 6.4.

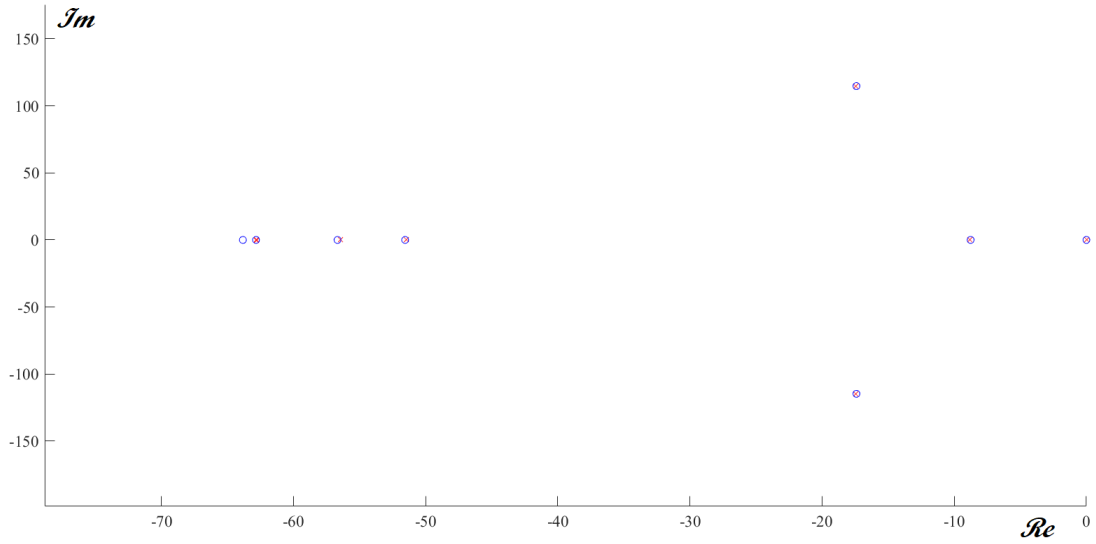

Figure 6.4: Full system eigenvalues (red crosses) and reduced system eigenvalues (blue dots); zoom on the area close to the imaginary axis.

Hence, the first step of the model reduction is assumed to be valid and to be working well with this kind of systems.

6.3.1.2 Small line inductance

The line inductances are small enough, in both inverters, to be considered $\mathcal{O}(\epsilon)$. However, proceeding with the approximations following from this assumption would mean turning the ODEs of the external currents $\boldsymbol{i_{o_{dq}1,2}}$ into algebraic equations. These equations describe the coupling between the actions of the inverters and are of primary importance concerning the stability of the system. Moreover, an eventual reduction would involve complicated algebraic expressions for the computation of the external currents; these expressions should substitute the external currents every time they appear in the other ODEs, increasing the complexity and number of nonlinearities.
For these reasons, a choice has been made, in contrast to the single-inverter case, to keep them as differential equations.

6.3.1.3 Small filter impedance

Considering, analogously to §5.3.2.4, the filter inductance and resistance to be $\mathcal{O}(\epsilon)$, two $\mathcal{O}(1)$ parameters can be defined as

$$\bar{L}_f = \epsilon^{-1} L_f = \mathcal{O}(1), \tag{6.41a}$$

$$\bar{R}_f = \epsilon^{-1} R_f = \mathcal{O}(1). \tag{6.41b}$$

Analogously to the single inverter case, the internal current ODEs can be approximated as follows:

$$\frac{\mathrm{d}i_{i_{d1,2}}(t)}{\mathrm{d}t} \sim \frac{V_{DC}\, m_{d1,2}(t)}{2\epsilon \bar{L}_f} - \frac{\bar{R}_f}{\bar{L}_f} i_{i_{d1,2}}(t) - \frac{v_{i_d 1,2}(t)}{\epsilon \bar{L}_f} i_{i_{d1,2}}(t) + \epsilon^{-1} \bar{\omega}_n\, i_{o_q 1,2}(t)\,, \tag{6.42a}$$

$$\frac{\mathrm{d}i_{i_{q1,2}}(t)}{\mathrm{d}t} \sim \frac{V_{DC}\, m_{q1,2}(t)}{2\epsilon \bar{L}_f} - \frac{\bar{R}_f}{\bar{L}_f} i_{i_{q1,2}}(t) - \frac{v_{i_q 1,2}(t)}{\epsilon \bar{L}_f} i_{i_{q1,2}}(t) - \epsilon^{-1} \bar{\omega}_n\, i_{o_d 1,2}(t)\,. \tag{6.42b}$$

Retaining the leading-order terms only in (6.42), four algebraic equations can be obtained:

$$v_{i_{d1,2}}(t) - \bar{L}_f \bar{\omega}_n i_{i_q 1,2}(t) \sim \frac{V_{DC}}{2} m_{d1,2}(t)\,, \tag{6.43a}$$

$$v_{i_{q1,2}}(t) - \bar{L}_f \bar{\omega}_n i_{i_d 1,2}(t) \sim \frac{V_{DC}}{2} m_{q1,2}(t), \tag{6.43b}$$

where the RHSs of (6.43) are given by

$$\begin{aligned} \frac{V_{DC}}{2} m_{d1,2}(t) &= K_{ip}[i_{ref_d 1,2}(t) - i_{i_d 1,2}(t)] + K_{ii}\, x_{int,i_d 1,2}(t) - \omega(t)\, L_f\, i_{i_q 1,2}(t) \\ &\sim K_{ip}[i_{ref_d 1,2}(t) - i_{i_d 1,2}(t)] + K_{ii}\, x_{int,i_d 1,2}(t) - \bar{\omega}_n\, \bar{L}_f\, i_{i_q 1,2}(t), \end{aligned} \tag{6.44a}$$

$$\begin{aligned} \frac{V_{DC}}{2} m_{q1,2}(t) &= K_{ip}[i_{ref_q 1,2}(t) - i_{i_q 1,2}(t)] + K_{ii}\, x_{int,i_q 1,2}(t) + \omega_{1,2}(t)\, L_f\, i_{i_d 1,2}(t) \\ &\sim K_{ip}[i_{ref_q 1,2}(t) - i_{i_q 1,2}(t)] + K_{ii}\, x_{int,i_d 1,2}(t) - \bar{\omega}_n\, \bar{L}_f\, i_{i_q 1,2}(t). \end{aligned} \tag{6.44b}$$

Substituting (6.44) into (6.43) leads to

$$v_{i_{d1,2}}(t) \sim K_{ip}[i_{ref_d1,2}(t) - i_{i_d1,2}(t)] + K_{ii}\, x_{int,i_d1,2}(t)\,, \tag{6.45a}$$

$$v_{i_{q1,2}}(t) \sim K_{ip}[i_{ref_q1,2}(t) - i_{i_q1,2}(t)] + K_{ii}\, x_{int,i_q1,2}(t)\,. \tag{6.45b}$$

Solving (5.85) for i_{i_d} and i_{i_q}, allows one to find the algebraic equations for the internal currents:

$$i_{i_d1,2}(t) \sim i_{ref_d1,2}(t) + \frac{K_{ii}\, x_{int,i_{d1,2}} - v_{i_d1,2}(t)}{K_{ip}}\,, \tag{6.46a}$$

$$i_{i_q1,2}(t) \sim i_{ref_q1,2}(t) + \frac{K_{ii}\, x_{int,i_{q1,2}} - v_{i_q1,2}(t)}{K_{ip}}\,. \tag{6.46b}$$

Considering the filter inductance and resistance to be "small" allows the reduction of the system by four ODEs (two for each inverter) and four corresponding state-space variables.

6.3.1.4 Neglect of integral error on the currents

Noting the analogies that have been achieved so far between the single-inverter reduction and the two-inverter reduction, and considering that the controllers of the two inverters are identical to the single inverter controller, for the sake of brevity some passages are omitted in this section.
Assuming

$$\bar{K}_{ii} = \epsilon\, K_{ii}\,, \tag{6.47}$$

$$\bar{x}_{int,i_d1,2}(t) = \epsilon^{-1}\, x_{int,i_d1,2}(t)\,, \tag{6.48}$$

four further ODEs can be eliminated from the system, analogously to §5.3.2.5.
In fact, following these assumptions leads to

$$i_{i_d1,2}(t) \sim i_{ref_d1,2}(t)\,, \tag{6.49a}$$

$$i_{i_q1,2}(t) \sim i_{ref_q1,2}(t)\,, \tag{6.49b}$$

while the state-space variables representing the integral errors on the currents are no longer present in the system, even though they are computable through the

following approximation:

$$\bar{x}_{int,i_d1,2}(t) \sim \frac{v_{i_d1,2}(t)}{\bar{K}_{ii}}\,, \tag{6.50a}$$

$$\bar{x}_{int,i_q1,2}(t) \sim \frac{v_{i_q1,2}(t)}{\bar{K}_{ii}}\,. \tag{6.50b}$$

The corresponding reduced system is formed of 21 ODEs and is given by

$$\frac{\mathrm{d}P_{lp1,2}(t)}{\mathrm{d}t} = \omega_{cd}[v_{i_d1,2}(t)\, i_{i_d1,2}(t) - v_{i_q1,2}(t)\, i_{i_q1,2}(t) - P_{lp1,2}(t)]\,, \tag{6.51a}$$

$$\frac{\mathrm{d}Q_{lp1,2}(t)}{\mathrm{d}t} = \omega_{cd}[v_{i_d1,2}(t)\, i_{i_q1,2}(t) - v_{i_q1,2}(t)\, i_{i_d1,2}(t) - Q_{lp1,2}(t)]\,, \tag{6.51b}$$

$$\frac{\mathrm{d}\alpha_2(t)}{\mathrm{d}t} = K_{dp}[P_{ref2} - P_{ref1} - P_{lp2}(t) + P_{lp1}(t)]\,, \tag{6.51c}$$

$$\frac{\mathrm{d}i_{lp_d1,2}(t)}{\mathrm{d}t} = \omega_{ci}[i_{o_d1,2}t) - i_{lp_d1,2}(t)]\,, \tag{6.51d}$$

$$\frac{\mathrm{d}i_{lp_q1,2}(t)}{\mathrm{d}t} = \omega_{ci}[i_{o_q1,2}(t) - i_{lp_q1,2}(t)]\,, \tag{6.51e}$$

$$\frac{\mathrm{d}x_{int,v_{d1,2}}(t)}{\mathrm{d}t} = v_{ref_{d1,2}}(t) - v_{i_{d1,2}}(t)\,, \tag{6.51f}$$

$$\frac{\mathrm{d}x_{int,v_{q1,2}}(t)}{\mathrm{d}t} = v_{ref_{q1,2}}(t) - v_{i_{q1,2}}(t)\,, \tag{6.51g}$$

$$\frac{\mathrm{d}v_{i_{d1,2}}(t)}{\mathrm{d}t} = \frac{i_{i_{d1,2}}(t)}{C_f} - \frac{i_{o_{d1,2}}(t)}{C_f} + \omega_n\, v_{i_q1,2}(t)\,, \tag{6.51h}$$

$$\frac{\mathrm{d}v_{i_{q1,2}}(t)}{\mathrm{d}t} = \frac{i_{i_{q1,2}}(t)}{C_f} - \frac{i_{o_{q1,2}}(t)}{C_f} - \omega_n\, v_{i_d1,2}(t)\,, \tag{6.51i}$$

$$\frac{\mathrm{d}i_{o_{d1}}(t)}{\mathrm{d}t} = \frac{v_{i_{d1}}(t)}{L_{l1}} - \frac{R_{l1}}{L_{l1}} i_{o_{d1}}(t) - \frac{R_{load}}{L_{l1}}\left[i_{o_{d1}}(t) + i_{o_{d21}}(t)\right] + \omega_n\, i_{o_{q1}}(t)\,, \tag{6.51j}$$

$$\frac{\mathrm{d}i_{o_{q1}}(t)}{\mathrm{d}t} = \frac{v_{i_{q1}}(t)}{L_{l1}} - \frac{R_{l1}}{L_{l1}} i_{o_{q1}}(t) - \frac{R_{load}}{L_{l1}}\left[i_{o_{q1}}(t) + i_{o_{q21}}(t)\right] - \omega_n\, i_{o_{d1}}(t)\,, \tag{6.51k}$$

$$\frac{\mathrm{d}i_{o_{d2}}(t)}{\mathrm{d}t} = \frac{v_{i_{d2}}(t)}{L_{l2}} - \frac{R_{l2}}{L_{l2}} i_{o_{d2}}(t) - \frac{R_{load}}{L_{l2}}\left[i_{o_{d2}}(t) + i_{o_{d12}}(t)\right] + \omega_n\, i_{o_{q2}}(t)\,, \tag{6.51l}$$

$$\frac{\mathrm{d}i_{o_{q2}}(t)}{\mathrm{d}t} = \frac{v_{i_{q2}}(t)}{L_{l2}} - \frac{R_{l2}}{L_{l2}} i_{o_{q2}}(t) - \frac{R_{load}}{L_{l2}}\left[i_{o_{q2}}(t) + i_{o_{q12}}(t)\right] - \omega_n\, i_{o_{d2}}(t)\,, \tag{6.51m}$$

where

$$v_{ref_d}1,2(t) = V_{d_n} + K_{dq}(Q_{ref} - Q_{lp1,2}(t)) \tag{6.52a}$$
$$+ L_v\{[\omega_n + K_{dp}(P_{ref} - P_{lp1,2}(t))]i_{lp_q}1,2(t) + \omega_{ci}(i_{lp_d}1,2(t) - i_{o_d}1,2(t))\},$$

$$v_{ref_q}1,2(t) = V_{q_n} + L_v\{ - [\omega_n + K_{dp}(P_{ref} - P_{lp1,2}(t))]i_{lp_d}1,2(t) \tag{6.52b}$$
$$+ \omega_{ci}(i_{lp_q}1,2(t) - i_{o_q}1,2(t))\},$$

$$i_{i_{d1,2}}(t) = K_{vp}[v_{ref_d}1,2(t) - v_{i_d}1,2(t)] + K_{vi}\, x_{int,v_d}1,2(t) - \omega_n\, C_f\, v_{i_q}1,2(t), \tag{6.52c}$$

$$i_{i_q}1,2(t) = K_{vp}[v_{ref_q}1,2(t) - v_{i_q}1,2(t)] + K_{vi}\, x_{int,v_q}1,2(t) + \omega_n\, C_f\, v_{i_d}1,2(t)\,, \tag{6.52d}$$

$$i_{o_{d12}}(t) = + \cos\alpha_2(t)\, i_{o_{d1}}(t) + \sin\alpha_2(t)\, i_{o_{q1}}(t)\,, \tag{6.52e}$$

$$i_{o_{q12}}(t) = - \sin\alpha_2(t)\, i_{o_{d1}}(t) + \cos\alpha_2(t)\, i_{o_{q1}}(t)\,, \tag{6.52f}$$

$$i_{o_{d21}}(t) = + \cos\alpha_2(t)\, i_{o_{d2}}(t) - \sin\alpha_2(t)\, i_{o_{q2}}(t)\,, \tag{6.52g}$$

$$i_{o_{q21}}(t) = + \sin\alpha_2(t)\, i_{o_{d2}}(t) + \cos\alpha_2(t)\, i_{o_{q2}}(t)\,. \tag{6.52h}$$

Simulating the system (6.51) in parallel with the full system, in a condition equal to the previous case, the maximum dimensionless error is still order 10^{-4}, while during transients dimensionless errors are order 10^{-1}, os observable in Figure 6.5.

LINEARISED SYSTEM

Considering the good steady-state agreement between (6.51) and the full system, the equilibrium point of the variables in common is assumed to be the same.
In this case, the linearised system is

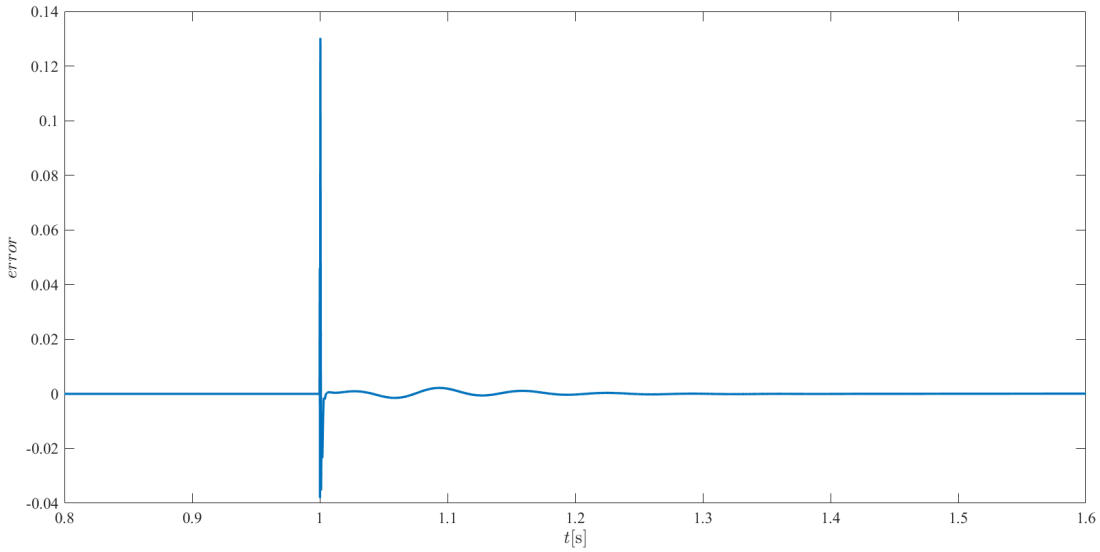

Figure 6.5: Dimensionless error on $i_{i_d 1}$, computed between the full system and the second reduced system.

$$\boldsymbol{A_{11}} = \begin{bmatrix} -\omega_{cd} & 0 & 0 & 0 & 0 & 0 & \cdots \\ 0 & -\omega_{cd} & 0 & 0 & 0 & 0 & \cdots \\ 0 & 0 & -\omega_{ci} & 0 & 0 & 0 & \cdots \\ 0 & 0 & 0 & -\omega_{ci} & 0 & 0 & \cdots \\ 0 & -K_{dq} & L_v\omega_{ci} & L_v w_n & 0 & 0 & \cdots \\ 0 & 0 & -L_v\omega_n & L_v\omega_{ci} & 0 & 0 & \cdots \\ 0 & -K_{dq} & \dfrac{K_{vp}}{C_f} & K_{vp}L_v\omega_{ci}C_f^{-1} & K_{vp}L_v\omega_n C_f^{-1} & K_{vi}C_f^{-1} & 0\cdots \\ 0 & 0 & -K_{vp}L_v\omega_n C_f^{-1} & K_{vp}L_v\omega_{ci}C_f^{-1} & 0 & K_{vi}C_f^{-1} & \cdots \\ 0 & 0 & 0 & 0 & 0 & 0 & \cdots \\ 0 & 0 & 0 & 0 & 0 & 0 & \cdots \end{bmatrix}$$

$$
\begin{matrix}
\cdots & \omega_{cd}\bar{\imath}_{o_d 1} & \omega_{cd}\bar{\imath}_{o_q 1} & \omega_{ci}\bar{v}_{i_d 1} & \omega_{cd}\bar{v}_{i_q 1} \\
\cdots & \omega_{cd}\bar{\imath}_{o_q 1} & -\omega_{cd}\bar{\imath}_{o_d 1} & -\omega_{cd}\bar{v}_{i_q 1} & \omega_{cd}\bar{v}_{i_d 1} \\
\cdots & 0 & 0 & \omega_{ci} & 0 \\
\cdots & 0 & 0 & 0 & \omega_{ci} \\
\cdots & -1 & 0 & -L_v\omega_{ci} & 0 \\
\cdots & 0 & -1 & 0 & -L_v\omega_{ci} \\
\cdots & -K_{vp}C_f^{-1} & 0 & -(1+K_{vp}L_v\omega_{ci})C_f^{-1} & 0 \\
\cdots & 0 & -K_{vp}C_f^{-1} & 0 & -(1+K_{vp}L_v\omega_{ci})C_f^{-1} \\
\cdots & L_{l1}^{-1} & 0 & -(R_{load}+R_{l1})L_{l1}^{-1} & \omega_n \\
0 & L_{l1}^{-1} & -\omega_n & -(R_{load}+R_{l1})L_{l1}^{-1} &
\end{matrix}
\Bigg],
\tag{6.53}
$$

$$
\boldsymbol{A_{12}} = \begin{bmatrix}
0 & 0 & 0 & 0 & 0 & 0 & 0 & 0 & 0 & 0 & 0 \\
0 & 0 & 0 & 0 & 0 & 0 & 0 & 0 & 0 & 0 & 0 \\
0 & 0 & 0 & 0 & 0 & 0 & 0 & 0 & 0 & 0 & 0 \\
0 & 0 & 0 & 0 & 0 & 0 & 0 & 0 & 0 & 0 & 0 \\
0 & 0 & 0 & 0 & 0 & 0 & 0 & 0 & 0 & 0 & 0 \\
0 & 0 & 0 & 0 & 0 & 0 & 0 & 0 & 0 & 0 & 0 \\
0 & 0 & 0 & 0 & 0 & 0 & 0 & 0 & 0 & 0 & 0 \\
0 & 0 & 0 & 0 & 0 & 0 & 0 & 0 & 0 & 0 & 0 \\
0 & 0 & \dfrac{R_{load}\,\bar{\imath}_{o_{q21}}}{L_{l1}} & 0 & 0 & 0 & 0 & 0 & 0 & -\dfrac{R_{load}\cos(\bar{\alpha}_2)}{L_{l1}} & \dfrac{R_{load}\sin(\bar{\alpha}_2)}{L_{l1}} \\
0 & 0 & -\dfrac{R_{load}\,\bar{\imath}_{o_{d21}}}{L_{l1}} & 0 & 0 & 0 & 0 & 0 & 0 & -\dfrac{R_{load}\sin(\bar{\alpha}_2)}{L_{l1}} & -\dfrac{R_{load}\cos(\bar{\alpha}_2)}{L_{l1}}
\end{bmatrix},
\tag{6.54}
$$

$$\boldsymbol{A_{21}} = \begin{bmatrix} 0 & 0 & 0 & 0 & 0 & 0 & 0 & 0 & 0 & 0 \\ 0 & 0 & 0 & 0 & 0 & 0 & 0 & 0 & 0 & 0 \\ K_{dp} & 0 & 0 & 0 & 0 & 0 & 0 & 0 & 0 & 0 \\ 0 & 0 & 0 & 0 & 0 & 0 & 0 & 0 & 0 & 0 \\ 0 & 0 & 0 & 0 & 0 & 0 & 0 & 0 & 0 & 0 \\ 0 & 0 & 0 & 0 & 0 & 0 & 0 & 0 & 0 & 0 \\ 0 & 0 & 0 & 0 & 0 & 0 & 0 & 0 & 0 & 0 \\ 0 & 0 & 0 & 0 & 0 & 0 & 0 & 0 & 0 & 0 \\ 0 & 0 & 0 & 0 & 0 & 0 & 0 & 0 & 0 & 0 \\ 0 & 0 & 0 & 0 & 0 & 0 & 0 & 0 & -\dfrac{R_{load}\cos(\bar{\alpha}_2)}{L_{l2}} & -\dfrac{R_{load}\sin(\bar{\alpha}_2)}{L_{l2}} \\ 0 & 0 & 0 & 0 & 0 & 0 & 0 & 0 & \dfrac{R_{load}\sin(\bar{\alpha}_2)}{L_{l2}} & -\dfrac{R_{load}\cos(\bar{\alpha}_2)}{L_{l2}} \end{bmatrix}, \tag{6.55}$$

$$\boldsymbol{A_{22}} = \begin{bmatrix} -\omega_{cd} & 0 & 0 & 0 & 0 & 0 & 0 & \cdots \\ 0 & -\omega_{cd} & 0 & 0 & 0 & 0 & 0 & \cdots \\ -K_{dp} & 0 & 0 & 0 & 0 & 0 & 0 & \cdots \\ 0 & 0 & 0 & -\omega_{cd} & 0 & 0 & 0 & \cdots \\ 0 & 0 & 0 & 0 & -\omega_{cd} & 0 & 0 & \cdots \\ 0 & -K_{dq} & 0 & L_v\omega_{cd} & L_v\omega_n & 0 & 0 & \cdots \\ 0 & 0 & 0 & -L_v\omega_n & L_v\omega_{cd} & 0 & 0 & \cdots \\ 0 & -\dfrac{K_{dq}K_{vp}}{C_f} & 0 & \dfrac{K_{vp}L_v\omega_{cd}}{C_f} & \dfrac{K_{vp}L_v\omega_n}{C_f} & \dfrac{K_vi}{C_f} & 0 & \cdots \\ 0 & 0 & 0 & -\dfrac{K_{vp}L_v\omega_n}{C_f} & \dfrac{K_{vp}L_v\omega_{cd}}{C_f} & 0 & \dfrac{K_{vi}}{C_f} & \cdots \\ 0 & 0 & \dfrac{R_{load}}{L_{l2}}(\bar{\imath}_{o_d1}\sin(\bar{\alpha}_2) - \bar{\imath}_{o_q1}\cos(\bar{\alpha}_2)) & 0 & 0 & 0 & 0 & \cdots \\ 0 & 0 & \dfrac{R_{load}}{L_{l2}}(\bar{\imath}_{o_d1}\cos(\bar{\alpha}_2) + \bar{\imath}_{o_q1}\sin(\bar{\alpha}_2)) & 0 & 0 & 0 & 0 & \cdots \end{bmatrix}$$

$$
\begin{bmatrix}
\cdots & \omega_{cd}\,\bar{\imath}_{o_d 2} & \omega_{cd}\,\bar{\imath}_{o_q 2} & \omega_{cd}\,\bar{v}_{i_d 2} & \omega_{cd}\,\bar{v}_{i_q 2} \\
\cdots & \omega_{cd}\,\bar{\imath}_{o_q 2} & -\omega_{cd}\,\bar{\imath}_{o_d 2} & \omega_{cd}\,\bar{v}_{i_q 2} & \omega_{cd}\,\bar{v}_{i_d 2} \\
\cdots & 0 & 0 & 0 & 0 \\
\cdots & 0 & 0 & \omega_{ci} & 0 \\
\cdots & 0 & 0 & 0 & \omega_{ci} \\
\cdots & -1 & 0 & -L_v\omega_{ci} & 0 \\
\cdots & 0 & -1 & 0 & -L_v\omega_{ci} \\
\cdots & -\dfrac{K_{vp}}{C_f} & 0 & -\dfrac{(1+K_{vp}L_v\omega_{cd})}{C_f} & 0 \\
\cdots & 0 & -\dfrac{K_{vp}}{C_f} & 0 & -\dfrac{(1+L_v\omega_{cd}K_{vp})}{C_f} \\
\cdots & L_{l2}^{-1} & 0 & -\dfrac{(R_{load}+R_{l2})}{L_{l2}} & \omega_n \\
\cdots & 0 & L_{l2}^{-1} & -\omega_n & -\dfrac{(R_{load}+R_{l2})}{L_{l2}}
\end{bmatrix}, \quad (6.56)
$$

STABILITY ANALYSIS

Again, the eigenvalues of the full linearised systems are compared with the eigenvalues of the second reduced system, as depicted in Figure 6.6.

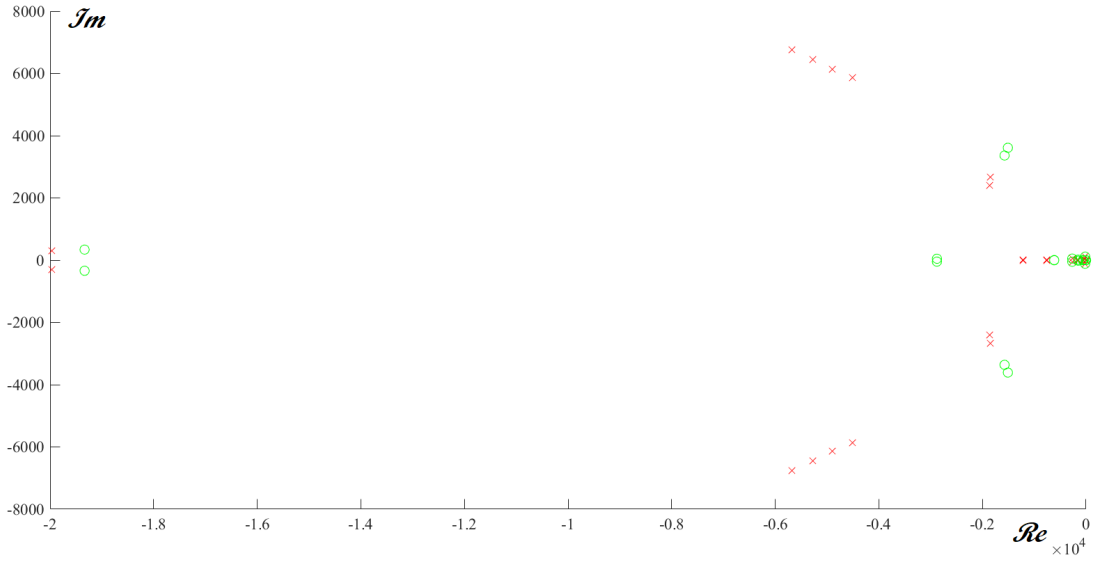

Figure 6.6: Full system eigenvalues (red crosses) and second reduced system eigenvalues (green circles).

In this case, the agreement between the two stability analyses show significant

discrepancies far from the imaginary axis. However, better agreement is observed closer to it, corresponding to the eigenvalues that are more critical for the system stability, as shown in Figure 6.7.

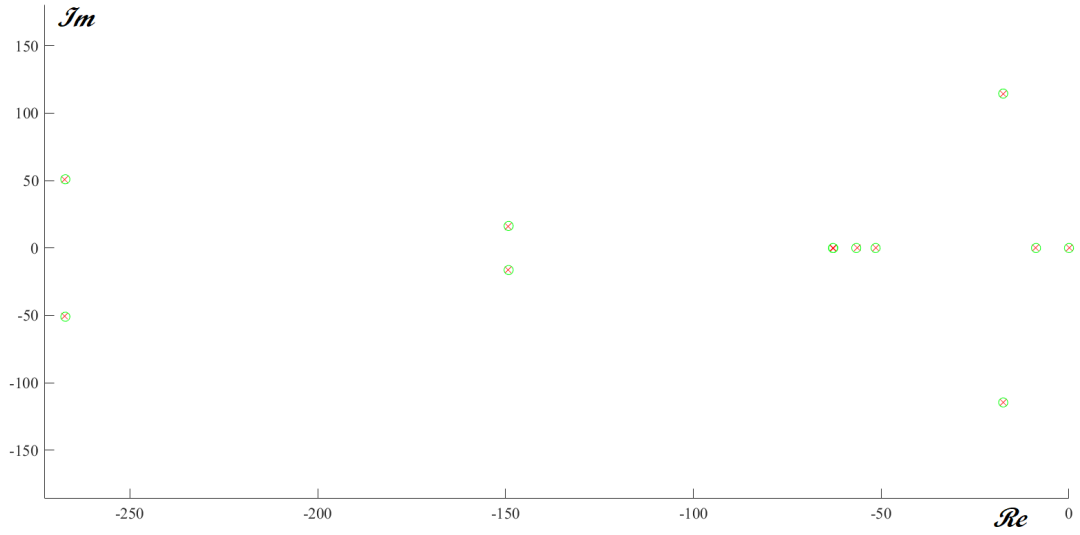

Figure 6.7: Full system eigenvalues (red crosses) and second reduced system eigenvalues (green circles); zoom on the area close to the imaginary axis.

Hence, some errors are likely to be present when fast transients are considered, while the steady-state behaviour of the system and its slower dynamics are well represented by the second reduced model.

6.3.1.5 Small filter capacitance

Since the value of the filter capacitance C_f is unchanged with respect with the single inverter model, analogous considerations can be taken into account and the system can be reduced further.
Considering the $\mathcal{O}(1)$ parameter $\bar{C}_f$, defined as

$$\bar{C}_f = \epsilon^{-1} C_f \,, \tag{6.57}$$

the dynamics described by the voltages ODEs can be approximated by algebraic equations, as well as examined in §5.3.2.6. In particular, this approximation gives new algebraic expressions for the internal currents, obtained through the retention of the leading order terms:

$$i_{i_d 1,2}(t) \sim i_{o_d 1,2}(t) - \bar{\omega}_n \bar{C}_f v_{i_q 1,2}(t)\,, \tag{6.58a}$$

$$i_{i_q 1,2}(t) \sim i_{o_q 1,2}(t) + \bar{\omega}_n \bar{C}_f v_{i_d 1,2}(t)\,. \tag{6.58b}$$

Substituting (6.52c)-(6.52d) into (6.58) and solving for v_{i_d} and v_{i_q} leads to the algebraic expressions of the voltages, while their four corresponding ODEs can be eliminated from the so-reduced system.

6.3.1.6 Neglect of voltage integral errors

Following the same considerations of §5.3.2.7, the integral errors on the voltages can drop from the system, while their corresponding ODEs are turned into algebraic equations. This follows from the assumption that the parameter K_{iv} is $\mathcal{O}(\epsilon^{-1})$, leading to

$$\epsilon \frac{\mathrm{d}\bar{x}_{int,v_d 1,2}(t)}{\mathrm{d}t} = v_{ref_d 1,2}(t) - v_{i_d 1,2}(t)\,, \tag{6.59a}$$

$$\epsilon \frac{\mathrm{d}\bar{x}_{int,v_q 1,2}(t)}{\mathrm{d}t} = v_{ref_q 1,2}(t) - v_{i_q 1,2}(t)\,, \tag{6.59b}$$

where $v_{ref_d 1,2}(t)$, $v_{i_d 1,2}(t)$, $v_{ref_q 1,2}(t)$ and $v_{i_q 1,2}(t)$ are $\mathcal{O}(1)$. Considering the leading orders only,

$$v_{i_d 1,2}(t) \sim v_{ref_d 1,2}(t)\,, \tag{6.60a}$$

$$v_{i_q 1,2}(t) \sim v_{ref_q 1,2}(t)\,, \tag{6.60b}$$

where $v_{ref_d 1,2}$ and $v_{ref_q 1,2}$ are given by

$$v_{ref_d 1,2}(t) \sim V_{d_n} + K_{dq}[Q_{ref} - Q_{lp1,2}(t)] + \bar{L}_v \bar{\omega}_n i_{lp_q 1,2}(t) \tag{6.61a}$$

$$v_{ref_q 1,2}(t) \sim V_{q_n} - \bar{L}_v \bar{\omega}_n i_{lp_d 1,2}(t)\,. \tag{6.61b}$$

Hence, this approximation allows a further reduction by four ODEs and variables,

leading to the following reduced state-space system:

$$\frac{\mathrm{d}P_{lp1,2}(t)}{\mathrm{d}t} = \omega_{cd}[v_{i_d}1,2(t)\, i_{i_d}1,2(t) - v_{i_q}1,2(t)\, i_{i_q}1,2(t) - P_{lp1,2}(t)]\,, \tag{6.62a}$$

$$\frac{\mathrm{d}Q_{lp1,2}(t)}{\mathrm{d}t} = \omega_{cd}[v_{i_d}1,2(t)\, i_{i_q}1,2(t) - v_{i_q}1,2(t)\, i_{i_d}1,2(t) - Q_{lp1,2}(t)]\,, \tag{6.62b}$$

$$\frac{\mathrm{d}\alpha_2(t)}{\mathrm{d}t} = K_{dp}[P_{ref2} - P_{ref1} - P_{lp2}(t) + P_{lp1}(t)]\,, \tag{6.62c}$$

$$\frac{\mathrm{d}i_{lp_d}1,2(t)}{\mathrm{d}t} = \omega_{ci}[i_{o_d}1,2t) - i_{lp_d}1,2(t)]\,, \tag{6.62d}$$

$$\frac{\mathrm{d}i_{lp_q}1,2(t)}{\mathrm{d}t} = \omega_{ci}[i_{o_q}1,2(t) - i_{lp_q}1,2(t)]\,, \tag{6.62e}$$

$$\frac{\mathrm{d}i_{o_{d1}}(t)}{\mathrm{d}t} = \frac{v_{i_{d1}}(t)}{L_{l1}} - \frac{R_{l1}}{L_{l1}} i_{o_{d1}}(t) - \frac{R_{load}}{L_{l1}}\left[i_{o_{d1}}(t) + i_{o_{d21}}(t)\right] + \omega_n\, i_{o_{q1}}(t)\,, \tag{6.62f}$$

$$\frac{\mathrm{d}i_{o_{q1}}(t)}{\mathrm{d}t} = \frac{v_{i_{q1}}(t)}{L_{l1}} - \frac{R_{l1}}{L_{l1}} i_{o_{q1}}(t) - \frac{R_{load}}{L_{l1}}\left[i_{o_{q1}}(t) + i_{o_{q21}}(t)\right] - \omega_n\, i_{o_{d1}}(t)\,, \tag{6.62g}$$

$$\frac{\mathrm{d}i_{o_{d2}}(t)}{\mathrm{d}t} = \frac{v_{i_{d2}}(t)}{L_{l2}} - \frac{R_{l2}}{L_{l2}} i_{o_{d2}}(t) - \frac{R_{load}}{L_{l2}}\left[i_{o_{d2}}(t) + i_{o_{d12}}(t)\right] + \omega_n\, i_{o_{q2}}(t)\,, \tag{6.62h}$$

$$\frac{\mathrm{d}i_{o_{q2}}(t)}{\mathrm{d}t} = \frac{v_{i_{q2}}(t)}{L_{l2}} - \frac{R_{l2}}{L_{l2}} i_{o_{q2}}(t) - \frac{R_{load}}{L_{l2}}\left[i_{o_{q2}}(t) + i_{o_{q12}}(t)\right] - \omega_n\, i_{o_{d2}}(t)\,, \tag{6.62i}$$

where

$$\begin{aligned} v_{i_d}1,2(t) = {} & V_{d_n} + K_{dq}(Q_{ref} - Q_{lp1,2}(t)) \\ & + L_v\{[\omega_n + K_{dp}(P_{ref} - P_{lp1,2}(t))]i_{lp_q}1,2(t) + \omega_{ci}(i_{lp_d}1,2(t) - i_{o_d}1,2(t))\}, \end{aligned} \tag{6.63a}$$

$$\begin{aligned} v_{i_q}1,2(t) = {} & V_{q_n} + L_v\{-[\omega_n + K_{dp}(P_{ref} - P_{lp1,2}(t))]i_{lp_d}1,2(t) \\ & + \omega_{ci}(i_{lp_q}1,2(t) - i_{o_q}1,2(t))\}, \end{aligned} \tag{6.63b}$$

$$i_{o_{d12}}(t) = +\cos\alpha_2(t)\, i_{o_{d1}}(t) + \sin\alpha_2(t)\, i_{o_{q1}}(t)\,, \tag{6.63c}$$

$$i_{o_{q12}}(t) = -\sin\alpha_2(t)\, i_{o_{d1}}(t) + \cos\alpha_2(t)\, i_{o_{q1}}(t)\,, \tag{6.63d}$$

$$i_{o_{d21}}(t) = +\cos\alpha_2(t)\, i_{o_{d2}}(t) - \sin\alpha_2(t)\, i_{o_{q2}}(t)\,, \tag{6.63e}$$

$$i_{o_{q21}}(t) = +\sin\alpha_2(t)\, i_{o_{d2}}(t) + \cos\alpha_2(t)\, i_{o_{q2}}(t)\,. \tag{6.63f}$$

This system is formed of 13 ODES.

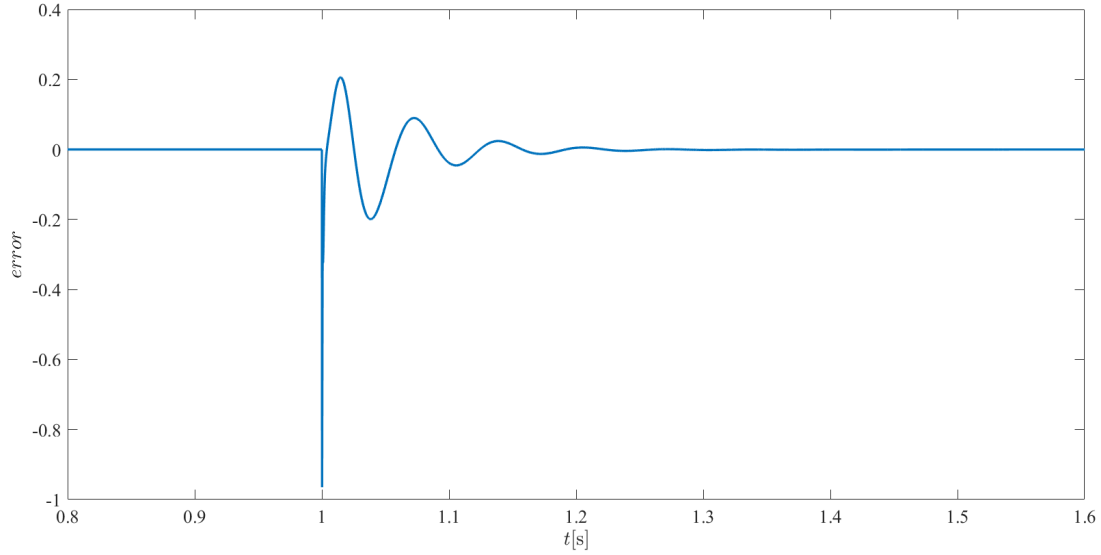

Figure 6.8: Dimensionless error on $i_{i_d 1}$, computed between the full system and the third reduced system.

As depicted in Figure 6.8, this reduced system does not agree very well with the full one during transients (dimensionless errors of order 1), but the steady-state behaviour show errors of order 10^{-3}. Even though the error of only one variable is shown in pictures, similar results are achieved in simulations for all the state-space variables of the system (including both inverters).

LINEARISED SYSTEM

Linearising the system (6.62) about its steady-state operating point leads to

$$\boldsymbol{A_{11}} = \begin{bmatrix} -\omega_{cd} & -\omega_{cd}K_{dq}\bar{\imath}_{o_d 1} & L_v\omega_{cd}(\omega_{ci}\bar{\imath}_{o_d 1} - \omega_n\bar{\imath}_{o_q 1}) & L_v\omega_{cd}(\omega_n\bar{\imath}_{o_d 1} + \omega_{ci}\bar{\imath}_{o_q 1}) & \cdots \\ 0 & -\omega_{cd}(1 + K_{dq}\bar{\imath}_{o_q 1} & L_v\omega_{cd}(\omega_{ci}\bar{\imath}_{o_q 1} + \omega_n\bar{\imath}_{o_d 1}) & L_v\omega_{cd}(\omega_n\bar{\imath}_{o_q 1} - \omega_{ci}\bar{\imath}_{o_d 1}) & \cdots \\ 0 & 0 & -\omega_{ci} & 0 & \cdots \\ 0 & 0 & 0 & -\omega_{ci} & \cdots \\ 0 & -K_{dq}/L_l 1 & \dfrac{L_v\omega_{ci}}{L_{l1}} & \dfrac{L_v\omega_n}{L_{l1}} & \cdots \\ 0 & 0 & -\dfrac{L_v\omega_n}{L_{l1}} & \dfrac{L_v\omega_{ci}}{L_{l1}} & \cdots \end{bmatrix}$$

$$
\begin{array}{c}
\cdots \quad \omega_{cd}(-L_v\omega_{ci}\bar{i}_{o_d1}+\bar{v}_{i_d1}) \quad \omega_{cd}(-L_v\omega_{ci}\bar{i}_{o_q1}+\bar{v}_{i_q1}) \\
\cdots \quad \omega_{cd}(-L_v\omega_{ci}\bar{i}_{o_d1}+\bar{v}_{i_d1}) \quad \omega_{cd}(-L_v\omega_{ci}\bar{i}_{o_q1}+\bar{v}_{i_q1}) \\
\cdots \quad \omega_{ci} \quad 0 \\
, \quad \cdots \quad 0 \quad \omega_{ci} \\
\cdots \quad -\dfrac{L_v\omega_{ci}+R_{l1}+R_{load}}{L_{l1}} \quad \omega_n \\
\cdots \quad -\omega_n \quad -\dfrac{R_{load}+R_{l1}+L_v\omega_{ci}}{L_{l1}}
\end{array}
\Bigg] \tag{6.64}
$$

$$
\boldsymbol{A_{12}} = \begin{bmatrix}
0 & 0 & 0 & 0 & 0 & 0 & 0 \\
0 & 0 & 0 & 0 & 0 & 0 & 0 \\
0 & 0 & 0 & 0 & 0 & 0 & 0 \\
0 & 0 & 0 & 0 & 0 & 0 & 0 \\
0 & 0 & \dfrac{R_{load}\,\bar{i}_{o_{q21}}}{L_{l1}} & 0 & 0 & -\dfrac{R_{load}\cos(\bar{\alpha}_2)}{L_{l1}} & \dfrac{R_{load}\sin(\bar{\alpha}_2)}{L_{l1}} \\
0 & 0 & -\dfrac{R_{load}\,\bar{i}_{o_{d21}}}{L_{l1}} & 0 & 0 & -\dfrac{R_{load}\sin(\bar{\alpha}_2)}{L_{l1}} & -\dfrac{R_{load}\cos(\bar{\alpha}_2)}{L_{l1}}
\end{bmatrix}, \tag{6.65}
$$

$$
\boldsymbol{A_{21}} = \begin{bmatrix}
0 & 0 & 0 & 0 & 0 & 0 \\
0 & 0 & 0 & 0 & 0 & 0 \\
K_{dp} & 0 & 0 & 0 & 0 & 0 \\
0 & 0 & 0 & 0 & 0 & 0 \\
0 & 0 & 0 & 0 & 0 & 0 \\
0 & 0 & 0 & 0 & -\dfrac{R_{load}\cos(\bar{\alpha}_2)}{L_{l2}} & -\dfrac{R_{load}\sin(\bar{\alpha}_2)}{L_{l2}} \\
0 & 0 & 0 & 0 & \dfrac{R_{load}\sin(\bar{\alpha}_2)}{L_{l2}} & -\dfrac{R_{load}\cos(\bar{\alpha}_2)}{L_{l2}}
\end{bmatrix}, \tag{6.66}
$$

$$\boldsymbol{A_{22}} = \begin{bmatrix} -\omega_{cd} & -\omega_{cd}K_{dq}\bar{\imath}_{o_d1} & L_v\omega_{cd}(\omega_{ci}\bar{\imath}_{o_d1} - \omega_n\bar{\imath}_{o_q1}) & L_v\omega_{cd}(\omega_n\bar{\imath}_{o_d1} + \omega_{ci}\bar{\imath}_{o_q1}) & \cdots \\ 0 & -\omega_{cd}(1 + K_{dq}\bar{\imath}_{o_q1} & L_v\omega_{cd}(\omega_{ci}\bar{\imath}_{o_q1} + \omega_n\bar{\imath}_{o_d1}) & L_v\omega_{cd}(\omega_n\bar{\imath}_{o_q1} - \omega_{ci}\bar{\imath}_{o_d1}) & \cdots \\ 0 & 0 & -\omega_{ci} & 0 & \cdots \\ 0 & 0 & 0 & -\omega_{ci} & \cdots \\ 0 & -K_{dq}/L_l1 & \frac{L_v\omega_{ci}}{L_{l1}} & \frac{L_v\omega_n}{L_{l1}} & \cdots \\ 0 & 0 & -\frac{L_v\omega_n}{L_{l1}} & \frac{L_v\omega_{ci}}{L_{l1}} & \cdots \end{bmatrix}$$

$$, \quad \begin{bmatrix} \cdots & \omega_{cd}(-L_v\omega_{ci}\bar{\imath}_{o_d1} + \bar{v}_{i_d1}) & \omega_{cd}(-L_v\omega_{ci}\bar{\imath}_{o_q1} + \bar{v}_{i_q1}) \\ \cdots & \omega_{cd}(-L_v\omega_{ci}\bar{\imath}_{o_d1} + \bar{v}_{i_d1}) & \omega_{cd}(-L_v\omega_{ci}\bar{\imath}_{o_q1} + \bar{v}_{i_q1}) \\ \cdots & \omega_{ci} & 0 \\ \cdots & 0 & \omega_{ci} \\ \cdots & -\frac{L_v\omega_{ci} + R_{l1} + R_{load}}{L_{l1}} & \omega_n \\ \cdots & -\omega_n & -\frac{R_{load} + R_{l1} + L_v\omega_{ci}}{L_{l1}} \end{bmatrix}. \quad (6.67)$$

STABILITY ANALYSIS

The comparison between the eigenvalues of the full linearised system and the eigenvalues of the third reduced system is depicted in Figure 6.9.

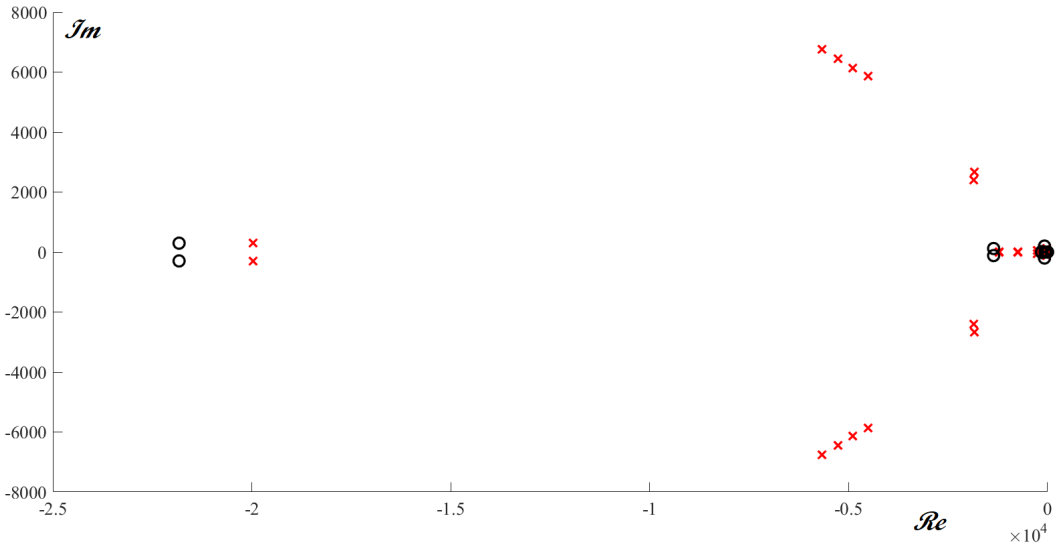

Figure 6.9: Full system eigenvalues (red crosses) and third reduced system eigenvalues (black circles).

Similarly to the previous case, some "fast" eigenvalues far from the imaginary axes are missing in the reduced model and some others are distorted. This time, how-

ever, a worse agreement is found also among the eigenvalues closer to the imaginary axis, as observed in Figure 6.10: a couple of complex conjugate eigenvalues are much further from the imaginary axis than the corresponding full-system pair. This would be problematic when assessing the system stability.

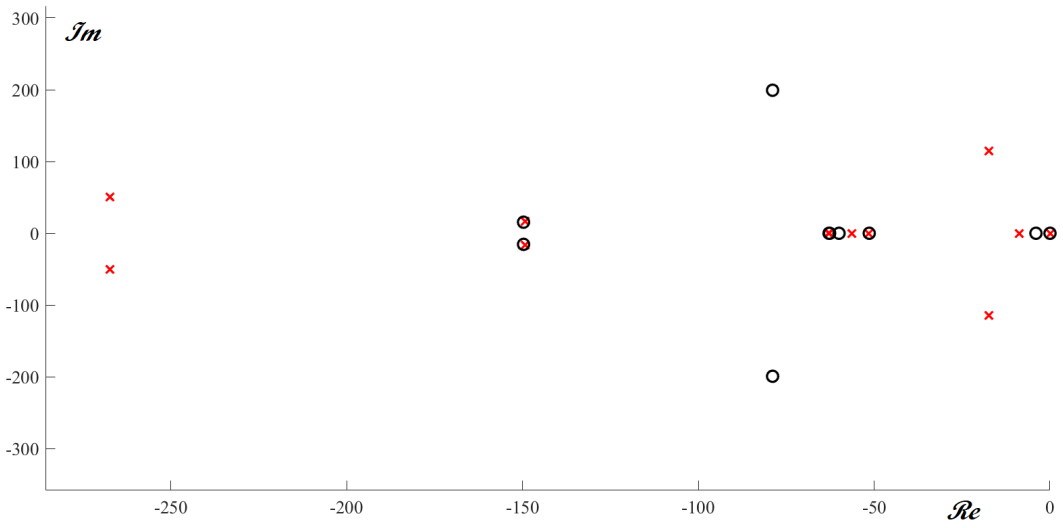

Figure 6.10: Full system eigenvalues (red crosses) and third reduced system eigenvalues (black circles); zoom on the area close to the imaginary axis.

In fact, if, for example, the value of the virtual inductance parameter is multiplied by a factor 5, the full system becomes unstable, while the third reduced system keeps its stable condition. This is observable in both time-domain simulations and eigenvalue plots (a zoom on the imaginary axis for this case is plotted in Figure 6.11). The complex conjugate eigenvalues that do not agree well in Figure 6.7 now are on the opposite sides of the imaginary axes.

Thus, the third reduced model might be used for a rough estimation of how the system behaves, but cannot be trusted for stability concerns.

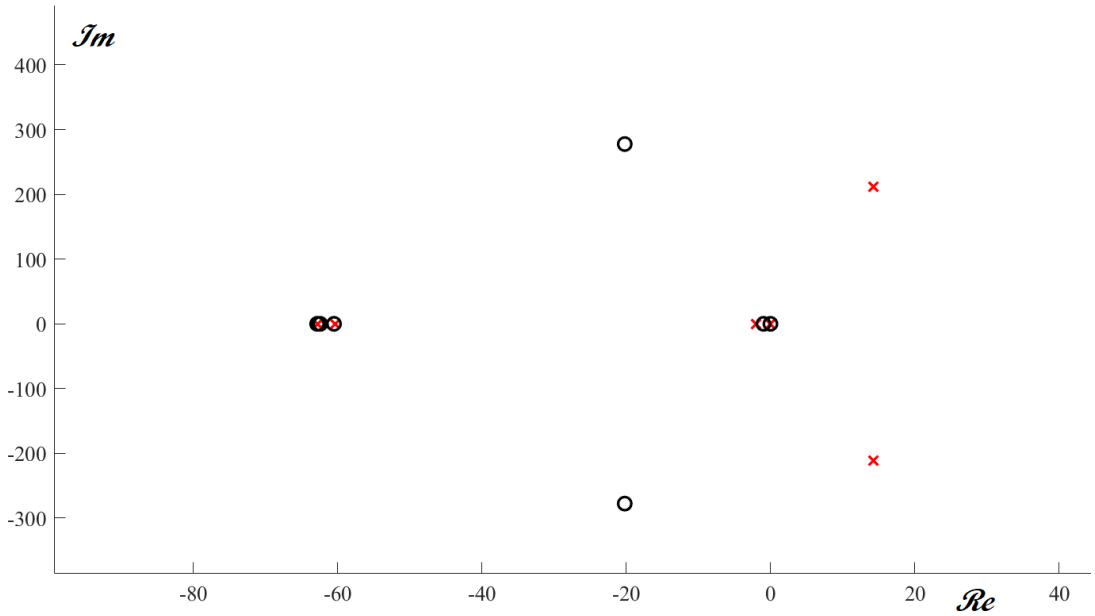

Figure 6.11: Stability disagreement: full system eigenvalues (red crosses) and third reduced system eigenvalues (black circles); zoom on the area close to the imaginary axis.

6.4 Chapter Summary

An AC microgrid system formed of two identical inverters connected to a resistive load by lines of different impedances has been considered in this section for a model reduction based on singular perturbation methods. The microgrid is assumed to run in island mode.

The full state-space system is formed of 30 ODEs and corresponding state-space variables.

A first approximation involved considering the frequency of the inverters as constant, despite it being dependent on the action of the droop controller in real systems. This allows a reduction of only one ODE, but reduces the number of nonlinearities and makes the linearisation of the system easier. Very good agreement is found between the full system and this first reduced system, in both time-domain simulations and stability analysis based on linearised-system eigenvalue computation.

A second reduction consisted in neglecting the current PI controller and its dynamics. The second reduced model is formed of 21 equations and agrees very well with the full model in steady-state, while some errors are present during transients. The stability analysis agrees well with that of the full system.

If a third reduction is performed, the voltage PI controller is neglected as well and the system is formed of 13 equations only. In this case, though, the reduced model behaves stably also in some conditions that cause the full model's instability. This can be observed in both simulations and stability analysis. This last finding is particularly interesting, as commonly used engineering model reductions involve the same procedure [29]. It is possible that this technique is more reliable when bigger systems (three or more inverters) are considered. The mutual interactions between the inverters, in fact, make AC microgrids sensitive to parameter changes and prone to instability, if not adequately controlled. As the number of inverters increases, the grid behaves more like an ideal grid with constant voltage and frequency, which is hardly influenced by the action of a single device. In particular, [29] considers three inverters and two loads. The importance of the number of devices for the validity of model reductions is currently under investigation.

The model reduction shown in the present chapter can be applied to other analogous microgrids, assuming that their parameters respect the assumptions made in terms of orders of magnitude. At each step of a new model reduction, if a parameter belongs to the same "size" with respect to ϵ, the same passages shown here can be followed. This offers a systematic way of reducing the state-space system models of AC microgrids, which might be expanded in the future once systems with more than two inverters will be analysed and reduced as well.

Chapter 7

Conclusions

7.1 Thesis Summary and General Conclusions

In this thesis, various applications of mathematical methods to power electronic systems have been considered. The aim of the work was to obtain effective models of such systems, perform reliable model reductions and assess their operating stability. Chapter §1 contains a short introduction to power electronic converters and explains the general structure of this thesis.

The following chapter concerns the mathematical modelling of average behaviour and the ripple of a Boost direct current (DC)-DC converter and a single-phase (SP) Full-Bridge inverter; this chapter was meant to be propaedeutic for the subsequent work. The average and ripple approximations, obtained through the application of perturbation theories, were observed to be effective in simulations. Similar approaches are found in the engineering literature; despite the lack of technical novelty, the procedure is here followed in a more rigorous manner. Since, in §2, the validity of the average model is proven when the switching period is negligible compared to the analysed time span, in the following chapters attention focuses on average models only, and the switching behaviour of the analysed devices is not considered further.

In chapter §3, a system reduction based on singular perturbation has been presented and applied to a SP-AFE. This kind of device is characterised by nonlinear time-periodic behaviour; the model reduction is achieved through nondimensionalisation, identification of a small dimensionless parameter, then retention of only leading-order terms. It can be observed that a moderate reduction in the size of

the model (reduction from 8 to 6 in the number of variables and ODEs) can be achieved through a rational reduction strategy based on identifying a small dimensionless parameter. This reduced model performs well and agrees with the full model in both time domain simulations and stability analysis. A further reduction leading to 5 or 4 degrees of freedom does not, in this case, perform so well. An acceptable model reduction for the system, then, involves a reduced model with 6 state-space variables and corresponding ODEs. This model reduction can be applied to any analogous device (in this case, SP-AFEs) whose physical and control parameters belong to the same categories as in the analysed converter. Partial model reductions can be used instead where only some parameters appear to be the same size, and the applicability of reduction procedure can be assessed stage by stage. This provides a flexible method of reducing the size of the system, that would not need to undergo further comparisons of full and reduced models in order to be validated.

Model reductions of AC microgrids are discussed in §5 and §6. First, a system formed of a single inverter is considered; subsequently, a system formed of two inverters. Results are achieved by applying perturbation theory to the system, and different degrees of reduction are proposed. Time-domain simulations and stability analyses are used to compare the reduced models with the full-model behaviour. The models are nondimensionalised, and a gradual reduction is applied according to assumptions on the "size" of some systems parameters. The variables are then split into "fast" and "slow", and the ODEs of the "fast" variables are approximated by algebraic equations. The reductions are validated at each stage through simulations comparing the behaviour of the full and of the reduced model, and computing the relative error between them.

About the single-inverter system, good results are found for reduced model with as few as four ODEs (the full system has fifteen). The smaller reduced model, having two ODEs only, does not perform so well, and hence should not be used to approximate the system's behaviour.

Concerning the two-inverter model reduction, a first approximation involved considering the frequency of the inverters as constant; very good agreement is found between the full system and this first reduced system, in both time-domain simu-

lations and stability analysis based on linearised-system eigenvalue computation. Neglecting the current PI controller and its dynamics allows a reduction to 21 equations (the full model is formed of 30 independent variables and corresponding ODEs); such reduced model agrees very well with the full model in steady-state, while some errors are present during transients. The stability analysis agrees well with that of the full system. If the voltage PI controller dynamics are neglected as well (and the system is formed of 13 equations), discrepancies are found between the full and reduced model stability analyses. This can be observed in both simulations and eigenvalue plots. This kind of reduction is relatively common in the engineering literature (e.g. [29] [27] [34] [38]). It is possible that this technique is more reliable when larger systems (three or more inverters, multiple loads) are considered: the mutual interactions between the inverters make AC microgrids sensitive to parameter changes and prone to instability, if not adequately controlled. As the number of inverters increases, the grid behaves more like an ideal grid with constant voltage and frequency, which is hardly influenced by the action of a single device. However, the overall reliability of reduced models obtained through this method should be investigated further, since there might be more cases where a more conservative approach (e.g. stopping the reduction after neglecting the current PI) should be recommended.

7.2 Future Work

In the model reduction performed in §3 on a SP-AFE, results could be improved by including further terms in the expansion of some of the variables. In the presented case, in fact, only the leading-order terms have been taken into account. However, the system describes some physical processes which sometimes cannot be neglected without affecting the model reliability. In general, drastic approximations of those phenomena are unlikely to be effective, but further attempt might be included in future work.

Results obtained in §6 differ from several AC microgrid model reductions found in the engineering literature. Further studies should be carried out to understand

how the reduction validity is affected by the number of devices included in the system. Different models can be considered according to the number of inverters and loads that are present in the analysed grid, in order to observe how this influences the disposition of the linearised systems' eigenvalues and, consequently, their stability analyses. Ideally, research should aim at identifying a minimum "threshold" number of devices, below which the voltage PI dynamics must be taken into account while computing reduced models for AC microgrids.

Besides this, more complex microgrids can be taken into account, involving inductive loads, constant-power loads, and eventually more intricate network topologies. Applying and analysing the same model reduction to a wide variety of microgrids should allow the identification of some parameter ranges that guarantee its reliability.

As a general result, this thesis presents some examples of how the application of perturbation theory (in particular, singular perturbation) can generate the computation of reduced models, together with a list of requirements about the system's parameters in order for the reduction to be valid. At each stage of the model reduction, some assumptions are made about the "size" of some parameters. If a similar system needs to be reduced in an analogous manner, the same model reduction can be directly applied to it, provided that its parameters belong to the same "sizes" as in the first model, which has been validated through simulations and stability analyses comparisons.

A "small" dimensionless parameter ϵ is used throughout this thesis. In the described works, ϵ is assumed to be 10^{-3}. Some attempts have been made assuming $\epsilon = 10^{-2}$, but the reduced models based on this assumptions do not perform very well in comparative simulations with the full systems. On the opposite side, the assumption that $\epsilon = 10^{-4}$ prevented the reduction from reaching the same stages as with $\epsilon = 10^{-3}$, and was hence considered too conservative. However, the possibility that a suitable value for ϵ depends on the nature of the analysed system cannot be excluded, and further studies can be conducted on that regard.

Collection of experimental results was beyond the main purposes of this work. The content of each chapter of this thesis might benefit from the addition of ex-

periments, which would prove that no mistake has been made in the various modelling stages (physical system-switching model, switching model-full average model, full average model-reduced average model). However, the main focus of this work concerns the mathematical modelling and model reduction of the analysed power electronic systems, and its validity is hence not affected by the lack of experiments.

Appendices

.1 Definition of Bandwidth in Control Theory

In control theory, the bandwidth of a closed-loop system is defined as the frequency range where the magnitude of the closed-loop gain in the frequency response is greater than -3.01 dB. The frequency which provides a -3.01 dB gain is defined as cutoff frequency (ω_B), where a gain equal to -3.01 dB corresponds to an attenuation of the input equal to half of its value.

Indeed, since a decibel ratio of the output power P_{out} of the input power P_{in} is defined as

$$G_P \;=\; 10\log_{10}\frac{P_{\text{out}}}{P_{\text{in}}}\,, \tag{1}$$

if P_{out} is half of the input, the corresponding dB gain is equal to

$$G_P \;=\; 10\log_{10}\frac{1}{2} \;\approx\; -3.01\text{dB}\,. \tag{2}$$

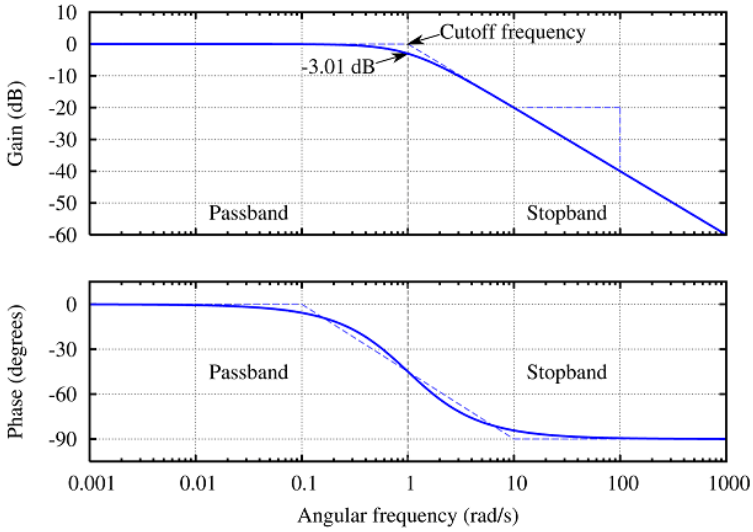

Figure 1: Bode plots of the frequency response of a low-pass filter

Bibliography

[1] N. Mohan, T. M. Undeland, and W. P. Robbins, *POWER ELECTRONICS, Converters, Applications, and Design*. JOHN WILEY & SONS, INC, 2nd ed., 1995.

[2] M. H. Rashid, *Power Electronics: Devices, Circuits, and Applications*. Pearson, 4th ed., 2013.

[3] N. M. Krylov and N. N. Bogoliubov, *Introduction to Nonlinear Mechanics*. Princeton: Princeton University Press, 1947.

[4] Y. A. Mitropolski, *Non-Stationary Processes in Non-Linear Oscillatory Systems*. Kiev: Izdvo AN, 1955.

[5] N. N. Bogoliubov and Y. A. Mitropolski, *Asymptotic Methods in the Theory of Non-Linear Oscillations*. New York: Gordon and Breach, 1961.

[6] P. V. Kokotović, "Applications of Singular Perturbation Techniques to Control Problems," *SIAM Review*, vol. 26, no. 4, October 1984.

[7] P. T. Krein, J. Bentsman, R. M. Bass, and B. L. Lesieutre, "On the Use of Averaging for the Analysis of Power Electronic Systems," *IEEE Transactions on Power Electronics*, vol. 5, no. 2, pp. 182–190, April 1990.

[8] B. Lehman and R. M. Bass, "Switching Frequency Dependent Averaged Models for PWM DC-DC Converters," *IEEE Transactions on Power Electronics*, vol. 11, no. 1, pp. 89–98, January 1996.

[9] J. W. Kimball and P. T. Krein, "Singular Perturbation Theory for DC–DC Converters and Application to PFC Converters," *IEEE Transactions on Power Electronics*, vol. 23, no. 6, pp. 2970–2981, November 2008.

[10] H. K. Khalil, *Nonlinear Systems*, ch. 9, 10, 11. Prentice Hall, 3rd ed., 1996.

[11] R. H. Park, "Two-Reaction Theory of Synchronous Machines, Generalized Method of Analysis — Part I," *Transactions of the American Institute of Electrical Engineers*, vol. 48, no. 3, pp. 717–727, July 1929.

[12] R. H. Park, "Two-Reaction Theory of Synchronous Machines — II," *Transactions of the American Institute of Electrical Engineers*, vol. 52, no. 2, pp. 352–354, June 1933.

[13] N. M. Wereley and S. R. Hall, "Frequency response of linear time periodic systems," in *Decision and Control, 29th IEEE Conference*, 1990.

[14] S. R. Hall and N. M. Wereley, "Generalized Nyquist stability criterion for linear time periodic systems," *American Control Conference*, pp. 1518–1525, May 1990.

[15] F. Umbría, J. Aracil, and F. Gordillo, "Singular perturbation stability analysis of three phase two-level power converters," in *18th Mediterranean Conference on Control and Automation*, 23th-25th June 2010.

[16] G. W. Hill, "On the Part of the Motion of Lunar Perigee Which is a Function of the Mean Motions of the Sun and Moon," *Acta mathematica*, no. 8, pp. 1–36, February 1886.

[17] P. L. Boyland, "Bifurcations of circle maps: Arnol'd tongues, bistability and rotation intervals," *Communications in Mathematical Physics*, vol. 106, no. 3, pp. 353–381, 1986.

[18] G. N. Love and A. R. Wood, "Harmonic State-Space model of power electronics," in *2008 13th International Conference on Harmonics and Quality of Power*, October 2008.

[19] J. R. Orillaza and A. R. Wood, "Harmonic State-Space Model of a Controlled TCR," *IEEE Transactions on Power Delivery*, vol. 28, no. 1, Jan 2013.

[20] J. Kwon, X. Wang, F. Blaaberg, C. L. Bak, V. S. Sularea, and B. C., "Harmonic Interaction Analysis in a Grid-Connected Converter Using Harmonic

State-Space (HSS) Modeling," *IEEE Transactions on Power Electronics*, vol. 32, no. 9, pp. 6823–6835, Sept 2017.

[21] E. Mollerstedt and B. Bernhardsson, "Out of control because of harmonics — an analysis of the harmonic response of an inverter locomotive," *IEEE Control Systems Magazine*, vol. 20, no. 4, pp. 70–81, Aug. 2017.

[22] V. Salis, A. Costabeber, S. M. Cox, and P. Zanchetta, "Stability Analysis of Single-Phase Grid-Feeding Inverters with PLL using Harmonic Linearisation and Linear Time Periodic (LTP) Theory," in *IEEE 17th Workshop on Control and Modeling for Power Electronics (COMPEL)*, 2016.

[23] V. Salis, A. Costabeber, S. M. Cox, A. Formentini, and P. Zanchetta, "Stability Assessment of High-Bandwidth DC Voltage Controllers in Single-Phase Active-Front-Ends: LTI vs LTP Models," *IEEE Journal of Emerging and Selected Topics in Power Electronics*, February 2018.

[24] R. C. Chaudhuri, R. Oliveira, and A. Yazdani, "Stability Analysis of Vector-Controlled Modular Multilevel Converters in Linear Time-Periodic Framework," *IEEE Transactions on Power Electronics*, vol. 31, no. 7, July 2016.

[25] N. Hatziargyrou, *Microgrids - Architectures and control.* Wiley, IEEE press, 1st ed., 2014.

[26] H. Bevrani, B. François, and T. Ise, *Microgrid Dynamics and control.* Wiley, 1st ed., 2017.

[27] V. Mariani, F. Vasca, J. C. Vásquez, and J. M. Guerrero, "Model Order Reductions for Stability Analysis of Islanded Microgrids With Droop Control," *IEEE Transactions on Industrial Electronics*, vol. 62, no. 7, pp. 4344–4354, July 2015.

[28] J. M. Guerrero, J. C. Vasquez, J. Matas, L. Garcia de Vicuna, and M. Castilla, "Hierarchical Control of Droop-Controlled AC and DC Microgrids — A General Approach Toward Standardization," *IEEE Transactions on Industrial Electronics*, vol. 58, no. 1, pp. 158–171, January 2011.

[29] N. Pogaku, M. Prodanović, and T. C. Green, "Modeling, Analysis and testing of Autonomous Operation of an Inverter-Based Microgrid," *IEEE Transactions on Power Electronics*, vol. 22, no. 2, pp. 613–625, March 2007.

[30] M. Rasheduzzaman, J. A. Mueller, and J. W. Kimball, "Reduced-Order Small-Signal Model of Microgrid Systems," *IEEE Transactions on Sustainable Energy*, vol. 6, no. 4, pp. 1292–1305, October 2015.

[31] J. Rocabert, A. Luna, F. Blaabjerg, and P. Rodriguez, "Control of Power COnverters in AC Microgrids," *IEEE Transactions on Power Electronics*, vol. 27, no. 11, pp. 4734–4749, November 2012.

[32] Y. W. Li and C. N. Kao, "An Accurate Power Control Strategy for Power-Electronics-Interfaced Distributed Generation Units Operating in a Low-Voltage Multibus Microgrid," *IEEE Transactions on Power Electronics*, vol. 24, no. 12, pp. 2977–2989, December 2009.

[33] V. Mariani, F. Vasca, J. C. Vásquez, and J. M. Guerrero, "Model order reductions for stability analysis of islanded microgrids with droop control," *IEEE Transactions on Industrial Electronics*, vol. 62, no. 7, pp. 4344–4354, 2015.

[34] K. Kodra, Ningfan Zhong, and Z. Gajić, "Model order reduction of an islanded microgrid using singular perturbations," in *2016 American Control Conference (ACC)*, pp. 3650–3655, 2016.

[35] L. Luo and S. V. Dhople, "Spatiotemporal Model Reduction of Inverter-Based Islanded Microgrids," *IEEE Transactions on Energy Conversion*, vol. 29, no. 4, pp. 823–922, December 2014.

[36] Y. Sun, X. Hou, J. Yiang, H. Han, S. M., and J. M. Guerrero, "New Perspectives on Droop Control in AC Microgrids," *IEEE Transactions on Energy Conversion*, vol. 29, no. 4, pp. 524–633, December 2014.

[37] K. Yao, K. Lee, M. Xu, and F. C. Lee, "Optimal Design of the Active Droop Control Method for the Transient Response," in *Eighteenth Annual IEEE Applied Power Electronics Conference and Exposition*, vol. 29, February 2003.

[38] L. Luo and S. V. Dhople, "Spatiotemporal Model Reduction of Inverter-Based Islanded Microgrids," *IEEE Transactions on Energy Conversions*, vol. 29, no. 4, pp. 823–832, Dec. 2014.